

New Strategies for Stereo- and Regiocontrol in Allene Hydrosilylation

by

Zachary D. Miller

**A dissertation submitted in partial fulfillment
of the requirements for the degree of
Doctor of Philosophy
(Chemistry)
in The University of Michigan
2015**

Doctoral Committee:

**Professor John Montgomery, Chair
Assistant Professor Pavel Nagorny
Professor Melanie S. Sanford
Assistant Professor Matthew B. Soellner**

Dedication

In memory of my grandfather Charles T. Pillichody.

Acknowledgments

I would like to acknowledge my thesis advisor, Prof. John Montgomery, for allowing me to join his research group. I have enjoyed working directly with him and I am grateful for his mentorship and patience throughout my graduate career. Additionally, I have been inspired by John's commitment to exploring truly intriguing and challenging problems in synthetic organic chemistry.

I am also grateful for the efforts of my graduate committee members who have made numerous contributions to my thesis work through their helpful suggestions. At the start of my career at Michigan, I had the excellent opportunity of working in Prof. Pavel Nagorny's lab. Through this experience, I learned many lab skills while working along side Pavel and I greatly benefited from his enthusiasm and excitement for chemistry. I would also like to express gratitude to Prof. Melanie Sanford for her insights and dedication to elevating the conversations during my committee meetings. In addition, I thank Prof. Matthew Soellner for serving as my cognate member and for offering his perspectives throughout this process. I appreciate all of your efforts in challenging and encouraging me to be a better scientist.

I have been very fortunate to work with many talented coworkers in the Montgomery research group. I would like to specifically thank Dr. Haz Malik, Dr. Grant Sormunen, Dr. Katie Partridge, Dr. Allison Knauff, Dr. Ben Thompson, Dr. Hengbin Wang, and Dr. Solymar Negretti for supporting me during my graduate career and for providing feedback to my questions regarding reaction design and experimental setup. I

would also like to acknowledge the work of visiting student Ruth Dorel from ICIQ for her tremendous contributions to the work in the fourth chapter.

I would also like to thank my friends and family for their support throughout this experience. I am grateful for my Ann Arbor friends: Eric Wortman, Mary Balconi, Daron Mills, Eric Wrestler, Sean Stalker, Caitlin Lackie, Chelsea Anderson, Mateo Carrillo, Dr. Sebastian Parlee, Allyson and Megan. I have so many great memories with all of you and I have been truly lucky to be surrounded by such a supportive group. I also thank my family for supporting me, especially my mother whose dedication in raising three children as a single parent has always been a source of inspiration for me. I would like to also acknowledge my fiancé, Alan Githens, for his love and support throughout graduate school. I am a better person because of you and I look forward to planning our wedding in the near future.

Table of Contents

Dedication.....	ii
Acknowledgments.....	iii
List of Figures	vii
List of Tables.....	viii
List of Schemes	ix
List of Abbreviations.....	xi
Abstract.....	xiii
Chapter 1	1
Strategies for Regiocontrol in Transition Metal-Catalyzed Multicomponent Couplings	
1.1 Introduction: Regioselectivity in Simple Coupling Reactions	
1.2 Nickel-Catalyzed Multicomponent Couplings.....	3
1.3 Nickel-Catalyzed Couplings with Allene Substrates.....	6
1.4 Regiodivergent Metal-Catalyzed Hydrometalations and Dimetalations	9
1.5 The Mechanisms of Alkyne Hydrosilylation: Two-Component Couplings	13
1.6 Examples of Terminal Alkyne Hydrosilylation Procedures.....	17
1.7 Methods for Regiocontrol in Alkyne and 1,3-Diene Hydrosilylation	20
1.8 Related Silane Functionalizations.....	26
1.9 Alkenyl- and Allylsilanes in Complex Molecule Synthesis	28
1.10 Conclusions and Outlook.....	30
Chapter 2	31
Metal-Directed Regioselective Allene Hydrosilylation Catalyzed by <i>N</i> -Heterocyclic Carbene Complexes of Ni(0) and Pd(0)	
2.1 Introduction: Allene Hydrosilylation	31
2.2 Allene Hydrosilylation and Related Metalation Protocols	32
2.3 Observation of Complementary Behavior in Regioselectivity	40
2.4 Evaluation of in situ generated NHC-M(0) catalysts	41
2.5 Substrate scope	43
2.6 Mechanistic Pathway and Crossover Study.....	46
2.7 Conclusions and outlook.....	49
2.8 Experimental.....	49
Chapter 3	91
Regioselective Allene Hydroarylation via One-Pot Regioselective Allene Hydrosilylation/ Pd(0)-Catalyzed Cross-Coupling	
3.1 Introduction	91
3.2 Hiyama-Denmark Cross-Couplings	92
3.3 One-Pot Hydroarylation Procedures Involving Hydrosilylation/ Cross-Coupling.....	94
3.4 NHC Ligand Evaluation with Pd(0) Precatalyst	96
3.5 Substrate Scope.....	98
3.6 Optimization of Allene Hydroarylation Protocol.....	101
3.7 Large-Scale Hydroarylation Operations.....	103
3.8 Proposed Mechanism and Origin of Regioselectivity	104
3.9 Conclusions and Outlook.....	105

3.10 Experimental.....	106
Chapter 4	124
Access to Regio- and Stereodefined E-Allylic- and Z-Alkenylsilanes via 1,3-Disubstituted Allene Hydrosilylation	
4.1 Introduction	124
4.2 Internal Alkyne Hydrosilylation Procedures.....	126
4.3 Methods for the Synthesis of Stereo- and Regiodefined Alkenylsilanes.....	129
4.4 Uncatalyzed Hydroalumination Methods Towards Z-Alkenylsilanes.....	131
4.5 Access to <i>E</i> -Allylsilanes.....	132
4.6 Research Plan	134
4.7 Evaluation of NHC Ligand Effects in 1,3-Disubstituted Allene Hydrosilylation	135
4.8 Allene Substrate Exploration	137
4.9 Synthetic Manipulations of Alkenylsilanes	140
4.10 Proposed Mechanisms.....	142
4.11 Conclusions and Outlook.....	145
4.12 Experimental.....	146
Chapter 5	193
Summary and Outlook	
References.....	197

List of Figures

Figure 1-1 Simple Coupling Reactions.....	2
Figure 1-2 Unbiased Substrates	2
Figure 1-3 Nickel-Catalyzed Reductive Couplings of Aldehydes and Alkynes.....	3
Figure 1-4 Hydrosilylations of Biased 1-Alkynes	18

List of Tables

Table 1 Evaluation of NHC Ligand Effects.....	42
Table 2 Metal-Directed Regiodivergent Allene Hydrosilylations	44
Table 3 Silane Scope for the Pd-Catalyzed Reaction	46
Table 4 Evaluation of NHC Ligands Effects	97
Table 5 Pd-Catalyzed Allene Hydrosilylation	100
Table 6 One-Pot Allene Hydroarylation	103
Table 7 Optimization Studies: 1,3-Disubstituted Allene Hydrosilylations	136
Table 8 Metal-Directed 1,3-Disubstituted Allene Hydrosilylation.....	138
Table 9 Additions to Unsymmetrically Substituted Allenes.....	140

List of Schemes

Scheme 1-1 Ligand-Controlled Regiocontrol Strategy.....	4
Scheme 1-2 Improving Regiocontrol Through Alterations in R.D.S.	5
Scheme 1-3 Reductive Couplings of Axially Chiral Allenes and Aldehydes	6
Scheme 1-4 Intramolecular Alkylative Reductive Couplings	7
Scheme 1-5 Key Fragment In Synthesis of Testudinariol A	8
Scheme 1-6 The Reductive Coupling of Allenes and Enones	9
Scheme 1-7 Nickel-Catalyzed Regiodivergent Hydroaluminations of Alkynes	10
Scheme 1-8 Regiodivergent 1,4-Hydroboration of 1,3-Dienes	11
Scheme 1-9 Regiodivergent Silaboration of Alkynes.....	12
Scheme 1-10 Regiocontrol Strategy: Alterations in R.D.S.....	12
Scheme 1-11 Metal-Catalyzed Hydrosilylations of Alkynes.....	14
Scheme 1-12 Chalk-Harrod Hydrometalation Alkyne Hydrosilylation Mechanism.....	14
Scheme 1-13 Modified Chalk-Harrod Mechansim.....	15
Scheme 1-14 <i>Trans</i> -Hydrosilylation Isomerization Pathways	16
Scheme 1-15 Pt-Catalyzed Hydrosilylations of Terminal Alkynes.....	19
Scheme 1-16 Cationic Ruthenium-Catalyzed Hydrosilylations of Terminal Alkynes.....	19
Scheme 1-17 Improving Regioselectivity via Substrate Electronic Bias	21
Scheme 1-18 Tethered Directing Group Regiocontrol Strategy	22
Scheme 1-19 Nickel-Catalyzed NHC Ligand-Controlled Hydrosilylations.....	23
Scheme 1-20 1,4-Hydrosilylation of Dienes.....	24
Scheme 1-21 1,2- Hydrosilylation of Dienes.....	25
Scheme 1-22 Copper-Catalyzed Protosilylations of Terminal Alkynes	26
Scheme 1-23 Mechanisms for Silyl-Heck Reaction	27
Scheme 1-24 Silyl-Heck Reaction Affording Alkenylsilanes	28
Scheme 1-25 Silyl-Heck Reaction Affording Allylsilanes.....	28
Scheme 1-26 Total Synthesis of Herboxidiene Employing Alkenyl- and Allylsilanes....	29
Scheme 2-1 Lewis-Acid Catalyzed Allene Hydrosilylation.....	32
Scheme 2-2 Lewis-Acid Catalyzed Allene Hydrosilylation Mechanism	33
Scheme 2-3 Hydrosilylation of Sugar Allenes.....	34
Scheme 2-4 Silaboration of Allenes	34
Scheme 2-5 Silaboration of 1,3-Disubstituted Allenes.....	35
Scheme 2-6 Silaborations of Unsymmetrically Substituted Allenes	35
Scheme 2-7 Mechanisms for Allene Silaboration	36
Scheme 2-8 Enantioselective Allene Diborations.....	37
Scheme 2-9 Mechanism for Allene Diboration	37
Scheme 2-10 Regiodivergent Hydroborations of Allenes	38
Scheme 2-11 Regiodivergent Pathways for Allene Hydroboration.....	39
Scheme 2-12 Metal-Directed Regiodivergent Hydrosilylations.....	41
Scheme 2-13 Hydrosilylations of 1,1-Disubstituted Allenes.....	45

Scheme 2-14 Proposed Hydrosilylation Pathways	47
Scheme 2-15 Double-Labeling Study with Ni-Catalyzed Protocol	48
Scheme 2-16 Double-Labeling Study with Pd-Catalyzed Protocol	48
Scheme 3-1 Heck-Type Cross-Couplings of Alkenylsilanes	92
Scheme 3-2 Pentacoordinate Silicon in Cross-Coupling Reactions	93
Scheme 3-3 Cross-Couplings of Silanoate Salts	94
Scheme 3-4 One-Pot Hydrosilylation/Cross-Coupling Protocol	95
Scheme 3-5 One-Pot Hydrosilylation/ Cross-Coupling in Total Synthesis	95
Scheme 3-6 Large-Scale Hydroarylation Example	104
Scheme 3-7 Origin of Regiocontrol: Ligand Sterics	105
Scheme 4-1 Challenge of Regiocontrol in Hydrosilylations of Internal Alkynes	125
Scheme 4-2 Pt-Catalyzed Hydrosilylations of Internal Alkynes	126
Scheme 4-3 Lewis-Acid-Catalyzed Hydrosilylations of Alkynes	127
Scheme 4-4 Hydrosilylations with Cationic Ruthenium Complexes	127
Scheme 4-5 Intramolecular <i>Trans</i> -Hydrosilylations	128
Scheme 4-6 Cyclocondensations of Aldehydes and Alkynes	129
Scheme 4-7 Reductive Couplings of Silylalkynes and Chiral Aldehydes	130
Scheme 4-8 Intramolecular Alkylative Couplings	130
Scheme 4-9 Rearrangement of Alkynols	131
Scheme 4-10 Hydroalumination/ Iodination Procedure	131
Scheme 4-11 Hydrometalations of Silyl Alkynes	132
Scheme 4-12 Disilylation Route to Chiral Allylsilanes	133
Scheme 4-13 Allylic Substitution Pathways to Allylsilanes	134
Scheme 4-14 Hydrosilylation of Cyclic Allenes	139
Scheme 4-15 Pd-Catalyzed Hydrosilylations of Unsymmetrical Substrates	140
Scheme 4-16 Synthetic Manipulations of Stereo- and Regiodefined Alkenylsilanes	141
Scheme 4-17 One-Pot Hydroarylation	142
Scheme 4-18 Proposed Hydrosilylation Mechanisms	143
Scheme 4-19 Origin of Selectivity with Unsymmetrical Substrates	144
Scheme 4-20 Additions to Enantioenriched Allenes	145

List of Abbreviations

AE	allylic ether
Ar	aryl
9-BBN	9-borabicyclo[3.3.1]nonane
B ₂ pin ₂	bis(pinacolato)diboron
Bn	benzyl
<i>n</i> -Bu	butyl
<i>t</i> -Bu	<i>tert</i> -butyl
COD	1,5-cyclooctadiene
°C	temperature in degrees centigrade
Cy	butyl
d	day(s)
<i>n</i> -Dec	decyne/decyl
DIBALH	<i>diisobutyl</i> aluminum hydride
dba	dibenzylideneacetone
dppf	1,1'-bis(diphenylphosphino)ferrocene
dr	diastereomeric ratio
% ee	percent enantiomeric excess
Et	ethyl
EtO	ethoxy
equiv	equivalent
EWG	electron-withdrawing group
GCMS	gas chromatography- mass spectrometry
h	hours
<i>n</i> -Hept	heptyl
<i>c</i> -Hex	cyclohexyl
<i>n</i> -Hex	hex

HPLC	high performance liquid chromatography
IMes	1, 3-bis-(1, 3, 5-trimethylphenyl)imidazol-2-ylidene
IPr.....	1, 3-bis-(2, 6-diisopropylphenyl)imidazol-2-ylidene
JohnPhos	(2-biphenyl)di- <i>tert</i> -butylphosphine
L•HX	ligand as hydrohalide salt
L _n	generalized ligand
Me	methyl
min	minute(s)
NHC	<i>N</i> -heterocyclic carbene
NMR	nuclear magnetic resonance
<i>n</i> -Pent	pentyl
Ph	phenyl
KO- <i>t</i> -Bu	potassium <i>tert</i> -butoxide
<i>i</i> -Pr.....	isopropyl
<i>n</i> -Pr.....	propyl
<i>i</i> -PrO.....	isopropoxyl
regiosel.....	regioselectivity
rds.....	rate-determining step
rt	room temperature
Sty	styrene
TBAF	<i>tetrabutylammonium fluoride</i>
TBS	<i>tert</i> -butyldimethylsilane
TMS	trimethylsilane
THF	tetrahydrofuran
TLC.....	thin-layer chromatography
Tol.....	toluene

Abstract

Controlling the regiochemistry in additions of silanes across π components is a significant challenge in route to important stereo- and regiodefined alkenyl- and allylsilane intermediates. In many cases the absence of substrate biases or appended directing groups, these reactions are unselective affording mixtures of inseparable constitutional isomers. With the aim to develop catalyst-controlled strategies to find solutions for these challenges, we investigated allene hydrosilylations due to the possibility of accessing either allyl- or alkenylsilanes from one substrate class.

Regioselective allene hydrosilylations with *N*-heterocyclic carbene (NHC) complexes of nickel and palladium have been developed and are described. In this reaction manifold, regioselectivity is governed primarily by choice of metal as alkenylsilanes are produced via nickel catalysis with larger NHC ligands and allylsilanes are produced via palladium catalysis with smaller NHC ligands. These complementary methods allow either regioisomeric product to be obtained with exceptional regiocontrol. Additional complementary access to the corresponding alkenylsilanes is accomplished with palladium catalysis via a novel ligand-controlled strategy with a class of large NHC ligands. In this approach, modification of NHC ligand structure from a common palladium pre-catalyst permits either regioisomeric product to be afforded in excellent regiocontrol via the reversal of a palladium hydrometalation to a silylmetalation. As an extension of this discovery, a one-pot hydroarylation protocol has been elucidated to afford functionalized branched alkene isomers. This process involves regioselective

allene hydrosilylation in tandem with a palladium-catalyzed cross-coupling reaction to furnish exclusively functionalized 1,1-disubstituted olefins.

Regio- and stereocontrolled additions to 1,3-disubstituted allenes affording either *E*-allylsilanes with palladium NHC catalysts or *Z*-alkenylsilanes with nickel NHC catalysts have been discovered. It was found that a variety of symmetrically and unsymmetrical 1,3-disubstituted allenes were tolerated with the optimized reaction conditions. The NHC nickel catalyst developed selectively affords only the *Z*-stereoisomer, which is typically the opposite stereochemistry experienced in normal mode transition-metal catalyzed hydrometalations. In addition, when the nickel reaction was conducted with unsymmetrical allenes differentiated by steric encumbrance result in only one isomer was afforded in high yields. These developments provide access to important stereo- and regiodefined, metalated intermediates useful in a variety of synthetic transformations.

Chapter 1

Strategies for Regiocontrol in Transition Metal-Catalyzed

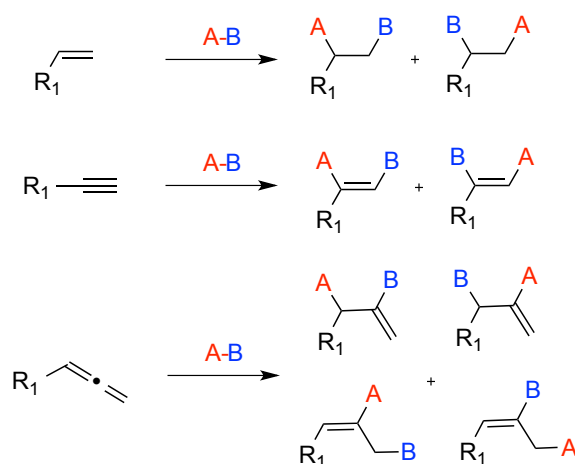
Multicomponent Couplings

1.1 Introduction: Regioselectivity in Simple Coupling Reactions

The research and development of molecular medicines is reliant upon the optimization and elaboration of efficient and selective chemical methods. Therefore, chemical reactions that are generally unselective or wasteful are a direct impediment to the discovery of biologically important molecules. For these reasons, chemical reactions that permit complexity to be rapidly constructed from widely available materials are especially attractive routes.

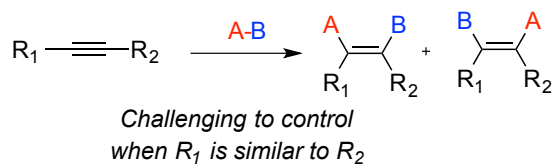
As a result of the need for efficient protocols, significant efforts have been dedicated towards the development of simple coupling reactions of π -components with coupling partners A-B (Figure 1-1). In this class of reactions, a variety of constitutional isomers (regioisomers) can be afforded depending on the mode of addition (*syn* or *trans*) and selection of π -component. Further complicating these processes is the likelihood for forming stereoisomeric products when substitution permits.

Figure 1-1 Simple Coupling Reactions



For biased substrates (Figure 1-1), the significant differences in steric and electronic environments make controlling regioselectivity significantly less challenging; however, reversing the inherent mode of addition for biased structures is typically difficult. In contrast, selection of a substrate with similar substitution patterns, such as internal alkynes, typically results in reaction outcomes that are often very challenging to control resulting in a mixture of regioisomers (Figure 1-2).

Figure 1-2 Unbiased Substrates



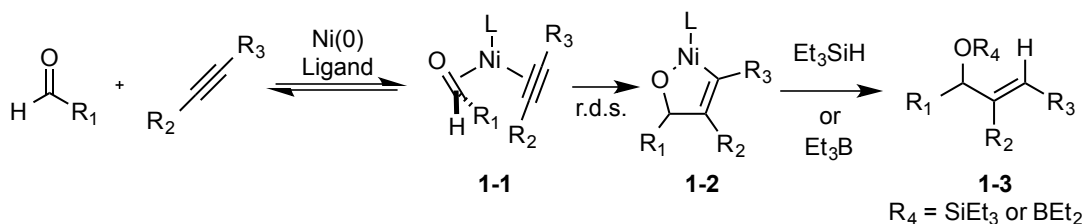
The design and implementation of catalyst systems that override inherent substrate biases would be an ideal solution for controlling the outcomes in simple coupling reactions, especially for otherwise difficult to control unbiased systems. In addition, the development of systems that permit a variety of substructures to be obtained from a common starting material by simple modification of catalyst structure would enable flexibility in synthetic planning. The remaining focus will be dedicated to metal-

catalyzed procedures that allow simple components to be translated into useful chemical commodities and the challenges associated with these processes.

1.2 Nickel-Catalyzed Multicomponent Couplings

A powerful method for the stereo- and regioselective synthesis of allylic alcohols is the nickel-catalyzed reductive coupling of aldehydes and alkynes (Figure 1-3). The most developed versions of this reaction involve reactions of Ni(0) precatalysts with either monodentate phosphine ligands with triethylborane¹ or with *N*-heterocyclic carbene ligands or monodentate phosphine ligands (NHC) with triethylsilane² as the reducing agent. This procedure is appealing due to the wide-availability of the starting materials and the sub-stoichiometric amounts of metal catalyst required to perform the reaction.

Figure 1-3 Nickel-Catalyzed Reductive Couplings of Aldehydes and Alkynes

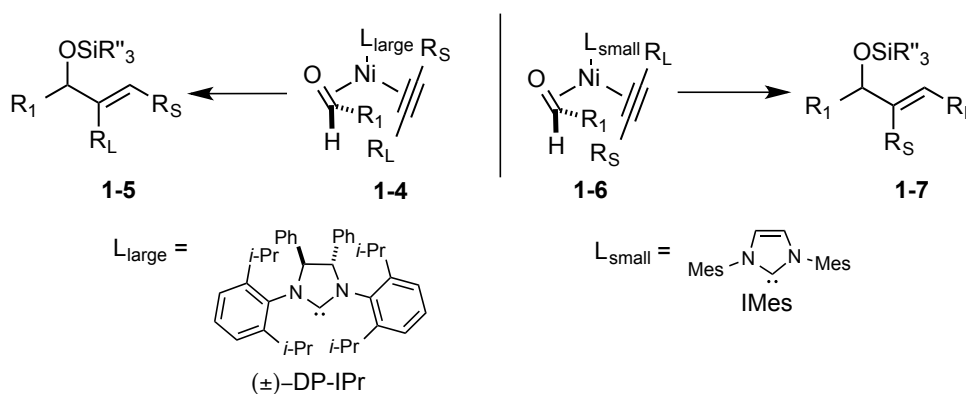


For these catalyst systems, the currently accepted mechanism begins with the reversible formation of π complex **1-1** followed by rate- and regiochemistry-determining oxidative cyclization affording nickelacycle **1-2** (Figure 1-3). After this step, sigma-bond metathesis with either an equivalent of triethylborane or triethylsilane restores the nickel catalyst while yielding allylic alcohol derivatives **1-3**. Evidence for this mechanistic model can be found in kinetic studies of the intramolecular reductive couplings of ynals employing Ni(COD)₂/PCy₃ catalyst which demonstrate that triethylsilane is not consumed until after the introduction of both π components (aldehyde and alkyne).^{3a}

Therefore, direct oxidative addition by catalyst into the Si-H bond is not observed under the catalytic conditions and the silane is consumed only after substantial metalacycle formation. As a result, the findings from this study outrule previously hypothesized hydro- or silylmetalative mechanisms and favor the metallacyclic pathway. Several other kinetic analyses as well as computational studies for both variants of this reaction are all in agreement with the current mechanistic model.^{3b-c}

A significant challenge in nickel-catalyzed aldehyde and alkyne reductive couplings is controlling the regiochemistry of the derived allylic alcohol products **1-5** and **1-7** (Scheme 1-1). Several successful approaches in harnessing regiocontrol have involved either applying substrate electronic and steric biases to the π components and also use of tethered alkene directing groups. A strategy for the reductive couplings of aldehydes and alkynes has recently been developed by Montgomery that utilizes NHC ligands to fine-tune and while also directing the regiochemical outcome in the reaction (Scheme 1-1).^{4a}

Scheme 1-1 Ligand-Controlled Regiocontrol Strategy

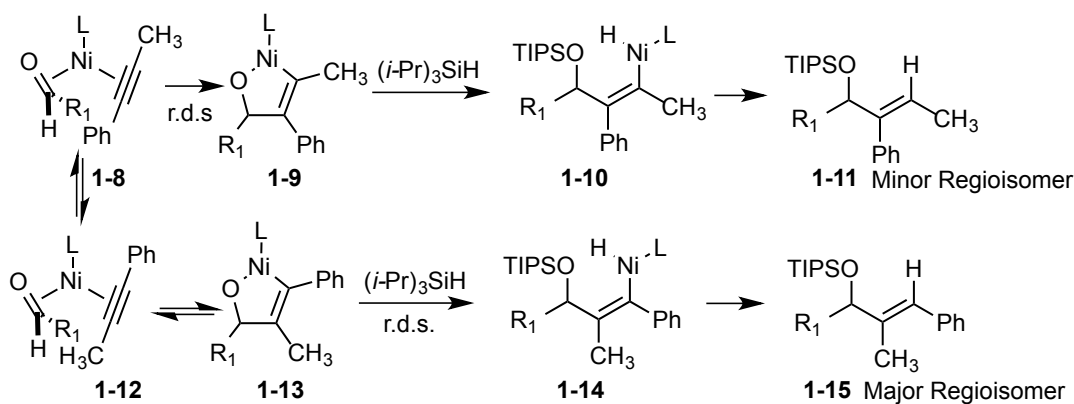


In this strategy, use of sterically-encumbered ligand DP-IPr forces nickel π complex **1-4** to adopt a geometry that minimize steric interactions between the larger substituent R_L and the large ligand. Conversely, employing smaller NHC ligand IMes imposes a less

significant steric penalty with the larger substituent R_L , so the nickel π complex **1-6**, where R_L is positioned closer to the NHC ligand, is instead favored (Scheme 1-1). Through adopting this pre-oxidative cyclization geometry, the complex simultaneously minimizes steric interactions between R_L and the R_1 substituent on the aldehyde. Computational studies plotting NHC contour maps describe the steric effects the ligands impose on the alkyne π ligands and are directly correlated with the percent buried volume ($\%V_{bur}$) of the Ni/NHC catalysts.^{4b}

A recently developed regiocontrol strategy in the nickel-catalyzed reductive couplings of aldehydes and alkynes involves changing the rate- and regiodetermining step by utilizing very bulky silane reducing agents (Scheme 1-2).^{4c} In this report by Jackson and Montgomery, use of bulky silanes (i.e. $i\text{-Pr}_3\text{SiH}$) effectively renders the oxidative cyclization (**1-12** to **1-13**) reversible and the sigma-bond metathesis step (**1-13** to **1-14**) in turn becomes the slow step in the reactive pathway for the formation of only isomer **1-15**.

Scheme 1-2 Improving Regiocontrol Through Alterations in R.D.S.



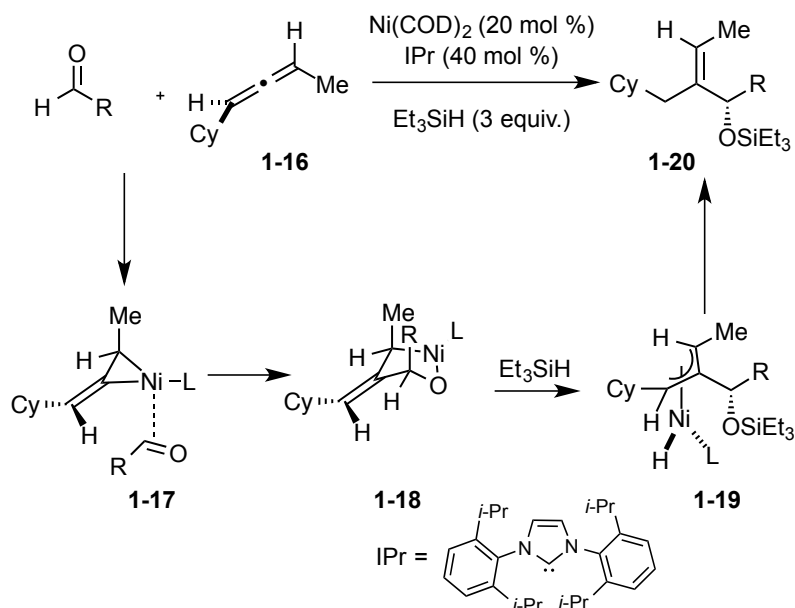
Evidence for the proposed mechanism can be found in the kinetic profiles for the formation of both **1-11** and **1-15** as it was found that the formation of isomer **1-11** is zero-order in silane while the formation of isomer **1-15** is first-order in silane, indicating that

the slow step for its formation is bimolecular and also involves the silane. This protocol, in contrast with the previously discussed ligand-controlled and substrate-directed approaches, bolsters regioselectivity without the use of exotic NHC ligands through the careful selection of silane reducing agent and reaction conditions.

1.3 Nickel-Catalyzed Couplings with Allene Substrates

The nickel-catalyzed couplings of allenes with aldehydes and enynes are powerful methods for transforming relatively simple starting materials into important stereodefined acyclic and cyclic motifs. In a report by the Jamison group,^{5a} it was discovered that Ni(0)/IPr catalysts effectively couple axially chiral allenes with aldehydes to afford chiral silyl-protected allylic alcohols **1-20** functionalized with *Z*-alkene stereochemistry (Scheme 1-3).

Scheme 1-3 Reductive Couplings of Axially Chiral Allenes and Aldehydes

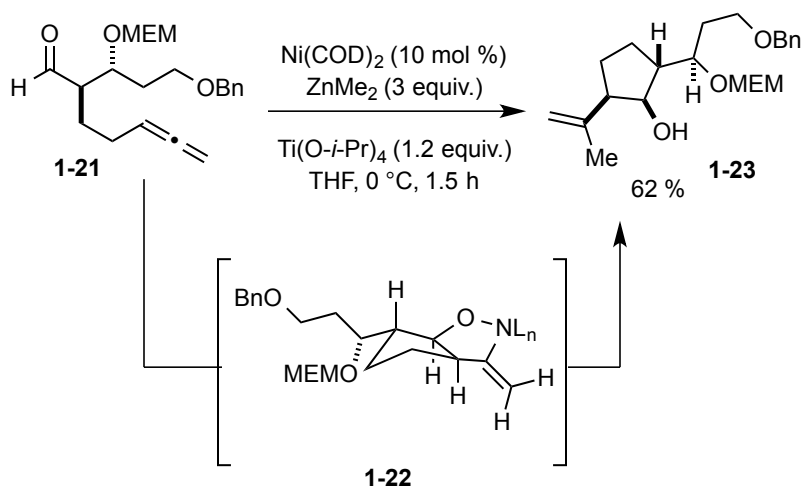


This process begins with the selective *anti*-coordination by the nickel catalyst to form the least hindered π complex **1-17**. The metal catalyst undergoes *anti*-additions to minimize unfavorable steric interactions experienced in a *syn*-addition with the

substituents (Cy or Me in this case). Another factor in the observed site selectivity is the selective *anti*-addition positioning the ligand closest to the Me group is favored over the analogous interaction with a larger Cy substituent. After this step, the oxidative cyclization with an aldehyde forms a five-membered nickellacycle **1-18**, with the C-C bond forming with the central carbon (Scheme 1-3). The stereochemistry of the silylether is imparted due to the lowest-energy approach of the aldehyde, with its substituent pointed away from the forming complex. Treatment with triethylsilane collapses nickellacycle **1-18** and forms the lowest energy π -allyl intermediate **1-19**, which simultaneously sets the *Z* stereochemistry. Subsequent reductive elimination at the methylene closest to the Cy substituent furnishes **1-20**. Evidence for this mechanism can be found in deuterium-incorporation studies.

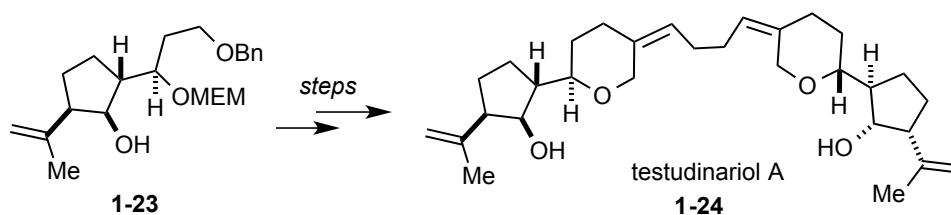
Intramolecular nickel-catalyzed allene and aldehyde alkylative couplings have also been developed and are useful for even complex substrates (Scheme 1-4).^{5b} In this sequence, addition across the internal double bond of allene **1-21** occurs, forming five-membered *exo*-metalacycle **1-22**, setting the stereochemistry of the alkene and alcohol.

Scheme 1-4 Intramolecular Alkylative Reductive Couplings



Upon treatment with dimethylzinc, a vinyl-nickel-methyl species is furnished and reductive elimination affords cyclopentanol **1-23** as one stereoisomer. The utility of this approach is further highlighted in the concise total synthesis of natural product testudinariol A **1-24** (Scheme 1-5). In this approach, rapid formation of rather complex fragments of this molecule is possible using this intramolecular alkylative allene/aldehyde coupling technology.

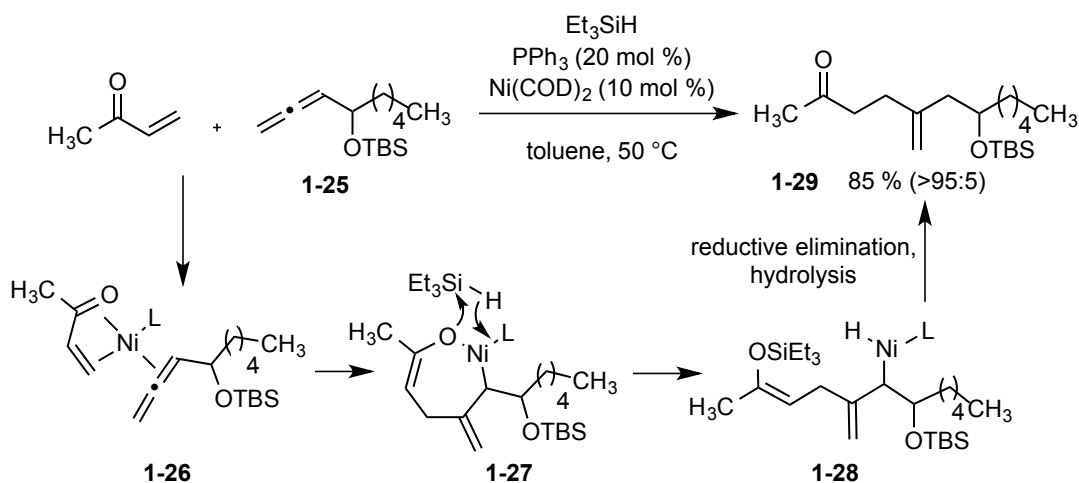
Scheme 1-5 Key Fragment In Synthesis of Testudinariol A



This example represents the potential utility of nickel-catalyzed coupling reactions in the synthesis of complex carbocyclic and acyclic molecules in a stereo- and regioselective fashion.

The nickel-catalyzed reductive coupling of allenes and enones is also a useful protocol to regioselectively afford ketone motifs (Scheme 1-6).^{5c} The optimized conditions employ triethylsilane, PPh₃, and Ni(COD)₂ precatalyst in toluene. In this reactive pathway, π complex **1-26** forms and oxidative cyclization affords seven-membered nickellacycle **1-27** with C-C bond formation to the central carbon of **1-25**.

Scheme 1-6 The Reductive Coupling of Allenes and Enones



Subsequent treatment with triethylsilane affords nickel-hydride **1-28** and upon reductive elimination and hydrolysis of enol silane **1-28**, compound **1-29** is formed in 85 % yield (Scheme 1-6). Benefits of this approach include the ability to simultaneously elaborate both the enone and allene to build up complex acyclic and cyclic alkene-containing keto motifs.

As demonstrated in the previous examples, the reductive and alkylative nickel-catalyzed couplings of allenes provide useful routes to stereodefined acyclic and cyclic functionalized motifs. For metallacyclic reactions, there is a continued theme of addition across the internal olefin of the contiguous double bonds. Use of allenes as substrates in these reactions permits the practitioner to take relatively simple starting materials and very selectively convert them to useful scaffolds.

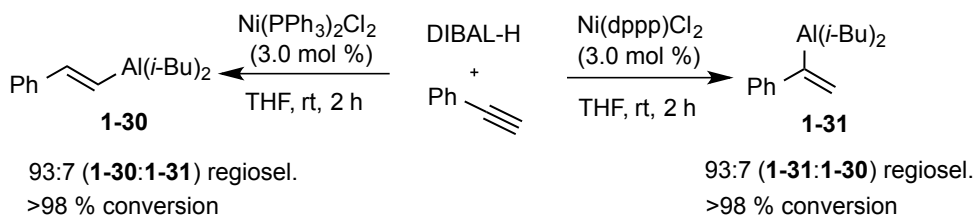
Section 1.4 Regiodivergent Metal-Catalyzed Hydrometalations and Dimetalations

The three-component nickel-catalyzed reductive couplings discussed in the previous section, with the exception of one recent example, undergo pathways where incorporation of the reducing agent occurs in a post rate-limiting step (after the oxidative cyclization). Therefore, the identity of the silane (or other reducing agent) typically has

insignificant impact on the regiochemical outcome since it is not intimately involved in the C-C bond-forming step. In contrast with these protocols, two-component couplings are a class of multicomponent coupling reactions where the reducing agent coupling partner is typically involved in the rate-determining and therefore also the regiochemistry-determining step. The subject of this section will focus on this class of transformations with a specific emphasis on procedures that permit a common starting material to be selectively converted into multiple regiodefined structures.

An example of such a protocol is the nickel-catalyzed hydroalumination of alkynes (Scheme 1-7).⁶ In this procedure, use of a Ni(II) ligand with PPh₃ affords linear hydrometalated product **1-30** while use of a similar catalyst modified with bidentate phosphine ligand dppp instead affords the branched regioisomer **1-31**.

Scheme 1-7 Nickel-Catalyzed Regiodivergent Hydroaluminations of Alkynes

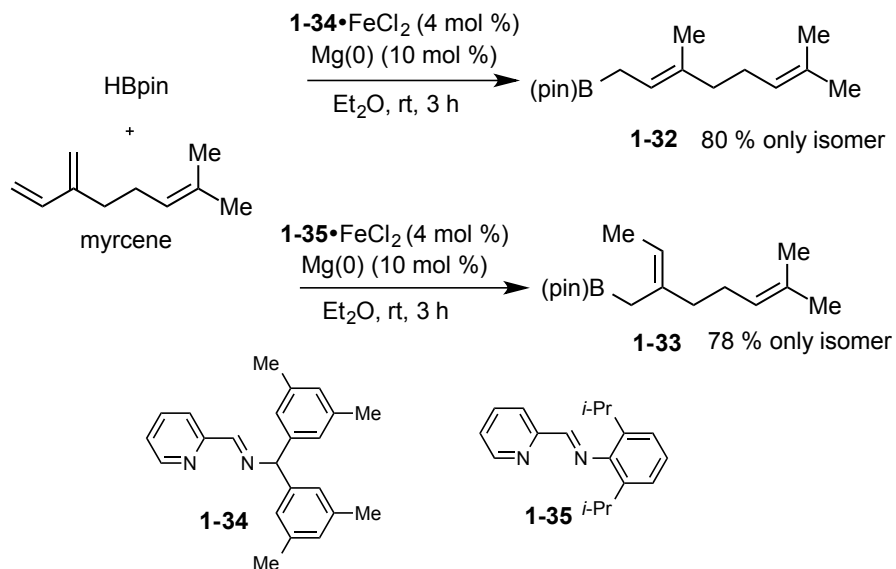


The exact role of the ligand and rationalization for why this regiodivergent behavior is observed is currently not well-understood; however, the authors do mention that they believe this to be a Ni(0)-catalyzed procedure as they observed *in situ* generated Ni(0) catalysts to also afford alkyne hydroalumination products. Products afforded in this manifold were coupled with a variety of electrophiles with excellent transfer of regio- and stereochemistry.

An iron-catalyzed hydroboration procedure was also reported that permits 1,3-dienes to be transformed to either 1,4-addition regioisomeric product as a function of

iminopyridine ligand (Scheme 1-8).⁷ For example, hydroboration of myrcene with iron (II) catalyst employing ligand **1-34** affords only linear allylborane **1-32** in excellent yield. Under the same reaction conditions, but instead simply modifying the iron catalyst with ligand **1-35** affords the opposite branched regioisomer **1-33** in 78 %.

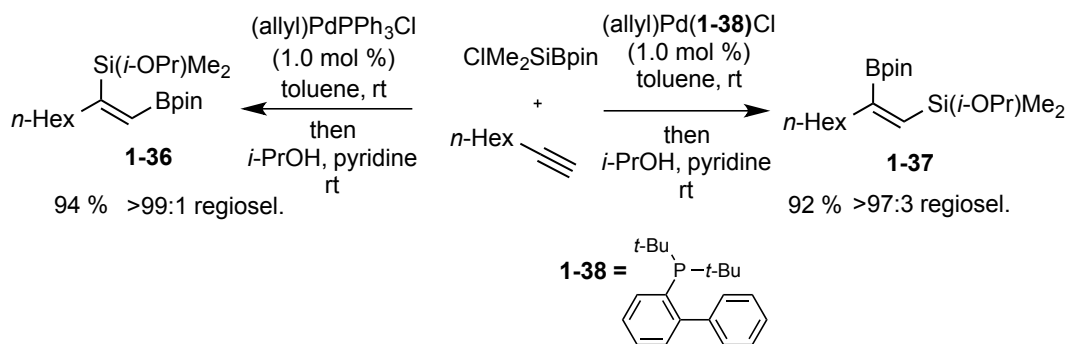
Scheme 1-8 Regiodivergent 1,4-Hydroboration of 1,3-Dienes



Although deuterium-labeling studies have helped narrow down the mechanism to a reasonable pathway, the exact role of the iminopyridine ligands and the factors that govern this regiodivergent behavior are not understood. KIE studies demonstrate that the rate-limiting step involves initial oxidative addition to the B-H.

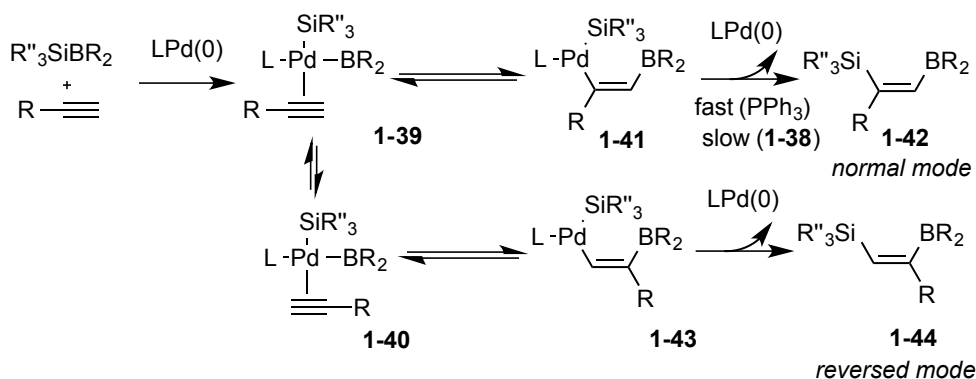
Advances have also been made in the development and optimization of palladium-catalyzed regiodivergent alkyne silaborations (Scheme 1-9).⁸ In this manifold, selection of phosphine ligand, either PPh_3 or **1-38**, directs the outcome to afford either **1-36** or **1-37** respectively in excellent yields.

Scheme 1-9 Regiodivergent Silaboration of Alkynes



Treatment with *i*-PrOH and pyridine after the reaction has completed then converts the Si-Cl into the isolable alkenyl siloxane. The authors propose a mechanism that commences with oxidative addition to the Si-B bond (Scheme 1-10). Coordination to the alkyne then affords intermediate **1-39**, which is the geometry prior to normal mode additions, whereby the more electrophilic boron ligand is positioned nearest the carbon with the most negative charge. For both processes, a common migratory insertion of the alkyne into the Pd-BR₂ bond affords **1-41**.

Scheme 1-10 Regiocontrol Strategy: Alterations in R.D.S.



When the ligand of choice is PPh₃, rapid reductive elimination from **1-41** furnishes the normal mode addition product **1-42**. However, with the use of bulkier ligand **1-38**, the rate of reductive elimination depresses and intermediate **1-41** reverts back to π -complex **1-39** via β -boryl elimination. From this intermediate, reorganization to afford π -complex **1-40** occurs and migratory insertion affords intermediate **1-43**. Reductive elimination

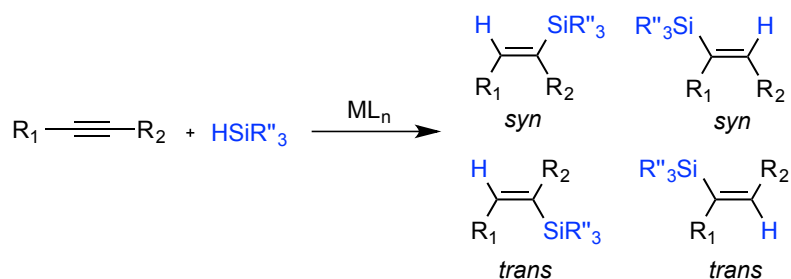
from intermediate **1-43** results in the formation of the reversed addition product **1-44** (observed only with ligand **1-38**). This mechanism is supported in the study of the cyclization of 1,6-enynes, where it was found that silaborations with PPh₃ resulted in less cyclized product, indicating that reductive elimination was fast thereby preventing a subsequent coordination/insertion event from occurring. In contrast with this result, the reaction with bulky ligand **1-38** resulted in substantially more cyclized product indicating that the reductive elimination is slow and the sigma-Pd species is less fleeting than in the normal mode addition pathway. In this example, changing the rate-determining step for one isomer in the pathway is also an effective mode for completely controlling the regiochemical outcome.

In the previously discussed two-component hydrometalation and dimetalation procedures, by simply changing catalyst structure one starting material can be regio- and stereoselectively transformed into a variety of useful functionalized scaffolds. Although in many cases the rationale for the observed regiodivergency is not completely understood, there is significant potential utility for practitioners interested in flexible routes to a variety of metalated intermediates.

1.5 The Mechanisms of Alkyne Hydrosilylation: Two-Component Couplings

Another class of reactions that is especially challenging in regard to controlling the stereo- and regiochemistry is the hydrosilylation of alkynes to afford alkenylsilanes (Scheme 1-11). The delivery of a silyl group and a hydride across unsymmetrical alkyne can potentially result in a mixture of stereoisomers and regioisomers depending on the mode of addition (either *syn* or *trans*) (Scheme 1-11).⁹

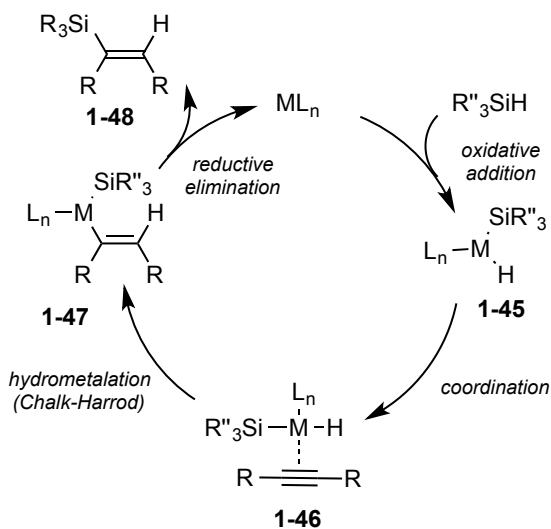
Scheme 1-11 Metal-Catalyzed Hydrosilylations of Alkynes



In these reactions, the outcome is typically significantly influenced by the metal-catalyst, silane structure, and alkyne identity. The majority of low-valent transition metal catalysts that undergo hydrosilylations with alkynes are known to deliver the hydride and silyl ligands *syn*

The mechanisms of hydrosilylation are some of the most studied in organometallic chemistry. One of the most commonly invoked mechanisms for alkyne hydrosilylation is the Chalk-Harrod hydrometalative pathway (Scheme 1-12).^{10a}

Scheme 1-12 Chalk-Harrod Hydrometalation Alkyne Hydrosilylation Mechanism

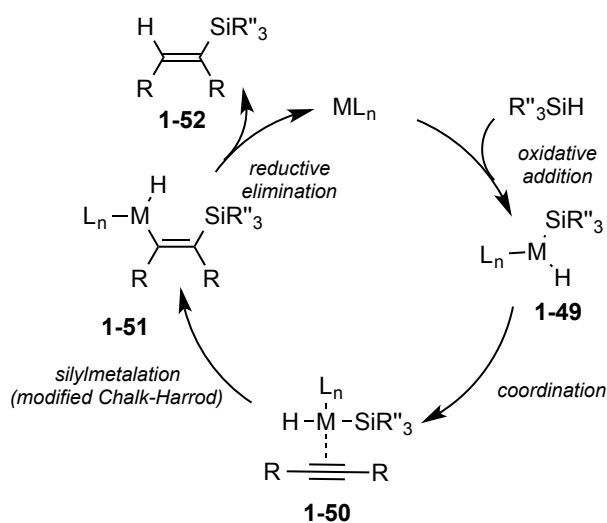


Metal catalysts that undergo this pathway include low-valent catalysts of Pt, Pd, and Ni.⁹ The process begins with oxidative addition to the silicon-hydride bond, generating intermediate **1-45**. Introduction of the alkyne substrate results in the formation of square

planar complex **1-46** and migratory insertion into the M-H bond (hydrometalation) affords species **1-47**. Reductive elimination from intermediate then affords alkenylsilane **1-48** while restoring the active catalyst.

Another commonly invoked hydrosilylation mechanism is the modified Chalk-Harrod mechanism (Scheme 1-13).^{10b} In this pathway, migratory insertion into the M-SiR₃ (silylmetalation) occurs instead of hydrometalation (Scheme 1-12) affording a vinyl-metal-hydride **1-51**. Reductive elimination of hydride from **1-51** affords alkenylsilane **1-52** while also restoring the catalyst.

Scheme 1-13 Modified Chalk-Harrod Mechanism

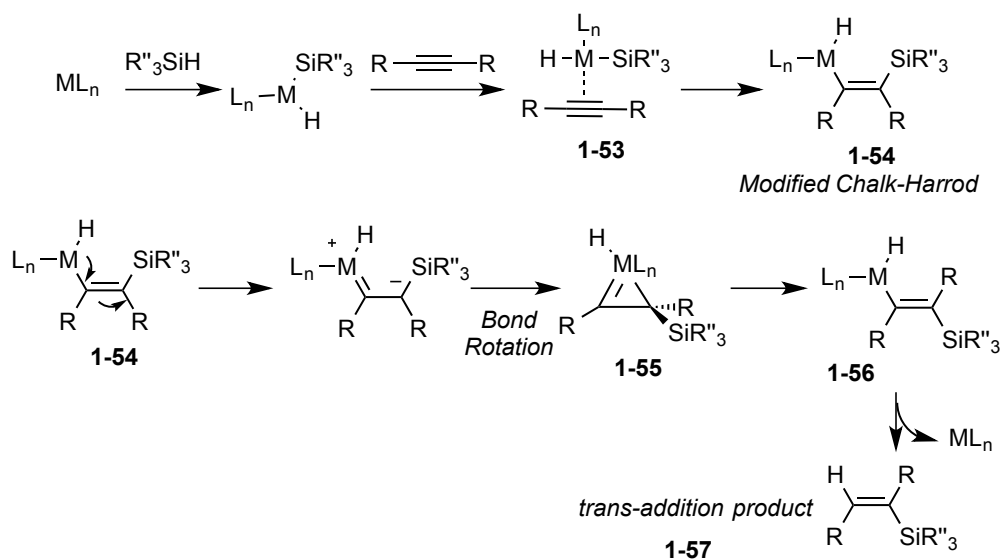


This mechanism was previously met with significant skepticism before numerous groups demonstrated that silylmetalation was the only explanation for their observed hydrosilylation products. A major reason for this critical reception was due to the seemingly unfavorable combination of reversed dipoles experienced in this step, where the more electrophilic ligand SiR₃ adds to an electropositive carbon. In addition, hydrometalation chemistry had previously been widely accepted in many other classes of coupling reactions (i.e. hydrostannanylation, hydrozirconation...) and was therefore a

reasonable explanation for these early observations. Nevertheless, the modified Chalk-Harrod mechanism has been attributed to the formation of alkenylsilanes for numerous hydrosilylation protocols.

In contrast with the previously discussed mechanisms (Scheme 1-12 and 1-13) that deliver the silyl and hydride ligands to the same face of the alkyne, there are also several catalysts that deliver the silyl and hydride ligands to opposite faces of the alkyne to afford *Z*-alkenylsilanes (Scheme 1-14).^{9b} There are considerably fewer catalysts that function under this manifold, but some of the most common are catalysts of Ru and Rh. The currently accepted mechanism involves a similar oxidative addition/ migratory insertion (either Chalk-Harrod or modified Chalk-Harrod) sequence seen in *syn* additions; however, the mechanism departs from these pathways when the reductive elimination from **1-54** is sluggish and isomerization instead furnishes metal carbenoid **1-55**.

Scheme 1-14 *Trans*-Hydrosilylation Isomerization Pathways



Free bond rotation and isomerization forms cyclopropyl carbenoid intermediate **1-55**. This intermediate subsequently collapses, forcing the silyl group to the opposite face of the alkene, forming vinyl-metal-hydride **1-56**. Then the reductive elimination of hydride

affords the *trans*-addition product **1-57**. Evidence for this mechanism can be found in deuterium-labeling studies as well as in the numerous computational studies.

1.6 Examples of Terminal Alkyne Hydrosilylation Procedures

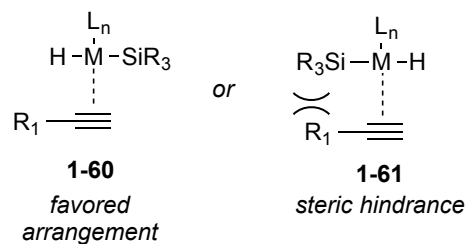
Hydrosilylations of terminal alkynes are some of the most efficient strategies for the synthesis of regio- and stereodefined alkenylsilanes. Although internal alkynes can be useful platforms for hydrosilylation reactions, they often are far less regioselective than their 1-alkyne counterparts, often affording mixtures of isomers in the absence of strong electronic or steric substrate biases (also discussed in further in Chapter 4). One of the major benefits to the use of 1-alkynes in this class of reactions is that monosubstitution effectively differentiates the electronics and sterics at both carbon atoms of the π system. A comparison for this type of substrate substitution-directed regioselectivity can be observed in acid-catalyzed hydration reactions of 1-alkynes and 1-alkenes, where the ability to stabilize electropositive charge build-up directs the regiochemistry in Markovnikov additions. Although the majority of transition-metal-catalyzed hydrosilylations are not described as going through carbocation intermediates, a similar argument that the more electropositive carbon atom receives a hydride ligand in order to align dipoles (**1-58** favored over **1-59**) (Figure 1-4, top portion). Terminal alkynes are also substantially sterically differentiated, which reinforces linear 1,2-migratory insertions affording a sigma-metal species that is significantly less hindered (**1-60** favored over **1-61**) (Figure 1-4, bottom portion).

Figure 1-4 Hydrosilylations of Biased 1-Alkynes

Electronic Effects:



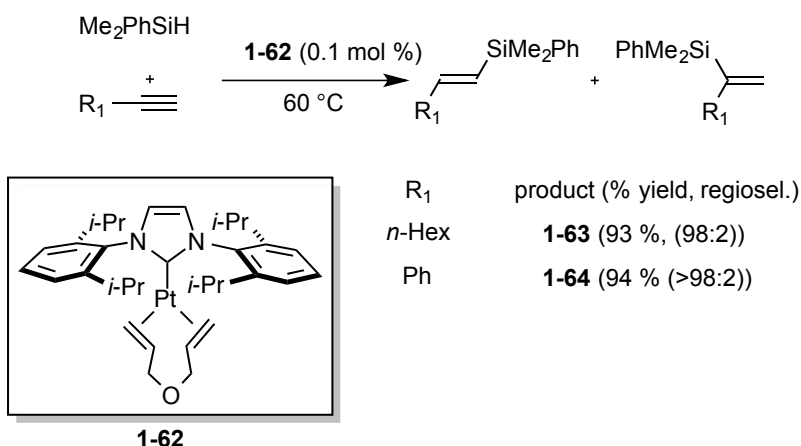
Steric Effects:



For these reasons, hydrosilylations of 1-alkynes are typically very regio- and stereoselective furnishing linear *E*-alkenylsilanes; however, reversing the preference to favor branched α -alkenylsilanes (via **1-59/1-60**) is challenging for group 10 metal catalysts and very few catalysts can achieve this across a broad range of structures.

One of the more popular protocols for terminal alkyne hydrosilylation involves use of a Pt catalyst with an IPr NHC ligand backbone affords linear *E*-alkenylsilanes (Scheme 1-15). In this protocol, excellent yields and high regioselectivities are achieved across a broad range of 1-alkynes.

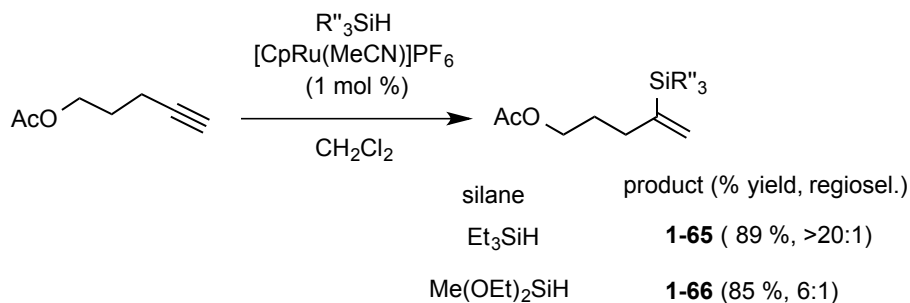
Scheme 1-15 Pt-Catalyzed Hydrosilylations of Terminal Alkynes



Additions catalyzed by this catalyst favor linear regioisomeric products over the branched isomers for unhindered aliphatics **1-63** and also aromatic containing alkynes **1-64**. An added benefit to use of this procedure is the catalyst loading is incredibly low (0.1 mol %) and reactions typically occur within 30 min. However, a challenge with this chemistry is that a variety of coupling silane partners are either not tolerated under the reaction conditions or they afford mixtures of regio- and stereoisomers.

A related catalyst system developed by Trost and coworkers is the cationic CpRu(MeCN) complex that in the presence of a 1-alkyne and hydrosilane partner, affords the branched α -alkenylsilane, the reversed mode product, in high selectivities (Scheme 1-16).¹²

Scheme 1-16 Cationic Ruthenium-Catalyzed Hydrosilylations of Terminal Alkynes



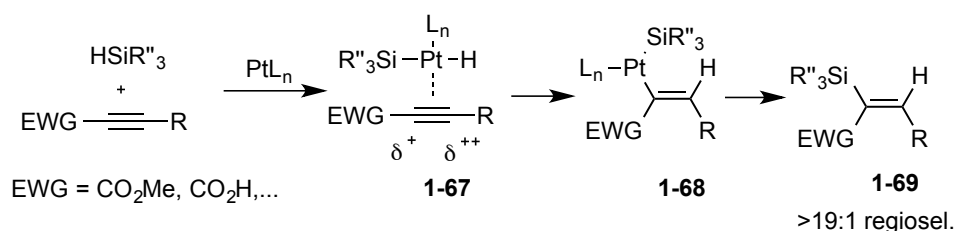
Currently, use of this catalyst is one of the only purely hydrosilylative protocols that provide access to this regioisomer for a broad range of 1-alkynes and silanes. However, one of the major challenges with this procedure is that the regioselectivity is also not consistently high for all silanecoupling partners (Scheme 1-16). For example, coupling a 1-alkyne with triethylsilane results in excellent regioselectivity (>20:1) for the branched isomer **1-65** while only changing the silane to Me(OEt)₂SiH affords **1-66** in 6:1 in eroded regiochemistry. This unexpected drop in regioselectivity is typically encountered in alkyne hydrosilylation and it makes the implementation of such protocols challenging, especially in complex molecule settings where subtle changes in either coupling structure can possibly have negative implications on the reaction outcome.

1.7 Methods for Regiocontrol in Alkyne and 1,3-Diene Hydrosilylation

One of the remaining challenges in the two-component couplings of π components and silanes is the lack of consistent regioselectivity achieved for even the most efficient hydrosilylation procedures across a broad range of unbiased substrates. This is especially problematic for the metal-catalyzed hydrosilylations of unsymmetrical internal alkynes and there have been several approaches to controlling the regioselectivity in these simple additions.

For example, a systematic study of Pt-catalyzed hydrosilylations of internal alkynes demonstrated that functionalizing an alkyne with a substituent that is electron-withdrawing (EWG) allows for predictable regioselectivity in the formation of *E*-alkenylsilanes **1-69** (Scheme 1-17).¹³ In this approach, including an EWG on the alkyne effectively enhances the electropositive dipole closest (intermediate **1-67**, Scheme 1-17) to the R substituent via inductive effects.

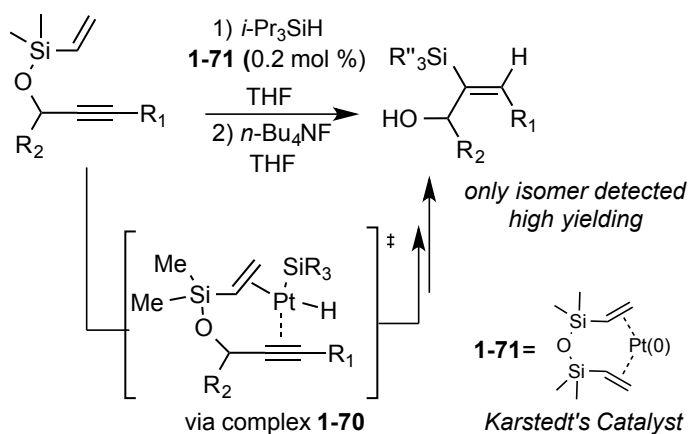
Scheme 1-17 Improving Regioselectivity via Substrate Electronic Bias



This substrate bias directs hydride addition to the more electrophilic carbon resulting in regioselectivities >19:1 favoring regioisomeric product **1-69**. In this report, predictable regioselectivity can be achieved for substrates where a large difference in the ¹³C-NMR chemical shifts (~17 ppm) is maintained. Although this approach provides a predictive model for reaction outcome, this protocol is currently limited to a small subset of similarly substituted structures so it is not a general solution.

Another creative approach for controlling the regioselectivity in alkyne hydrosilylations involves tethering a directing group to propargyl alcohol substrates to reinforce catalyst geometry prior to the insertion (Scheme 1-18).¹⁴ It was found that in the absence of the vinylsiloxane directing group, additions to the alkyne were generally unselective, affording an inseparable mixture of regio- and stereoisomeric alkenylsilanes. However, by attaching the coordinating group by the treatment of the propargyl alcohol with dimethylvinylsilylchloride and pyridine, pre-insertion complex **1-70** is selectively formed in the presence of a silane and Karstedt's catalyst.

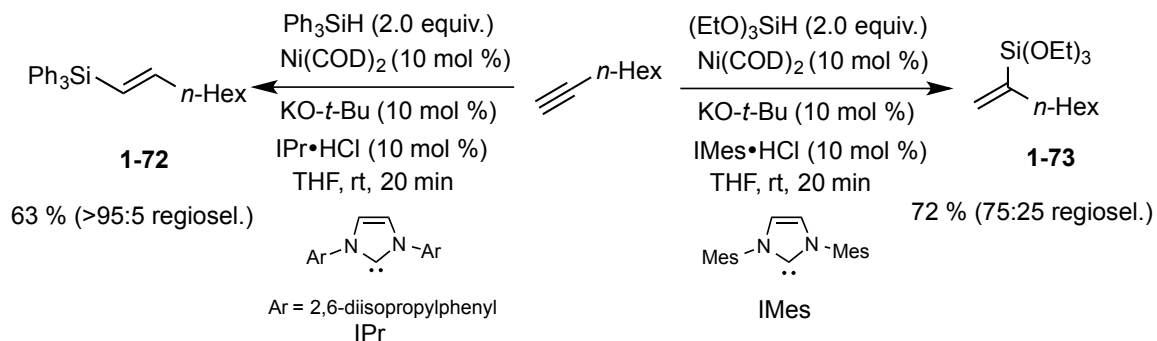
Scheme 1-18 Tethered Directing Group Regiocontrol Strategy



The Pt catalyst favors a specific geometry before insertion that reinforces one hydrometalation pathway over a pathway that is conformationally more restrictive. After the reaction is complete, the directing group can be readily cleaved via hydrolysis affording only one isomer in excellent yields. It was discovered that having the alcohol functionality further removed from the appended alkyne resulted in a lack of regiocontrol.

Another successful regiocontrol strategy that has been developed in the hydrosilylation of terminal alkynes is fine-tuning regioselectivity by choice of silane and NHC ligand with nickel-catalysts (Scheme 1-19).¹⁵ As previously discussed, hydrosilylations of terminal alkynes typically favor the linear product **1-72** in order to minimize the steric interactions of the sigma-alkenylmetal complex with the alkyne substituent.

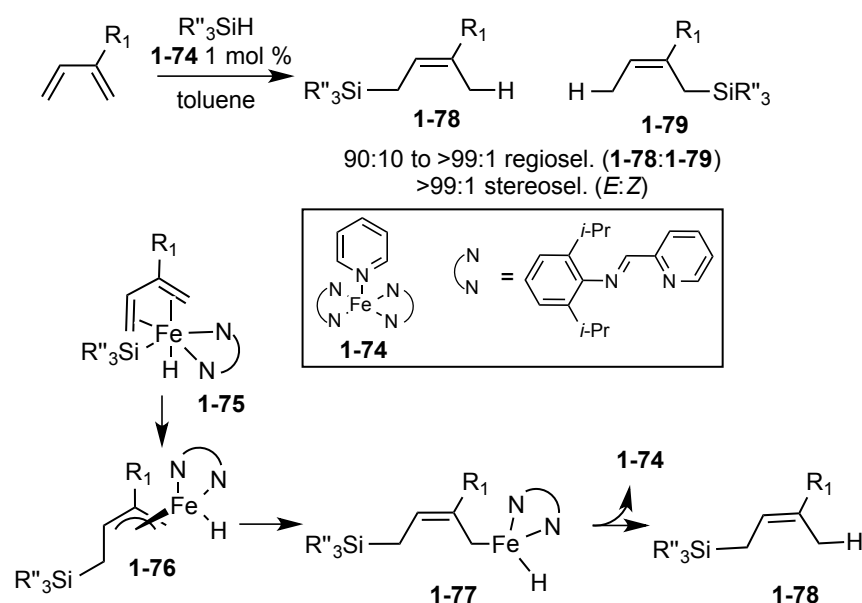
Scheme 1-19 Nickel-Catalyzed NHC Ligand-Controlled Hydrosilylations



The use of the larger NHC ligand IPr reinforces this steric destabilization and results in highly regioselective formation of linear isomer **1-72** (Scheme 1-19). However, employing the same precatalyst and simply changing the silane to smaller coupling reagent $(\text{EtO})_3\text{SiH}$ in conjunction with a smaller NHC ligand IMes, the opposite branched regioisomeric product **1-73** is afforded in good selectivity (75:25) and 72 % yield. However, reversing the regioselectivity via silane and ligand identity with nickel-catalysis could not be successfully achieved with internal alkynes.

In contrast with the additions of silanes to alkynes, the hydrosilylations of 1,3-dienes can potentially undergo mechanisms that potentially involve 1,2- or 1,4-additions resulting in a mixture of regio- and stereoisomers depending on the catalyst employed. In the iron-catalyzed hydrosilylation of 1,3-dienes, the Ritter group discovered that 1,4-hydrosilylation could be controlled through use of discrete iron catalysts containing iminopyridine ligands (Scheme 1-20).^{16a}

Scheme 1-20 1,4-Hydrosilylation of Dienes

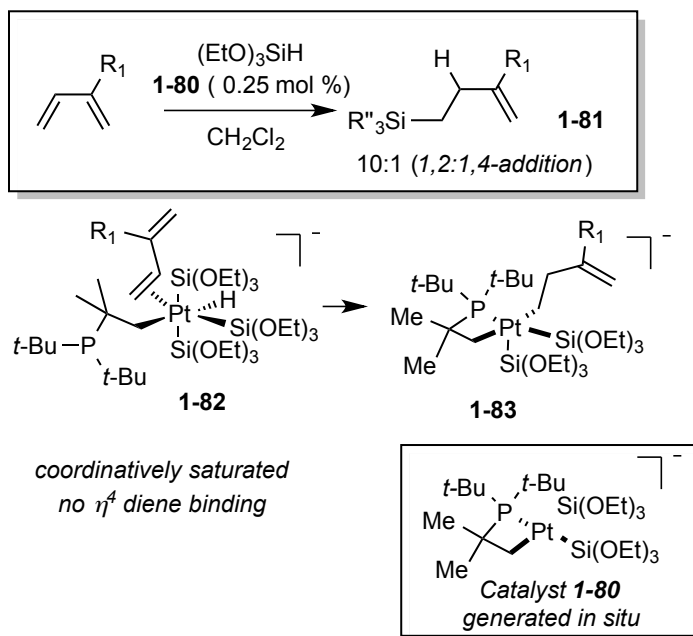


After initial oxidative addition of the iron catalyst to the Si-H bond, silylmetalation occurs at the least sterically encumbered π bond to form π -allyl **1-76**, in the same fashion as in the modified Chalk-Harrod pathway. Reductive elimination of hydride from **1-77** then affords allylsilane isomer **1-78** in excellent regio- and stereoselectivities (>99:1). Determination of the kinetic order of silane has shown that the slow step involves the first-order dependence of silane, suggesting that oxidative addition to the silane is the slow step in the pathway.

Recent developments from the Ritter group have also demonstrated that selective 1,2-addition is possible with 1,3-dienes through careful catalyst design (Scheme 1-21).^{16b} Through the use of a coordinatively saturated Pt catalyst with a weakly coordinated phosphine ligand, oxidative addition to the silane occurs from intermediate **1-82**. Dissociation of the phosphine ligand and subsequent coordination to the least sterically-encumbered π bond followed by insertion affords complex **1-83**

that is coordinatively saturated and therefore cannot bind to the other π bond of the diene due to the lack of open sites.

Scheme 1-21 1,2- Hydrosilylation of Dienes



The inability to undergo η^4 coordination reinforces the catalyst to undergo 1,2-hydrometalation with the same regiochemistry observed with normal mode alkyne hydrometalation (Scheme 1-21). Reductive elimination of the silyl moiety affords allylsilane **1-81** in high selectivities (10:1).

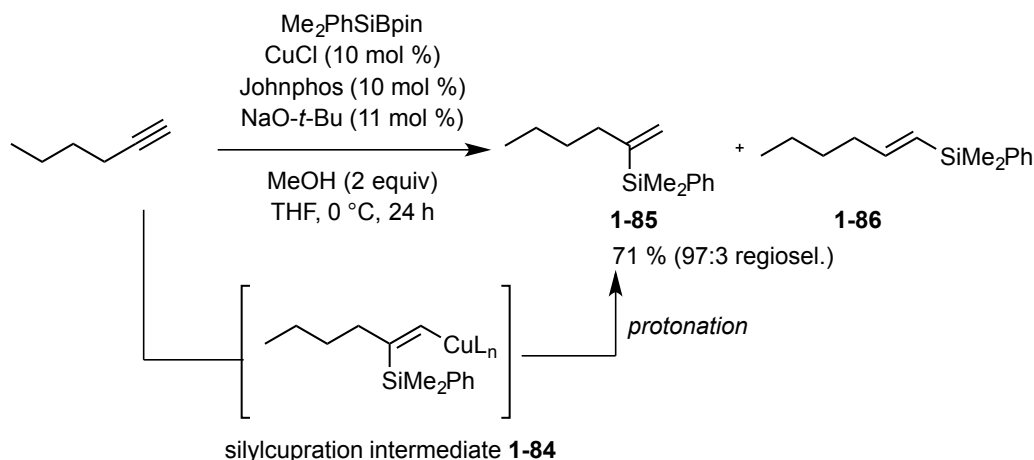
There are numerous successful approaches for controlling the regio- and stereoselectivity in the hydrosilylations of alkynes and 1,3-dienes. In these cases, it is effective to apply either inherent substrate biases or use directing groups to direct the site of hydrosilylation. Careful design of catalyst systems is also an effective means for controlling the outcome in these reactions, either by development of silane and NHC ligands with nickel-catalysis or through the use of coordinatively saturated Pt catalysts that cannot undergo further isomerization. One of the major challenges experienced in

these classes of additions is reversing inherent preferences for a particular mode of addition.

1.8 Related Silane Functionalizations

As a result of the challenges experienced in achieving predictable regio- and stereocontrol for many hydrosilylation procedures, catalytic methods that introduce silyl groups through alternate mechanisms have been extensively developed. For example, the use of copper(I) pre-catalysts with silylboranes and Johnphos ligand catalyzes the protosilylation of 1-alkynes to favor primarily branched alkenylsilanes **1-85** in high yields (Scheme 1-22).¹⁷

Scheme 1-22 Copper-Catalyzed Protosilylations of Terminal Alkynes

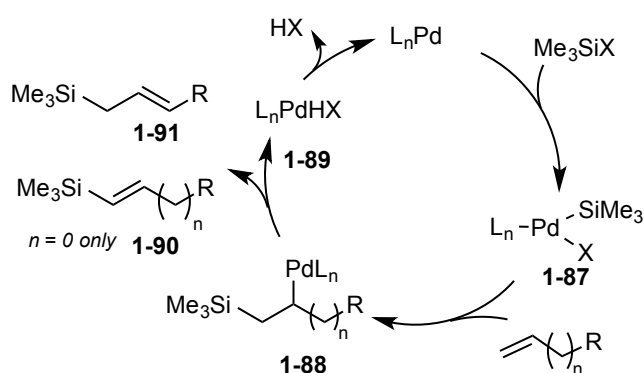


This pathway proceeds by a mechanism distinctive from the previously discussed hydrosilylation pathways. The use of CuCl with NaO-*t*-Bu affords Cu-O-*t*-Bu which transmetalates with an equivalent of Me₂PhSiBpin to create the active catalyst Cu-SiMe₂Ph. Silylcupration (migratory insertion into Si-Cu) of 1-hexyne then affords **1-84** with the same 1,2-regiochemistry that is favored in other migratory insertions with alkynes. Protonation of intermediate **1-84** affords branched isomer **1-85** and the formation of Cu-OMe further turns the catalytic cycle. Although this procedure furnishes

branched silyl alkenes more consistently than many other hydrosilylation procedures, the use of a silylborane is less atom-economical than a hydrosilane and also limits the silane scope to silylboranes that are either commercially or synthetically available.

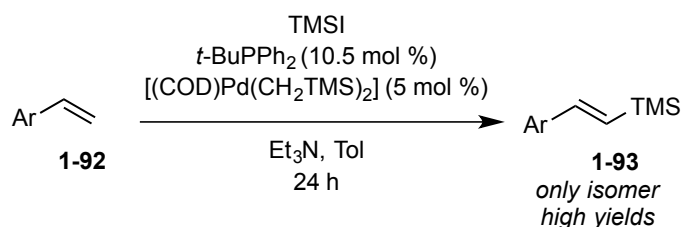
Watson and coworkers have also developed a useful procedure, termed the silyl-Heck reaction, with Pd-catalysis that efficiently functionalizes alkenes with silanes in access to stereodefined alkenyl- and allylsilanes (Scheme 1-23).¹⁸ In this process, instead of a hydrosilane starting material, TMSI serves as an oxidative addition partner with Pd-catalysts to afford intermediate **1-87**.

Scheme 1-23 Mechanisms for Silyl-Heck Reaction



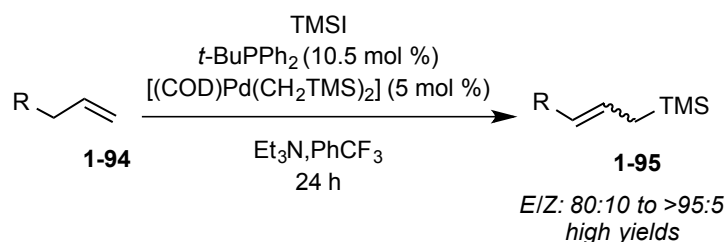
Introduction of terminal alkenes results in silylmatalation with the same regiochemistry experienced in traditional Heck reactions affords **1-88**. However, depending on the substrate, either alkenyl- or allylsilanes are furnished based on the favored site of β -hydride elimination. Reductive elimination of HX from **1-89** restores the active catalyst. If the alkene substrate is an aryl alkene, β -hydride elimination affords only *E*-alkenylsilanes **1-93** in high yields (Scheme 1-24).

Scheme 1-24 Silyl-Heck Reaction Affording Alkenylsilanes



Recent developments have broadened the scope of silyl coupling reagents to include siloxane functional groups that are useful in cross-coupling reactions and other useful technology.^{18b} Under similar reaction conditions, *E*-allylsilanes **1-95** are afforded for substrates containing allylic protons (Scheme 1-25).

Scheme 1-25 Silyl-Heck Reaction Affording Allylsilanes



It was found that this reaction afforded allylsilanes in higher yields when the solvent was changed to electron-deficient PhCF₃ that stabilizes the sigma-alkyl intermediate **1-88**. Advantages to the use of this method include the wide-availability of a feedstock reagent and the degree of unsaturation of the starting materials does not change during the course of the transformation.

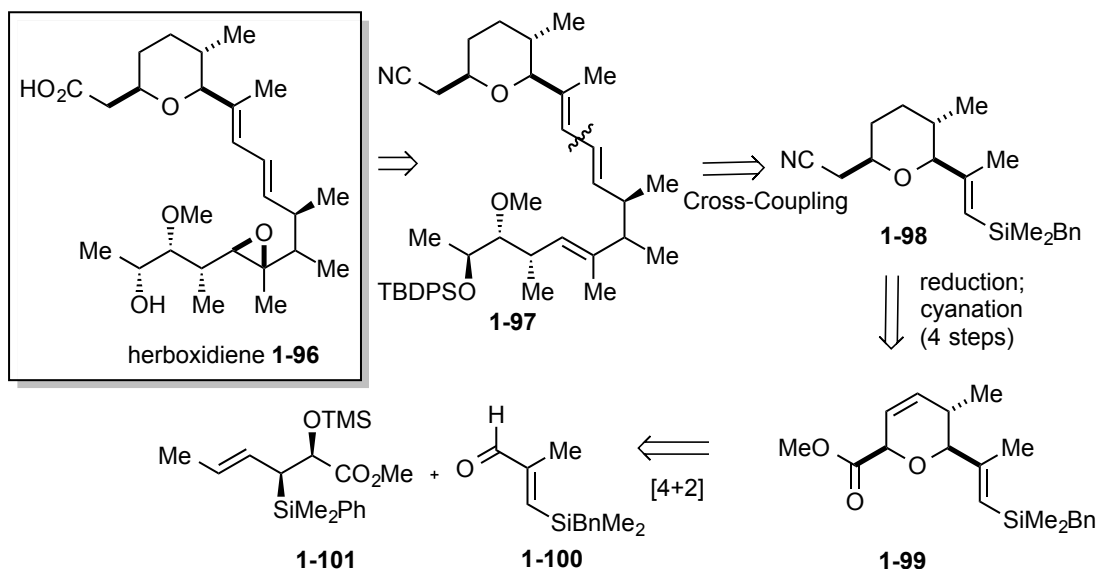
1.9 Alkenyl- and Allylsilanes in Complex Molecule Synthesis

Hydrosilylation is an attractive transformation due to the flexibility of alkenyl- and allylsilanes as synthetic intermediates. For example, alkenylsilanes are useful in the C-C bond-forming Hiyama-Denmark cross-coupling reactions, iodination reactions, electrophilic additions, and can be oxidized under Fleming-Tamao conditions.⁹

Allylsilanes are also useful in Hiyama-Denmark cross-couplings, Fleming-Tamao oxidations, numerous cycloaddition procedures, and also serve as allylation and crotylation reagents. A major benefit to the use of alkenyl- and allylsilanes in synthesis involves their stability and translatability in comparison to coupling reagents of boron, tin, and aluminum.⁹

The total synthesis of herboxidiene **1-96** is an example of the flexible applications of alkenyl- and allylsilane intermediates in complex molecule settings (Scheme 1-26).¹⁹ In this route, an important disconnection in access to the diene in the phytotoxic compound is furnished through a Hiyama-Denmark cross-coupling reaction of alkenylsilane **1-98** with an aryl iodide to afford **1-97**, an advanced intermediate.

Scheme 1-26 Total Synthesis of Herboxidiene Employing Alkenyl- and Allylsilanes



An advantage to use of cross-coupling nucleophilic intermediate **1-98** over other available cross-coupling reagents is the ease for alkenylsilane to be translated through multiple synthetic sequences (4 steps in this instance), including very acidic and basic conditions, without the observation of appreciable decomposition. Strategic use of a [4+2] cycloaddition of allylsilane **1-101** and alkenylsilane **1-100** results in the formation of

alkenylsilane **1-99** as only one stereoisomer. This example of the synthesis of herboxidiene demonstrates the synergy and practicality that results from the employment of allyl- and alkenylsilanes in synthesis.

1.10 Conclusions and Outlook

The development of regioselective metal-catalyzed multicomponent coupling reactions has allowed molecular complexity to be established from simple starting materials. Numerous achievements in aldehyde/alkyne reductive couplings have demonstrated that NHC ligands and also the judicious choice of reducing agents can result in fine-tuning of the regioselectivity in access to allylic alcohol derivatives.

Related developments in two-component coupling reactions in the hydrometalations and dimetalations of alkynes have also demonstrated that catalyst engineering can enable access to a variety of structures from a common starting material. In contrast with the majority of three-component reactions, in this class of reactions the role of the reductant is typically involved in the same step as the regiochemistry-determining step.

Despite the numerous efficient protocols for the hydrosilylations of alkynes and 1,3-dienes, there is still a considerable challenge in harnessing stereo- and regiocontrol for unbiased and undirected substrates. Improvements in the understanding of the factors that govern the regio- and stereochemistry in these reactions will enable more widespread use of these intermediates in chemical synthesis. Therefore, further exploration of the factors that govern the additions of hydrosilanes to π -component is warranted.

Chapter 2

Metal-Directed Regioselective Allene Hydrosilylation Catalyzed by *N*-Heterocyclic Carbene Complexes of Ni(0) and Pd(0)

2.1 Introduction: Allene Hydrosilylation

Access to metalated synthetic intermediates is most efficiently accomplished by metal-catalyzed hydrometalations of π components.²⁰ These procedures are benefited by use of simple starting materials and highly atom-economical steps, where all reagent molecules are incorporated in the product. In contrast with procedures of boron and tin, hydrometalations with silicon afford stable intermediates that are non-toxic and readily carried through multiple synthetic sequences without degradation. Despite these advantages, the tremendous challenge in harnessing predictable selectivity in metal-catalyzed hydrosilylations of unsymmetrical π components limits their applications in organic synthesis. For example, even the most efficient hydrosilylation procedures are plagued by the lack of regiocontrol for a variety of π components and silane precursors, resulting in mixtures of inseparable constitutional isomers. As part of our laboratory's broader interests in developing catalytic regioselective processes,²¹ we set out to develop a hydrosilylation protocol with the aim to discover a process that would allow predictable access to a diverse range of structures from a single substrate class.

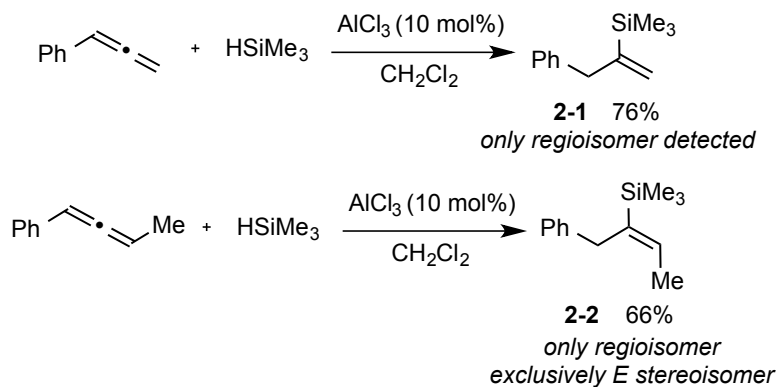
The need for new regiocontrolled methods that provide streamlined access to useful alkenyl- and allylsilane reagent classes encouraged us to investigate allene

hydrosilylation. The inspiration for selection of allenes originated from the observation that allene hydrosilylation had only rarely been examined. In addition, allene hydrosilylation posed a great challenge and opportunity since 1,2- or 2,1-addition to either of the two contiguous π -systems can occur, potentially providing two regioisomeric allylsilanes and two regioisomeric vinylsilanes, in some cases as mixtures of alkene stereoisomers.

2.2 Allene Hydrosilylation and Related Metalation Protocols

At the start of our study of allene hydrosilylation, we were interested in the previous reports of allene hydrosilylation. In a report by Yamamoto, Lewis-acids were observed to catalyze the hydrosilylation of allenes regioselectively to afford branched alkenylsilanes **2-1** (Scheme 2-1).²²

Scheme 2-1 Lewis-Acid Catalyzed Allene Hydrosilylation

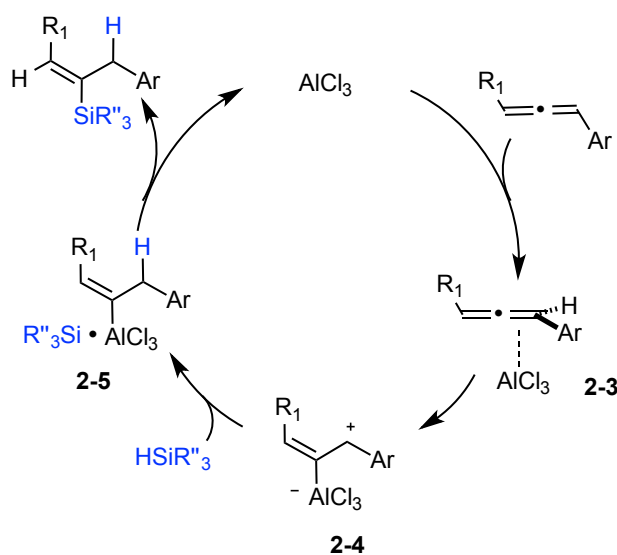


Monosubstituted and 1,3-disubstituted aryl allenes functioned under these conditions and it was observed that addition occurs across the central allene carbon for all cases affording **2-2** in good yields. Unsymmetrically substituted allenes were also tolerated to selectively afford *E*-alkenylsilanes in excellent yields. However, the scope of allenes was limited to substrates with aryl groups and issues with substrate compatibilities with the use of strong Lewis-acids limits the broad applications of this procedure in more complex

settings. In addition, the silane coupling partners were limited to trialkylsilanes that are not typically suitable for Hiyama-Denmark cross-couplings and other classes of transformations.

The authors propose that the allene hydrosilylation proceeds via initial coordination by the aluminum catalyst to the π bond closest to the aryl substituent to afford π complex **2-3** (Scheme 2-2).

Scheme 2-2 Lewis-Acid Catalyzed Allene Hydrosilylation Mechanism

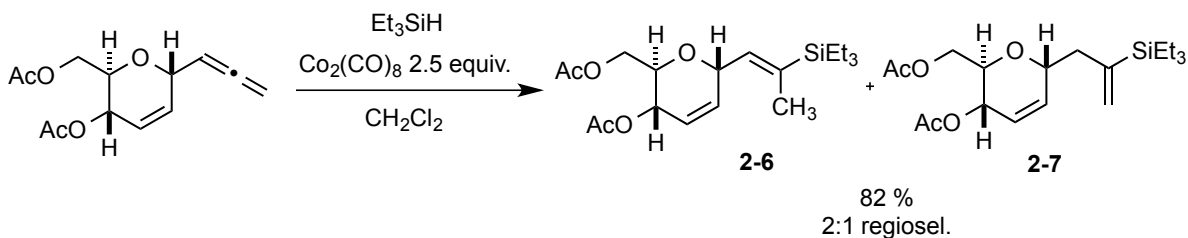


After aluminum coordinates to the *anti*-face of the allene, zwitterionic intermediate **2-4** and treatment with silane results in addition of the hydride to the carbocation affording complexed silane structure **2-5**. Elimination of the aluminum catalyst generates the alkenylsilane product while restoring the active catalyst. The observed alkene configuration in the product is a direct result of the migratory insertion pathway and is conserved in the following steps due to the vinyl-aluminum species' (**2-4**) inability to isomerize.

The hydrosilylation of sugar allenes by action of super-stoichiometric *bis*-cobaltocarbonyl has also been previously developed (Scheme 2-3).²³ In this procedure,

a catalytic amount of the cobalt species did not afford alkenylsilanes; however, increasing the metal species to 250 mol% resulted in a 2:1 mixture of alkenylsilane **2-6** and **2-7** in 82 % yield (Scheme 2-3).

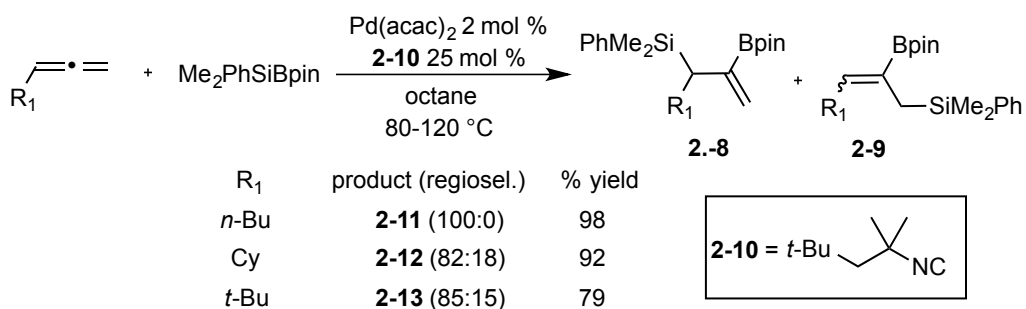
Scheme 2-3 Hydrosilylation of Sugar Allenes



Although this procedure afforded alkenylsilanes in high yields, the lack of regioselectivity achieved in this reaction is a significant drawback. Unfortunately, in the absence of a mechanistic proposal no conclusion can be drawn from the observed distribution of regioisomeric products, although it is very interesting that the major regioisomer is afforded in addition to the terminal double bond of the allene.

In contrast with the limited background for allene hydrosilylation, the silaboration of allenes has been extensively studied.²⁴ For example, the additions of silylboranes across allenes occurs under catalytic conditions with 2 mol % Pd catalyst with a variety of isocyanide ligands to afford primarily silyboranes **2-11** through **2-13** (Scheme 2-4)

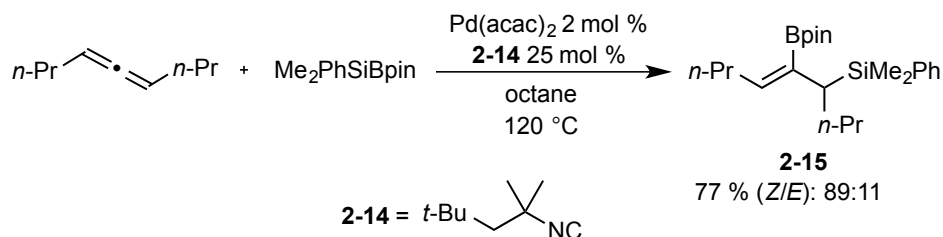
Scheme 2-4 Silaboration of Allenes



This reaction tolerates a broad substrate scope with unhindered aliphatics **2-11**, cyclic aliphatics **2-12**, and bulky groups **2-13** in excellent yields and regioselectivities. In

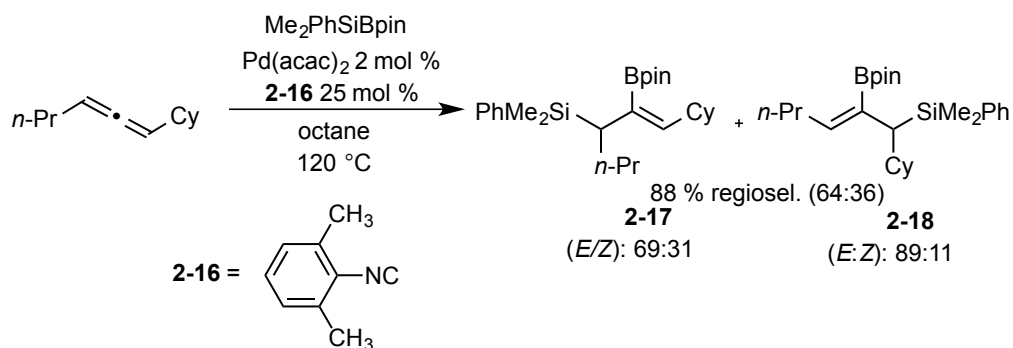
addition, a stereoselective variant of this reaction was reported that employed phosphoramidite ligands with Pd-catalysis. In this protocol, 1,3-disubstituted allene substrates were also tolerated with the reaction conditions to afford regio- and stereodefined silylboranes (Scheme 2-5).

Scheme 2-5 Silaboration of 1,3-Disubstituted Allenes



For example, additions to symmetrically substituted *n*-Pr allene favored the formation of compound **2-15** in 89:11 d.r.. However, the use of unsymmetrically substituted allenes results in mixtures of regioisomers **2-17** and **2-18** in moderate regioselectivity (64:36) and stereoselectivity (Scheme 2-6). As demonstrated in this example, allenes serve as an efficient handle for the construction of complex metalated intermediates not readily available by other direct methods.

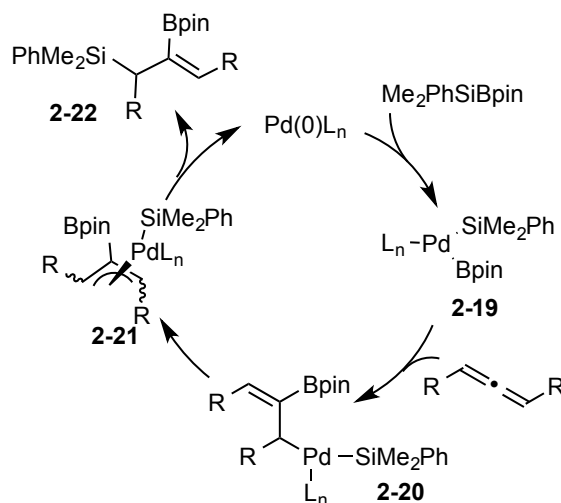
Scheme 2-6 Silaborations of Unsymmetrically Substituted Allenes



The currently accepted mechanism for this transformation is analogous to those discussed in Chapter 1 in additions to alkynes and 1,3-dienes in that the reaction undergoes similar oxidative addition/migratory insertion sequences. In this mechanism,

the Pd catalyst undergoes oxidative addition to the silylborane to afford intermediate **2-19** (Scheme 2-7). Subsequent migratory insertion of the allene into the Pd-BR₂ results in the addition of the boronate ester to the central carbon atom to form sigma-allyl intermediate **2-20**.

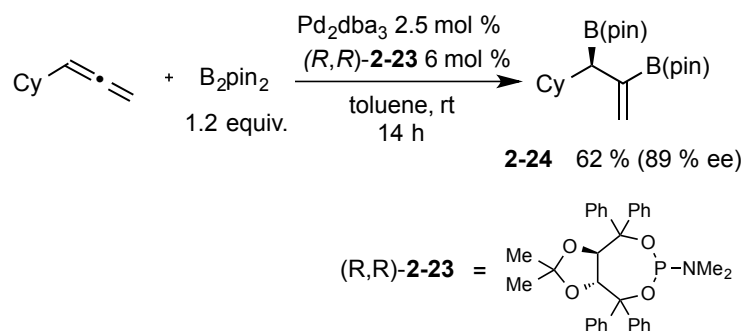
Scheme 2-7 Mechanisms for Allene Silaboration



Intermediate **2-20** then undergoes isomerization to form π -allyl **2-21** and reductive elimination directly from intermediate **2-21** furnishes **2-22**. This mechanism is evidenced by computational DFT experiments.

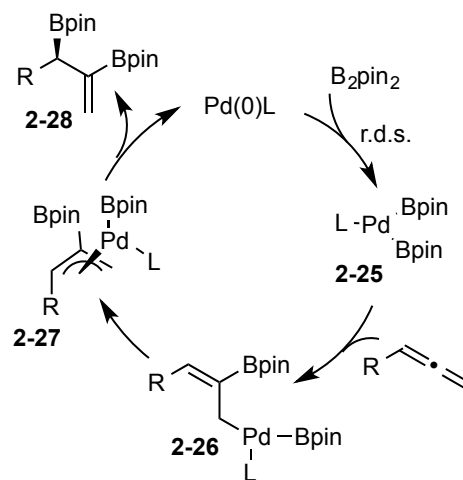
In related developments in the additions to allenes, Morcken and coworkers have reported the enantioselective diboration of allenes (Scheme 2-8).²⁵ In this reaction, B₂pin₂ is added across the central allene double bond through the use of a Pd/ chiral phosphoramidite ligand **2-23** catalyst system. This procedure affords chiral diborylated compound **2-24** in moderate yield and excellent enantiomeric excesses, which can be transformed to useful oxidized, cross-coupled, and allylation products in one step.

Scheme 2-8 Enantioselective Allene Diborations



Significant efforts in elucidating the operative pathway was undertaken both in the form of computational studies and classical kinetic studies. Based on their findings, the rate of reactions is first order in B_2pin_2 suggesting that the rate-limiting step was the oxidative addition of the Pd catalyst to form **2-25** (Scheme 2-9).

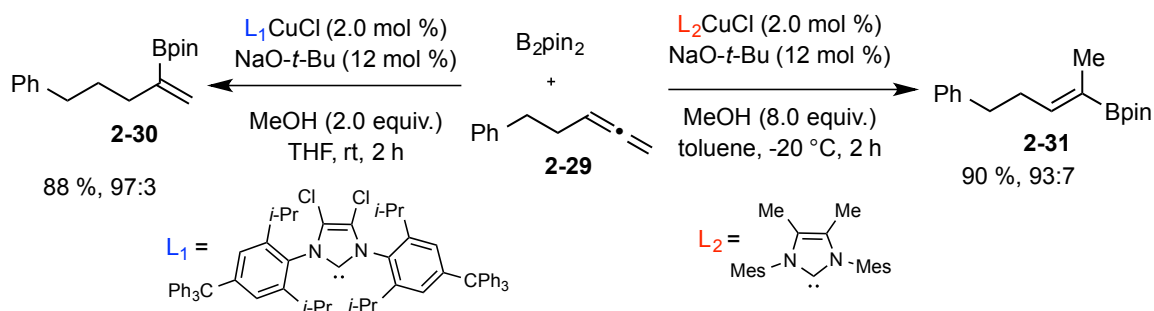
Scheme 2-9 Mechanism for Allene Diboration



Introduction of the allene to the catalytic cycle results in the migratory insertion into the Pd-Bpin bond to form sigma-allyl complex **2-26**. The next step involves subsequent isomerization to π -allyl intermediate **2-27**, as evidenced by allene deuterium-labeling studies. Reductive elimination then affords chiral allylic boronate ester **2-28**. Studies conducted in this report provided significant insight into the mode of π -allyl isomerization in transition-metal catalyzed additions to allenes.

Numerous allene hydrometalation methodologies have also been developed including the hydroboration of allenes with reports of both catalyzed and uncatalyzed protocols.²⁶ The outcomes for uncatalyzed variants are largely affected by allene sterics and electronics. However, metal-catalyzed procedures typically result in more consistent outcomes. For example, the copper-catalyst hydroboration of allenes permits regiodivergent access to either branched **2-30** or linear **2-31** alkenyl boranes (Scheme 2-10).^{8a}

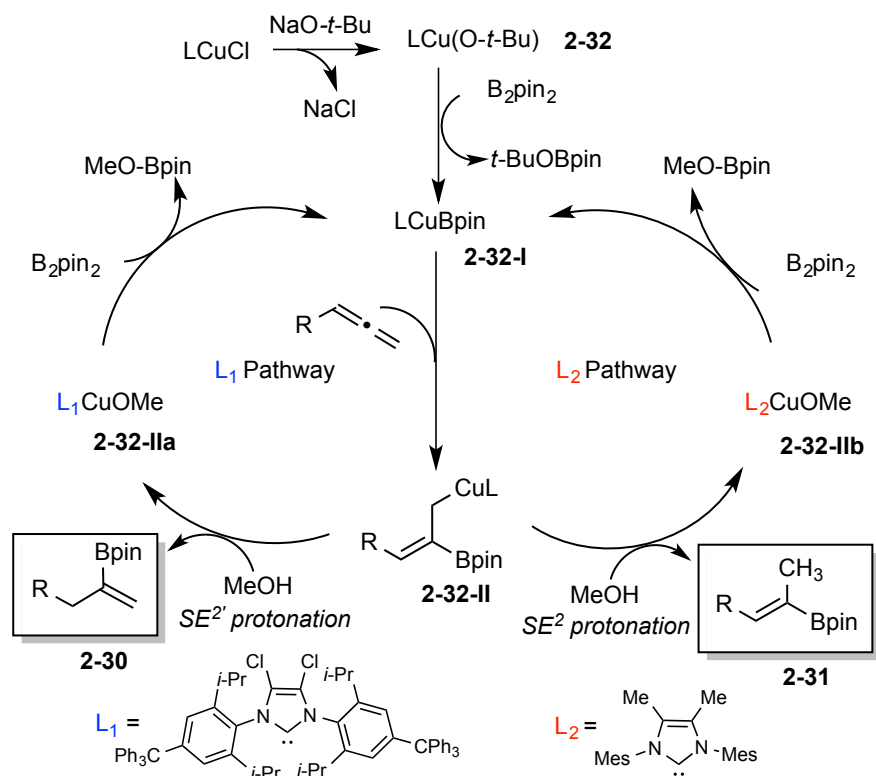
Scheme 2-10 Regiodivergent Hydroborations of Allenes



In this pathway, use of B_2pin_2 with an allene substrate permits access to branched isomer **2-30** in 97:3 regioselectivity in 88 % yield when a Cu catalyst with large NHC ligand L_1 is employed. However, the use of the same catalyst system only with small NHC IMes affords the opposite regioisomer **2-31** in 93:7 regioselectivity and in 90 % yield.

The proposed pathway for the Cu-catalyzed allene hydroboration protocol involves regiodivergent pathways depending on the choice of NHC ligand (Scheme 2-11).

Scheme 2-11 Regiodivergent Pathways for Allene Hydroboration



Formation of pre-catalyst **2-32** occurs after ligand substitution of the chloride with an equivalent of $\text{KO-}t\text{-Bu}$. Subsequent transmetalation of **2-32** with B_2pin_2 affords Cu-Bpin active catalyst **2-32-I**. For both pathways, migratory insertion of the allene into the Cu-B bond affords a common sigma-allyl Cu intermediate **2-32-II**. In the presence of bulky NHC ligand L_1 , direct protonation of the Cu is unfavored due to the steric crowding; therefore, an $\text{SE}^{2'}$ protonation pathway predominates to afford branches isomer **2-30**. When the ligand is IMes L_2 , direct SE^2 protonation of the Cu species is favored and instead affords isomer **2-31**. Further transmetalation of the generated LCu-OMe species **2-32-IIa** and **2-32-IIb** with B_2pin_2 further turns the catalytic cycle regenerating active catalyst **2-32-I**.

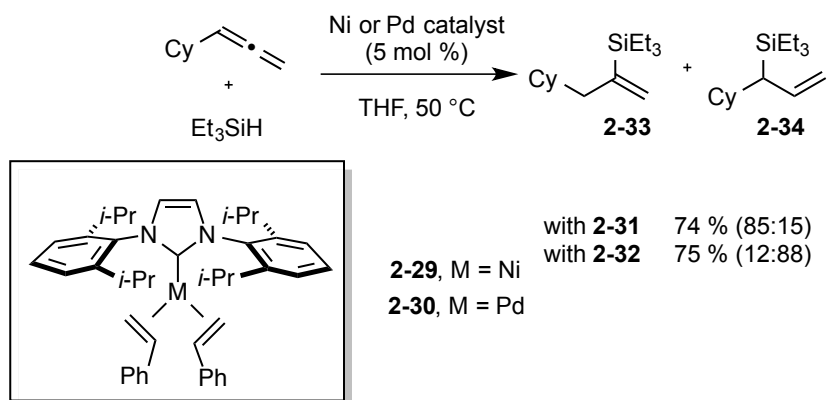
Despite the numerous pioneering advances in diborations, silaborations, and hydroborations of allenes, significantly less attention has been directed to simple allene

hydrosilylation reactions. Previous successes in allene hydrosilylation were limited to either strongly Lewis-acidic conditions with aluminum catalysts or were reported to be generally unselective with super-stoichiometric cobalt species. It is with this gap in developed methodology that we became interested in developing a regiocontrolled allene hydrosilylation reaction with nickel-catalysis with the goal to establish regiodivergent pathways to a variety of useful structures.

2.3 Observation of Complementary Behavior in Regioselectivity

We began our hydrosilylation study with the initial goal to develop ligand-controlled regioselectivity reversal in the nickel-catalyzed hydrosilylation of allenes. However, upon screening a broad range of nickel catalysts modified with *N*-heterocyclic carbene (NHC) or phosphine ligands failed to provide access to high-yielding and highly regioselective access to both alkenyl- and allylsilane regioisomers. In the course of our exploratory studies, we became interested in the use of recently disclosed well-defined NHC catalysts of nickel and palladium.²⁸ Initially we anticipated that the metal complexes would either both display similar reactivities in the hydrosilylation of cyclohexylallene or one of the two metals would be ineffective in the transformation. However, much to our surprise, simply changing the metal identity while maintaining identical ligand scaffold and reaction conditions, resulted in a promising new direction for routes to both alkenyl- and allylsilane regioisomers.

Scheme 2-12 Metal-Directed Regiodivergent Hydrosilylations

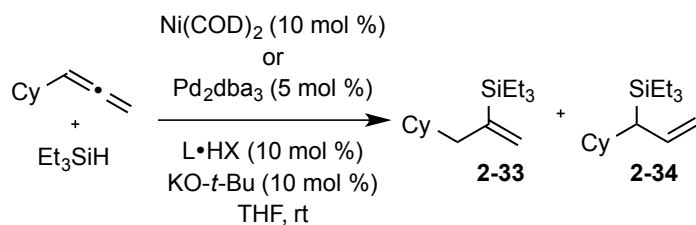


For example, the hydrosilylation of cyclohexylallene with triethylsilane using nickel complex **2-29** favored predominantly alkenylsilane **2-33** in 85:15 regioselectivity (Scheme 2-12). In contrast with the nickel-catalyzed reaction, under the same reaction conditions and with the same ligand scaffold, use of palladium complex **2-30** afforded primarily allylsilane regioisomeric product **2-34** in 88:12 regioselectivity in similar yield (Scheme 2-12). In this unusual example of metal-directed regiocontrol, careful selection of metal identity is an effective strategy for accessing either regioisomer from a common allene precursor.

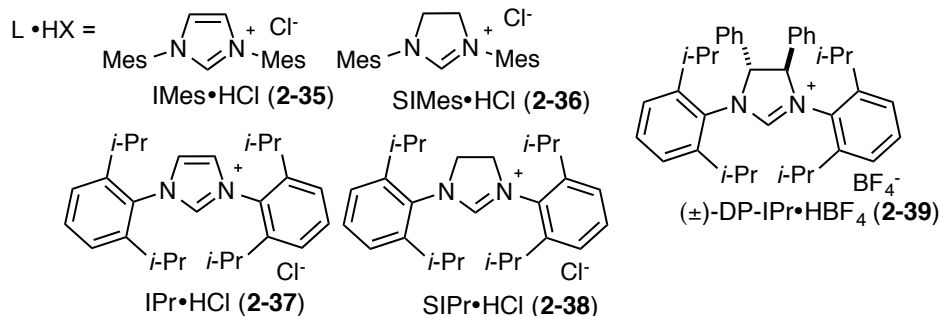
2.4 Evaluation of in situ generated NHC-M(0) catalysts

With the aim to improve the regioselectivities for these complementary processes, we explored the effects of altering NHC ligand structure with reactions of nickel and palladium. An in situ protocol that utilizes NHC hydrochloride salts with KO-*t*-Bu base, with either $\text{Ni}(\text{COD})_2$ or Pd_2dba_3 precatalysts was developed to streamline the evaluation of the reaction outcome. To our satisfaction, this reaction setup successfully duplicated the results with pre-synthesized complexes **2-29** and **2-30** with identical regioselectivities and similar chemical yields (comparing Scheme 2-12 to Table 1, entries 3 and 8).

Table 1 Evaluation of NHC Ligand Effects



entry	precatalyst	L•HX	% yield	regioisel. (2-33 : 2-34)
1	Ni(COD)_2	2-35	22	33:67
2	Ni(COD)_2	2-36	15	40:60
3	Ni(COD)_2	2-37	58	85:15
4	Ni(COD)_2	2-38	47	81:19
5	Ni(COD)_2	2-39	84	>98:<2
6	Pd_2dba_3	2-39	trace	n.d.
7	Pd_2dba_3	2-38	56	14:86
8	Pd_2dba_3	2-37	75	12:88
9	Pd_2dba_3	2-36	74	2:98
10	Pd_2dba_3	2-35	80	<2:>98



Alterations in NHC ligand selection along with metal precatalysts revealed an interesting trend, whereas nickel-catalyzed reactions with larger ligands boosted regioselectivity for alkenylsilanes, smaller ligands with palladium-catalysis improved regioselectivity favoring allylsilanes. To illustrate this, hydrosilylations with smaller ligands IMes **2-35** and SIMes **2-36** with Ni(COD)_2 only slightly favored regioisomer allylsilane **2-34** in low yields (Table 1, entries 1 and 2). The selection of large ligands IPr **2-37** and SIPr **2-38** with nickel-catalysis favored the formation of alkenylsilane **2-33** in moderate regioselectivities (Table 1, entries 3 and 4). The nickel reaction with bulky DP-

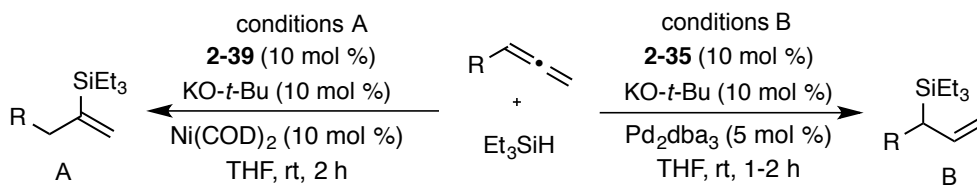
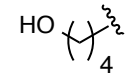
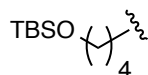
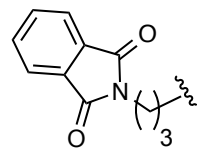
IPr ligand **2-39** afforded the optimal result, with the formation of alkenylsilane **2-33** with >98:2 regioselectivity in 84% yield (Table 1, entry 5). However, the reaction with DP-IPr **2-39** and Pd₂dba₃ resulted in very low conversion of a mixture of regioisomers (Table 1, entry 6) while the reactions with large IPr **2-37** and SIPr **2-38** ligands afforded predominantly allylsilane **2-34** in moderate regioselectivities (Table 1, entries 7 and 8). Exceptional regioselectivities were achieved in the palladium-catalyzed reaction with SIMes ligand **2-36** where use of IMes ligand **2-35** resulted in 80% of allylsilane **2-34** with >98:2 regioselectivity (Table 1, entries 8 and 9).

2.5 Substrate scope

The above guidelines for the in situ-generated Ni(0) and Pd(0) hydrosilylation catalysts were utilized in the reactions for a variety of allene substrate classes (Table 2). In addition to the use of cyclohexylallene (entries 1 and 2), allenes containing less hindered aliphatic groups (Table 2, entries 3 and 4), aromatic groups (Table 2, entries 5 and 6), unprotected hydroxyls (Table 2, entries 7 and 8), and silyloxy groups (Table 2, entries 9 and 10) were successfully hydrosilylated using either Ni(COD)₂ with ligand **2-35** (DP-IPr; conditions A) or Pd₂(dba)₃ with ligand **2-39** (IMes; conditions B) with consistently excellent regioselectivities (>98:2) and in high chemical yields. In addition, an allene containing a phthalimido moiety underwent smooth hydrosilylation to afford either regioisomeric product (Table 2, entries 11 and 12). To further explore the scaleup and utility in reactions not using glovebox manipulations, the palladium-catalyzed procedure with cyclohexyl allene was optimized on a 6 mmol scale, which proceeded in 98% isolated yield in >98:2 regioselectivity (Table 2, entry 13). Additionally, a procedure conducted with a standard benchtop assembly purged with a nitrogen line proceeds in

74% isolated yield with slightly eroded (96:4) regioselectivity (Table 2, entry 14). Finally, an experiment with a reduced catalyst loading (2.5 mol % Pd₂(dba)₃) proceeded in 72% isolated yield (Table 2, entry 15), whereas attempts to lower the catalyst loading further resulted in more significant drops in chemical yield.

Table 2 Metal-Directed Regiodivergent Allene Hydrosilylations

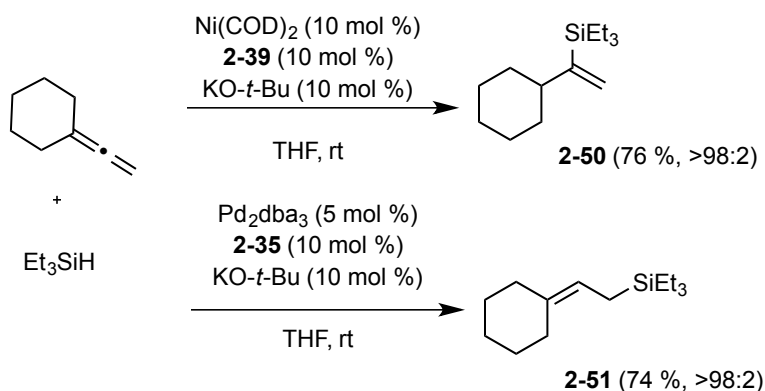
				
entry	R	conditions	product (% yield)	regiosel. (A:B)
1	Cy	A	2-33 (84)	>98:<2
2		B	2-34 (80)	<2:>98
3	<i>n</i> -Oct	A	2-40 (80)	>98:<2
4		B	2-41 (98)	<2:>98
5	Ph	A	2-42 (78)	>98:<2
6		B	2-43 (94)	<2:>98
7		A	2-44 (62)	>98:<2
8		B	2-45 (88)	<2:>98
9		A	2-46 (73)	>98:<2
10		B	2-47 (97)	<2:>98
11		A	2-48 (78)	>98:<2
12		B	2-49 (97)	<2:>98
13	Cy	B	2-34 (98)	<2:>98 ^a
14	Cy	B	2-34 (74)	<2:>98 ^b
15	Cy	B	2-34 (72)	4:96 ^c

^a Reaction conducted on 4.0 mmol scale ^b Lower catalyst loading of 2.5 mol % Pd₂(dba)₃ ^c Reaction conducted with standard bench assembly

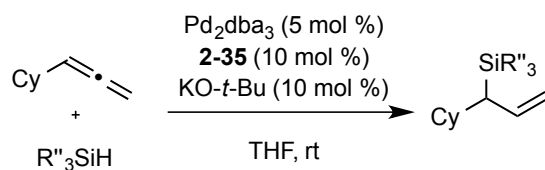
In order to evaluate the effects of introducing 1,1-allene disubstitution, we subjected commercial vinylidenecyclohexane to both Pd(0) and Ni(0) reaction conditions

(Scheme 2-13). Reactions with palladium afforded a new observed allylic silane isomer **2-51**, with the C-Si bond forming at the least substituted allenic carbon. This observation offers a new entry to a useful allylic silane traditionally accessed via 1,3-diene hydrosilylation. The Ni(0) reaction resulted in an outcome consistent with the previous observations for monosubstituted allenes, where the C-Si bond is installed at the central allenic carbon forming **2-50**.

Scheme 2-13 Hydrosilylations of 1,1-Disubstituted Allenes



Another feature of the Pd-catalyzed variant is its broad scope in silane coupling partners (Table 3). For example, in additions to cyclohexylallene, silanes containing aromatic (**2-52**), benzyl groups (**2-53**), siloxanes (**2-54**), and silanes with more than one Si-H bond (**2-55**) were tolerated with consistently high regioselectivities >98:2 and excellent chemical yields. The substrate scope for the nickel procedure is, however, is currently limited to trialkylsilanes. As an example of catalyst-controlled additions, by engineering catalyst structure to override inherent structural biases, consistent regioselectivity is achieved across a range of substrates and coupling partners.

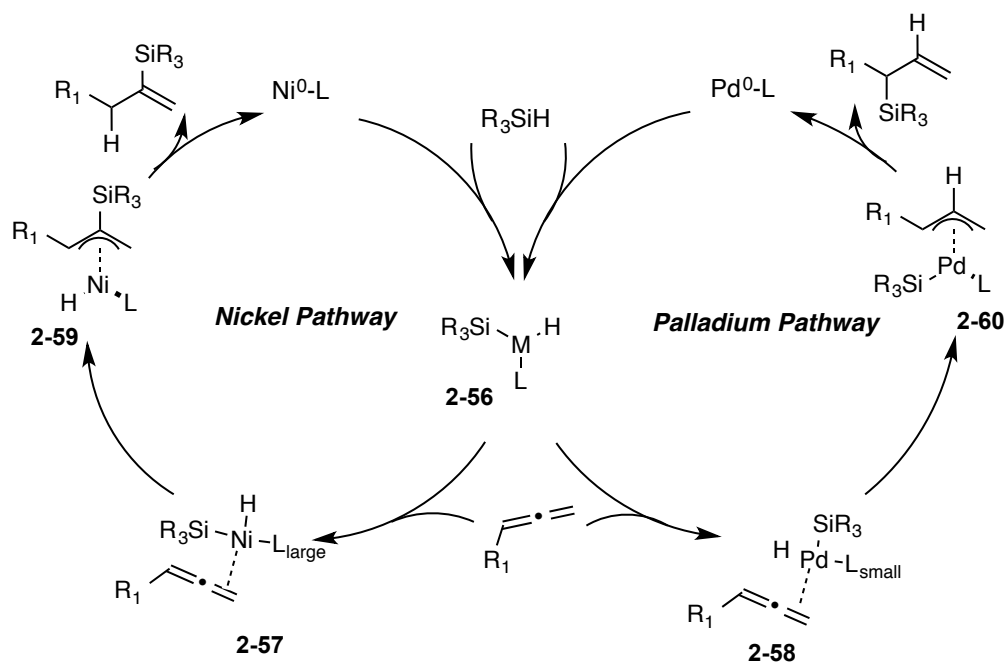
Table 3 Silane Scope for the Pd-Catalyzed Reaction

entry	silane	product (% yield)	regioSEL.
1	HSiMe ₂ Ph	2-52 (91)	>98:2
2	HSiMe ₂ Bn	2-53 (93)	>98:2
3	HSiMe(OSiMe ₃) ₂	2-54 (82)	>98:2
4	H ₂ Si(<i>t</i> -Bu) ₂	2-55 (75)	>98:2

2.6 Mechanistic Pathway and Crossover Study

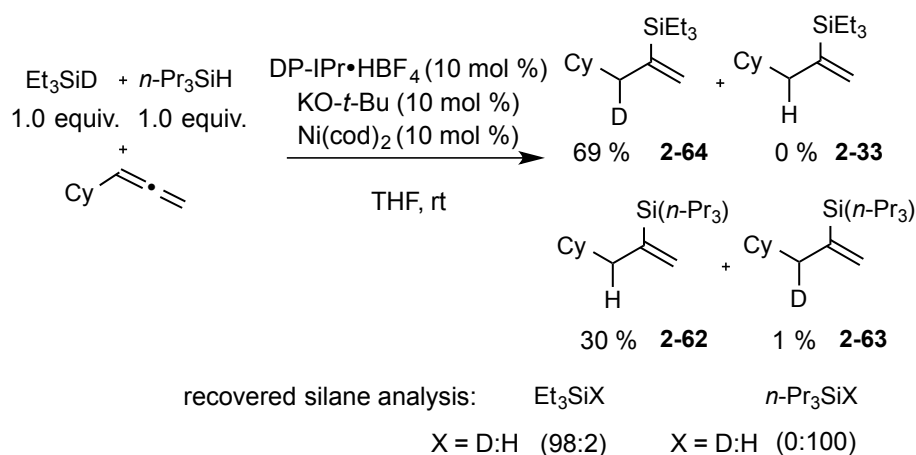
The origin of regiocontrol is at present uncertain; however, our working hypothesis involves allene silylmethylation pathways with nickel catalysts to produce alkenylsilane and allylsilanes production by allene hydromethylation pathways with palladium catalysts (Scheme 2-14). Migratory insertions to allenes typically favor addition to the central allene carbon with the formation of a metal π -allyl complex as depicted (Scheme 2-14). The use of bulky NHC ligands such as DP-IPr **2-39** orient position the silyl and L_{large} groups trans to minimize steric interactions prior to the migratory insertion (Scheme 2-14). In contrast, use of smaller NHC ligand IMes **2-35** reinforces the hydromethylation route by minimizing the steric interaction between silyl and L_{small} ligand. After silylmethylation (forming **2-57** with Ni) and hydromethylation (forming **2-58** with Pd), π allyl complexes **2-59** and **2-60** form and reductive elimination occurs at the most sterically-encumbered carbon, which is likely due to the high kinetic barrier for exchange of the L and silyl ligands.

Scheme 2-14 Proposed Hydrosilylation Pathways



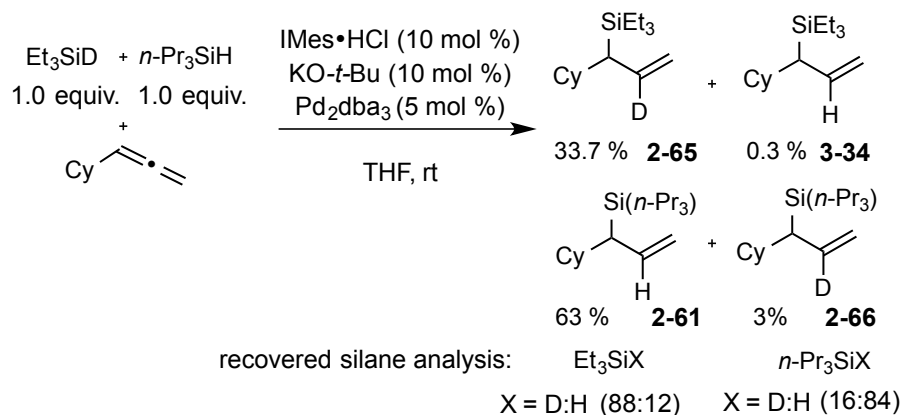
A series of double-labeling studies were performed to gain mechanistic insight into the regiodivergent additions involving cyclohexylallene and catalysts of Ni and Pd (Scheme 2-15 and 2-16). The reactions were carried out with an equivalent each of Et_3SiD and $n-Pr_3SiH$ and the distribution of products were determined via GCMS analysis (more details included in the experimental portion of this chapter). It was found that in the nickel variant (Scheme 2-15), the majority of the products formed were non-crossover products **2-64** in 69 % and **2-62** in 30 %. Crossover product **2-33** was not observed while **2-63** was detected in only 1 % abundance. The starting silanes (Et_3SiD and nPr_3SiH) were recovered and it was observed that the starting materials were recovered without observed scrambling.

Scheme 2-15 Double-Labeling Study with Ni-Catalyzed Protocol



The results of the crossover experiments for the Pd/IMes system resulted in the observation of primarily non-crossover products **2-65** in 33.7 % and **2-61** in 63 % (Scheme 2-16). Crossover products **2-66** and **3-34** were formed in only very small amounts (3 % and 0.3 % respectively). The recovered silane equivalents were observed to scramble in roughly equal amounts, 88:12 for Et_3SiD and 16:84 for $n\text{Pr}_3\text{SiH}$ starting materials.

Scheme 2-16 Double-Labeling Study with Pd-Catalyzed Protocol



From the above study, several conclusions can be gleaned about the mechanism. First, as a result of the observation of primarily non-crossover products, the equivalent of silane introduced to the reactive manifolds stays associated with the metal catalysts as

crossover products are not detected to an appreciable level for both catalysts. This also outrules potential mechanisms involving disproportionation to M-H or M-SiR₃ species as these scenarios would afford significant crossover products. This study also clearly demonstrates that more complex processes, such as dehydrogenative silylation, are not operative pathways for the developed reaction conditions.

2.7 Conclusions and outlook

In summary, the complementary use of metals (Ni vs Pd) results in dramatic regiochemical reversals in allene hydrosilylation with triethylsilane. Alterations in NHC ligand structure can drastically improve the regioselectivities to provide metal-divergent access to a wide range of either alkenyl silane regioisomer in high yields. Further enhancements are potentially possible with NHC ligand alterations, i.e. the development of even smaller ligands for Ni(0) reactions; however, the above study demonstrates the special relationship metal identity can play in governing catalytic reactions that are sensitive to substrate electronics and sterics. Our lab will conduct a full exploration of these intriguing effects, in order to elucidate the synergy that can be realized by combining changes in metal identity with structure of the precatalyst, ligand, and silane. The results from this study demonstrate that metal identity can be an effective strategy in controlling the regioselectivity in simple two-component reactions.

The content of this chapter was published in The Journal of the American Chemical Society.⁴⁴

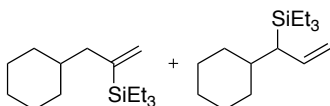
2.8 Experimental

General: All reagents were used as received unless otherwise noted. Solvents were purified under nitrogen using a solvent purification system (Innovative Technology, Inc.

Model # SPS-400-3 and PS-400-3). IPr-Ni-sty₂ (**2-29**) and IPr-Pd-sty₂ (**2-30**) catalysts were synthesized according to established procedures and stored in a glovebox.²⁸ Tris(dibenzylideneacetone)-dipalladium (Pd₂dba₃) was purchased from Sigma Aldrich and stored in a glovebox. Cyclohexylallene and vinylidenecyclohexane were purchased (Sigma Aldrich), while all remaining allenes were synthesized according to established procedures from the respective 1-alkyne precursors.²⁹ All reactions were conducted under an atmosphere of nitrogen with magnetic stirring in flame-dried or oven dried (120 °C) glassware. Racemic **3-29** (DP-IPr•HBF₄) was synthesized according to the established procedure and was subsequently stored and weighed in a glovebox.³⁰ All other utilized *N*-heterocyclic carbene salts (**2-35**, **2-36**, **2-37**, **2-38**) and *t*-BuOK (purchased from Sigma-Aldrich and Strem) were stored and weighed in an inert atmosphere glovebox. Triethylsilane (Sigma-Aldrich) was passed through alumina and degassed before use. Benzyldimethylsilane (Sigma-Aldrich), dimethylphenylsilane (Sigma-Aldrich), di-*tert*-butylsilane (Sigma-Aldrich), and 1,1,1,3,5,5,5-heptamethyltrisiloxane (TCI chemicals) were used as received. ¹H and ¹³C spectra were obtained in CDCl₃ at rt (25 °C), unless otherwise noted, on a Varian Mercury 400 MHz instrument, Varian Unity 500 MHz instrument, or Varian Unity 700 MHz instrument. Chemical shifts of ¹H NMR spectra were recorded in parts per million (ppm) on the δ scale from an internal standard of residual chloroform (7.24 ppm). Chemical shifts of ¹³C NMR spectra were recorded in ppm from the central peak of CDCl₃ (77.0 ppm) on the δ scale. High resolution mass spectra (HRMS) were obtained on a VG-70-250-s spectrometer manufactured by Micromass Corp. (Manchester UK) at the University of Michigan Mass Spectrometry Laboratory. Regioisomeric ratios were determined on crude reaction mixtures using

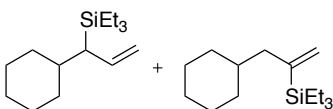
NMR or GC. GC analyses were carried out on an HP 6980 Series GC System with HP-5MS column (30 m x 0.252 mm x 0.25 μ m).

[2-(Triethylsilyl)-2-propen-1-yl]-cyclohexane (2-33) and [3-(triethylsilyl)-2-propen-1-yl]-cyclohexane (2-34) from nickel complex 2-29 (Scheme 2)



THF (1.0 mL) was added to IPr-Ni-sty₂ complex **2-29** (9.83 mg, 0.015 mmol) at 50 °C. After stirring for 10 min at 50 °C, triethylsilane (48 μ L, 0.3 mmol) was added. The reaction mixture was stirred for 10 min at 50 °C followed by addition of cyclohexylallene (36.6 mg, 0.3 mmol) in THF (4.0 mL) via syringe pump addition over 2 h. The reaction mixture was stirred at 50 °C for 1 h. The reaction mixture was filtered through silica gel eluting with 50% v/v EtOAc/hexanes. The solvent was removed *in vacuo*, and the crude residue was purified via flash column chromatography (100% hexanes) affording a clear oil (53 mg, 74 % yield) as a mixture of regioisomers (85:15 regioselectivity). Full characterization data for the major product (**2-33**) is provided below (Table 1, entry 5).

[3-(Triethylsilyl)-2-propen-1-yl]-cyclohexane (2-34) and [2-(triethylsilyl)-2-propen-1-yl]-cyclohexane (2-33) from palladium complex 2-30 (Scheme 2)



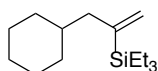
THF (1.0 mL) was added to IPr-Pd-sty₂ complex **2-30** (10.6 mg, 0.015 mmol) at 50 °C. After stirring for 10 min at 50 °C, triethylsilane (48 μ L, 0.3 mmol) was added. The reaction mixture stirred for 10 min at 50 °C followed by addition of cyclohexylallene (36.6 mg, 0.3 mmol) in THF (4.0 mL) via syringe pump addition over 2 h (syringe-drive

addition is optional, but was used for consistent comparison). The reaction mixture stirred at 50 °C for 1 h. The reaction mixture was filtered through silica gel eluting with 50% v/v EtOAc/hexanes. The solvent was removed *in vacuo*, and the crude residue was purified via flash column chromatography (100% v/v hexanes) affording a clear oil (54 mg, 75 % yield) as a mixture of regioisomers (88:12 regioselectivity). Full characterization data for the major product (**2-34**) is provided below (Table 1, entry 10).

General procedure I for the Ni(COD)₂/DP-IPr-promoted hydrosilylation of monosubstituted and 1,1-disubstituted allenes:

THF (1.0 mL) was added to a solid mixture of DP-IPr·HBF₄ **2-39** (0.03 mmol), *t*-BuOK (0.03 mmol), and Ni(COD)₂ (0.03 mmol) at rt. After stirring for 10 min at rt, the reaction mixture turned light brown, and silane (0.3 mmol) was added. The reaction mixture was stirred for 10 min at rt followed by the addition of allene (0.3 mmol) in THF (4.0 mL) over 2 h by syringe pump. The reaction mixture was stirred at rt until TLC analysis indicated disappearance of the allene. The reaction mixture was filtered through silica gel eluting with 50% v/v EtOAc/hexanes. The solvent was removed *in vacuo*, and the crude residue was purified via flash column chromatography on silica gel to afford the desired product.

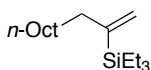
[2-(Triethylsilyl)-2-propen-1-yl]-cyclohexane (2-33) (Table 1, Entry 5)



General procedure I was followed with Ni(COD)₂ (8.25 mg, 0.03 mmol), DP-IPr·HBF₄ **2-39** (18.9 mg, 0.03 mmol), *t*-BuOK (3.4 mg, 0.03 mmol), triethylsilane (48 μL, 0.3 mmol), and cyclohexylallene (36.6 mg, 0.3 mmol). The crude residue was purified by flash chromatography (100% hexanes) affording a clear oil (60 mg, 84 % yield). ¹H NMR (400 MHz, CDCl₃): δ 5.56 (dt, *J* = 3.6, 1.2 Hz, 1H), 5.30 (dt, *J* = 3.2, 0.4 Hz, 1H), 1.96 (d, *J* = 7.2 Hz, 2H), 1.56-1.74 (m, 5H), 1.30-1.39 (m, 1H), 1.10-1.21 (m, 3 H), 0.91 (t, *J* = 8 Hz,

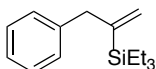
9H), 0.71-0.86 (m, 2H), 0.58 (q, $J = 4.4$ Hz, 6H); ^{13}C NMR (125 MHz, CDCl_3): δ 147.4, 126.4, 45.2, 36.4, 33.4, 26.7, 26.4, 7.3, 3.0; IR (thin film): ν 3045, 2920, 2874, 2851, 1449, 1416, 1237, 1008, 923, 719 cm^{-1} ; HRMS (EI) (m/z): $[\text{M}]^+$ calc for $\text{C}_{15}\text{H}_{30}\text{Si}$, 238.2117; found, 238.2117.

Triethyl(1-methylenenonyl)-silane (2-40) (Table 2, Entry 3)



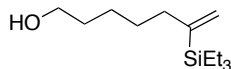
General procedure I was followed with $\text{Ni}(\text{COD})_2$ (8.25 mg, 0.03 mmol), DP-IPr· HBF_4 **2-39** (18.9 mg, 0.03 mmol), t -BuOK (3.4 mg, 0.03 mmol), triethylsilane (48 μL , 0.3 mmol), and undeca-1,2-diene (45.7 mg, 0.3 mmol). The crude residue was purified by flash chromatography (100% hexanes) affording a clear oil (64 mg, 80 % yield). Spectral data matched that previously reported.³¹

[2-(Triethylsilyl)-2-propen-1-yl]-benzene (2-42) (Table 2, Entry 5)



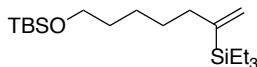
General procedure I was followed with $\text{Ni}(\text{COD})_2$ (8.25 mg, 0.03 mmol), DP-IPr· HBF_4 **2-39** (18.9 mg, 0.03 mmol), t -BuOK (3.4 mg, 0.03 mmol), triethylsilane (48 μL , 0.3 mmol), and phenylallene (34.8 mg, 0.3 mmol). The crude residue was purified by flash chromatography (100% hexanes) affording a clear oil (54 mg, 78% yield). ^1H NMR (500 MHz, CDCl_3): δ 7.24-7.25 (m, 2H), 7.12-7.14 (m, 3H), 5.48 (dt, $J = 3.0, 1.2$ Hz, 1H), 5.39 (dt, $J = 3.0, 1.2$ Hz, 1H), 3.41 (s, 2H), 0.86 (t, $J = 8.0$ Hz, 9H), 0.51 (q, $J = 8.0$ Hz, 6H); ^{13}C NMR (175 MHz, CDCl_3): δ , 148.2, 140.0, 129.3, 128.1, 127.2, 125.9, 43.0, 7.2, 2.8; IR (thin film): ν 3085, 2953, 1495, 1237, 1008, 721, 673, 586 cm^{-1} ; HRMS (EI) (m/z): $[\text{M}-\text{C}_2\text{H}_5]^+$ calcd for $\text{C}_{12}\text{H}_{24}\text{Si}$, 203.1256; found, 203.1252.

(6-(Triethylsilyl))hept-6-en-1-ol (2-44) (Table 2, Entry 7)



General procedure I was followed with Ni(COD)₂ (8.25 mg, 0.03 mmol), DP-IPr·HBF₄ **2-39** (18.9 mg, 0.03 mmol), *t*-BuOK (3.4 mg, 0.03 mmol), triethylsilane (48 μL, 0.3 mmol), and hexa-4,5-dien-1-ol (33.6 mg, 0.3 mmol). The crude residue was purified by flash chromatography (25% v/v EtOAc:hexanes) affording a clear oil (43 mg, 62 % yield). ¹H NMR (400 MHz, CDCl₃): δ 5.61 (m, 1H), 5.27 (m, 1H), 3.63 (t, *J* = 6.5 Hz, 2H), 2.07 (t, *J* = 6.5 Hz, 2H), 1.57 (quint, *J* = 6.5 Hz, 2H), 1.42 (m, 2H), 1.34 (quint, *J* = 6.5 Hz, 2H), 0.90 (t, *J* = 8.0 Hz, 9H), 0.58 (q, *J* = 8.0 Hz, 6H); ¹³C NMR (175 MHz, CDCl₃): δ 149.0, 125.1, 63.0, 36.2, 32.7, 28.6, 25.6, 7.4, 2.9; IR (thin film): ν 3359.8, 2934.6, 2875.0, 1458.6, 1416.2, 1237.4, 1052.4, 1017.3, 720.6 cm⁻¹; HRMS (EI) (*m/z*): [M-Et]⁺ calc for C₁₃H₂₈OSi, 199.1518; found, 199.1522.

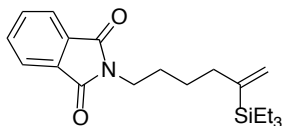
***tert*-Butyldimethoxy(6-(triethylsilyl))hept-6-ene (2-46) (Table 2, Entry 9)**



General procedure I was followed with Ni(COD)₂ (8.25 mg, 0.03 mmol), DP-IPr·HBF₄ **2-39** (18.9 mg, 0.03 mmol), *t*-BuOK (3.4 mg, 0.03 mmol), triethylsilane (48 μL, 0.3 mmol), and *tert*-butyl(hexa-4,5-dien-1-yloxy)dimethylsilane (68 mg, 0.3 mmol). The crude residue was purified by flash chromatography (100% hexanes) affording a slightly yellow oil (75.0 mg, 73% yield). ¹H NMR (500 MHz, CDCl₃): δ 5.64 (s, 1H), 5.30 (s, 1H), 3.62 (td, *J* = 6.5, 1.8 Hz, 2H), 2.09 (t, *J* = 7.5 Hz, 2H), 1.52-1.56 (m, 2H), 1.40-1.44 (m, 2H), 1.31-1.37 (m, 2H), 0.93 (t, *J* = 8.0 Hz, 9H), 0.91 (s, 9H), 0.61 (q, *J* = 8.0 Hz, 6H), 0.06 (s, 6H); ¹³C NMR (175 MHz, CDCl₃): δ 149.1, 125.0, 63.3, 36.3, 32.8, 28.7, 26.0, 25.8, 18.4, 7.4, 2.9, -5.3; IR (thin film): ν 2952.7, 2928.3, 2856.1, 1462.1, 1384.2,

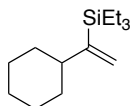
12551.1, 1103.6, 1005.3, 834.9, 719.9 cm^{-1} ; HRMS (EI) (m/z): $[\text{M}-t\text{-Bu}]^+$ calc for $\text{C}_{15}\text{H}_{33}\text{OSi}_2$, 285.2070; found, 285.2069.

2-(5-Triethylsilyl)hex-5-en-1-yl)isoindoline-1,3-dione (2-48) (Table 2, Entry 11)



General procedure I was followed with $\text{Ni}(\text{COD})_2$ (8.25 mg, 0.03 mmol), $\text{DP-IPr}\cdot\text{HBF}_4$ **2-39** (18.9 mg, 0.03 mmol), $t\text{-BuOK}$ (3.4 mg, 0.03 mmol), triethylsilane (48 μL , 0.3 mmol), and 2-(hexa-4,5-dien-1-yl)isoindoline-1,3-dione (68.2 mg, 0.3 mmol). The crude residue was purified by flash chromatography (10% v/v EtOAc/hexanes) affording a clear oil (80 mg, 78% yield). ^1H NMR (700 MHz, CDCl_3): δ 7.81-7.83 (m, 2H), 7.68-7.69 (m, 2H), 5.60 (dt, $J = 2.8, 1.4$ Hz, 1H), 5.27 (d, $J = 3.0$ Hz, 1H), 3.67 (t, $J = 7.7$ Hz, 2H), 2.11 (t, $J = 7.7$ Hz, 2), 1.67 (quint, $J = 7.7$ Hz, 2H), 1.44 (quint, $J = 7.7$ Hz, 2H), 0.87 (t, $J = 8.4$ Hz, 9H), 0.55 (q, $J = 8.4$ Hz, 6H); ^{13}C NMR (175 MHz, CDCl_3): δ 168.4, 148.4, 133.8, 132.1, 125.5, 123.1, 37.9, 35.7, 28.4, 25.9, 7.3, 2.9; IR (thin film): ν 2975, 2866, 1772, 1719, 1457, 1382, 1151, 1121, 925, 720 cm^{-1} ; HRMS (APCI) (m/z): $[\text{M}+\text{H}]^+$ calcd for $\text{C}_{20}\text{H}_{29}\text{NO}_2\text{Si}$ 344.2040; found, 344.2039.

[1-(Triethylsilyl)ethenyl]-cyclohexane (2-50) (Scheme 3)

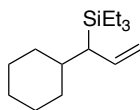


General procedure I was followed with $\text{Ni}(\text{COD})_2$ (8.25 mg, 0.03 mmol), $\text{DP-IPr}\cdot\text{HBF}_4$ **2-39** (18.9 mg, 0.03 mmol), $t\text{-BuOK}$ (3.4 mg, 0.03 mmol), triethylsilane (48 μL , 0.3 mmol), and vinylidenecyclohexane (32.5 mg, 0.3 mmol). The crude residue was purified by flash chromatography (100% hexanes) affording a clear oil (51 mg, 76% yield). Spectral data matched that previously reported.³²

General procedure II for the Pd₂dba₃/ IMes –promoted hydrosilylation of monosubstituted and 1,1-disubstituted allenes:

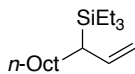
THF (1.0 mL) was added to a solid mixture of IMes·HCl **2-35** (0.03 mmol), *t*-BuOK (0.03 mmol), and Pd₂dba₃ (0.015 mmol) at rt. After stirring for 10 min at rt, the reaction mixture turned bright red and triethylsilane (0.3 mmol) was added. The reaction mixture was stirred for 10 min at rt followed by dilution with THF (4.0 mL) and addition of the allene (0.3 mmol) neat by syringe. The reaction mixture was stirred at rt for 2 h. The reaction mixture was filtered through silica gel eluting with 50% v/v EtOAc/hexanes. The solvent was removed *in vacuo*, and the crude residue was purified via flash column chromatography on silica gel to afford the desired product.

[3-(Triethylsilyl)-2-propen-1-yl]-cyclohexane (2-34) (Table 1, Entry 10)



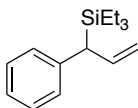
General procedure II was followed with Pd₂dba₃ (13.7 mg, 0.015 mmol), IMes·HCl salt **2-35** (10.2 mg, 0.03 mmol), *t*-BuOK (3.4 mg, 0.03 mmol), triethylsilane (48 μL, 0.3 mmol), and cyclohexylallene (36.6 mg, 0.3 mmol). The crude residue was purified by flash chromatography (100% hexanes) affording a clear oil (57 mg, 80% yield). ¹H NMR (400 MHz, CDCl₃): δ 5.70 (dt, *J* = 16.8, 10.4 Hz, 1H), 4.82 (dd, *J* = 8.0, 1.6 Hz, 1H), 4.77 (dd, *J* = 16.8, 2.4 Hz, 1H), 1.63-1.75 (m, 3H), 1.41-1.63 (m, 4 H), 0.98-1.25 (m, 5H), 0.93 (t, *J* = 8.0 Hz, 9H), 0.55 (q, *J* = 8.0 Hz, 6H); ¹³C NMR (175 MHz, CDCl₃): δ 138.6, 112.7, 39.9, 38.3, 34.3, 31.7, 26.89, 26.88, 26.3, 7.7, 3.3; IR (thin film): ν 3072, 2918, 2850, 1622, 1448, 1415, 1238, 1009, 894, 765, 728, 599 cm⁻¹; HRMS (EI) (*m/z*): [M]⁺ calc for C₁₅H₃₀Si, 238.2117; found, 238.2113.

Triethyl(undec-1-en-3-yl)silane (2-51) (Table 2, Entry 4)



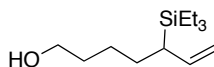
General procedure II was followed with Pd₂dba₃ (13.7 mg, 0.015 mmol), IMes·HCl salt **2-35** (10.2 mg, 0.03 mmol), *t*-BuOK (3.4 mg, 0.03 mmol), triethylsilane (48 μL, 0.3 mmol), and undeca-1,2-diene (45.7 mg, 0.3 mmol). The crude residue was purified by flash chromatography (100% hexanes) affording a clear oil (79 mg, 98 % yield). ¹H NMR (500 MHz, CDCl₃): δ 5.62 (dt, *J* = 16.0, 10.0 Hz, 1H), 4.82 (dd, *J* = 10.4, 1.5 Hz, 1H), 4.79 (dd, *J* = 16.5, 1.0 Hz, 1H), 1.63 (td, *J* = 13.0, 4.0 Hz, 1H), 1.33-1.43 (m, 2H), 0.97-1.23 (m, 12H), 0.92 (t, *J* = 8.0 Hz, 9H), 0.86 (t, *J* = 8.0 Hz, 3H), 0.52 (q, *J* = 8.0 Hz, 6H); ¹³C NMR (175 MHz, CDCl₃): δ 140.8, 111.4, 32.1, 31.9, 29.5, 29.46, 29.45, 29.3, 28.6, 22.7, 14.0, 7.6, 2.1; IR (thin film): ν 3074, 2920, 2853, 1625, 1465 1415, 1239, 1017, 893, 776, 730, 615 cm⁻¹; HRMS (EI) (*m/z*): [M]⁺ calc for C₁₅H₃₀Si, 268.2586; found, 268.2583.

Triethyl(1-phenylallyl)silane (**2-53**) (Table 2, Entry 6)



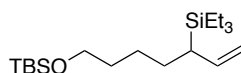
General procedure II was followed with Pd₂dba₃ (13.7 mg, 0.015 mmol), IMes·HCl salt **2-35** (10.2 mg, 0.03 mmol), *t*-BuOK (3.4 mg, 0.03 mmol), triethylsilane (48 μL, 0.3 mmol), and phenylallene (34.8 mg, 0.3 mmol). The crude residue was purified by flash chromatography (100% hexanes) affording a clear oil (66 mg, 94 % yield). Spectral data matched that previously reported.³³

5-(Triethylsilyl)hept-6-en-1-ol (**2-55**) (Table 2, Entry 8)



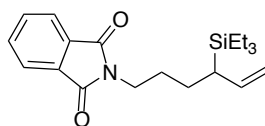
General procedure II was followed with Pd₂dba₃ (13.7 mg, 0.015 mmol), IMes·HCl salt **2-35** (10.3 mg, 0.03 mmol), *t*-BuOK (3.4 mg, 0.03 mmol), triethylsilane (48 μL, 0.3 mmol), and hexa-4,5-dien-1-ol (33.6 mg, 0.3 mmol). The crude residue was purified by flash chromatography (100% hexanes) affording a clear oil (60 mg, 88 % yield). ¹H NMR (500 MHz, CDCl₃): δ 5.61 (dt, *J* = 17.0, 10.0 Hz, 1H), 4.82 (dd, *J* = 10.4, 1.5 Hz, 1H), 4.79 (dd, *J* = 16.5, 1.0 Hz, 1H), 3.61 (q, *J* = 5.6 Hz, 2H), 1.41-1.65 (m, 6H), 1.16-1.20 (m, 1H), 0.92 (t, *J* = 8.0 Hz, 9H), 0.52 (q, *J* = 8.0 Hz, 6H); ¹³C NMR (175 MHz, CDCl₃): δ 140.4, 111.8, 63.3, 32.7, 32.1, 28.5, 25.6, 7.6, 2.2; IR (thin film): ν 3337.6, 2952.0, 1625.5, 1458.0, 1239.8, 1054.0, 893.1, 732.4, 615.8; HRMS (EI) (*m/z*): [M-*t*-Bu]⁺ calc for C₁₃H₂₈OSi, 199.1518; found, 199.1523.

***tert*-Butyldimethyl(5-(triethylsilyl)hept-6-en-1-yl)oxy)silane (2-57) (Table 2, Entry 10)**



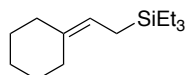
General procedure II was followed with Pd₂dba₃ (13.7 mg, 0.015 mmol), IMes·HCl salt **2-35** (10.3 mg, 0.03 mmol), *t*-BuOK (3.4 mg, 0.03 mmol), triethylsilane (48 μL, 0.3 mmol), and *tert*-butyl(hexa-4,5-dien-1-yloxy)dimethylsilane (67.9 mg, 0.3 mmol). The crude residue was purified by flash chromatography (100% hexanes) affording a slightly yellow oil (100 mg, 97 % yield). ¹H NMR (400 MHz, CDCl₃): δ 5.61 (dt, 1H, *J* = 17.0 10.0 Hz, 1H), 4.82 (dd, *J* = 10.4, 1.5 Hz, 1H), 4.79 (dd, *J* = 16.5, 1.0 Hz, 1H), 3.61 (t, *J* = 5.6 Hz, 2H), 1.41-1.65 (m, 6H), 1.16-1.20 (m, 1H), 0.92 (t, *J* = 8.0 Hz, 9H), 0.87 (s, 9H), 0.52 (q, *J* = 8.0 Hz, 6H), 0.02 (s, 6H); ¹³C NMR (175 MHz, CDCl₃): δ 140.5, 111.7, 63.3, 32.7, 32.1, 28.5, 26.0, 25.6, 18.4, 7.6, 2.2, -5.2; IR (thin film): ν 3074.1, 2952.8, 1624.9, 1471.3, 1360.2, 1255.1, 1101.4, 1005.3, 836.1, 730.1; HRMS (EI) (*m/z*): [M-*t*-Bu]⁺ calc for C₁₅H₃₃OSi₂, 285.2070; found, 285.2072.

2-(4-(Triethylsilyl)hex-5-en-1-yl)isoindoline-1,3-dione (2-59) (Table 2, Entry 12)



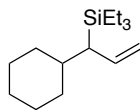
General procedure II was followed with Pd₂dba₃ (13.7 mg, 0.015 mmol), IMes·HCl salt **2-35** (10.2 mg, 0.03 mmol), *t*-BuOK (3.4 mg, 0.03 mmol), triethylsilane (48 μL, 0.3 mmol), and 2-(hexa-4,5-dien-1-yl)isoindoline-1,3-dione (68.2 mg, 0.3 mmol). The crude residue was purified by flash chromatography (10% v/v EtOAc:hexanes) affording a yellow solid (mp = 56-58 °C) (100 mg, 97 % yield). ¹H NMR (400 MHz, CDCl₃): δ 7.80-7.82 (m, 2H), 7.66 (m, 2H), 5.59 (dt, *J* = 16.8, 10.0 Hz, 1H), 4.84 (dd, 1H, *J* = 4.0, 1.6 Hz), 4.80 (dd, *J* = 10.8, 1.6 Hz, 1H), 3.62 (t, *J* = 7.6 Hz, 2H), 1.76-1.86 (m, 1H), 1.62-1.70 (m, 2H), 1.39-1.58 (m, 2H), 0.90 (t, *J* = 8.0 Hz, 9H), 0.51 (q, *J* = 8.0 Hz, 6H); ¹³C (100 MHz, CDCl₃): δ 168.4, 139.8, 133.8, 132.1, 123.1, 112.3, 37.8, 31.8, 28.4, 25.9, 7.5, 2.0; IR (thin film): ν 2949, 1771, 1716, 1622, 1399, 1370, 1004, 718, 531 cm⁻¹; HRMS (APCI) (*m/z*): [M+H]⁺ calc for C₂₀H₂₉NO₂Si, 344.2040; found, 344.2044.

(2-Cyclohexylideneethyl)triethylsilane (**2-51**) (Scheme 3)



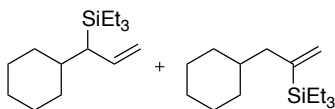
General procedure II was followed with Pd₂dba₃ (13.7 mg, 0.015 mmol), IMes·HCl salt **2-35** (10.2 mg, 0.03 mmol), *t*-BuOK (3.4 mg, 0.03 mmol), triethylsilane (48 μL, 0.3 mmol), and vinylidenecyclohexane (32.5 mg, 0.3 mmol). The crude residue was purified by flash chromatography (100% hexanes) affording a clear oil (50 mg, 74 % yield). Spectral data matched that previously reported.³⁴

[3-(Triethylsilyl)-2-propen-1-yl]-cyclohexane (**2-34**) (Table 2, Entry 13)



THF (25 mL) was added to a solid mixture of IMes·HCl **2-35** (205 mg, 0.6 mmol), *t*-BuOK (67.2 mg, 0.6 mmol), and Pd₂dba₃ (275 mg, 0.3 mmol) at rt. After stirring for 10 min at rt, the reaction mixture turned bright red and triethylsilane (1.0 mL, 6.0 mmol) was added. The reaction mixture was stirred for 10 min at rt followed by dilution with THF (75 mL) and addition of cyclohexylallene (732 mg, 6.0 mmol) neat by syringe. The reaction mixture was stirred at rt for 2 h. The reaction mixture was filtered through silica gel eluting with 50% v/v EtOAc/hexanes. The solvent was removed *in vacuo*, and the crude residue was purified via flash column chromatography (100% hexanes) on silica gel to afford the desired product as a clear oil (1.4 g, 98%). Full characterization data is provided above (Table 1, entry 10).

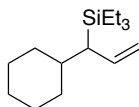
[3-(Triethylsilyl)-2-propen-1-yl]-cyclohexane (2-34) and [2-(triethylsilyl)-2-propen-1-yl]-cyclohexane (2-33) (Table 2, Entry 14)



IMes·HCl **2-35** (10.3 mg, 0.03 mmol), *t*-BuOK (3.4 mg, 0.03 mmol), and Pd₂dba₃ (13.7 mg, 0.015 mmol) were added to a 6.0 mL dram vial in air. The vial was fitted with a septum and underwent 3 pump/purge manifold cycles with nitrogen. THF (1.0 mL) was then added. After stirring for 10 min at rt, the reaction mixture turned bright red and triethylsilane (48 μL, 0.3 mmol) was added. The reaction mixture was stirred for 10 min at rt followed by dilution with THF (4.0 mL) and addition of cyclohexylallene (36.6 mg, 0.3 mmol) neat by syringe. The reaction mixture was stirred at rt for 2 h. The reaction mixture was filtered through silica gel eluting with 50% v/v EtOAc/hexanes. The solvent was removed *in vacuo*, and the crude residue was purified via flash column chromatography on silica gel affording a clear oil (54 mg, 75 % yield) as a mixture of

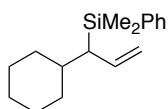
regioisomers (96:4 regioselectivity). Full characterization data for the major product (**2-34**) is provided above (Table 1, entry 10).

[3-(Triethylsilyl)-2-propen-1-yl]-cyclohexane (2-34) (Table 2, Entry 15)



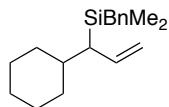
THF (1.0 mL) was added to a solid mixture of IMes·HCl **2-35** (5.11 mg, 0.015 mmol), *t*-BuOK (1.7 mg, 0.015 mmol), and Pd₂dba₃ (6.9 mg, 7.5 μmol) at rt. After stirring for 10 min at rt, the reaction mixture turned bright red and triethylsilane (48 μL, 0.3 mmol) was added. The reaction mixture was stirred for 10 min at rt followed by dilution with THF (4.0 mL) and addition of cyclohexylallene (36.6 mg, 0.3 mmol) neat by syringe. The reaction mixture was stirred at rt for 3 h. The reaction mixture was filtered through silica gel eluting with 50% v/v EtOAc/hexanes. The solvent was removed *in vacuo*, and the crude residue was purified via flash column chromatography (100 % hexanes) on silica gel to afford the desired product as a clear oil (51 mg, 72%). Full characterization data is provided above (Table 1, entry 10).

(1-Cyclohexylallyl)dimethyl(phenyl)silane (2-52) (Table 3, Entry 1)



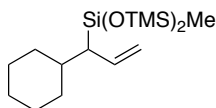
General procedure II was followed with Pd₂dba₃ (13.7 mg, 0.015 mmol), IMes·HCl salt **2-35** (10.2 mg, 0.03 mmol), *t*-BuOK (3.4 mg, 0.03 mmol), dimethylphenylsilane (48 μL, 0.3 mmol), and cyclohexylallene (36.6 mg, 0.3 mmol). The crude residue was purified by flash chromatography (100% hexanes) affording a clear oil (70 mg, 91 % yield). Spectral data matched that previously reported.³⁵

Benzyl(1-cyclohexylallyl)dimethylsilane (2-53) (Table 3, Entry 2)



General procedure II was followed with Pd₂dba₃ (13.7 mg, 0.015 mmol), IMes·HCl salt **2-35** (10.2 mg, 0.03 mmol), *t*-BuOK (3.4 mg, 0.03 mmol), benzyldimethylsilane (47.5 μL, 0.3 mmol), and cyclohexylallene (36.6 mg, 0.3 mmol). The crude residue was purified by flash chromatography (100% hexanes) affording a clear oil (76 mg, 93 % yield). ¹H NMR (400 MHz, CDCl₃): δ 7.18 (t, *J* = 7.6 Hz, 2H), 7.04 (t, *J* = 7.6 Hz, 1H), 6.98 (d, *J* = 7.6 Hz, 2H), 5.70 (dt, *J* = 16.8, 10.4 Hz, 1H), 4.92 (dd, *J* = 10.4, 2.2 Hz, 1H), 4.82 (dd, *J* = 17.2, 2.2 Hz, 1H), 2.09 (s, 2H), 1.41-1.63 (m, 5 H), 0.98-1.25 (m, 7H), -0.056 (s, 3H), -0.071 (s, 3H); ¹³C (125 MHz, CDCl₃): δ 140.3, 137.8, 128.3, 128.1, 123.9, 113.7, 41.6, 38.5, 34.2, 31.3, 26.86, 26.83, 26.3, 24.7, -3.64, -3.71; IR (thin film): ν 2921, 2850, 1600, 1492, 1449, 1246, 827, 697 cm⁻¹; HRMS (EI) (*m/z*): [M]⁺ calc for C₁₈H₂₈Si, 272.1960; found, 272.1955.

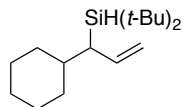
3-(1-Cyclohexylallyl)-1,1,1,3,5,5,5-heptamethyltrisiloxane (2-54) (Table 3, Entry 3)



General procedure II was followed with Pd₂dba₃ (13.7 mg, 0.015 mmol), IMes·HCl salt **2-35** (10.2 mg, 0.03 mmol), *t*-BuOK (3.4 mg, 0.03 mmol), 1,1,1,3,5,5,5-heptamethyltrisiloxane (105 μL, 0.3 mmol), and cyclohexylallene (36.6 mg, 0.3 mmol). The crude residue was purified by flash chromatography (100% hexanes) affording a yellow oil (85 mg, 82 % yield). ¹H NMR (400 MHz, CDCl₃): δ 5.65 (dt, *J* = 16.8, 10 Hz, 1H), 4.88 (dd, *J* = 10, 2.6 Hz, 1H), 4.82 (dd, *J* = 10, 2.4 Hz, 1H), 1.53-1.84 (m, 5H), 0.94-1.41 (m, 7H), 0.066 (s, 18H), -0.014 (s, 3H); ¹³C (100 MHz, CDCl₃): δ 137.9, 113.9, 43.9, 37.8, 33.7, 31.4, 26.9, 26.4, 1.87, 1.85, -0.4; IR (thin film): ν 2922, 1251, 1045,

836, 781, 752 cm^{-1} ; HRMS (EI) (m/z): $[\text{M}^+]^+$ calc for $\text{C}_{15}\text{H}_{33}\text{O}_2\text{Si}_3$, 329.1788; found, 329.1788.

di-*tert*-Butyl(1-cyclohexylallyl)silane (2-55) (Table 3, Entry 4)



General procedure II was followed with Pd_2dba_3 (13.7 mg, 0.015 mmol), IMes·HCl salt **2-35** (10.2 mg, 0.03 mmol), *t*-BuOK (3.4 mg, 0.03 mmol), di-*tert*-butylsilane (59.4 μL , 0.3 mmol), and cyclohexylallene (36.6 mg, 0.3 mmol). The crude residue was purified by flash chromatography (100% hexanes) affording a clear oil (60 mg, 75 % yield). ^1H NMR (400 MHz, CDCl_3): δ 5.90 (dt, $J = 16, 11.2$ Hz, 1H), 4.91 (m, 1H), 4.88 (m, 1H), 3.46 (s, 1H), 1.45-1.92 (m, 7H), 1.10-1.26 (m, 3H), 1.05 (s, 9H), 1.03 (s, 9H), 0.79-0.91 (m, 2H); ^{13}C NMR (100 MHz, CDCl_3): δ 139.5, 113.7, 39.5, 39.0, 33.9, 32.4, 30.0, 29.5, 26.7, 26.5, 20.6, 20.0; IR (thin film): ν 2924, 2854, 2097, 1623, 1469, 1002, 896, 852, 819, 803, 508, 459 cm^{-1} ; HRMS (EI) (m/z): $[\text{M}-\text{H}]^+$ calc for $\text{C}_{17}\text{H}_{34}\text{Si}$, 265.2352; found, 265.2356.

Double-Labeling Study Data:

General procedure III for the $\text{Ni}(\text{COD})_2/\text{DP-IPr}$ -promoted hydrosilylation of monosubstituted allenes affording alkenylsilane authentic standards:

THF (1.0 mL) was added to a solid mixture of DP-IPr· HBF_4 **2-39** (0.03 mmol), *t*-BuOK (0.03 mmol), and $\text{Ni}(\text{COD})_2$ (0.03 mmol) at rt. After stirring for 10 min at rt, the silane (0.3 mmol) was added. The reaction mixture was stirred for 10 min at rt followed by the addition of allene (0.3 mmol) in THF (4.0 mL) over 2 h by syringe pump. The reaction mixture was stirred at rt until TLC analysis indicated disappearance of the allene. The reaction mixture was filtered through silica gel eluting with 50% v/v EtOAc/hexanes. The solvent was removed *in vacuo*, and the crude residue was purified via flash column chromatography on silica gel to afford the desired product.

General procedure IV for the Pd₂dba₃/IMes –promoted hydrosilylation of monosubstituted allenes affording allylsilane authentic standards:

THF (1.0 mL) was added to a solid mixture of IMes·HCl **2-35** (0.03 mmol), KO-*t*-Bu (0.03 mmol), and Pd₂dba₃ (0.015 mmol) at rt. After stirring for 10 min at rt, the reaction mixture turned bright red and triethylsilane (0.3 mmol) was added. The reaction mixture was stirred for 10 min at rt followed by dilution with THF (4.0 mL) and addition of the allene (0.3 mmol) neat by syringe. The reaction mixture was stirred at rt for 2 h. The reaction mixture was filtered through silica gel eluting with 50% v/v EtOAc/hexanes. The solvent was removed *in vacuo*, and the crude residue was purified via flash column chromatography on silica gel to afford the desired product.

General procedure V for the Ni(COD)₂/DP-IPr-promoted hydrosilylation crossover experiment:

THF (1.0 mL) was added to a solid mixture of DP-IPr·HBF₄ **2-39** (0.03 mmol), KO-*t*-Bu (0.03 mmol) and Ni(COD)₂ (0.03 mmol) at rt. After stirring for 10 min at rt, the Et₃SiD (0.3 mmol) and *n*-Pr₃SiH (0.3 mmol) and cyclohexylallene (0.3 mmol) were added in THF (4.0 mL) over 2 h by syringe pump. The reaction mixture was filtered through silica gel eluting with 50% v/v EtOAc/hexanes. The solvent was removed *in vacuo*, and the crude residue was directly analyzed by GCMS.

General procedure VI for the Pd₂dba₃/IMes –promoted hydrosilylation crossover experiment:

THF (1.0 mL) was added to a solid mixture of IMes·HCl **2-35** (0.03 mmol), and Pd₂dba₃ (0.015 mmol) at rt. Then *n*-BuLi (0.03 mmol) was slowly added to the stirring solution. After stirring for 10 min at rt, the Et₃SiD (0.3 mmol) and *n*-Pr₃SiH (0.3 mmol) addition of cyclohexylallene (0.3 mmol) in THF (4.0 mL) over 2 h by syringe pump. The reaction mixture was filtered through silica gel eluting with 50% v/v EtOAc/hexanes. The solvent was removed *in vacuo*, and the crude residue was directly analyzed by GCMS.

Analysis of the crossover experiment:

Pure samples of products derived from Et₃SiH (MW 238), Et₃SiD (MW 239), and Pr₃SiH (MW 280) were independently prepared and GCMS analysis was performed. Based on

the similarity of the molecular ion minus ethyl regions (M-Et = 209) of the Et₃SiH and Et₃SiD derived product, the molecular ion region of the Pr₃SiD derived product was assumed to appear as the molecular ion minus propyl (M = 280) region of the Pr₃SiH-derived product, shifted by one mass unit. Relative peak heights in the molecular ion minus ethyl region of the spectra of each pure compound were normalized, with a value of 1 assigned to the base peak. In the crude product of an experiment that employed 0.5 equiv each of Et₃SiD and Pr₃SiH, the ratio of Et₃Si products to Pr₃Si products was determined by GC. From the crude GCMS, the relative intensity of the products were normalized, with the value of 1 assigned to the base peak. The ratio of the Et₃Si-(H) product to Et₃Si-(D) product was determined as follows:

$$\frac{\text{intensity of 209 peak in crossover experiment}}{\text{intensity of 210 peak in crossover experiment}} = \frac{[X] [\text{rel. height of 209 peak for Et}_3\text{Si-(H) product}] + [Y] [\text{rel. height of 209 peak for Et}_3\text{Si-(D) product}]}{[X] [\text{rel. height of 210 peak for Et}_3\text{Si-(H) product}] + [Y] [\text{rel. height of 210 peak for Et}_3\text{Si-(D) product}]}$$

$$X = 1/100 \times \text{relative \% of Et}_3\text{Si-(H) product}$$

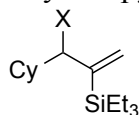
$$Y = 1/100 \times \text{relative \% of Et}_3\text{Si-(D) product} = 1-X$$

In the above equation, after substitution of [1-X] for [Y], the experimental values were inserted and the equation was solved for [X]. The ratio of Pr₃Si-(H) product to the intensity of 280 peak in crossover experiment and Pr₃Si-(D) products was determined in a similar fashion. Merging the GCFID ratios of Et₃Si products to Pr₃Si products with the data calculated from the above equation, an overall ratio of the products were obtained.

Product ratios detected with ion ratios: (*chromatograms for authentic samples and crossover experiments are included in the appendix following the spectra*):

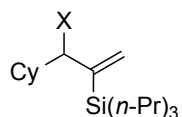
GCFID ratio Ethyl:Propyl products (nickel crossover): [69:31]

GCFID ratio Ethyl:Propyl products (palladium crossover): [34:66]



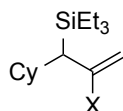
Ni crossover experiment

Authentic H Sample		Authentic D Sample		Crossover Experiment		Calculation Results	
Ion 209	Ion 210	Ion 209	Ion 210	Ion 209	Ion 210	% H:	% D:
1654272	378496	117712	2918912	72912	1783296	0 %	100 %



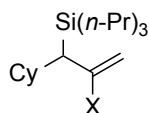
Ni crossover experiment

Authentic H Sample		Authentic D Sample		Crossover Experiment		Calculation Results	
Ion 280	Ion 281	Ion 280	Ion 281	Ion 280	Ion 281	% H:	% D:
2186	710	0	2186	276	100	96 %	4 %



Pd crossover experiment

Authentic H Sample		Authentic D Sample		Crossover Experiment		Calculation Results	
Ion 209	Ion 210	Ion 209	Ion 210	Ion 209	Ion 210	% H:	% D:
285888	56432	17680	107760	587	21952	1 %	99 %



Pd crossover experiment

Authentic H Sample		Authentic D Sample		Crossover Experiment		Calculation Results	
Ion 280	Ion 281	Ion 280	Ion 281	Ion 280	Ion 281	% H:	% D:
53264	12224	154	53264	7333	1956	96 %	4 %

Collected Et₃SiX (from nickel crossover experiment)

Authentic H Sample		Authentic D Sample		Crossover Experiment		Calculation Results	
Ion 116	Ion 117	Ion 116	Ion 117	Ion 116	Ion 117	% H:	% D:
662848	115800	57608	594304	85144	703616	2	98

Collected nPr₃SiX (from nickel crossover experiment)

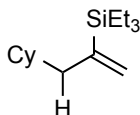
Authentic H Sample		Authentic D Sample		Crossover Experiment		Calculation Results	
Ion 158	Ion 159	Ion 158	Ion 159	Ion 158	Ion 159	% H:	% D:
177536	29160	29160	177536	201856	32168	100	0

Collected Et₃SiX (from Pd crossover experiment)

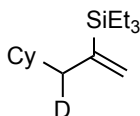
Authentic H Sample		Authentic D Sample		Crossover Experiment		Calculation Results	
Ion 116	Ion 117	Ion 116	Ion 117	Ion 116	Ion 117	% H:	% D:
662848	115800	57608	594304	16824	74376	12	88

Collected $n\text{Pr}_3\text{SiX}$ (from Pd crossover experiment)

Authentic H Sample		Authentic D Sample		Crossover Experiment		Calculation Results	
Ion 158	Ion 159	Ion 158	Ion 159	Ion 158	Ion 159	% H:	% D:
177536	29160	29160	177536	42800	14671	84	16

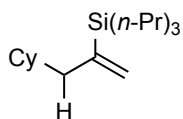
[2-(Triethylsilyl)-2-propen-1-yl]-cyclohexane (2-33) (Table 1, entry 5)

General procedure I was followed with $\text{Ni}(\text{COD})_2$ (8.25 mg, 0.03 mmol), DP-IPr· HBF_4 **2-39** (18.9 mg, 0.03 mmol), KO-*t*-Bu (3.4 mg, 0.03 mmol), triethylsilane (48 μL , 0.3 mmol), and cyclohexylallene (36.6 mg, 0.3 mmol). The crude residue was purified by flash chromatography (100% hexanes) affording a clear oil (60 mg, 84 % yield). Spectral data matched that previously reported.

(3-Cyclohexylprop-1-en-2-yl-3-*d*)triethylsilane (2-64) (Scheme 2-15)

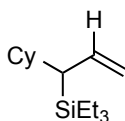
General procedure I was followed with $\text{Ni}(\text{COD})_2$ (8.25 mg, 0.03 mmol), DP-IPr· HBF_4 **2-39** (18.9 mg, 0.03 mmol), *n*-BuLi (12 μL , 0.03 mmol, 2.5 M in hexanes), *d*-triethylsilane (47.7 μL , 0.3 mmol), and cyclohexylallene (36.6 mg, 0.3 mmol). The crude residue was purified by flash chromatography (100% hexanes) affording a clear oil (60 mg, 83 % yield). ^1H NMR (700 MHz, CDCl_3): δ 5.56 (dd, $J = 3.3, 1.1$ Hz, 1H), 5.31 (d, $J = 3.3$ Hz, 1H), 1.94 (d, $J = 7$ Hz, 1H), 1.64 – 1.72 (m, 5H), 1.11-1.20 (m, 4H), 0.91 (t, $J = 8.0$ Hz, 9H), 0.77 – 0.83 (m, 2H), 0.58 (q, $J = 8.0$ Hz, 6H); ^{13}C NMR (175 MHz, CDCl_3): δ 147.3, 126.5, 36.3, 33.43, 33.41, 26.7, 26.4, 7.3, 3.0; IR (thin film): ν 2922.3, 2874.8, 2850.5, 1447.7, 1415.9, 1348.1, 1261.0 1236.3, 1012.0, 923.5, 892.9 cm^{-1} ; HRMS (EI) (m/z): $[\text{M}]^+$ calc for $\text{C}_{13}\text{H}_{24}\text{DSi}$, 210.1788; found, 210.1789.

(3-Cyclohexylprop-1-en-2-yl)tripropylsilane (2-62) (Scheme 2-15)



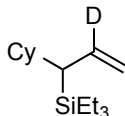
General procedure I was followed with Ni(COD)₂ (8.25 mg, 0.03 mmol), DP-IPr·HBF₄ **2-39** (18.9 mg, 0.03 mmol), *t*-BuOK (3.4 mg, 0.03 mmol), tripropylsilane (μL, 0.3 mmol), and cyclohexylallene (36.6 mg, 0.3 mmol). The crude residue was purified by flash chromatography (100% hexanes) affording a clear oil (47 mg, 56 % yield). ¹H NMR (700 MHz, CDCl₃): δ 5.54 (m, 1H), 5.30 (d, *J* = 3.4 Hz, 1H), 1.96 (d, *J* = 5.9 Hz, 2H), 1.60-1.71 (m, 6H), 1.25-1.32 (m, 6H), 1.10-1.22 (m, 3H), 0.943 (t, *J* = 8.0 Hz, 9 H), 0.77 – 0.84 (m, 2H), 0.55 (m, 6H); ¹³C NMR (175 MHz, CDCl₃): δ 148.0, 126.2, 45.1, 36.4, 33.5, 26.7, 26.4, 18.6, 17.4, 15.0; IR (thin film): ν 2922.4, 2954.2, 2867.7, 1449.6, 10654, 923, 806.5 cm⁻¹; HRMS (EI⁺) (*m/z*): [M-propyl]⁺ calc for C₁₅H₂₉Si, 237.2039; found, 237.2041.

[3-(Triethylsilyl)-2-propen-1-yl]-cyclohexane (**2-34**) (Table 1, entry 10)



General procedure II was followed with Pd₂dba₃ (13.7 mg, 0.015 mmol), IMes·HCl salt **2-35** (10.2 mg, 0.03 mmol), *t*-BuOK (3.4 mg, 0.03 mmol), triethylsilane (48 μL, 0.3 mmol), and cyclohexylallene (36.6 mg, 0.3 mmol). The crude residue was purified by flash chromatography (100% hexanes) affording a clear oil (57 mg, 80% yield). Spectral data matched that previously reported.

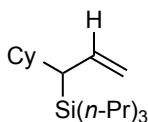
(1-Cyclohexylallyl-2-d)triethylsilane (**2-65**) (Scheme 2-16)



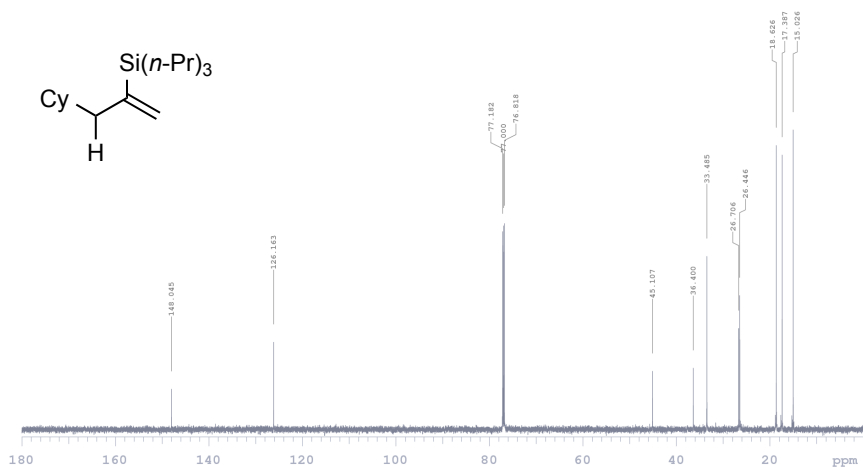
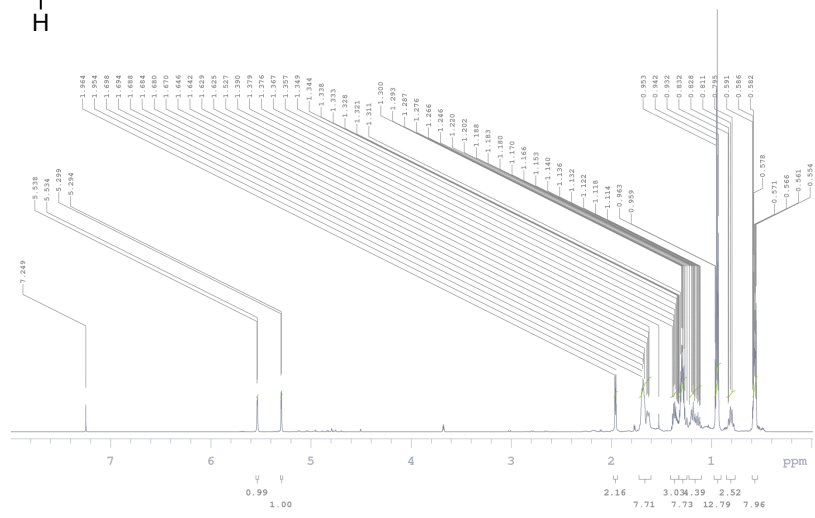
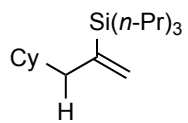
General procedure II was followed with Pd₂dba₃ (13.7 mg, 0.015 mmol), IMes·HCl salt **2-35** (10.2 mg, 0.03 mmol), *n*-BuLi (12 μL, 0.03 mmol, 2.5 M in hexanes), triethylsilane (47.7 μL, 0.3 mmol), and cyclohexylallene (36.6 mg, 0.3 mmol). The crude residue was

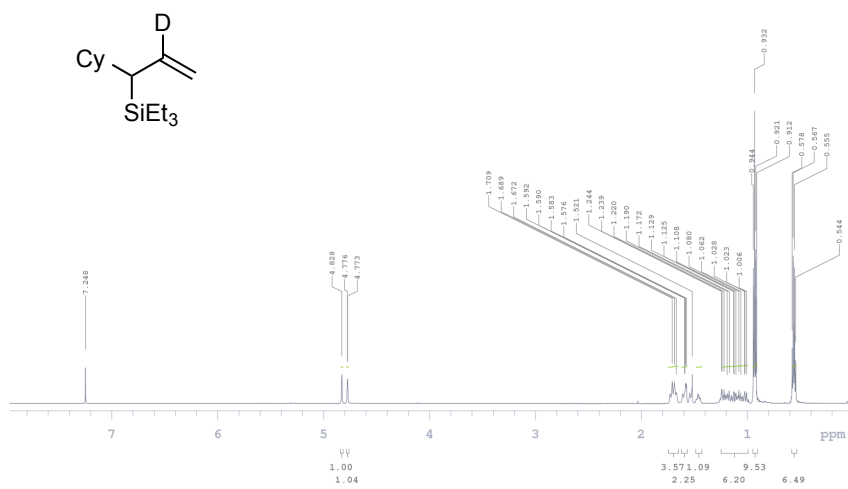
purified by flash chromatography (100% hexanes) affording a clear oil (50 mg, 70 % yield). ^1H NMR (700 MHz, CDCl_3): δ 4.83 (s, 1H), 4.77 (s, 1H), 1.65 – 1.74 (m, 3H), 1.44 – 1.63 (m, 2H), 0.986 – 1.27 (m, 6H), 0.93 (t, $J = 8.9$ Hz, 9H), 0.561 (q, $J = 8.9$ Hz, 6H); ^{13}C NMR (174 MHz, CDCl_3): δ 112.6, 39.8, 38.3, 34.3, 31.6, 26.90, 26.89, 26.3, 7.7, 3.3; IR (thin film): ν 2922.1, 1259.9, 1088.6, 799.9 cm^{-1} ; HRMS (EI^+) (m/z): $[\text{M}]^+$ calc for $\text{C}_{15}\text{H}_{29}\text{DSi}$, 239.2180; found, 239.2185.

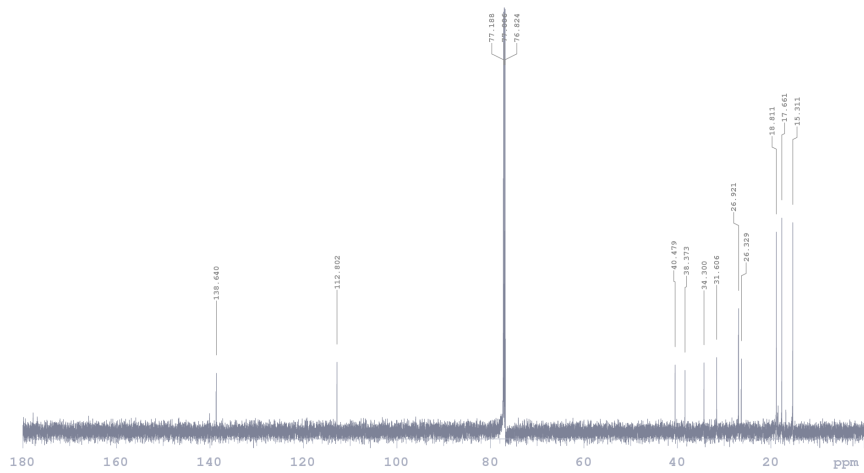
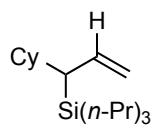
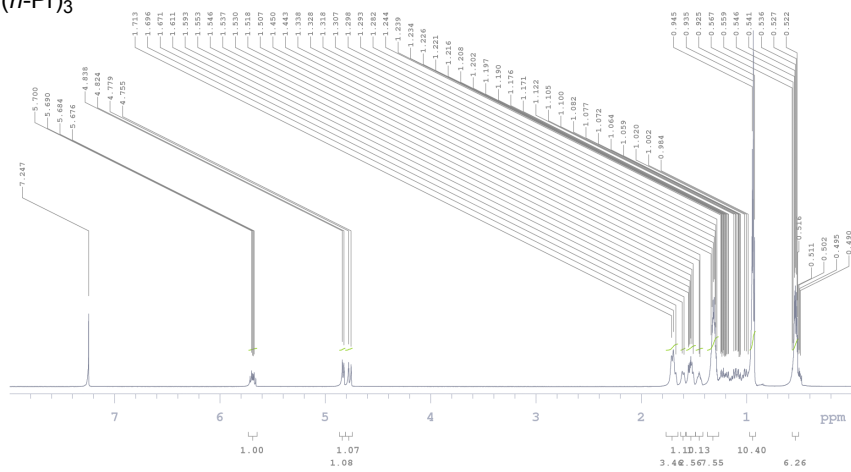
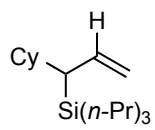
(1-Cyclohexylallyl)tripropylsilane (2-61) (Scheme 2-16)



General procedure II was followed with Pd_2dba_3 (13.7 mg, 0.015 mmol), $\text{IMes}\cdot\text{HCl}$ salt **2-35** (10.2 mg, 0.03 mmol), $t\text{-BuOK}$ (3.4 mg, 0.03 mmol), triethylsilane (48 μL , 0.3 mmol), and cyclohexylallene (36.6 mg, 0.3 mmol). The crude residue was purified by flash chromatography (100% hexanes) affording a clear oil (49 mg, 58.56 % yield). ^1H NMR (700 MHz, CDCl_3): 5.69 (dt, $J = 17.2, 9.5$ Hz, 1H), 4.83 (dd, $J = 10.5, 2.7$ Hz, 1H), 4.77 (dd, $J = 17.2, 2.3$ Hz, 1H), 1.66 (m, 3H), 1.58 - 1.60 (m, 1H), 1.50 – 1.57 (m, 3H), 1.41 – 1.48 (m, 1H), 1.27 – 1.37 (m, 6H), 1.00 – 1.22 (m, 1H), 0.935 (t, $J = 8.0$ Hz, 9H), 0.513 – 0.569 (m, 6H); ^{13}C NMR (175 MHz, CDCl_3): 138.6, 112.8, 40.5, 38.4, 34.3, 31.6, 26.9, 26.3, 18.8, 17.7, 15.3; IR (thin film): ν 3073.1, 2954.5, 2924.1, 2867.7, 2661.8, 1623.3, 1450.1, 1331.9, 1203.2, 1067.5, 998.8, 894.7, 740.4 cm^{-1} ; HRMS (EI^+) (m/z): $[\text{M}]^+$ calc for $\text{C}_{18}\text{H}_{36}\text{Si}$, 280.2586; found, 280.2588.

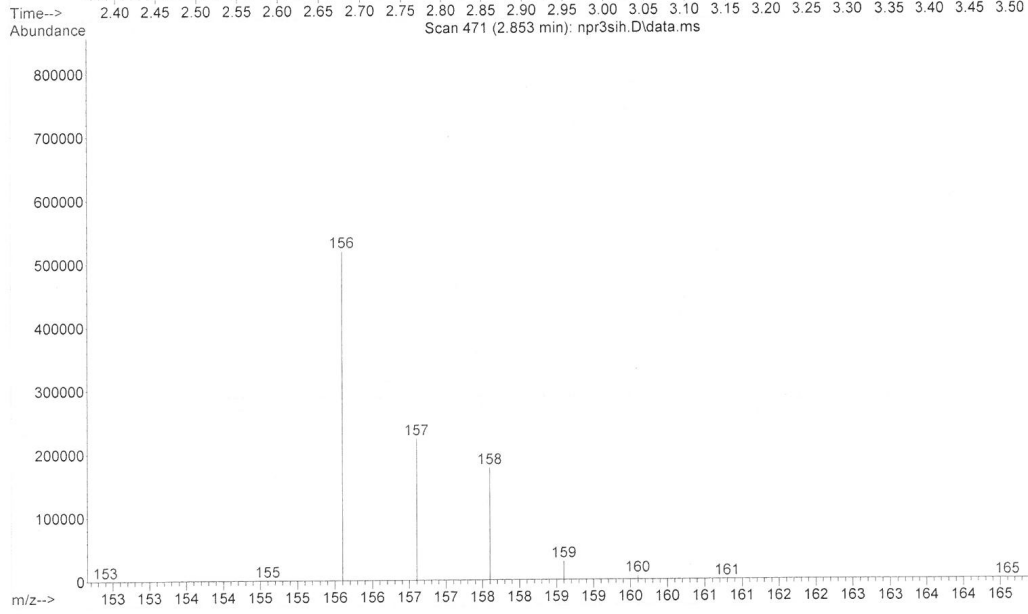
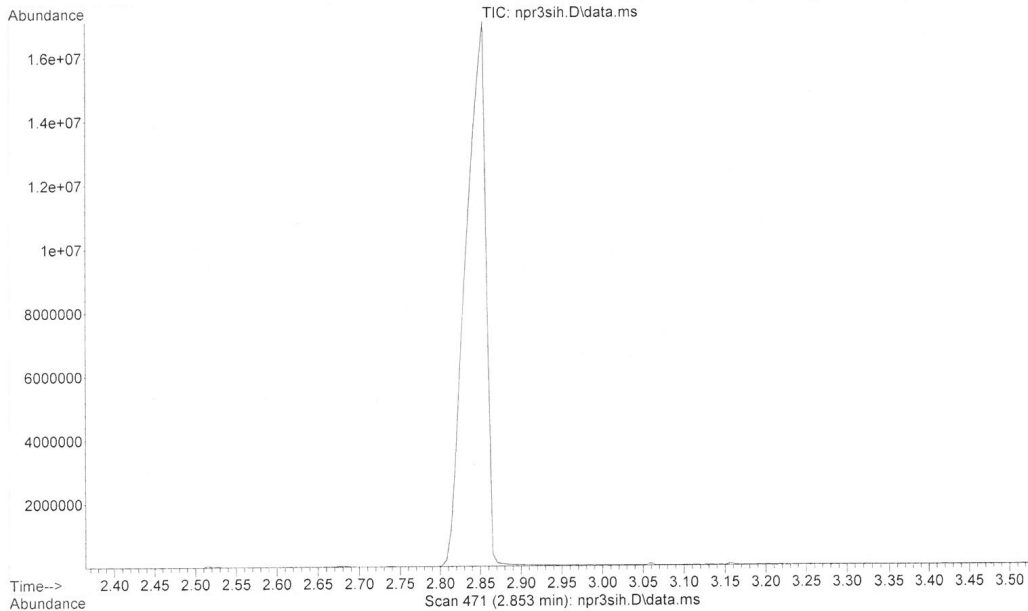






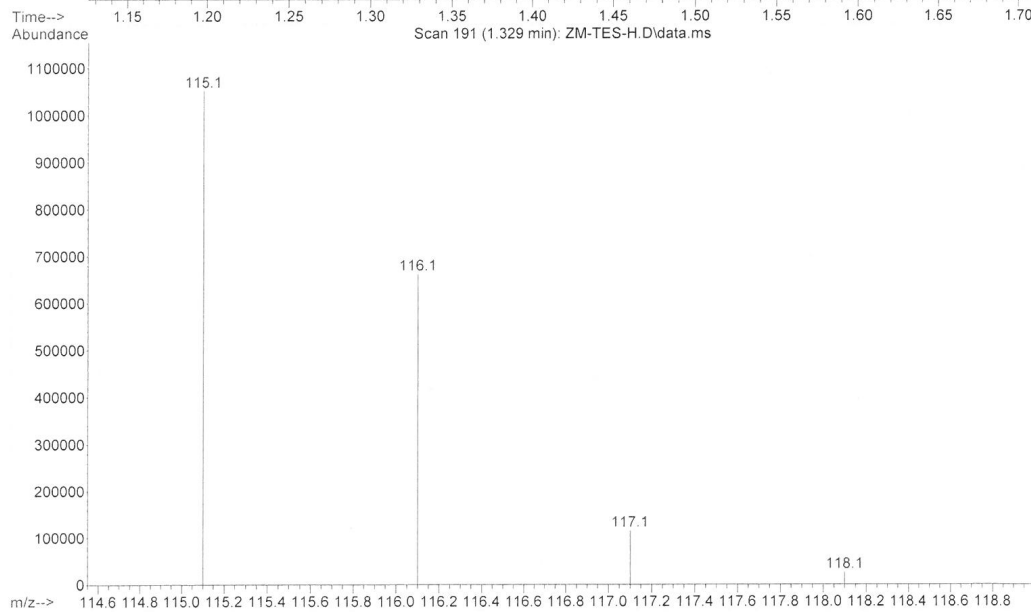
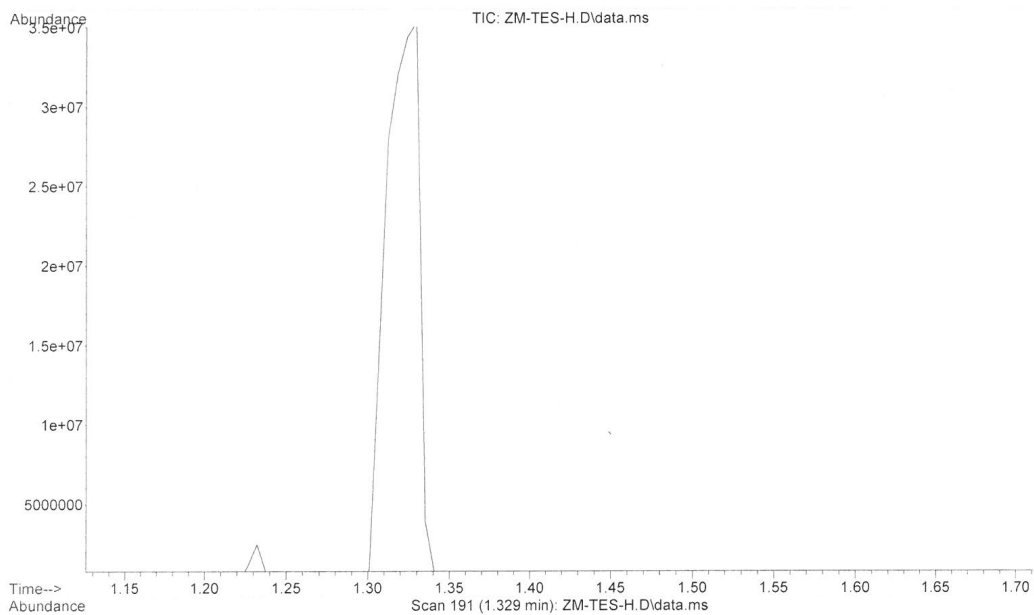
***n*-Pr₃SiH authentic standard:**

File : C:\msdchem\1\DATA\Zach\npr3sih.D
Operator : zm
Acquired : 18 Mar 2015 12:27 using AcqMethod RYANRAMP.M
Instrument : GC
Sample Name: pr3sih
Misc Info :
Vial Number: 98



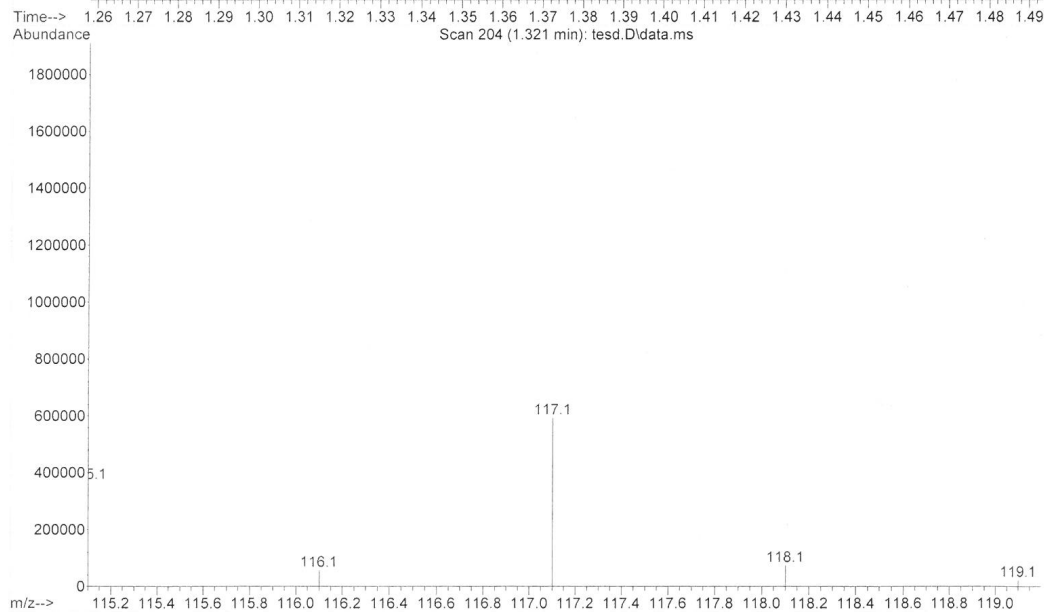
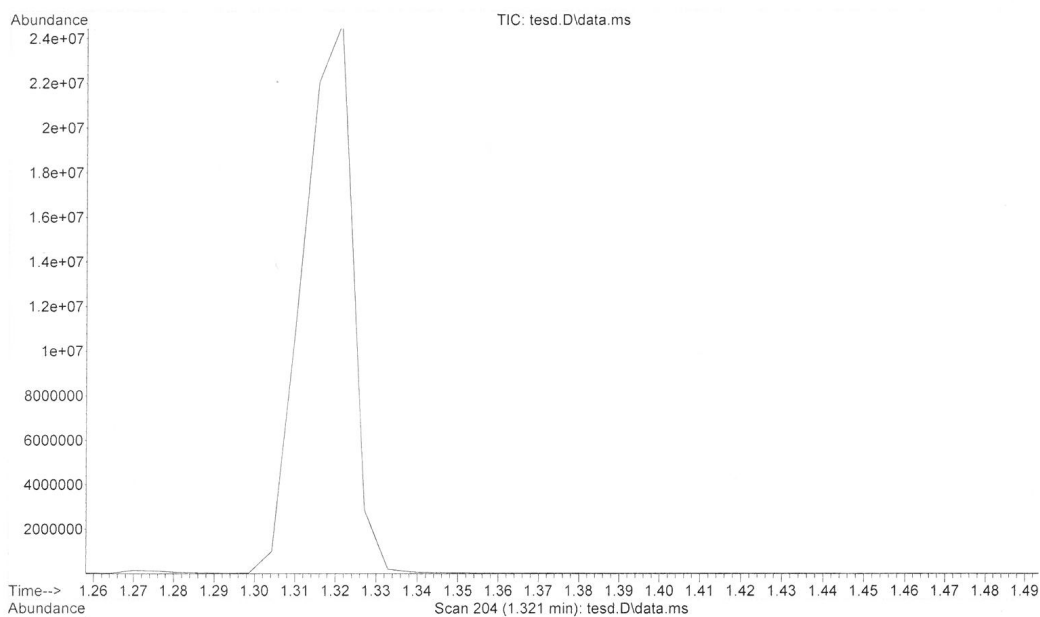
Et₃SiH authentic standard:

File : C:\msdchem\1\DATA\Zach\ZM-TES-H.D
Operator : zm
Acquired : 23 Mar 2015 15:14 using AcqMethod RYANRAMP.M
Instrument : GC
Sample Name: zm-v-tes-h
Misc Info :
Vial Number: 93



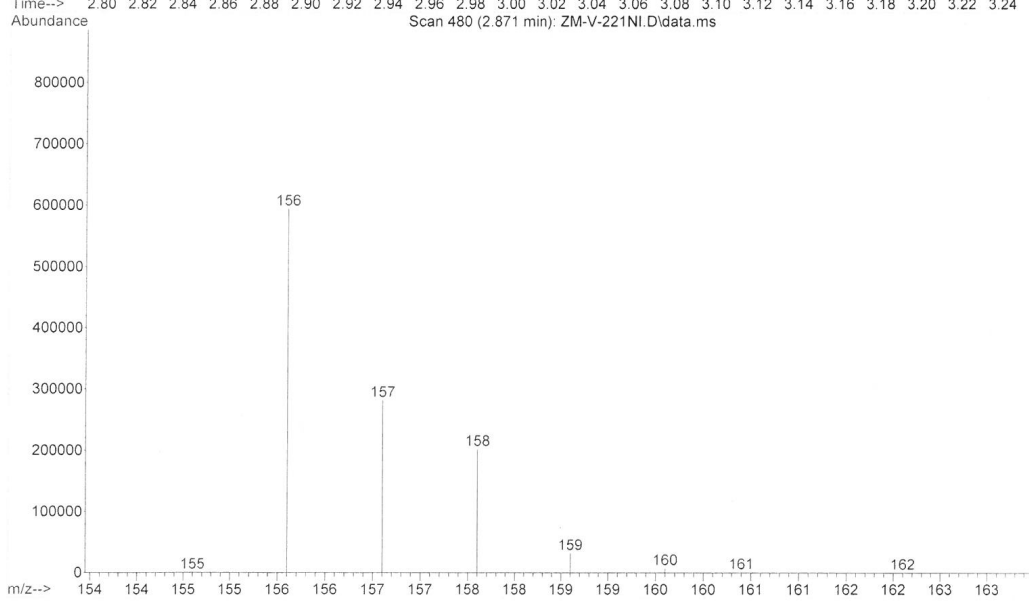
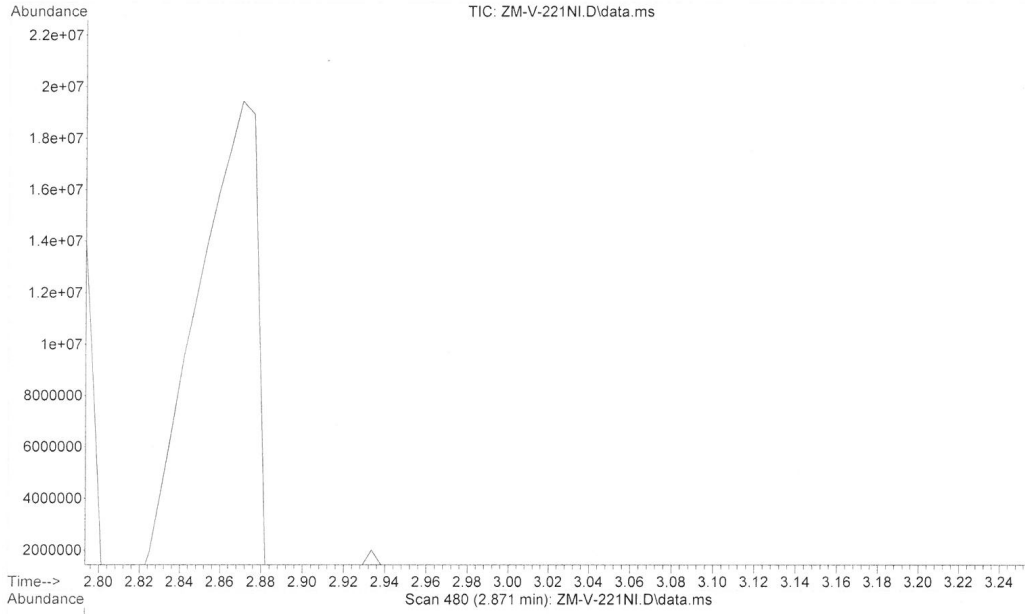
Et₃SiD Authentic Standard:

File : C:\msdchem\1\DATA\Zach\tesd.D
Operator : zm
Acquired : 18 Mar 2015 12:34 using AcqMethod RYANRAMP.M
Instrument : GC
Sample Name: tesd
Misc Info :
Vial Number: 99



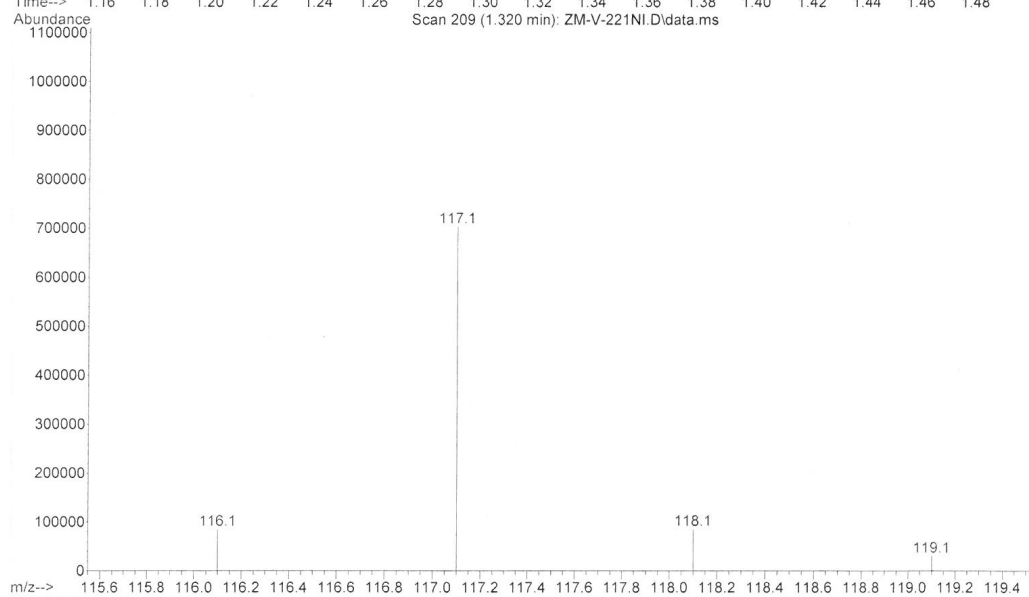
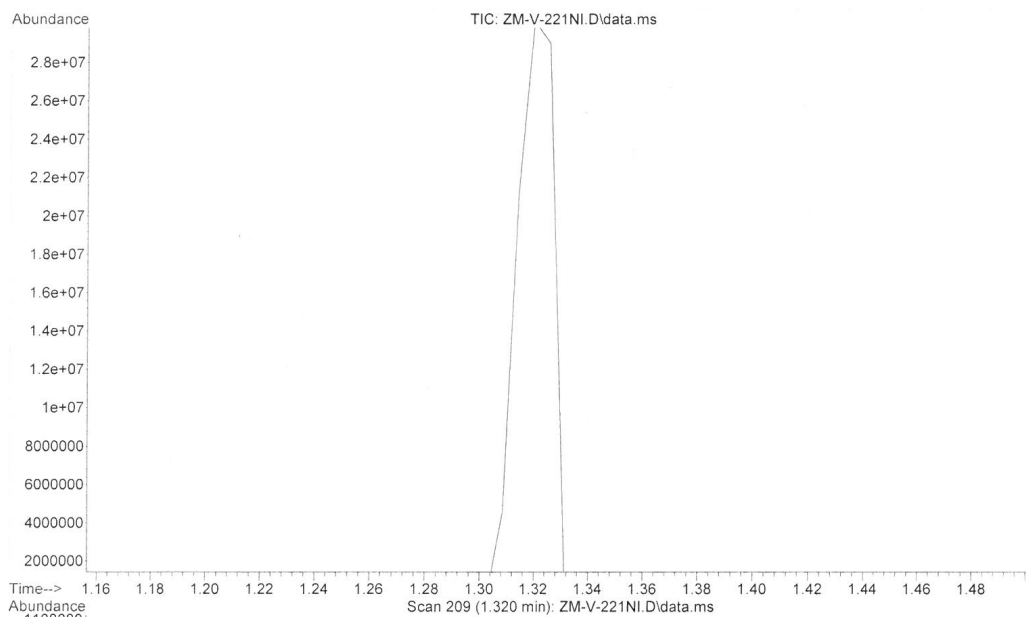
Collected $n\text{-Pr}_3\text{SiX}$ – Nickel Crossover Experiment:

File :C:\msdchem\1\DATA\Zach\ZM-V-221NI.D
Operator : zm
Acquired : 20 Mar 2015 15:42 using AcqMethod RYANRAMP.M
Instrument : GC
Sample Name: ZM-V-221NI
Misc Info :
Vial Number: 75



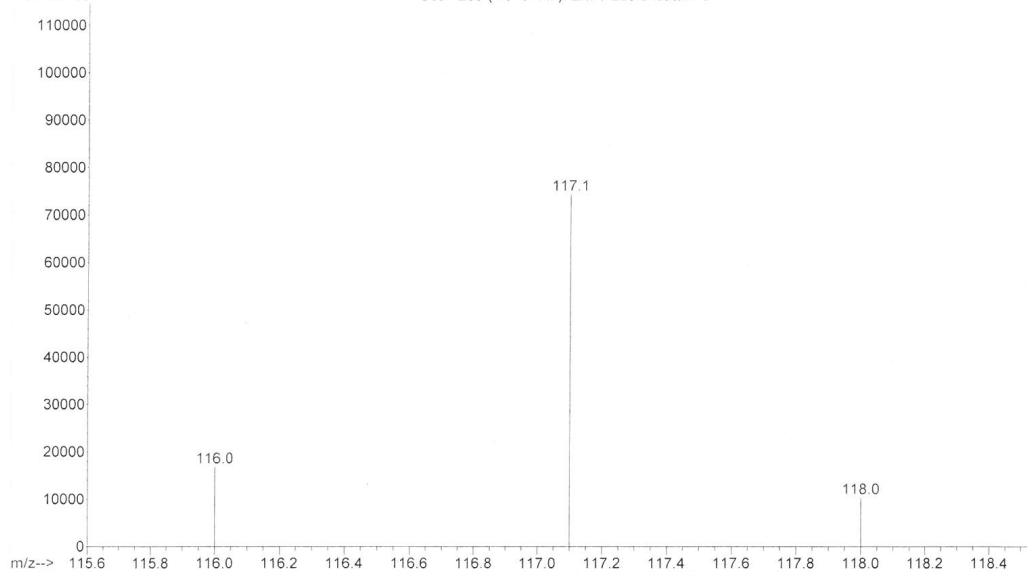
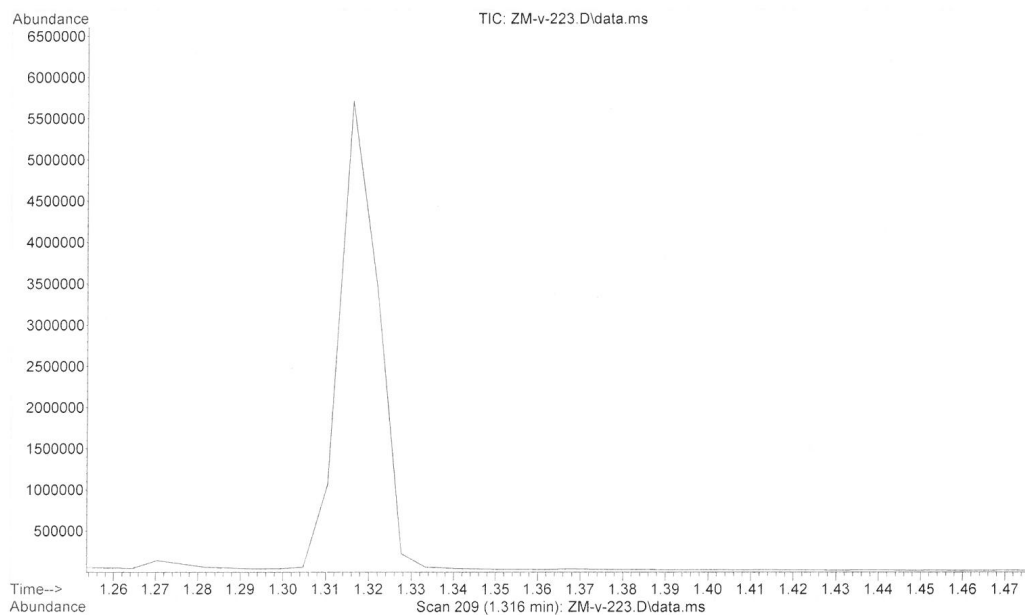
Collected Et₃SiX: Nickel Crossover Experiment:

File :C:\msdchem\1\DATA\Zach\ZM-V-221NI.D
Operator : zm
Acquired : 20 Mar 2015 15:42 using AcqMethod RYANRAMP.M
Instrument : GC
Sample Name: ZM-V-221NI
Misc Info :
Vial Number: 75



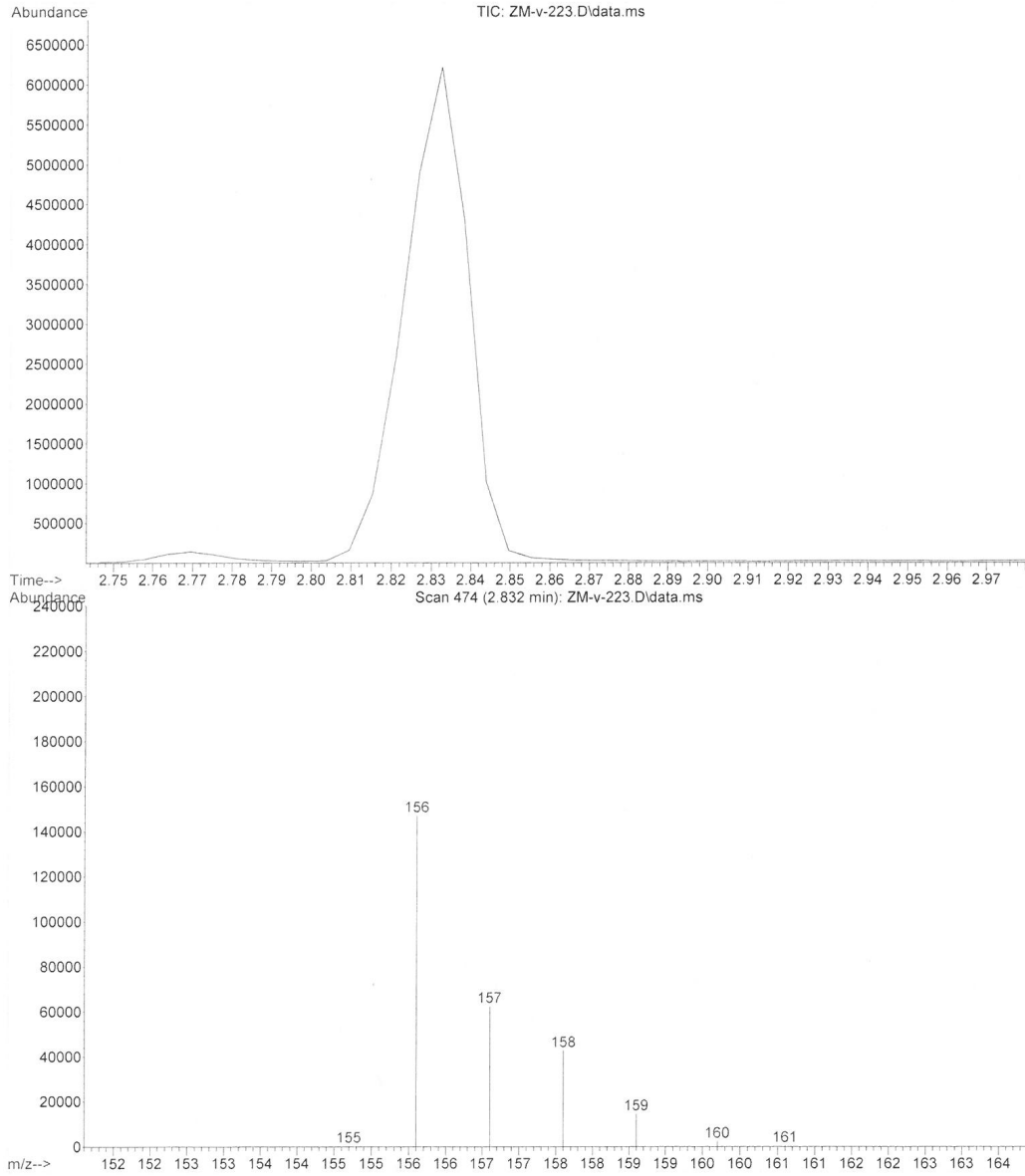
Collected Et₃SiX: Palladium Crossover Experiment:

File :C:\msdchem\1\DATA\Zach\ZM-v-223.D
Operator : ZM
Acquired : 21 Mar 2015 13:33 using AcqMethod RYANRAMP.M
Instrument : GC
Sample Name: ZM-v-223
Misc Info :
Vial Number: 64



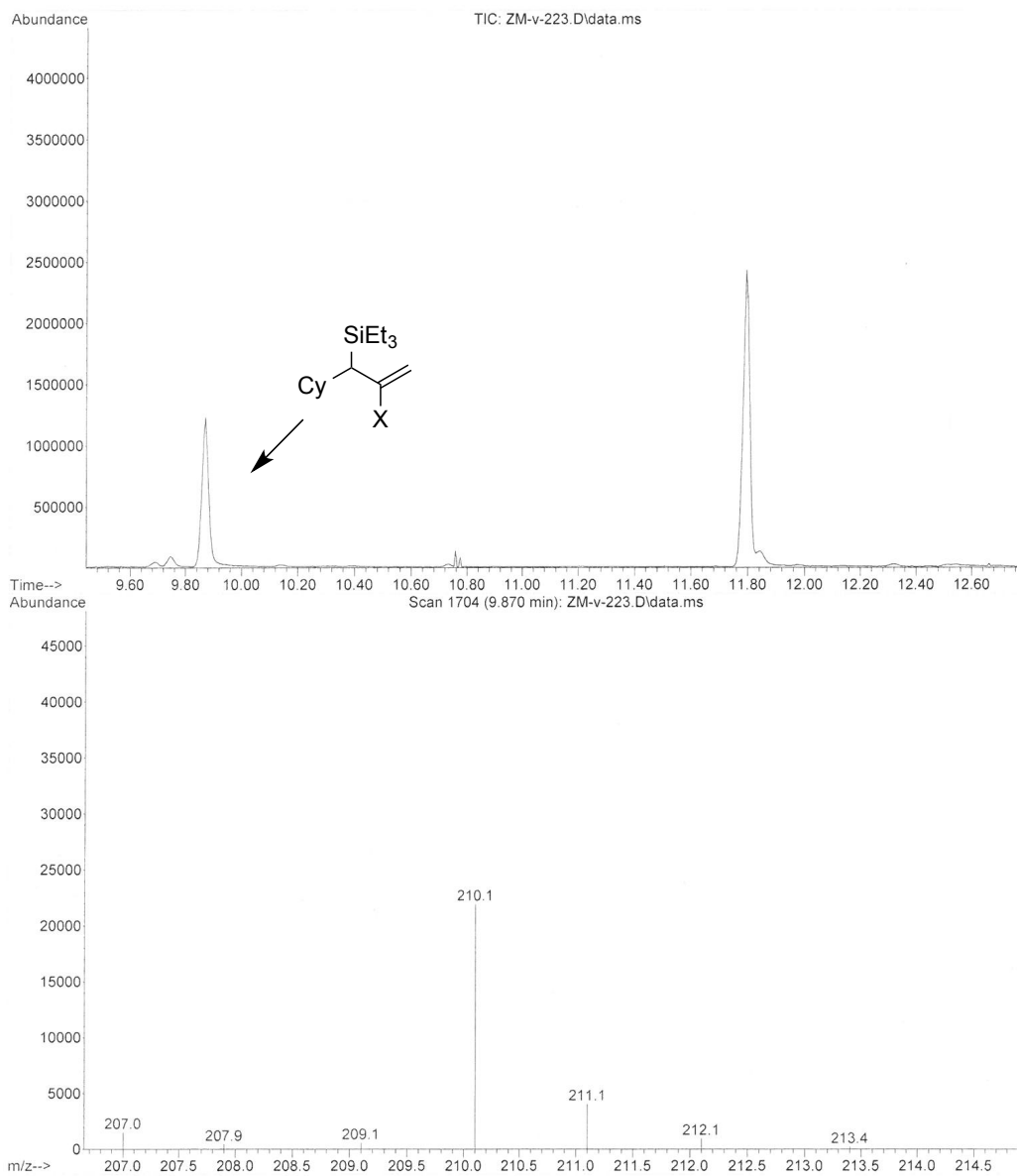
Collected *n*-Pr₃SiX: Palladium Crossover Experiment:

File :C:\msdchem\1\DATA\Zach\ZM-v-223.D
Operator : ZM
Acquired : 21 Mar 2015 13:33 using AcqMethod RYANRAMP.M
Instrument : GC
Sample Name: ZM-v-223
Misc Info :
Vial Number: 64



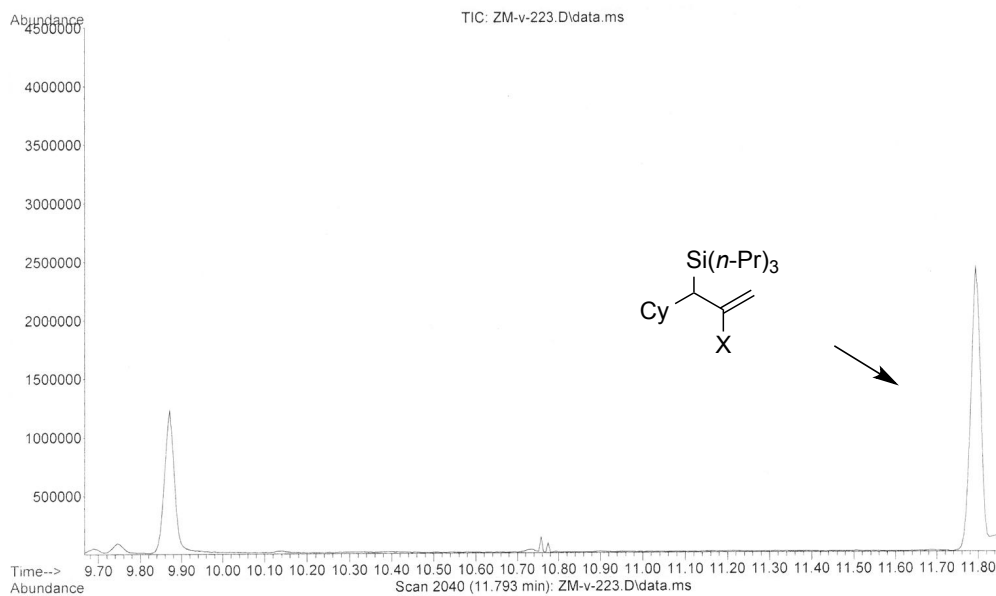
Palladium Crossover Experiment:

File :C:\msdchem\1\DATA\Zach\ZM-v-223.D
Operator : ZM
Acquired : 21 Mar 2015 13:33 using AcqMethod RYANRAMP.M
Instrument : GC
Sample Name: ZM-v-223
Misc Info :
Vial Number: 64



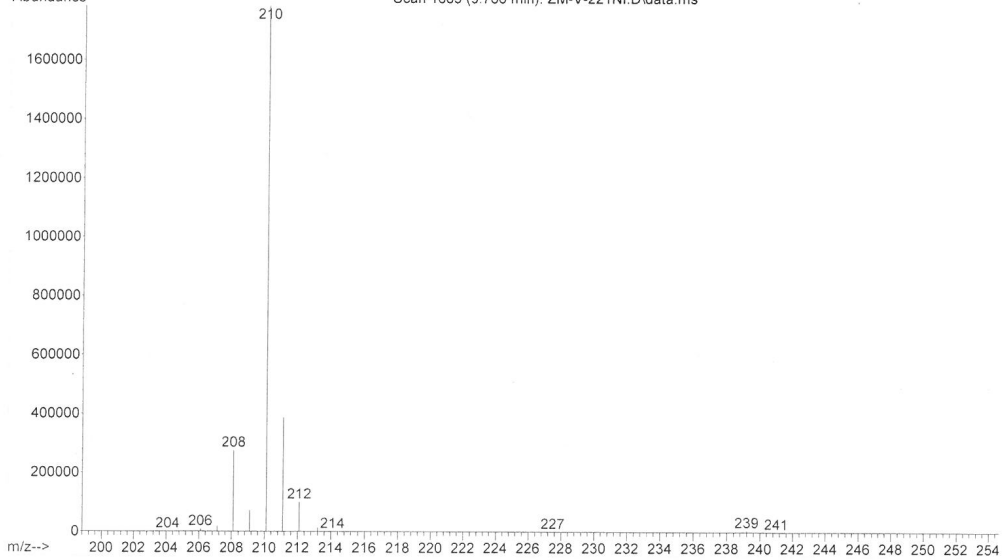
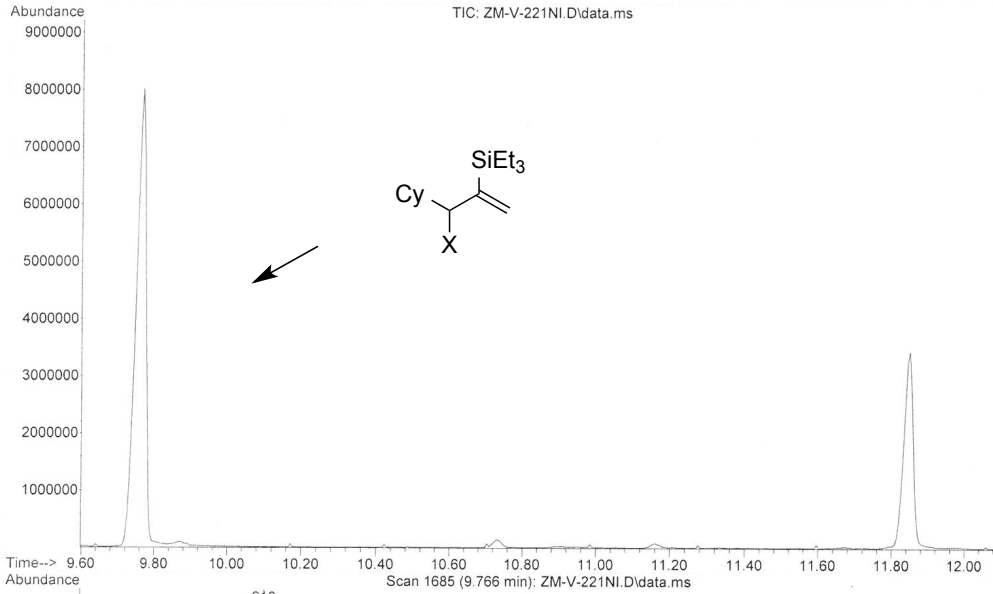
Palladium Crossover Experiment:

File : C:\msdchem\1\DATA\Zach\ZM-v-223.D
Operator : ZM
Acquired : 21 Mar 2015 13:33 using AcqMethod RYANRAMP.M
Instrument : GC
Sample Name: ZM-v-223
Misc Info :
Vial Number: 64



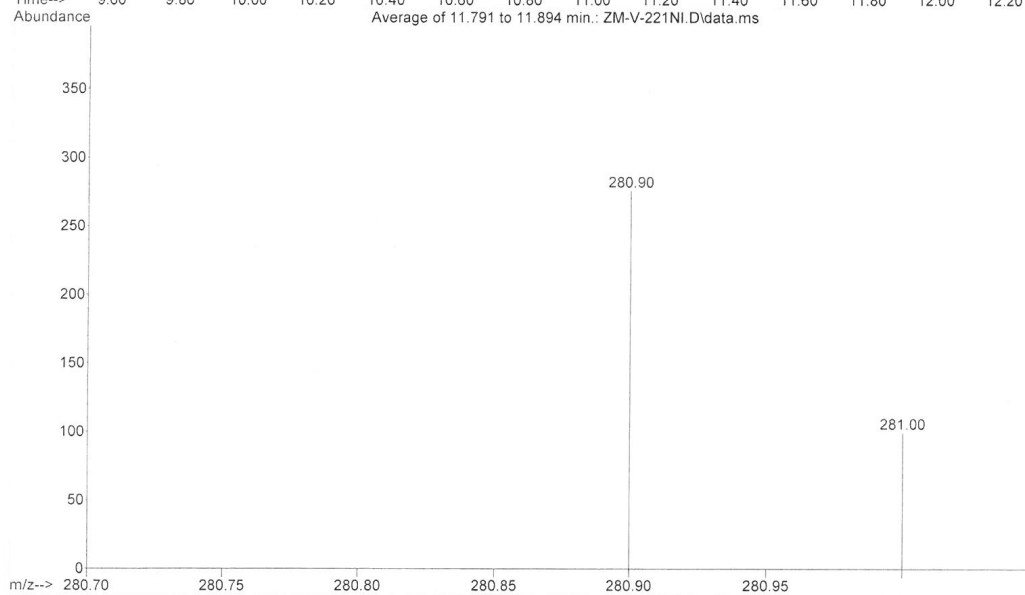
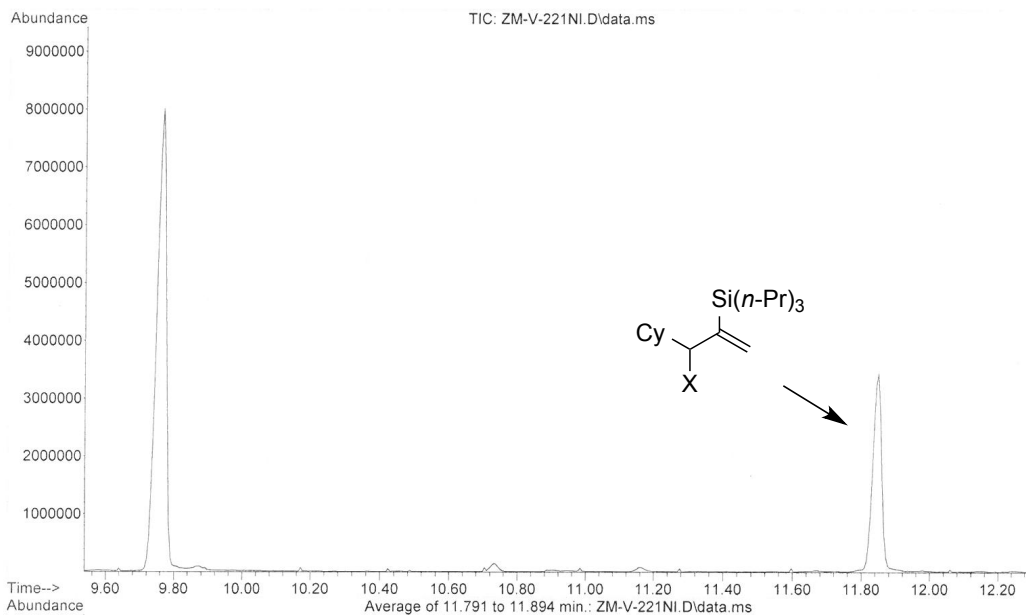
Nickel Crossover Experiment:

File : C:\msdchem\1\DATA\Zach\ZM-V-221NI.D
Operator : zm
Acquired : 20 Mar 2015 15:42 using AcqMethod RYANRAMP.M
Instrument : GC
Sample Name : ZM-V-221NI
Misc Info :
Vial Number : 75



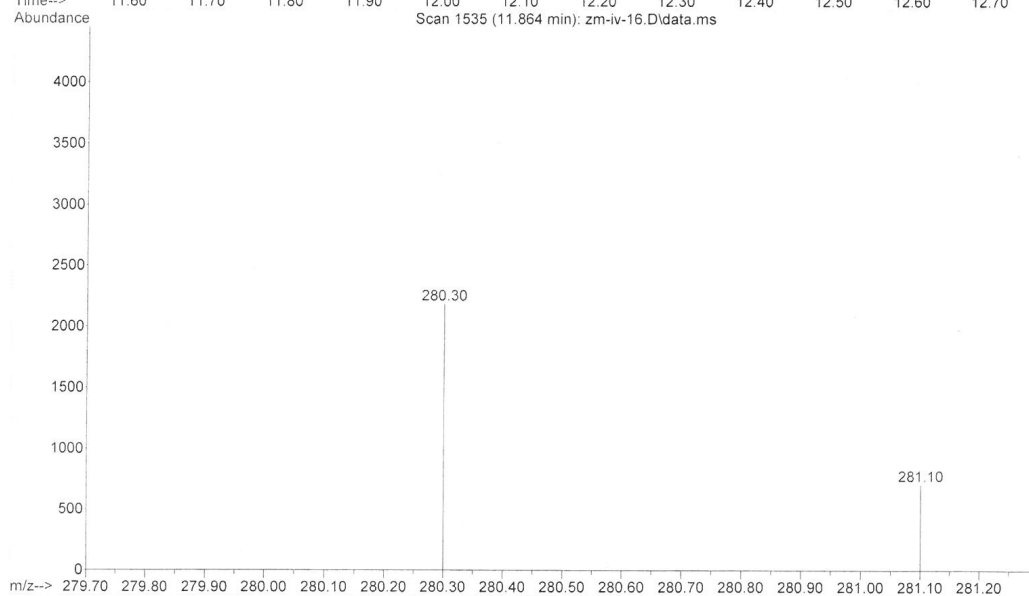
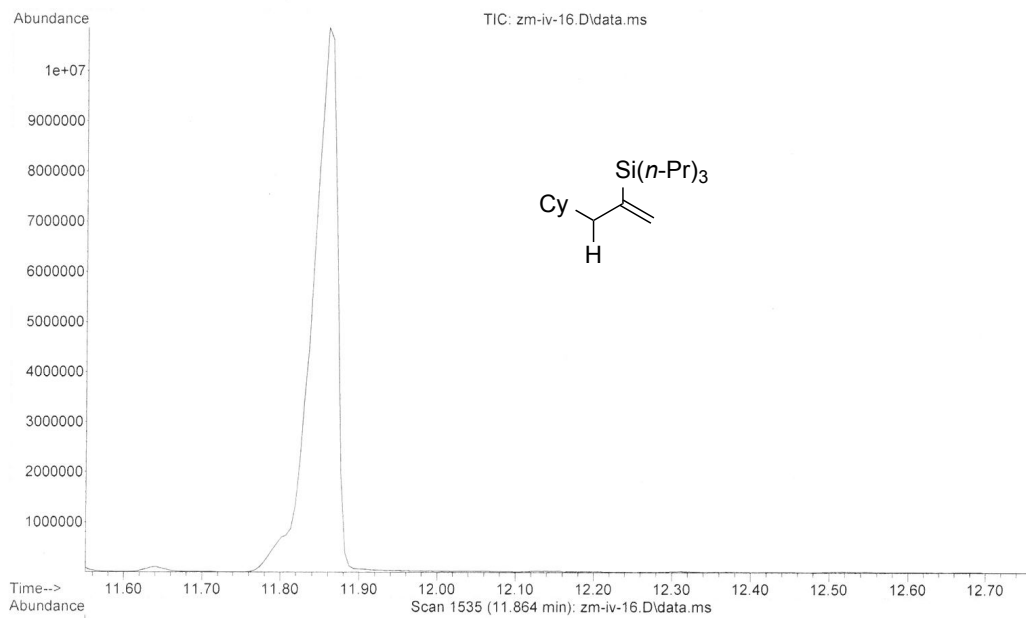
Nickel Crossover Experiment:

File :C:\msdchem\1\DATA\Zach\ZM-V-221NI.D
Operator : zm
Acquired : 20 Mar 2015 15:42 using AcqMethod RYANRAMP.M
Instrument : GC
Sample Name: ZM-V-221NI
Misc Info :
Vial Number: 75

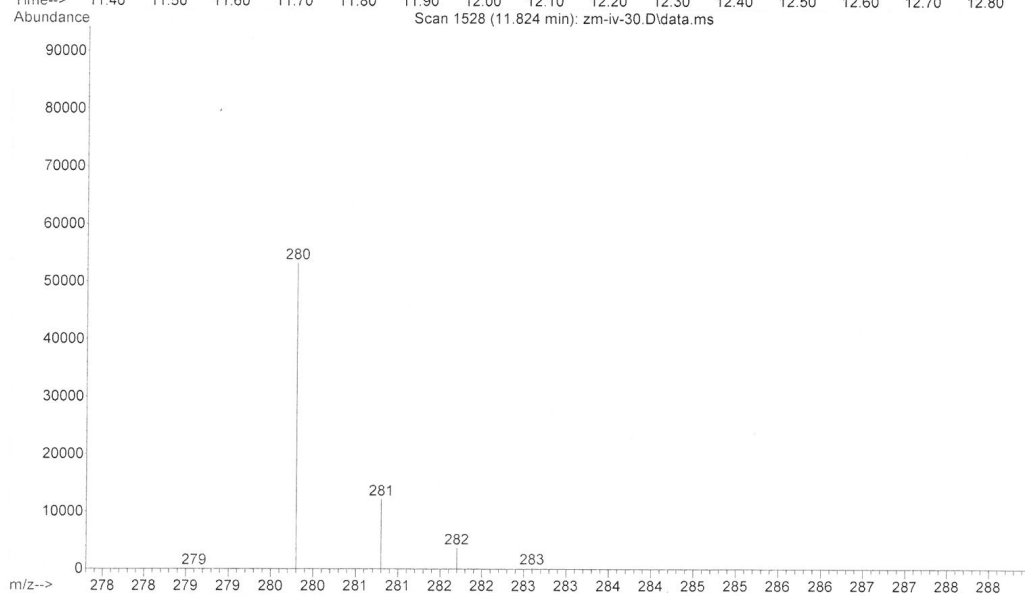
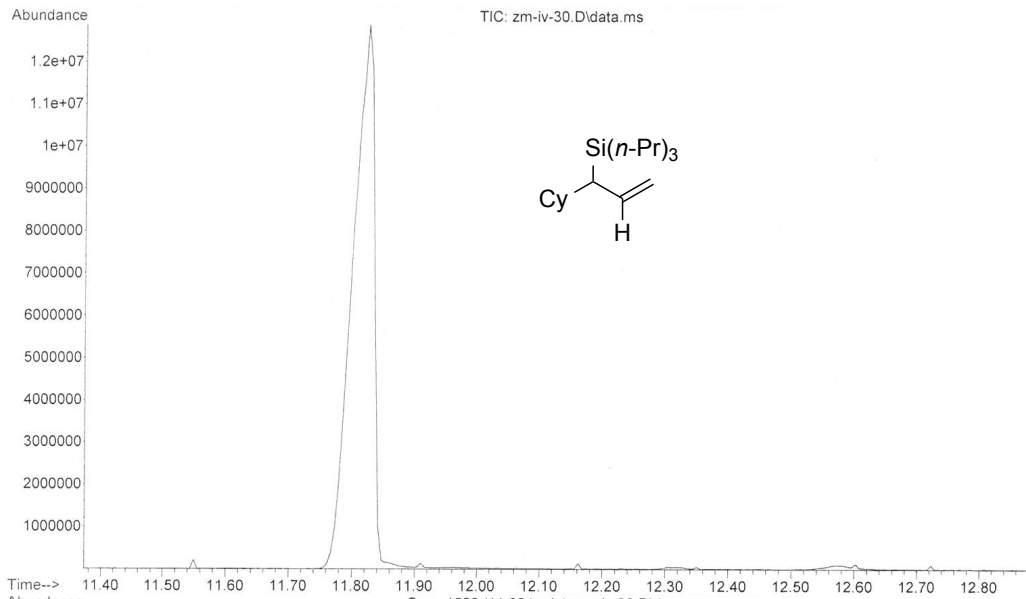


Chromatograms for Authentic Standards:

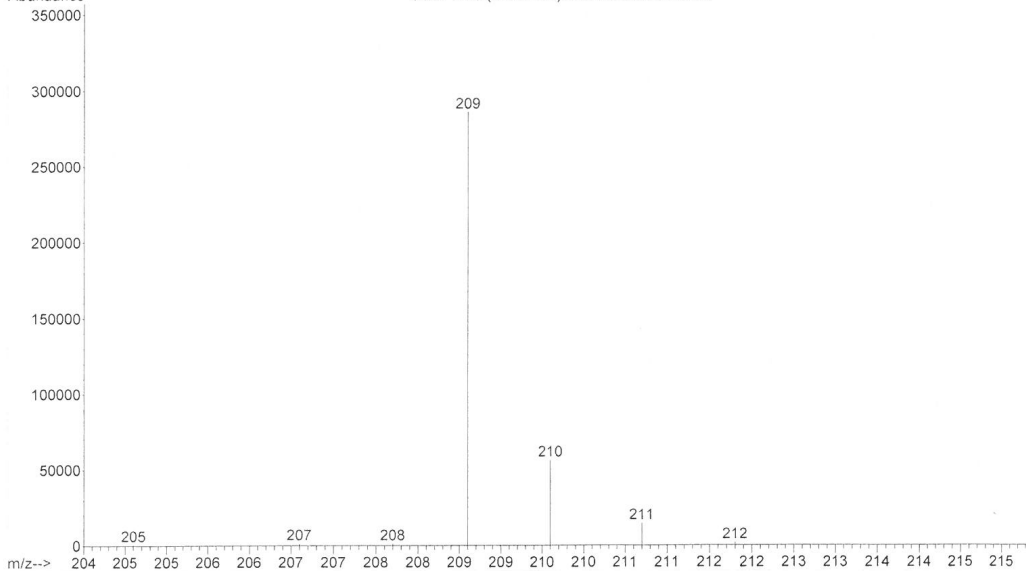
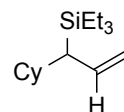
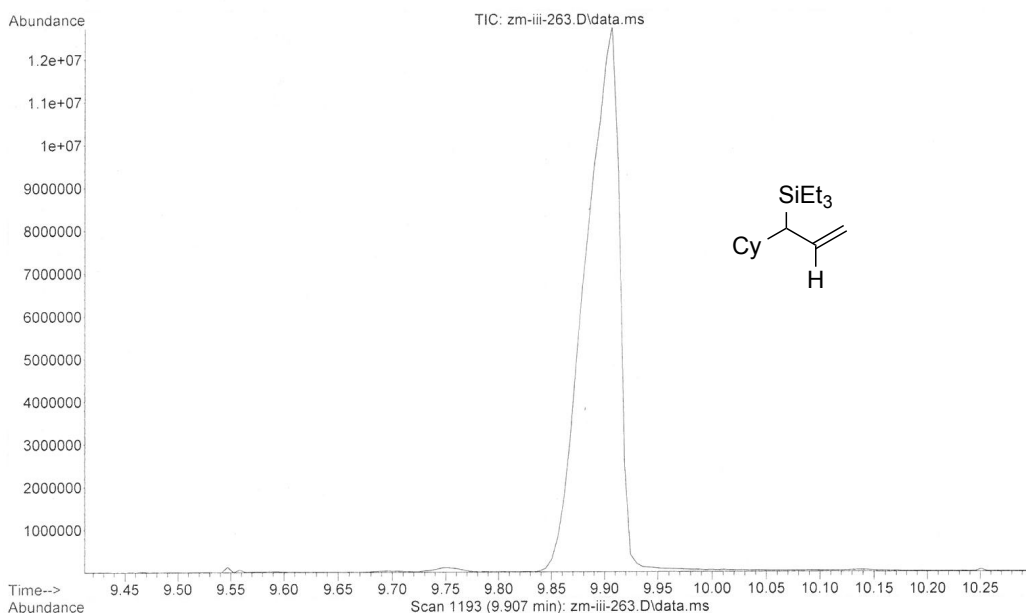
File :C:\msdchem\1\DATA\Zach\zm-iv-16.D
Operator : zm
Acquired : 17 Mar 2015 12:36 using AcqMethod RYANRAMP.M
Instrument : GC
Sample Name: zm-iv-16
Misc Info : vinyl-propylsilane-H
Vial Number: 70



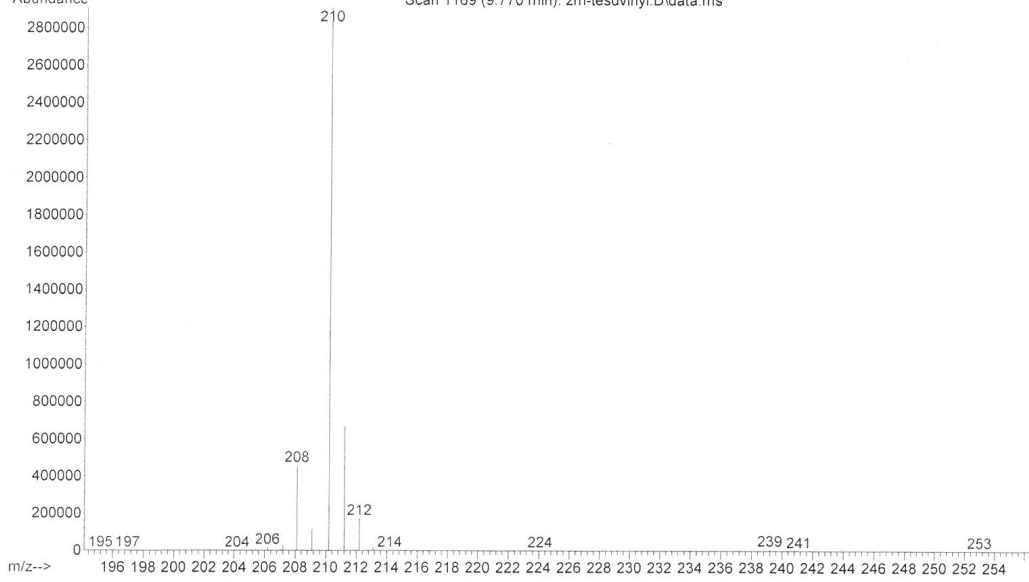
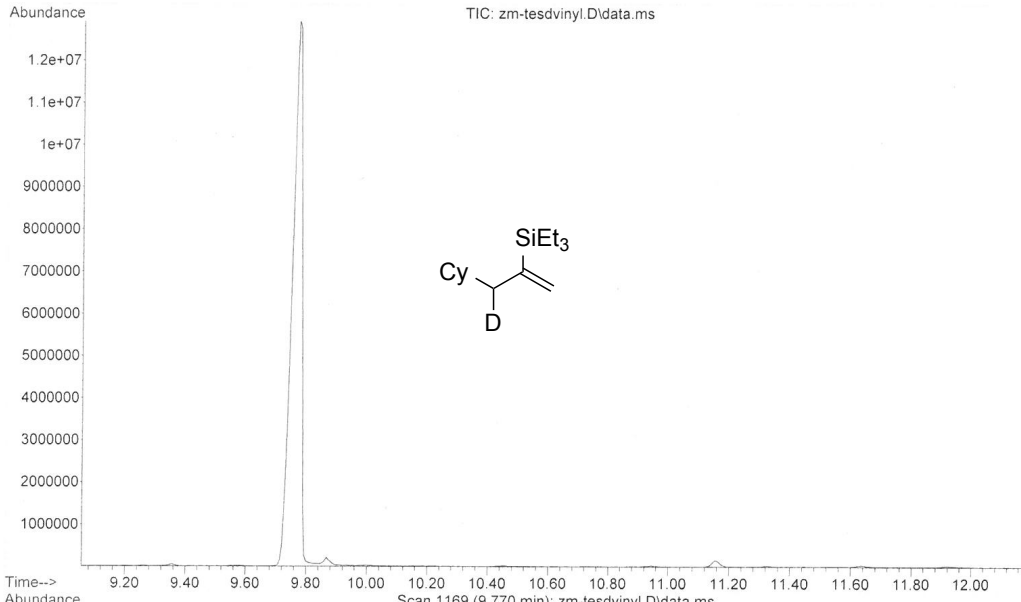
File :C:\msdchem\1\DATA\Zach\zm-iv-30.D
Operator : zm
Acquired : 17 Mar 2015 15:07 using AcqMethod RYANRAMP.M
Instrument : GC
Sample Name: zm-iv-30
Misc Info : allyl-ethylsilane-D
Vial Number: 75



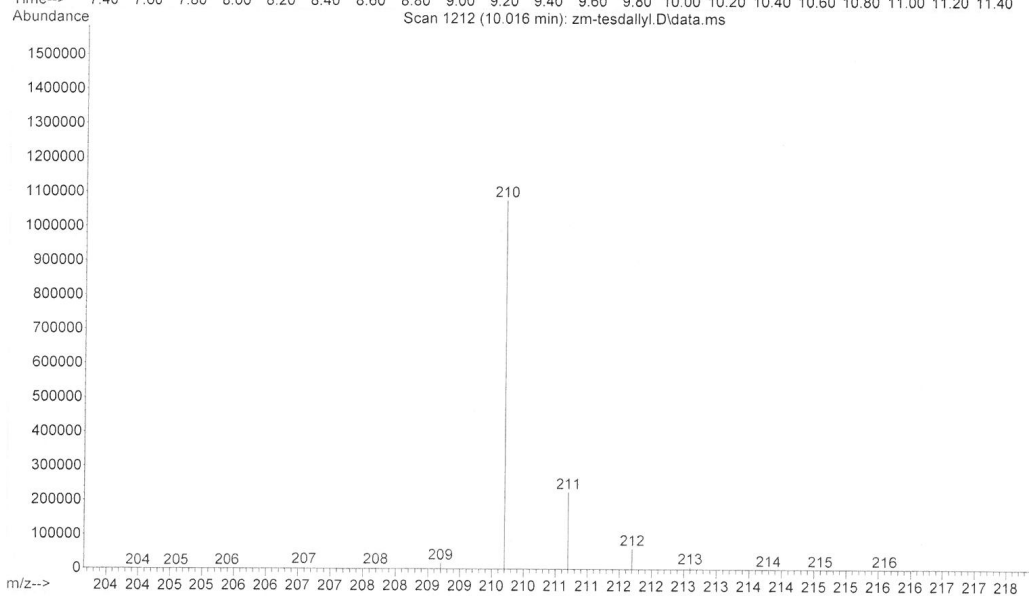
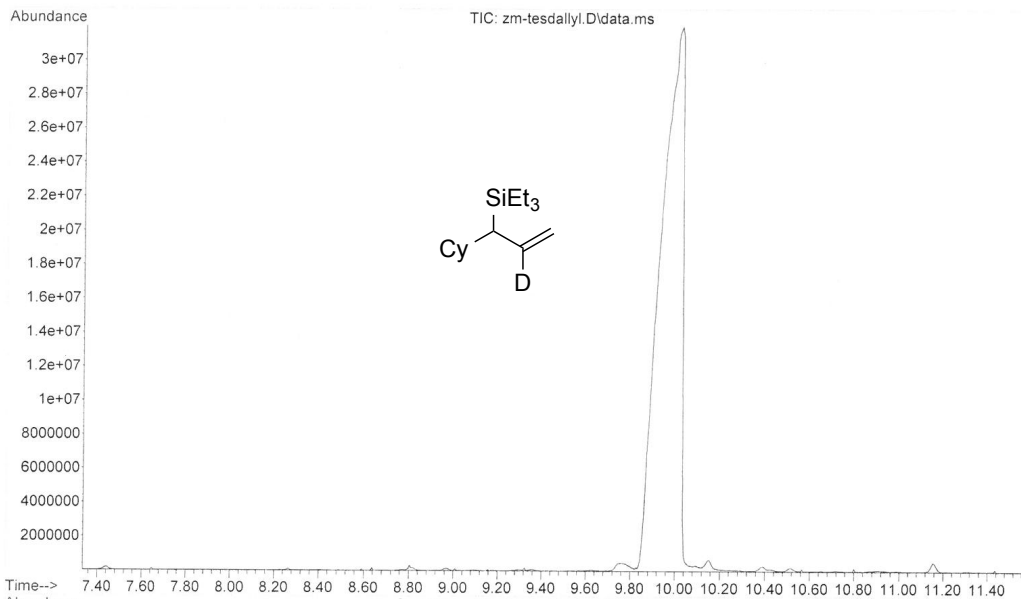
File : C:\msdchem\1\DATA\Zach\zm-iii-263.D
Operator : zm
Acquired : 17 Mar 2015 14:07 using AcqMethod RYANRAMP.M
Instrument : GC
Sample Name: zm-iii-263
Misc Info : allyl-ethylsilane-H
Vial Number: 67



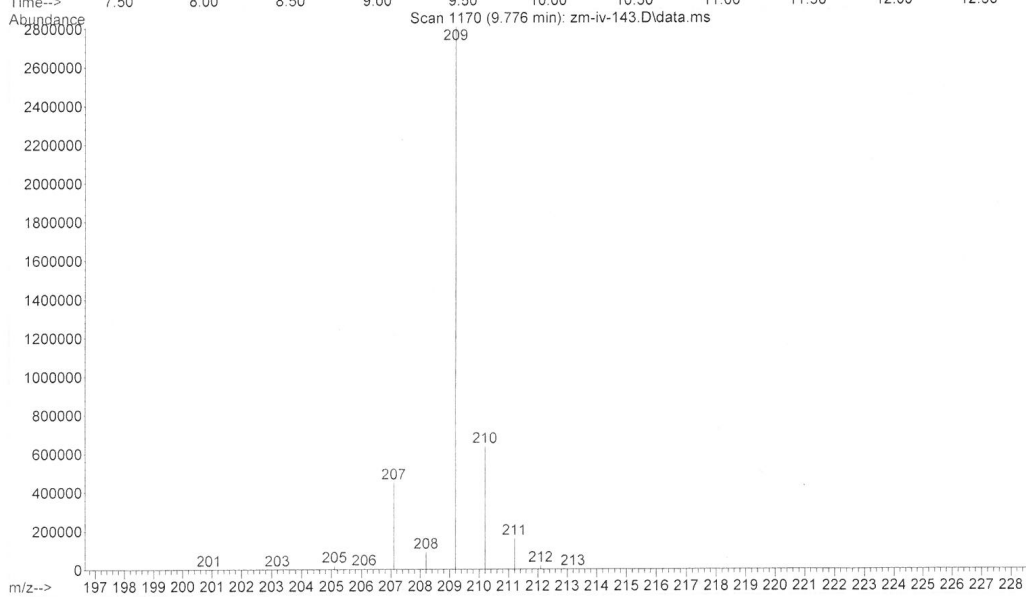
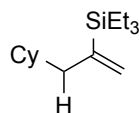
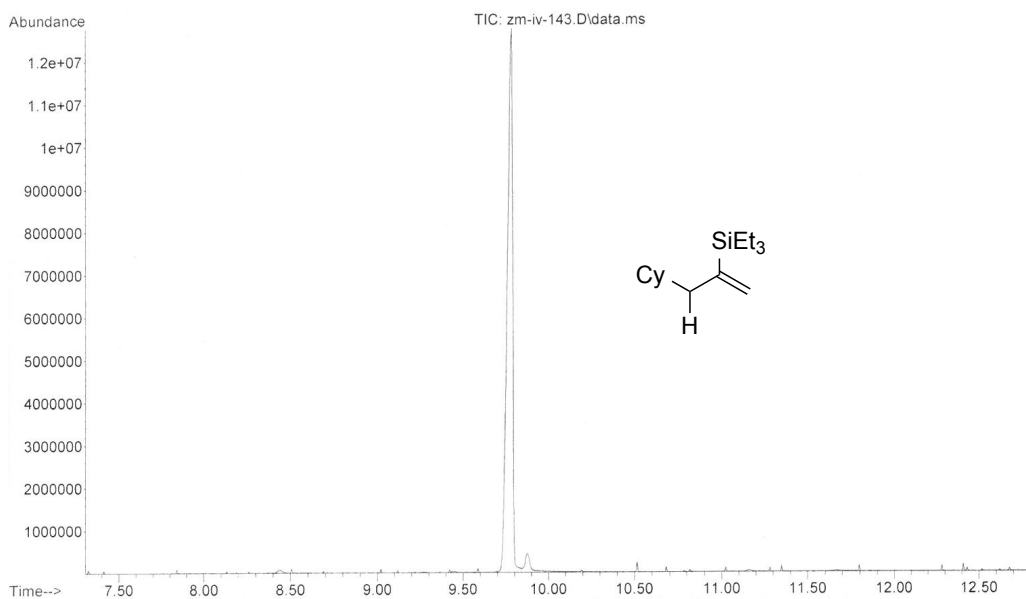
File :C:\msdchem\1\DATA\Zach\zm-tesdvinyl.D
Operator : zm
Acquired : 18 Mar 2015 15:41 using AcqMethod RYANRAMP.M
Instrument : GC
Sample Name: zm-tesdvinyl
Misc Info :
Vial Number: 97



File : C:\msdchem\1\DATA\Zach\zm-tesdallyl.D
Operator : zm
Acquired : 18 Mar 2015 16:11 using AcqMethod RYANRAMP.M
Instrument : GC
Sample Name: zm-tesdallyl
Misc Info :
Vial Number: 96



File :C:\msdchem\1\DATA\Zach\zm-iv-143.D
Operator : zm
Acquired : 17 Mar 2015 13:36 using AcqMethod RYANRAMP.M
Instrument : GC
Sample Name: zm-iv-143
Misc Info : vinyl-ethylsilane-H
Vial Number: 68



Chapter 3

Regioselective Allene Hydroarylation via One-Pot Regioselective Allene Hydrosilylation/ Pd(0)-Catalyzed Cross-Coupling

3.1 Introduction

As part of our interests in developing regioselective catalytic processes, our lab has gained interest in regioselective allene hydrosilylation. Our previous discoveries in this area have demonstrated that regiocontrol can be achieved by selection of metal, where reactions with nickel catalysis form alkenylsilanes and reactions of palladium catalysis form allylsilanes with exceptional regioselectivities. The palladium-based procedure tolerates a variety of silane coupling partners with minimal erosion of regioselectivity while the nickel-based procedure is limited to only trialkylsilanes. As an effort to expand access to a variety of alkenylsilanes useful in cross-coupling and related transformations,³⁶ we expanded our efforts to discovering the reaction conditions with palladium catalysis that would result in a complete regioinversion upon alteration of ligand identity.

As an additional motivation, we were inspired by the possibility of performing regioselective allene hydrosilylation followed in tandem with a Pd(0) cross-coupling reaction to afford hydroarylated products. Performing two catalytic cycles in tandem is a powerful technique for improving efficiency in synthesis.³⁷ Functionalizing a molecule that then undergoes additional manipulations in a one-pot scenario is especially attractive

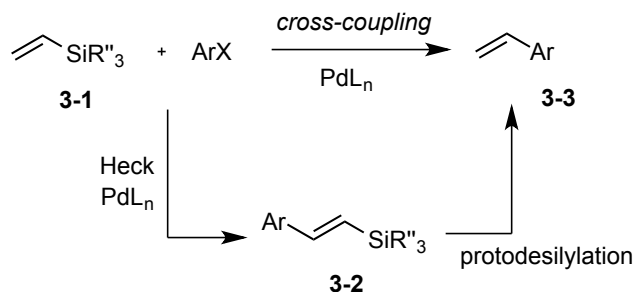
as it removes the necessity to isolate intermediates; streamlining access to important motifs.

3.2 Hiyama-Denmark Cross-Couplings

As a result of the pioneering work independently developed in the labs of Hiyama and Denmark, alkenyl- and allylsilane intermediates have been established as effective nucleophiles in metal-catalyzed cross-coupling chemistry. Compared with other nucleophiles in related cross-coupling procedures, these intermediates are generally of low toxicity, derived from relatively cheap precursors, and are typically stable to isolation and storage.³⁸

The mechanisms for the silicon-based cross-coupling reaction vary depending on the catalyst system, mode of activation, and silyl group. Although allylsilanes are also useful in these protocols, this topic of this chapter will focus on the cross-couplings of alkenylsilanes due to the importance of sp^2 - sp^2 C-C bond-forming. At the time of the first reports of vinylsilane cross-couplings, the mechanisms were not well-studied. In fact, many of the first reports were later found to undergo a coupling reaction analogous to the Heck reaction,³⁹ not via a direct transmetalation mechanism with the silyl group (Scheme 3-1).²

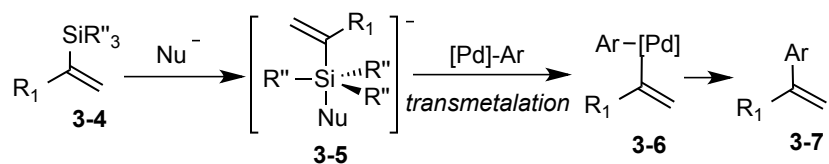
Scheme 3-1 Heck-Type Cross-Couplings of Alkenylsilanes



In this reaction, a palladium catalyst undergoes oxidative addition to an aryl halide and then migratory insertion with vinylsilane **3-1** and subsequent β -hydride elimination affords **3-2**. Subsequent protodesilylation of the *E*-alkenylsilane affords vinylarene product **3-3** with the regiochemistry that would falsely imply a direct cross-coupling at the silyl group.

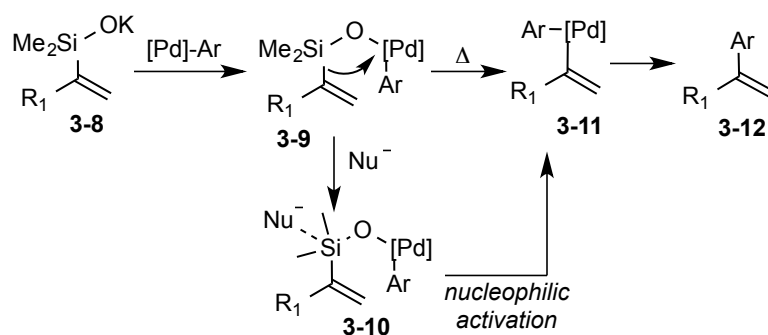
For reactions that actually undergo direct cross-coupling with the silyl group, there are currently two accepted mode of activation for the transmetalation. The most commonly employed methods utilize a nucleophile, such as anionic fluoride (TBAF), to activate the silane affording pentacoordinate species **3-5** (Scheme 3-2).

Scheme 3-2 Pentacoordinate Silicon in Cross-Coupling Reactions



This activated intermediate then undergoes transmetalation to afford **3-6** and reductive elimination furnishes vinylarene **3-7**. The 1,1-substitution of the product demonstrates that the C-C bond-forming step does not involve a Heck reaction since linear *E*-alkenes form in Heck reactions with the majority of 1-alkene substrates. One drawback to this procedure is use of a corrosive nucleophile (i.e. TBAF) can often simultaneously remove silyl-protective groups. As a result of the challenges presented by this, Denmark and coworkers have extensively developed mild methods for activation through the use of potassium silanoate salts that are activated through the treatment of silanols with strong bases (i.e. KH) (Scheme 3-3).⁴¹

Scheme 3-3 Cross-Couplings of Silanoate Salts



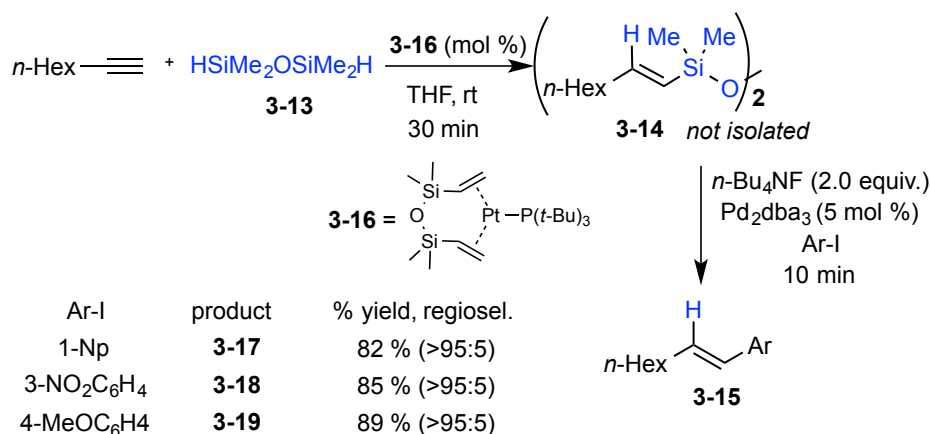
Upon transmetalation, intermediate **3-9** rearranges with heat to afford **3-11**, which reductively eliminates to afford **3-12**. It has been discovered that use of a nucleophile (i.e. TBAF, or TMSOK) in conjunction with a silanoate salt dramatically increases the rate of transmetalation and therefore decreases overall reaction time.⁴¹

Although numerous advances have been made in the mild activation of silane cross-coupling partners, a remaining challenge is gaining access to regio- and stereodefined alkenyl and allylsilanes for use in this class of transformations and related procedures. Improving the efficiency in access to a variety of alkenylsilanes not readily available by other methods would therefore be a significant accomplishment and practical handle for cross-coupling protocols.

3.3 One-Pot Hydroarylation Procedures Involving Hydrosilylation/ Cross-Coupling

Although there are numerous alkyne hydroarylation protocols with boron and tin, there are relatively scarce reports of one-pot hydrosilylation/ cross-coupling reactions. For example, Denmark and coworkers reported a hydroarylation protocol that involves the hydrosilylation of alkynes with silane **3-13** to regioselectively afford linear dimer **3-14** (Scheme 3-4).⁴²

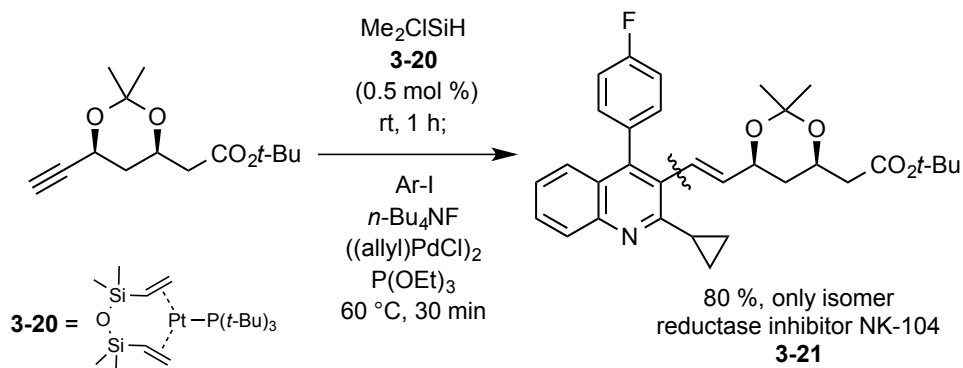
Scheme 3-4 One-Pot Hydrosilylation/Cross-Coupling Protocol



Subsequent activation with TBAF and treatment with an aryliodide results in rapid cross-coupling to afford linear arylated product **3-15** with excellent retention of regio- and stereochemistry. It was found that this procedure was general for a variety of aryliodide coupling partners to afford *E*-alkene isomers with extended aromatics (**3-17**), electron withdrawing groups (**3-18**) and electron-donating groups (**3-19**).

Hiyama and coworkers also demonstrated that one-pot hydroarylation procedures employing tandem hydrosilylation/ cross-coupling protocols were effective in access to reductase inhibitor NK-104 (**3-21**) (Scheme 3-5).⁴³

Scheme 3-5 One-Pot Hydrosilylation/ Cross-Coupling in Total Synthesis



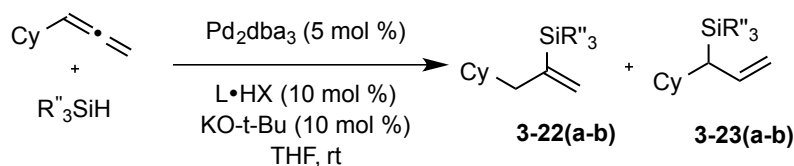
Through the use of Pt/monodentate phosphine complex **3-20**, the hydrosilylation reaction occurs to favor the 1,2-addition product that upon activation with TBAF can be coupled with an aryl iodide to establish the core of the natural product in one-step.

As discussed, hydroarylation one-pot hydrosilylation/cross-coupling protocols typically favor 1,2-addition to alkynes favoring linear scaffolds. Other hydrosilylation protocols in access to 1,1-disubstituted functionalized alkenes require subsequent isolation and purification steps followed by a separate cross-coupling reaction. Therefore, development of a one-pot allene hydroarylation protocol in access to 1,1-disubstituted branched alkenes would streamline access to this reagent class.

3.4 NHC Ligand Evaluation with Pd(0) Precatalyst

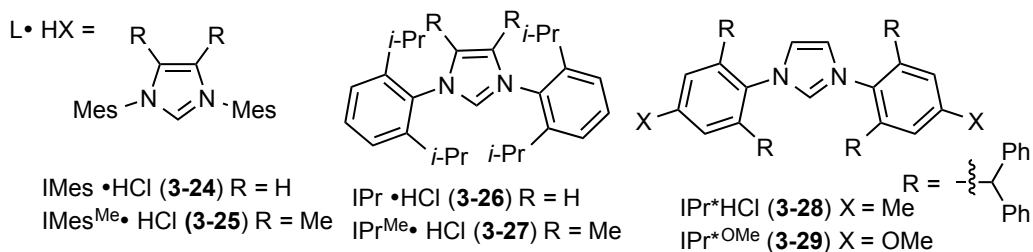
Our efforts to identify the conditions that favor alkenylsilanes in palladium-catalyzed allene hydrosilylation began with an evaluation of the effects of structural modification of NHC ligands on reaction outcome. To facilitate rapid screening, we utilized a protocol where the active catalyst is formed by the deprotonation of the NHC hydrochloride salt with an equivalent of KO-*t*-Bu base and Pd₂dba₃ precatalyst (Table 4). Our preliminary experiments resulted in the observation that methyl substitution of the backbone of *N*-mesityl ligands resulted in a slight erosion of regioselectivity, with allylsilanes strongly preferred in analogy with our prior findings.⁴⁴ For example, the hydrosilylation of cyclohexylallene with triethylsilane using IMes (**3-24**) as a ligand resulted in excellent regioselectivities (>98:2) favoring allylsilane **3-23a**, while use of IMes^{Me} (**3-25**) as a ligand proceeded with slightly decreased regioselectivity (98:2) in an excellent chemical yield of 85% (Table 4, entries 1 and 2). The effects of NHC ligand variation were further explored with bulkier ligands (Table 4, entries 3– 5).

Table 4 Evaluation of NHC Ligands Effects



entry	silane	L•HX	major product (% yield)	regioselectivity (3-22:3-23)
1	Et ₃ SiH	3-24	3-23a (80)	<2:>98
2	Et ₃ SiH	3-25	3-23a (85)	2:98
3	Et ₃ SiH	3-26	3-23a (75)	12:88
4	Et ₃ SiH	3-27	3-22a (83)	>98:2
5	Et ₃ SiH	3-28	3-22a (50)	>98:2
6	Et ₃ SiH	3-29^a	3-22a (90)	>98:2
7	BnMe ₂ SiH	3-26	3-23b (77)	3:97
8	BnMe ₂ SiH	3-27	3-22b (73)	75:25 ^b
9	BnMe ₂ SiH	3-28	3-22b (62)	81:19
10	BnMe ₂ SiH	3-29^a	3-22b (79)	95:5

^a Reaction conducted in absence of KO-*t*-Bu. ^b Reaction conducted with 2.5 mol % Pd₂dba₃ and 5.0 mol % ligand.



The reaction with the comparatively large IPr (**3-26**) as the ligand still resulted in the allylsilane **3-23a** as the major product with triethylsilane in 88:12 regioselectivity (Table 4, entry 3). However, use of IPr^{Me} (**3-27**) as the ligand, modified from its IPr variant by simple dimethyl substitution of the backbone, afforded alkenylsilane **3-22a** with triethylsilane in >98:2 regioselectivity in 83% yield. While the steric differences of IPr and IPr^{Me} have been previously recognized including a description of %V_{bur} for silver and gold complexes,⁴⁵ this dramatic regiochemical reversal is nonetheless surprising.

Additionally, variation of *N*-aryl rather than the backbone substituent also allows alkenyl silanes to be produced with exceptional regiocontrol. Specifically, the use of commercially available NHC carbene ligand IPr*(**3-28**) or IPr*^{OMe} (**3-29**) also provided a highly selective entry to alkenyl silanes, with product being obtained again in >98:2 regioselectivity in both instances.

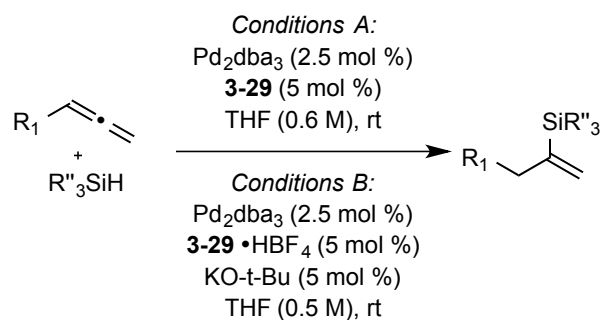
Given that an important objective of the current study is the utilization of organosilicon structures that perform well in cross-couplings, related hydrosilylations using BnMe₂SiH were next examined (Table 4, entries 6– 8). The comparison of IPr (**3-26**), IPr^{Me} (**3-27**), IPr* (**3-28**), and IPr*^{OMe} (**3-29**) exhibited similar trends, with ligand **3-26** providing allylsilane **3-23b** with 97:3 regioselectivity, ligand **3-27** providing a 75:25 mixture favoring alkenylsilane **3-22b**, ligand **3-28** favoring alkenylsilane **3-22b** with 81:19 selectivity, and ligand **3-29** favoring alkenylsilane **3-22b** with optimum 95:5 regiocontrol. The **3-28/3-29** comparison illustrates that both the steric and electronic environment play an important role in regioselectivity. Given the superior regioselection of alkenylsilane production with IPr*^{OMe} (**3-29**) across the two different silane structures, this procedure was adopted as the standard procedure for alkenylsilane synthesis for the remainder of this study.

3.5 Substrate Scope

With the most selective conditions for the formation of alkenylsilanes in hand, we further explored variations in silane coupling partners along with allene substitution. In the air-free reaction conditions employing free carbene ligand IPr*OMe **3-29** (conditions A), hydrosilylations occurred in 1-2 h at room temperature with palladium-catalysis to afford alkenylsilanes (Table 5). Coupling partners Me₂PhSiH and BnMe₂SiH were

explored due to their previous applications as “safety-catch” silanes in cross-couplings.⁴⁶ Reactions with Me₂EtOSiH were also examined as recent studies have demonstrated that this motif is effective in both fluoride-promoted and fluoride-free cross-couplings. The hydrosilylation of cyclohexylallene with dimethylphenylsilane afforded product **3-30** in 90% yield (Table 5, entry 1) while the reaction with dimethylethoxysilane afforded alkenylsilane **3-31** in 81% yield in high regioselectivity (96:4) (Table 5, entry 2). Aromatic allene substituents were well-tolerated with exceptional regioselectivity (>98:<2) for both dimethylethoxysilane and benzyldimethylsilane to afford **3-32** and **3-33** in excellent yields (Table 5, entries 4 and 5). Allenes with directly attached benzoxyl motifs were also well-tolerated for all silanes screened to yield alkenylsilanes **3-35**, **3-36**, **3-37** in excellent yields and regioselectivities (Table 5, entries 6-8). The reaction setup also is benefited by ease of scale-up as **3-35** was afforded in 95% yield at the 6.8 mmol scale (Table 5, entry 6). Unhindered *n*-aliphatics were also well-tolerated with a slight erosion of regioselectivity to form dimethylphenylsilane **3-38**, dimethylethoxysilane **3-39** and benzyldimethylsilane **3-40** in excellent yields.

Table 5 Pd-Catalyzed Allene Hydrosilylation



entry	R ₁	conditions	silane	product (% yield)	regiosel. (X:X)
1	Cy	A	Me ₂ PhSiH	3-30 (90)	>98:2
2	Cy	A	Me ₂ EtOSiH	3-31 (81)	96:4
3	Ph	A	Me ₂ PhSiH	3-32 (83)	>98:2
4	Ph	A	Me ₂ EtOSiH	3-33 (88)	>98:2
5	Ph	A	BnMe ₂ SiH	3-34 (90)	>98:2
6	BnO	A	Me ₂ PhSiH	3-35 (95) ^a	>98:2
7	BnO	A	Me ₂ EtOSiH	3-36 (84)	>98:2
8	BnO	A	BnMe ₂ SiH	3-37 (85)	>98:2
9	<i>n</i> -Oct	A	Me ₂ PhSiH	3-38 (83)	98:2
10	<i>n</i> -Oct	A	Me ₂ EtOSiH	3-39 (87)	96:4
11	<i>n</i> -Oct	A	BnMe ₂ SiH	3-40 (91)	93:7
12	Cy	B	BnMe ₂ SiH	3-22b (94)	98:2
13	Cy	B	Me ₂ EtOSiH	3-31 (99)	98:2
14	Ph	B	Me ₂ EtOSiH	3-33 (94)	>98:2
15	Ph	B	BnMe ₂ SiH	3-34 (92)	>98:2

^a Reaction was conducted on a 6.8 mmol scale

Improved reaction conditions were optimized to include standard benchtop assembly, without the use of air-free technology such as use of a glovebox (conditions B, Table 6). This protocol employs IPr*^{OMe}•HBF₄ salt **3-29**, KO-*t*-Bu base, Pd₂dba₃ precatalyst, and more concentrated reaction conditions (0.5 M). Reactions performed with conditions B were faster than with conditions A, with reactions occurring within 30 min at room temperature (Table 5). Likewise, reactions with conditions B were also

higher yielding than with conditions A (Table 5). For example, in entries 12 and 13, reactions with dimethylethoxysilane and benzyldimethylsilane resulted in much higher yields of 99% and 97% respectively with slightly improved regioselectivities 98:2 for both **3-31** and **3-22b**. Alterations in allene functionality were also tolerated under the conditions B, as aromatic substitution resulted in improved yields for both dimethylethoxysilane **3-33** in 94% and benzyldimethylsilane **3-34** in 92% with exceptional regioselectivities >98:<2 (Table 5, comparing entries 11 and 12 with entries 3 and 4).

3.6 Optimization of Allene Hydroarylation Protocol

To demonstrate the utility of ligand-controlled allene hydrosilylation, a one-pot hydroarylation procedure was developed. Optimization of the hydrosilylation reaction to function with benchtop assembly was accomplished through the use of ligand **3-29**•HBF₄ salt, KO-*t*-Bu and Pd₂dba₃ precatalyst. This reaction is followed by Hiyama-Denmark cross-couplings with aryl iodides (Table 6). Numerous attempts to utilize the IPr*OMe/Pd(0) in situ catalyst to promote the hydrosilylation and also the cross-coupling reaction resulted in low chemical yields. A solution to this problem involved the addition of an additional 2.5 mol % equivalent of the same Pd₂dba₃ precatalyst upon completion of the hydrosilylation reaction. This procedure affords α -branched isomers with no detection of proto-desilyl-Heck intermediates or any other regioisomers of Heck cross-coupling reactions.

The scope of the one-pot hydroarylation reaction is general and provides access to a variety of functionalized 1,1-disubstituted alkenes. This method tolerates variation in silane structure, as BnMe₂SiH and Me₂EtOSiH were successfully coupled with PhI in

high yields of 95% and 85% respectively (Table 6, entries 1 and 2). The reaction sequence likewise tolerates a variety of electrophile iodides with no observed erosion of regioselectivity. Aryl iodides with electron-withdrawing substituents (Table 6, entries 3 and 4) and electron-rich groups (Table 6, entry 5) were successfully coupled in excellent yields. In addition, a variety of heterocyclic-containing iodides functioned under the reaction conditions, as reactions with uracil-containing (Table 6, entry 6) and thienyl-containing (Table 6, entry 7) iodides were tolerated with excellent yields 81% and 77%. Sterically hindered substrates that typically exhibit low tolerance in Stille cross-couplings were also tolerated in the hydroarylation protocol, as a reaction with 2-iodotoluene successfully yielded **3-27** in excellent yield (Table 6, entry 8). Alterations in allene substitution had insignificant impact on the outcome of the reaction, as aromatic allenes were coupled with PhI (Table 6, entry 9) and dioxine-containing moieties (Table 6, entry 10) in excellent yields of 76% and 83%. Additionally, directly attached benzoxyl substituted allene was successfully coupled with PhI in exceptional yield of 89% (Table 6, entry 11). To further demonstrate the utility in catalyst-controlled hydrosilylation, a phthalimido-containing allene was coupled with pyrrole-containing iodide to furnish hydroarylation product **3-51** in excellent yield 89% (Table 6, entry 12).

Table 6 One-Pot Allene Hydroarylation

1.) Pd₂dba₃ (2.5 mol %)
3-29 • HBF₄ (5 mol %)
 KO-t-Bu (5 mol %)
 THF (0.5 M), rt

2.) Ar-I (1.0 equiv.)
 n-Bu₄NF (2.0 equiv.)
 Pd₂dba₃ (2.5 mol %)
 THF, 50 °C

single regioisomer

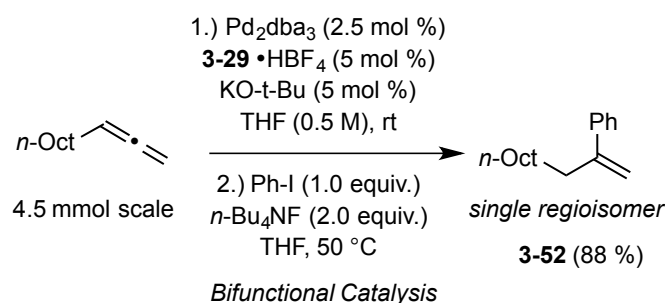
entry	R ₁	silane	Ar-I	major product (% yield)
1	Cy	Me ₂ EtOSiH	Ph	3-41 (95)
2	Cy	BnMe ₂ SiH	Ph	3-41 (85)
3	Cy	Me ₂ EtOSiH	<i>p</i> -NO ₂ Ph	3-42 (77)
4	Cy	Me ₂ EtOSiH	<i>p</i> -MeCOPh	3-43 (90)
5	Cy	Me ₂ EtOSiH	<i>p</i> -MeOPh	3-44 (74)
6	Cy	Me ₂ EtOSiH		3-45 (81)
7	Cy	Me ₂ EtOSiH		3-46 (77)
8	<i>n</i> -Oct	Me ₂ EtOSiH	<i>o</i> -tolyl	3-47 (92)
9	Ph	Me ₂ EtOSiH	Ph	3-48 (76)
10	Ph	Me ₂ EtOSiH		3-49 (83)
11	BnO	Me ₂ EtOSiH	Ph	3-50 (89)
12		Me ₂ EtOSiH		3-51 (89)

3.7 Large-Scale Hydroarylation Operations

It was found that large-scale one-pot hydrocarbations could be performed without the addition of a second batch of palladium precatalyst (Scheme 3-6). In one synthetic step, undeca-1,2-diene was successfully transformed to **3-52** on the gram-scale without the use of additional palladium precatalyst. This is likely due to the different coordinating

environment of the palladium catalyst at the larger scale, potentially liberating trace amounts of free Pd(0) without an appended NHC ligand. It was found that this reaction was not general, as other large-scale experiments failed to consistently afford cross-coupling products for a variety of electrophiles. However, use of a second batch of palladium precatalyst on the smaller scale permitted predictable access to 1,1-disubstituted alkene products (see Table 6 conditions).

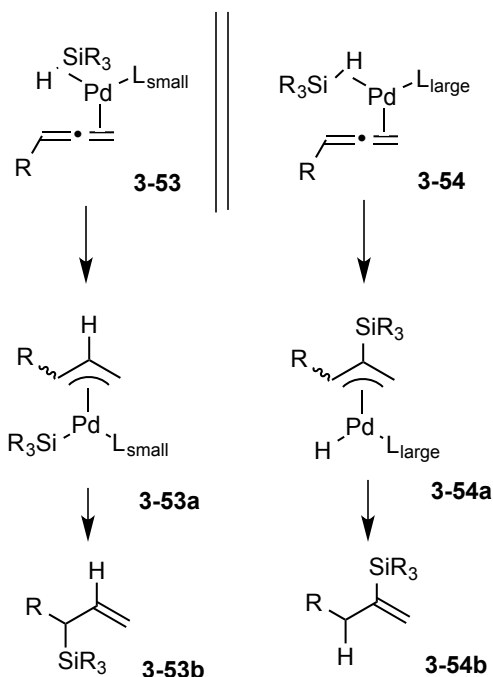
Scheme 3-6 Large-Scale Hydroarylation Example



3.8 Proposed Mechanism and Origin of Regioselectivity

The mechanism and origin of regioselectivity is likely a result from ligand-controlled alterations from a hydrometalation pathway to a silylmetalation pathway (Scheme 3-7). In our previous studies, we found that traditional NHC ligands (IMes/IPr) favor hydride donation to the central allene carbon and reductive elimination of the silyl group (**3-53a** to **3-53b**). This trend was also observed in our preliminary screenings; however, upon use of incredibly bulky NHC ligand IPr*OMe **3-29** this pathway reverses due to increased steric repulsions between the silyl ligand and the ligand (**3-54a** to **3-54c**, Scheme 3-7). Recent computational studies on allene hydrosilylation have demonstrated that the oxidative-addition/migratory insertion steps occur in the same step.

Scheme 3-7 Origin of Regiocontrol: Ligand Sterics



These observations demonstrate that fine-tuning the structures of NHC ligands can have profound effects on the regiochemical outcomes in simple two-component couplings.

3.9 Conclusions and Outlook

Careful selection of NHC ligand structure is a successful strategy for achieving regiocontrol in allene hydro-silylation with palladium-catalysis. This methodology utilizes bulky NHC IPr*OMe ligand **3-29** to predictably favor the formation of a variety of alkenylsilanes with exceptional regiocontrol (95:5 to >98:2) and without the use of a directing group or electronic substrate bias. Synthetic benefits to this approach have been demonstrated in the development of a one-pot hydroarylation reaction that couples the regioselective hydro-silylation strategy with an optimized Pd-catalyzed cross-coupling reaction with aryl iodides. This method streamlines access to α -branched isomers in excellent yields without isolation of alkenylsilane intermediates. Future work will be

dedicated to evaluating the subtle mechanistic factors that govern the regioselectivity in this reaction and related classes of reactions.

The contents of this chapter were published in the journal *Organic Letters*.⁵¹

3.10 Experimental

General: All reagents were used as received unless otherwise noted. Solvents were purified under nitrogen using a solvent purification system (Innovative Technology, Inc. Model # SPS-400-3 and PS-400-3). *Tris*(dibenzylideneacetone)-dipalladium (Pd₂dba₃) was purchased from Sigma Aldrich and was stored in a glovebox (for conditions A) and on the benchtop (for conditions B). Cyclohexylallene was purchased (Sigma-Aldrich) and (propa-1,2-dien-1-yloxy)methylbenzene was synthesized by isomerization of the respective propargyl ether, according to previously published methods.⁴⁷ All remaining allenes were synthesized from the respective 1-alkyne precursors according to established procedures.⁴⁸ All reactions were conducted under an atmosphere of nitrogen with magnetic stirring in flame-dried or oven-dried (120 °C) glassware. Ligand **3-29** (IPr*^{OMe}) was purchased from Strem and was stored in a glovebox and **3-29**·HBF₄ (IPr*^{OMe}·HBF₄) was synthesized according to known methods and stored on the benchtop in a dessicator.⁴⁹ NHC Ligands **3-25** (DM-IMes·HCl), **3-27** (DM-IPr·HCl), and **3-28** (IPr*·HCl) were synthesized according to established methods and were stored and weighed out in a glovebox.⁵⁰ All other utilized *N*-heterocyclic carbene salts (**3-24** and **3-26**) and *t*-BuOK (purchased from Sigma-Aldrich and Strem) were stored and weighed in an inert atmosphere glovebox. Triethylsilane (purchased from Sigma-Aldrich) was passed through alumina and degassed before use. Benzyltrimethylsilane (purchased from Sigma-Aldrich) and dimethylphenylsilane (purchased from Sigma-Aldrich) were used as received. Dimethylethoxysilane (purchased from Acros) was stored in a Schlenk flask. Iodobenzene, 1-iodo-4-nitrobenzene, 4-iodoacetophenone, 4-iodoanisole, 5-iodo-1,3-dimethyluracil, 2-iodothiophene, 1-(4-iodophenyl)pyrrole, 2-iodotoluene and 6-iodo-2,4-dihydrobenzo[b][1,4]dioxine were used as received and purchased from Sigma-Aldrich. Allylsilanes **2a** and **2b** were afforded by previously reported procedures.⁵¹ A solution of tetra-*n*-butylammonium (TBAF, 1.0 M in THF, purchased from Sigma-Aldrich). ¹H and ¹³C spectra were obtained in CDCl₃ at rt (25 °C), unless otherwise noted, on a Varian

Mercury 400 MHz instrument, Varian Unity 500 MHz instrument, or Varian Unity 700 MHz instrument. Chemical shifts of ^1H NMR spectra were recorded in parts per million (ppm) on the δ scale from an internal standard of residual chloroform (7.24 ppm). Chemical shifts of ^{13}C NMR spectra were recorded in ppm from the central peak of CDCl_3 (77.0 ppm) on the δ scale. High-resolution mass spectra (HRMS) were obtained on a VG-70-250-s spectrometer manufactured by Micromass Corp. (Manchester UK) at the University of Michigan Mass Spectrometry Laboratory. Regioisomeric ratios were determined on crude reaction mixtures using NMR or GC. GC analyses were carried out on an HP 6980 Series GC System with HP-5MS column (30 m x 0.252 mm x 0.25 μm). When noted, a Biotage purification system (model # SP1) was utilized with SNAP (10 g) silica columns. Reported regioselectivities were determined by GCMS analysis and confirmed by ^1H NMR analysis by comparing the ratios of detectable geminal protons of the major and minor regioisomers in the crude reaction mixture. In cases where >98:2 regioselectivity is reported, minor isomers were not detected by either GCMS or NMR based methods.

General procedure I for the $\text{Pd}_2\text{dba}_3/\text{IPr}^{\text{OMe}}$ -promoted hydrosilylation of monosubstituted allenes (table 4):

THF (1.0 mL) was added to a solid mixture of IPr^{OMe} **3-29** (0.03 mmol) and Pd_2dba_3 (0.015 mmol) at rt. After stirring for 10 min at rt, the reaction mixture turned dark red, and silane (0.3 mmol) was added. The reaction mixture was stirred for 10 min at rt followed by dilution with THF (4.0 mL) and addition of the allene (0.3 mmol) neat by syringe. The reaction mixture was stirred at rt for 2 h. The reaction mixture was filtered through silica gel eluting with 50 % v/v EtOAc/hexanes. The solvent was removed *in vacuo*, and the crude residue was purified via flash column chromatography on silica gel or by Biotage to afford the desired product.

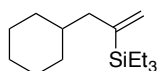
General procedure II for the $\text{Pd}_2\text{dba}_3/\text{IPr}^{\text{OMe}}$ -promoted hydrosilylation of monosubstituted allenes (conditions A, table 5):

THF (1.0 mL) was added to a solid mixture of IPr*^{OMe} **3-29** (0.015 mmol) and Pd₂dba₃ (0.0075 mmol) at rt. After stirring for 10 min at rt, the reaction mixture turned dark red, and silane (0.3 mmol) was added. The reaction mixture was stirred for 10 min at rt followed by dilution with THF (4.0 mL) and addition of the allene (0.3 mmol) neat by syringe. The reaction mixture was stirred at rt for 2 h. The reaction mixture was filtered through silica gel eluting with 50 % v/v EtOAc/hexanes. The solvent was removed *in vacuo*, and the crude residue was purified via flash column chromatography on silica gel or by Biotage to afford the desired product.

General procedure III for the Pd₂dba₃/IPr*^{OMe}·HBF₄ -promoted hydrosilylation of monosubstituted allenes (conditions B, table 5):

IPr*^{OMe}·HBF₄ **3-29** (0.025 mmol), *t*-BuOK (0.025 mmol), and Pd₂dba₃ (0.0125 mmol) were added to a 6.0 mL dram vial in air. The vial was fitted with a septum and underwent 3 pump/purge manifold cycles with nitrogen. THF (1.0 mL) was then added to the solid mixture. After stirring for 10 min at rt, the reaction mixture turned dark red, and silane (0.5 mmol) was added. The reaction mixture was stirred for 10 min at rt followed by addition of the allene (0.5 mmol) neat by syringe. The reaction mixture was stirred at rt for 30 min. The reaction mixture was filtered through silica gel eluting with 50 % v/v EtOAc/hexanes. The solvent was removed *in vacuo*, and the crude residue was purified via flash column chromatography on silica gel or by Biotage to afford the desired product.

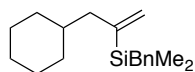
(3-Cyclohexylprop-1-en-2-yl)triethylsilane (3-22a) (Table 4, Entry 6)



General procedure II was followed with Pd₂dba₃ (6.9 mg, 0.0075 mmol), IPr*^{OMe} **3-29** (14.2 mg, 0.015 mmol), triethylsilane (48 μ L, 0.3 mmol), and cyclohexylallene (36.7 mg,

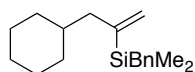
0.3 mmol). The crude residue was purified by flash chromatography (100 % hexanes) affording a clear oil (64.3 mg, 90 %). Spectral data matched that previously reported.⁵¹

Benzyl(3-cyclohexylprop-1-en-2-yl)dimethylsilane (3-22b) (Table 4, Entry 10)



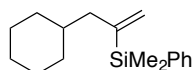
Conditions A: General procedure I was followed with Pd₂dba₃ (13.8 mg, 0.015 mmol), IPr^{*OMe} **3-29** (28.4 mg, 0.03 mmol), benzyldimethylsilane (47.5 μL, 0.3 mmol), and cyclohexylallene (36.7 mg, 0.3 mmol). The crude residue was purified by flash chromatography (100% hexanes) affording a clear oil (65 mg, 79 %). Full characterization of major product (**1b**) is provided below (with 95:5 regioselectivity).

Benzyl(3-cyclohexylprop-1-en-2-yl)dimethylsilane (3-22b) (Table 4, Entry 12)



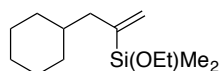
Conditions B: General procedure III was followed with Pd₂dba₃ (11.4 mg, 0.0125 mmol), IPr^{*OMe}·HBF₄ **3-29**·HBF₄ (25.8 mg, 0.025 mmol), *t*-BuOK (2.8 mg, 0.025 mmol), benzyldimethylsilane (54.8 μL, 0.5 mmol), and cyclohexylallene (72.7 μL, 0.5 mmol). The crude residue was purified by flash chromatography (100% hexanes) affording a clear oil (132 mg, 97 %) (with 98:2 regioselectivity). ¹H NMR (700 MHz, CDCl₃): δ 7.18 (t, *J* = 7.0 Hz, 2 H), 7.05 (t, *J* = 7.0 Hz, 1 H), 6.98 (d, *J* = 7.0 Hz, 2 H), 5.54 (m, 1 H), 5.33 (m, 1H), 2.13 (s, 2 H), 1.997 (d, *J* = 6.3 Hz, 2 H), 1.15-1.19 (m, 5 H), 1.33 (m, 1H), 1.11-1.19 (m, 3 H), 0.803 (q, *J* = 9.8 Hz, 2 H), 0.016 (s, 6 H); ¹³C NMR (100 MHz, CDCl₃): δ 149.0, 140.1, 128.3, 128.1, 126.4, 123.9, 44.9, 36.6, 33.4, 26.6, 26.4, 25.5, -3.4; IR (thin film): ν 3082, 2919, 2850, 1938, 1863, 1600, 1449, 1246, 923 cm⁻¹; HRMS (EI) (m/z): [M]⁺ calc for C₁₈H₂₉Si, 272.1960; found, 272.1960.

(3-Cyclohexylprop-1-en-2-yl)dimethyl(phenyl)silane (3-30) (Table 5, Entry 1)



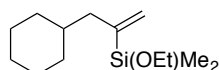
General procedure II was followed with Pd₂dba₃ (6.9 mg, 0.0075 mmol), IPr*^{OMe} **3-29** (14.2 mg, 0.015 mmol), dimethylphenylsilane (46 μL, 0.3 mmol), and cyclohexylallene (36.7 mg, 0.3 mmol). The crude residue was purified by flash chromatography (100% hexanes) affording a clear oil (70 mg, 90 %). ¹H NMR (500 MHz, CDCl₃): δ 7.48-7.50 (m, 2 H), 7.31-7.33 (m, 3 H), 5.60 (dt, *J* = 3.0, 1.5 Hz, 1 H), 5.40 (dt, *J* = 3.0, 0.5 Hz, 1 H), 1.98 (d, *J* = 7.2 Hz, 2 H), 1.57-1.59 (m, 5 H), 1.20-1.27 (m, 1 H), 1.02-1.08 (m, 3 H), 0.72 (m, 2 H), 0.34 (s, 6H); ¹³C NMR (125 MHz, CDCl₃): δ 148.8, 138.6, 133.8, 128.8, 127.6, 127.1, 44.9, 36.4, 33.3, 26.6, 26.3, -2.8; IR (thin film): ν 2999, 2919, 2849, 1876, 1447, 1427, 1247, 1111, 814 cm⁻¹; HRMS (EI) (*m/z*): [M]⁺ calc for C₁₇H₂₆Si, 258.1804, found, 258.1794.

(3-Cyclohexylprop-1-en-2-yl)(ethoxy)dimethylsilane (3-31) (Table 5, Entry 2)



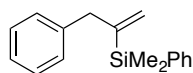
Conditions A: General procedure II was followed with Pd₂dba₃ (6.9 mg, 0.0075 mmol), IPr*^{OMe} **3-29** (14.2 mg, 0.015 mmol), dimethylethoxysilane (47.5 μL, 0.3 mmol), and cyclohexylallene (36.7 mg, 0.3 mmol). The crude residue was purified by flash chromatography (10 % v/v EtOAc/hexanes) affording a clear oil (55 mg, 81 %) (with 96:4 regioselectivity). Full characterization for the major product (**3-31**) is provided below (Table 5, Entry 12).

(3-Cyclohexylprop-1-en-2-yl)(ethoxy)dimethylsilane (3-31) (Table 5, Entry 13)



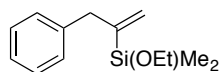
Conditions B: General procedure III was followed with Pd₂dba₃ (11.4 mg, 0.0125 mmol), IPr*^{OMe}·HBF₄ **3-29**·HBF₄ (25.8 mg, 0.025 mmol), *t*-BuOK (2.8 mg, 0.025 mmol), dimethylethoxysilane (69.3 μL, 0.5 mmol), and cyclohexylallene (72.7 μL, 0.5 mmol). The crude residue was purified by flash chromatography (10 % v/v EtOAc/hexanes) affording a clear oil (112.5 mg, 99 %) (with 98:2 regioselectivity). ¹H NMR (500 MHz, CDCl₃): δ 5.58 (dt, *J* = 3.0, 1.0 Hz, 1 H), 5.45 (dt, *J* = 3.0, 0.5 Hz, 1 H), 3.63 (q, *J* = 7.0 Hz, 2 H), 2.03 (d, *J* = 7.0 Hz, 2 H), 1.65-1.71 (m, 5 H), 1.39-1.46 (m, 1 H), 1.10-1.26 (m, 3 H) 1.18 (t, *J* = 7.0 Hz, 3 H), 0.82 (m, 2 H), 0.18 (s, 6 H); ¹³C NMR (125 MHz, CDCl₃): δ 148.9, 127.1, 58.3, 44.5, 36.5, 33.4, 26.7, 26.4, 18.4, -2.0; IR (thin film): ν 2971, 2921, 2851, 1448, 1389, 1256, 1102, 1076, 795 cm⁻¹; HRMS (EI) (*m/z*): [M-CH₃]⁺ calc for C₁₂H₂₃OSi, 211.1518; found, 211.1519.

Dimethyl(phenyl)(3-phenylprop-1-en-2-yl)silane (**3-32**) (Table 5, Entry 3)



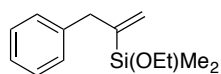
General procedure II was followed with Pd₂dba₃ (6.9 mg, 0.0075 mmol), IPr*^{OMe} **3-29** (14.2 mg, 0.015 mmol), dimethylphenylsilane (46 μL, 0.3 mmol), and phenylallene (34.9 mg, 0.3 mmol). The crude residue was purified by Biotage system (100% hexanes) affording a clear oil (63 mg, 83 %). Spectral data matched that previously reported.⁵²

Ethoxydimethyl(3-phenylprop-1-en-2-yl)silane (**3-33**) (Table 5, Entry 4)



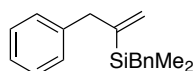
Conditions A: General procedure II was followed with Pd₂dba₃ (6.9 mg, 0.0075 mmol), IPr*^{OMe} **3-29** (14.2 mg, 0.015 mmol), dimethylethoxysilane (31.2 mg, 0.3 mmol), and phenylallene (34.9 mg, 0.3 mmol). The crude residue was purified by flash chromatography (5 % v/v EtOAc/hexanes) affording a clear oil (58 mg, 88 %). Full characterization for the major product (**6b**) is provided below (Table 5, Entry 14).

Ethoxydimethyl(3-phenylprop-1-en-2-yl)silane (3-33) (Table 5, Entry 4)



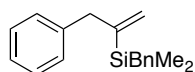
Conditions B: General procedure III was followed with Pd₂dba₃ (11.4 mg, 0.0125 mmol), IPr*^{OMe}·HBF₄ **3-29**·HBF₄ (25.8 mg, 0.025 mmol), *t*-BuOK (2.8 mg, 0.025 mmol), dimethylethoxysilane (69.3 μL, 0.5 mmol), and phenylallene (58 mg, 0.5 mmol). The crude residue was purified by Biotage system (0 to 10% gradient v/v EtOAc/hexanes) affording a clear oil (103 mg, 94 %). ¹H NMR (400 MHz, CDCl₃): δ 7.29-7.25 (m, 2 H), 7.19-7.13 (m, 3 H), 5.52 (m, 2 H), 3.56 (q, *J* = 7.2 Hz, 2 H), 3.47 (s, 2 H), 1.14 (t, *J* = 7.2 Hz, 3 H), 0.07 (s, 6 H); ¹³C NMR (125 MHz, CDCl₃): δ 149.6, 139.9, 129.3, 128.2, 127.5, 125.9, 58.4, 42.1, 18.4, 18.4, -2.1; IR (thin film): 3027, 2968, 1600, 1493, 1390, 1250, 1104, 1075, 828, 696 cm⁻¹; HRMS (EI) (*m/z*): [M]⁺ calc for C₁₃H₂₀OSi, 220.1283; found, 220.1283.

Benzoyldimethyl(3-phenylprop-1-en-2-yl)silane (3-34) (Table 5, Entry 5)



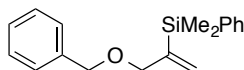
Conditions A: General procedure II was followed with Pd₂dba₃ (6.9 mg, 0.0075 mmol), IPr*^{OMe} **3-29** (14.2 mg, 0.015 mmol), benzoyldimethylsilane (47.5 μL, 0.3 mmol), and phenylallene (34.9 mg, 0.3 mmol). The crude residue was purified by flash chromatography (100% hexanes) affording a clear oil (71 mg, 90 %). Full characterization for the major product (**6c**) is provided below (Table 5, Entry 15).

Benzoyldimethyl(3-phenylprop-1-en-2-yl)silane (3-34) (Table 5, Entry 15)



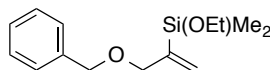
Conditions B: General procedure III was followed with Pd₂dba₃ (11.4 mg, 0.0125 mmol), IPr*^{OMe}·HBF₄ **3-29**·HBF₄ (25.8 mg, 0.025 mmol), *t*-BuOK (2.8 mg, 0.025 mmol), benzyldimethylsilane (54.8 μL, 0.5 mmol), and phenylallene (58 mg, 0.5 mmol). The crude residue was purified by silica plug (100% hexanes) affording a clear oil (125 mg, 92 %). ¹H NMR (500 MHz, CDCl₃): δ 7.27 (t, *J* = 8.5 Hz, 2 H), 7.17 (t, *J* = 8.5 Hz, 3 H), 7.11 (d, *J* = 7.5 Hz, 2 H), 7.04 (t, *J* = 7.5 Hz, 1 H), 6.92 (d, *J* = 8.5 Hz, 2 H), 5.49 (m, 1 H), 5.40 (m, 1 H), 3.41 (s, 2 H), 2.02 (s, 2 H), -0.05 (s, 6 H); ¹³C NMR (125 MHz, CDCl₃): δ 149.7, 139.9, 129.3, 128.3, 128.2, 128.1, 127.1, 126.0, 124.0, 42.9, 25.4, -3.6; IR (thin film): 2956, 3024, 1600, 1492, 1452, 1247, 1205, 1056, 696 cm⁻¹; HRMS (EI) (*m/z*): [M-CH₃]⁺ calc for C₁₈H₂₂Si, 251.1256; found, 251.1261.

(3-(Benzyloxy)prop-1-en-2-yl)dimethyl(phenyl)silane (3-35) (Table 5, Entry 6)



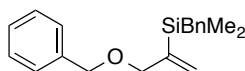
THF (25 mL) was added to a solid mixture of IPr*^{OMe} **3-29** (321 mg, 0.34 mmol) and Pd₂dba₃ (156 mg, 0.17 mmol) at rt. After stirring for 5 min at rt, the reaction mixture turned bright red and dimethylphenylsilane (1.0 mL, 6.8 mmol) was added. The reaction mixture was stirred for 10 min at rt followed by dilution with THF (75 mL) and addition of (propa-1,2-dien-1-yloxy)methylbenzene (1.0 g, 6.8 mmol) neat by syringe. The reaction mixture was stirred at rt for 2 h. The reaction mixture was filtered through silica gel eluting with 50% v/v EtOAc/hexanes. The solvent was removed *in vacuo*, and the crude residue was purified via flash column chromatography (10% v/v EtOAc/hexanes) on silica gel to afford the desired product as a yellow oil (1.8 g, 95%). Spectral data matched that previously published.⁵⁴

(3-(Benzyloxy)prop-1-en-2-yl)(ethoxy)dimethylsilane (3-36) (Table 5, Entry 7)



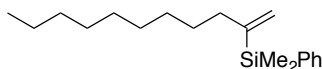
General procedure II was followed with Pd₂dba₃ (6.9 mg, 0.0075 mmol), IPr*^{OMe} **3-29** (14.2 mg, 0.015 mmol), dimethylethoxysilane (47.5 μL, 0.3 mmol), and (propa-1,2-dien-1-yloxy)methylbenzene (43.9 mg, 0.3 mmol). The crude residue was purified by flash chromatography (20 % v/v EtOAc/hexanes) affording a clear oil (63 mg, 84 %). ¹H NMR (500 MHz, CDCl₃): δ 7.25-7.34 (m, 5 H), 5.90 (dt, *J* = 3.0, 1.5 Hz, 1 H), 5.57 (dt, *J* = 3.5 Hz, 1.0 Hz, 1 H), 4.50 (s, 2 H), 4.14 (s, 2 H), 3.65 (q, *J* = 7.5 Hz, 2 H), 1.16 (t, *J* = 7.5 Hz, 3 H), 0.21 (s, 6 H); ¹³C NMR (125 MHz, CDCl₃): δ 147.1, 138.5, 128.3, 127.6, 127.4, 126.8, 73.7, 72.2, 58.5, 18.4, -1.9; IR (thin film): 2963, 2862, 1617, 1388, 1251, 1081, 941, 824, 732 cm⁻¹; HRMS (ESI) (*m/z*): [M+Na]⁺ calc for C₁₄H₂₂O₂Si, 273.1281; found, 273.1286.

Benzyl(3-(benzyloxy)prop-1-en-2-yl)dimethylsilane (3-37) (Table 5, Entry 8)



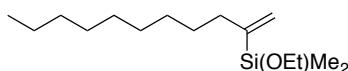
General procedure II was followed with Pd₂dba₃ (6.9 mg, 0.0075 mmol), IPr*^{OMe} **3-29** (14.2 mg, 0.015 mmol), benzyldimethylsilane (47.5 μL, 0.3 mmol), and (propa-1,2-dien-1-yloxy)methylbenzene (43.9 mg, 0.3 mmol). The crude residue was purified by flash chromatography (20% EtOAc/hexanes) affording a clear oil (75.6 mg, 85 %). ¹H NMR (400 MHz, CDCl₃): δ 7.25-7.33 (m, 5 H), 7.17 (t, *J* = 7.2 Hz, 2 H), 7.04 (t, *J* = 7.0 Hz, 1 H), 6.96 (d, *J* = 6.4 Hz, 2 H), 5.85 (s, 1 H), 5.42 (s, 1 H), 4.47 (s, 2 H), 4.08 (s, 2 H), 2.18 (s, 2 H), 0.06 (s, 6 H); ¹³C NMR (175 MHz, CDCl₃): δ 147.3, 139.9, 138.5, 128.33, 128.30, 128.1, 127.6, 127.5, 126.5, 124.0, 74.6, 72.2, 25.5, -3.7; IR (thin film): 2955, 1599, 1493, 1452, 1248, 1206, 908 cm⁻¹; HRMS (*m/z*): [M-CH₃]⁺ calc for C₁₉H₂₄OSi, 205.1049; found, 205.1054.

Dimethyl(phenyl)(undec-1-en-2-yl)silane (3-38) (Table 5, Entry 9)



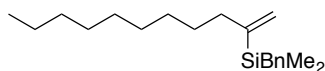
General procedure II was followed with Pd₂dba₃ (6.9 mg, 0.0075 mmol), IPr*^{OMe} **3-29** (14.2 mg, 0.015 mmol), dimethylphenylsilane (47.5 μL, 0.3 mmol), and undeca-1,2-diene (45.7 mg, 0.3 mmol). The crude residue was purified by flash chromatography (100% hexanes) affording a clear oil (72 mg, 83 %) (with 98:2 regioselectivity). Spectral data matched that previously reported.⁵⁵

Ethoxydimethyl(undec-1-en-2-yl)silane (3-39) (Table 5, Entry 10)



General procedure II was followed with Pd₂dba₃ (6.9 mg, 0.0075 mmol), IPr*^{OMe} **3-29** (14.2 mg, 0.015 mmol), dimethylethoxysilane (47.5 μL, 0.3 mmol), and undeca-1,2-diene (45.7 mg, 0.3 mmol). The crude residue was purified by flash chromatography (10 % v/v EtOAc/hexanes) affording a clear oil (67 mg, 87 %) (with 96:4 regioselectivity). ¹H NMR (400 MHz, CDCl₃): δ 5.61 (m, 1 H), 5.40 (m, 1 H), 3.62 (q, *J* = 7.2 Hz, 2 H), 2.11 (t, *J* = 9.0 Hz, 2 H), 1.35-1.46 (m, 2 H), 1.26 (s, 14 H), 1.17 (t, *J* = 7.2 Hz, 0.86 (t, *J* = 7 Hz, 3 H), 0.18 (s, 6 H); ¹³C NMR (100 MHz, CDCl₃): δ 150.6, 125.6, 58.4, 35.7, 31.9, 29.59, 29.55, 29.3, 28.9, 22.7, 18.4, 14.1, -2.1; IR (thin film): 2957, 2923, 2854, 1465, 1389, 1249, 1106, 1079, 928, 828, 781 cm⁻¹; HRMS (EI) (*m/z*): [M-CH₃]⁺ calc for C₁₅H₃₂OSi, 241.1988; found, 241.1999.

Benzoyldimethyl(undec-1-en-2-yl)silane (3-40) (Table 5, Entry 11)



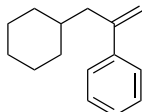
General procedure II was followed with Pd₂dba₃ (6.9 mg, 0.0075 mmol), IPr*^{OMe} **3-29** (14.2 mg, 0.015 mmol), benzoyldimethylsilane (47.5 μL, 0.3 mmol), and undeca-1,2-diene (45.7 mg, 0.3 mmol). The crude residue was purified by flash chromatography (100% hexanes) affording a clear oil (82.6 mg, 91%) (with 93:7 regioselectivity). ¹H NMR (400

MHz, CDCl₃): δ 7.18 (t, J = 7.0 Hz, 2 H), 7.04 (t, J = 7.0 Hz, 1 H), 6.97 (d, J = 7.6 Hz, 2 H), 5.58 (m, 1 H), 5.28 (m, 1 H), 2.14 (s, 2 H), 2.07 (t, J = 9.6 Hz, 2 H), 1.30-1.40 (m, 2 H), 1.26 (s, 14 H), 0.87 (t, J = 6.8 Hz, 3 H), 0.02 (s, 6 H); ¹³C NMR (125 MHz, CDCl₃): δ 150.7, 140.1, 128.2, 128.1, 124.8, 123.9, 36.1, 31.9, 29.6, 29.54, 29.53, 29.3, 28.9, 25.5, 22.7, 14.1, -3.6; IR (thin film): 3025, 2955, 2923, 2853, 1601, 1493, 1452, 1247, 1206, 1153, 1056, 696 cm⁻¹; HRMS (EI) (m/z): [M]⁺ calc for C₂₀H₃₄Si, 302.2430; found, 302.2434.

General procedure IV for the Pd₂dba₃/IPr*^{OMe}·HBF₄ -promoted hydroarylation of monosubstituted allenes:

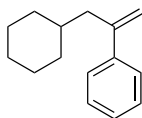
IPr*^{OMe}·HBF₄ **3-29** (0.025 mmol), Pd₂dba₃ (0.0125 mmol), and *t*-BuOK (0.025 mmol) were added to a 6.0 mL dram vial in air. The vial was fitted with a septum and underwent 3 pump/purge manifold cycles with nitrogen. THF (1.0 mL) was then added to the solid mixture. After stirring for 10 min at rt, the reaction mixture turned dark red, and silane (0.5 mmol) was added. The reaction mixture was stirred for 10 min at rt followed by addition of the allene (0.5 mmol) neat by syringe. The reaction mixture was stirred at rt until reaction was determined complete by disappearance of starting material, within 30 min, as observed by thin-layer chromatography. TBAF (1 mmol, 2.0 equiv., 1.0 M in THF) was then added slowly by hand with a syringe over 5 minutes (**caution, a strong exotherm is generated!**) to the stirring solution. After 10 min at rt, the iodide (0.5 mmol) was added followed by Pd₂dba₃ (0.0125 mmol). The reaction vessel was then heated at 50 °C in an oil bath until the reaction was determined complete by the disappearance of iodide, within 30 min, as determined by thin-layer chromatography. The solvent was removed *in vacuo*, and the crude residue was purified via flash column chromatography on either silica gel or by Biotage purification system to afford the desired product.

(3-Cyclohexylprop-1-en-2-yl)benzene (3-41) (Table 6, Entry 1)



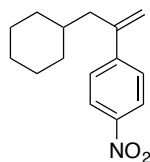
General procedure IV was followed with Pd₂dba₃ (11.4 mg, 0.0125 mmol), IPr*^{OMe}·HBF₄ **3-29** (25.8 mg, 0.025 mmol), *t*-BuOK (2.8 mg, 0.025 mmol), dimethylethoxysilane (68.8 μL, 0.5 mmol), cyclohexylallene (72.7 μL, 0.5 mmol), iodobenzene (102 mg, 0.5 mmol), TBAF (1 mL, 1 mmol), and a second batch of Pd₂dba₃ (11.4 mg, 0.025 mmol). The crude residue was purified by flash chromatography (100% hexanes) affording a clear oil (95 mg, 95 %). Spectral data matched that previously reported.⁵⁶

(3-Cyclohexylprop-1-en-2-yl)benzene (3-41) (Table 6, Entry 2)



General procedure IV was followed with Pd₂dba₃ (11.4 mg, 0.0125 mmol), IPr*^{OMe}·HBF₄ **3-29** (25.8 mg, 0.025 mmol), *t*-BuOK (2.8 mg, 0.025 mmol), benzyldimethylsilane (54.8 μL, 0.5 mmol), cyclohexylallene (72.7 μL, 0.5 mmol), iodobenzene (102 mg, 0.5 mmol), TBAF (1 mL, 1 mmol), and a second batch of Pd₂dba₃ (11.4 mg, 0.025 mmol). The crude residue was purified by flash chromatography (100% hexanes) affording a clear oil (85 mg, 85 %). Spectral data matched that previously reported.⁵⁶

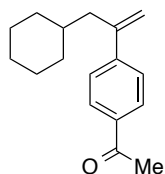
1-(3-Cyclohexylprop-1-en-2-yl)-4-nitrobenzene (3-42) (Table 6, Entry 3)



General procedure IV was followed with Pd₂dba₃ (11.4 mg, 0.025 mmol), IPr*^{OMe}·HBF₄ **3-29** (25.8 mg, 0.025 mmol), *t*-BuOK (2.8 mg, 0.025 mmol), dimethylethoxysilane (68.8

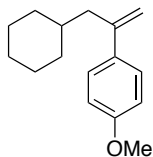
μL , 0.5 mmol), cyclohexylallene (72.7 μL , 0.5 mmol), 1-iodo-4-nitrobenzene (124.5 mg, 0.5 mmol), TBAF (1 mL, 1 mmol), and a second batch of Pd_2dba_3 (11.4 mg, 0.025 mmol). The crude residue was purified by flash chromatography (100 % v/v hexanes) to afford (94 mg, 77 %). ^1H NMR (400 MHz, CDCl_3): δ 8.17 (d, $J = 8.4$ Hz, 2 H), 7.51 (d, $J = 8.4$ Hz, 2 H), 5.38 (s, 1 H), 5.18 (s, 1 H), 2.40 (d, $J = 10.4$ Hz, 2 H), 1.56-1.71 (m, 5 H), 1.19-1.32 (m, 1 H), 1.03-1.15 (m, 5 H), 0.80-0.94 (m, 2 H); ^{13}C NMR (175 MHz, CDCl_3): δ 148.1, 146.9, 145.5, 127.0, 123.6, 116.9, 43.3, 35.8, 33.1, 26.4, 26.1; IR (thin film): 2921, 2849, 1595, 1515, 1341, 856, 712 cm^{-1} ; HRMS (EI) (m/z): $[\text{M}]^+$ calc for $\text{C}_{15}\text{H}_{19}\text{NO}_2$, 245.1416; found, 245.1426.

1-(4-(3-Cyclohexylprop-1-en-2-yl)phenyl)ethan-1-one (3-43) (Table 6, Entry 4)



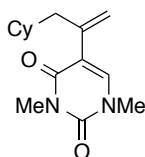
General procedure IV was followed with Pd_2dba_3 (11.4 mg, 0.025 mmol), $\text{IPr}^{\text{OMe}}\cdot\text{HBF}_4$ **3-29** (25.8 mg, 0.025 mmol), *t*-BuOK (2.8 mg, 0.025 mmol), dimethylethoxysilane (68.8 μL , 0.5 mmol), cyclohexylallene (72.7 μL , 0.5 mmol), 4-iodoacetophenone (123 mg, 0.5 mmol), TBAF (1 mL, 1 mmol), and a second batch of Pd_2dba_3 (11.4 mg, 0.025 mmol). The crude residue was purified by flash chromatography (20 % v/v EtOAc/hexanes) affording a clear oil (110 mg, 90 %). Spectral data matched that previously reported.⁵⁷

1-(3-Cyclohexylprop-1-en-2-yl)-4-methoxybenzene (3-44) (Table 6, Entry 5)



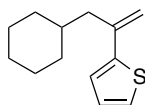
General procedure IV was followed with Pd₂dba₃ (11.4 mg, 0.025 mmol), IPr*^{OMe}·HBF₄ **3-29** (25.8 mg, 0.025 mmol), *t*-BuOK (2.8 mg, 0.025 mmol), dimethylethoxysilane (68.8 μL, 0.5 mmol), cyclohexylallene (72.7 μL, 0.5 mmol), 4-iodoanisole (117 mg, 0.5 mmol), TBAF (1 mL, 1 mmol), and a second batch of Pd₂dba₃ (11.4 mg, 0.025 mmol). The crude residue was purified by flash chromatography (100% hexanes) affording a clear oil (85 mg, 74 %). Spectral data matched that previously reported.⁵⁸

5-(3-Cyclohexylprop-1-en-2-yl)-1,3-dimethylpyrimidine-2,4(1*H*,3*H*)-dione (3-45)
(Table 6, Entry 6)



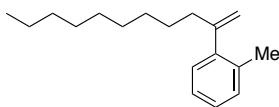
General procedure IV was followed with Pd₂dba₃ (11.4 mg, 0.025 mmol), IPr*^{OMe}·HBF₄ **3-29** (25.8 mg, 0.025 mmol), *t*-BuOK (2.8 mg, 0.025 mmol), dimethylethoxysilane (68.8 μL, 0.5 mmol), cyclohexylallene (72.7 μL, 0.5 mmol), 5-iodo-1,3-dimethyluracil (133 mg, 0.5 mmol), TBAF (1 mL, 1 mmol), and a second batch of Pd₂dba₃ (11.4 mg, 0.025 mmol). The crude residue was purified by flash chromatography (10 to 25 % gradient v/v EtOAc:Hex) affording a yellow oil (106 mg, 81 %). ¹H NMR (500 MHz, CDCl₃): δ 7.05 (s, 1 H), 5.20 (s, 1 H), 5.00 (s, 1 H), 3.40 (d, *J* = 1.7 Hz, 3 H), 3.34 (d, *J* = 1.7 Hz, 3 H), 2.32 (d, *J* = 8.2 Hz, 2 H), 1.56-1.74 (m, 5 H), 1.09-1.28 (m, 3 H), 0.80-0.90 (m, 3 H); ¹³C NMR (175 MHz, CDCl₃): δ 162.1, 151.6, 141.4, 139.4, 116.2, 115.4, 42.8, 37.0, 35.9, 33.0, 28.0, 26.5, 26.2; IR (thin film): 2921, 2849, 1702, 1650, 1448, 1343, 1031 cm⁻¹; HRMS (ESI) (*m/z*): [M+H]⁺ calc for C₁₅H₁₉NO₂, 263.1754; found, 263.1754.

2-(3-Cyclohexylprop-1-en-2-yl)thiophene (3-46) (Table 6, Entry 7)



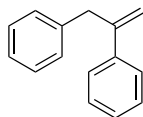
General procedure IV was followed with Pd₂dba₃ (11.4 mg, 0.025 mmol), IPr*^{OMe}·HBF₄ **3-29** (25.8 mg, 0.025 mmol), *t*-BuOK (2.8 mg, 0.025 mmol), dimethylethoxysilane (68.8 μL, 0.5 mmol), cyclohexylallene (72.7 μL, 0.5 mmol), 2-iodothiophene (105 mg, 0.5 mmol), TBAF (1 mL, 1 mmol), and a second batch of Pd₂dba₃ (11.4 mg, 0.025 mmol). The crude residue was purified by flash chromatography (100% hexanes) affording a clear oil (80 mg, 77 %). ¹H NMR (400 MHz, CDCl₃): δ 7.14 (dd, *J* = 5.2, 1.0 Hz, 1 H), 7.00 (dd, *J* = 3.7, 1.0 Hz, 1 H), 6.95 (dd, *J* = 5.5, 3.7 Hz, 1 H), 5.38 (s, 1 H), 4.87 (s, 1 H), 2.32 (d, *J* = 7.6 Hz, 2 H), 1.58-1.79 (m, 5 H), 1.46-1.55 (m, 1 H), 1.08-1.24 (m, 3 H), 0.84-0.96 (m, 2 H); ¹³C NMR (125 MHz, CDCl₃): δ 145.7, 140.2, 127.3, 123.9, 123.4, 112.0, 44.0, 36.4, 33.4, 26.5, 26.3; IR (thin film): 2921, 2849, 1518, 1447, 1344, 1032, 852, 694 cm⁻¹; HRMS (EI) (*m/z*): [*M*]⁺ calc for C₁₃H₁₈S, 206.1129; found, 206.1127.

1-Methyl-2-(undec-1-en-2-yl)benzene (**3-47**) (Table 6, Entry 8)



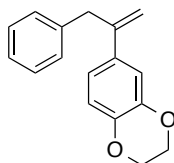
General procedure IV was followed with Pd₂dba₃ (11.4 mg, 0.025 mmol), IPr*^{OMe}·HBF₄ **3-29** (25.8 mg, 0.025 mmol), *t*-BuOK (2.8 mg, 0.025 mmol), dimethylethoxysilane (68.8 μL, 0.5 mmol), undeca-1,2-diene (76.1 mg, 0.5 mmol), 2-iodotoluene (109 mg, 0.5 mmol), TBAF (1 mL, 1 mmol), and a second batch of Pd₂dba₃ (11.4 mg, 0.025 mmol). The crude residue was purified by flash chromatography (100% hexanes) affording a clear oil (112 mg, 92 %). ¹H NMR (400 MHz, CDCl₃): δ 7.11-7.20 (m, 3 H), 7.04-7.09 (m, 1 H), 5.16 (s, 1 H), 4.84 (s, 1 H), 2.31 (t, *J* = 8.0 Hz, 2 H), 2.29 (s, 3 H), 1.34-1.43 (m, 2 H), 1.20-1.34 (m, 14 H), 0.88 (t, *J* = 8.0 Hz, 3 H); ¹³C NMR (100 MHz, CDCl₃): δ 150.3, 143.3, 134.7, 130.0, 128.3, 126.6, 125.3, 113.4, 37.8, 31.9, 29.56, 29.48, 29.39, 29.29, 27.8, 22.7, 19.9, 14.1; IR (thin film): 2922, 2851, 1486, 1455, 1259, 1078, 898, 728 cm⁻¹; HRMS (EI) (*m/z*): [*M*]⁺ calc for C₁₈H₂₈ 244.2129; found, 244.2185.

Prop-2-ene-1,2-diylidibenzene (**3-48**) (Table 6, Entry 9)



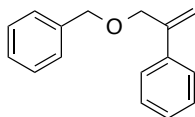
General procedure IV was followed with Pd₂dba₃ (11.4 mg, 0.025 mmol), IPr*^{OMe}·HBF₄ **3-29** (25.8 mg, 0.025 mmol), *t*-BuOK (2.8 mg, 0.025 mmol), dimethylethoxysilane (68.8 μL, 0.5 mmol), phenylallene (58.1 mg, 0.5 mmol), iodobenzene (102 mg, 0.5 mmol), TBAF (1 mL, 1 mmol), and a second batch of Pd₂dba₃ (11.4 mg, 0.025 mmol). The crude residue was purified by flash chromatography (100% hexanes) affording a clear oil (73.7 mg, 76 %). Spectral data matched that previously reported.⁵⁹

6-(3-Phenylprop-1-en-2-yl)-2,3-dihydrobenzo[*b*][1,4]dioxine (3-49) (Table 6, Entry 10)



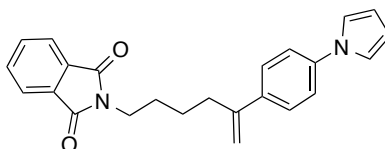
General procedure IV was followed with Pd₂dba₃ (11.4 mg, 0.025 mmol), IPr*^{OMe}·HBF₄ **3-29** (25.8 mg, 0.025 mmol), *t*-BuOK (2.8 mg, 0.025 mmol), dimethylethoxysilane (68.8 μL, 0.5 mmol), phenylallene (58.1 mg, 0.5 mmol), 6-iodo-2,4-dihydrobenzo[*b*][1,4]dioxine (131 mg, 0.5 mmol), TBAF (1 mL, 1 mmol), and a second batch of Pd₂dba₃ (11.4 mg, 0.025 mmol). The crude residue was purified by flash chromatography (100% hexanes) affording a clear oil (105 mg, 83 %). ¹H NMR (400 MHz, CDCl₃): δ 7.15-7.28 (m, 5 H), 7.0 (s, 1 H), 6.93 (d, *J* = 8.7 Hz, 1 H), 6.76 (d, *J* = 9.1 Hz, 1 H), 5.40 (s, 1 H), 4.92 (s, 1 H), 4.21 (s, 4 H), 3.76 (s, 2 H); ¹³C NMR (175 MHz, CDCl₃): δ 145.9, 143.1, 139.6, 134.3, 128.8, 128.3, 119.3, 116.9, 115.0, 113.4, 64.4, 64.3, 41.6; IR (thin film): 3025, 2924, 2875, 1578, 1505, 1494, 1423, 1306, 1282, 1246, 1066, 893, 696 cm⁻¹; HRMS (ESI) (*m/z*): [M+H]⁺ calc for C₁₇H₁₆O₂, 253.1223; found, 253.1223.

(3-(Benzyloxy)prop-1-en-2-yl)benzene (3-50) (Table 6, Entry 11)



General procedure IV was followed with Pd₂dba₃ (11.4 mg, 0.025 mmol), IPr*^{OMe}·HBF₄ **3-29** (25.8 mg, 0.025 mmol), *t*-BuOK (2.8 mg, 0.025 mmol), dimethylethoxysilane (68.8 μL, 0.5 mmol), ((propa-1,3-dien-1-yloxy)methyl)benzene (73.1 mg, 0.5 mmol), iodobenzene (102 mg, 0.5 mmol), TBAF (1 mL, 1 mmol), and a second batch of Pd₂dba₃ (11.4 mg, 0.025 mmol). The crude residue was purified by flash chromatography (100% hexanes) affording a clear oil (100 mg, 89 %). Spectral data matched that previously reported.⁴⁷

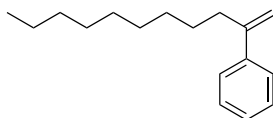
2-(5-(4-(1*H*-Pyrrol-1-yl)phenyl)hex-5-en-1-yl)isoindoline-1,3-dione (3-51) (Table 6, Entry 12)



General procedure IV was followed with Pd₂dba₃ (11.4 mg, 0.025 mmol), IPr*^{OMe}·HBF₄ **3-29** (25.8 mg, 0.025 mmol), *t*-BuOK (2.8 mg, 0.025 mmol), dimethylethoxysilane (68.8 μL, 0.5 mmol), 2-(hexa-4,5-dien-1-yl)isoindoline-1,3-dione (114 mg, 0.5 mmol), 1-(4-iodophenyl)pyrrole (134.6 mg, 0.5 mmol), TBAF (1 mL, 1 mmol), and a second batch of Pd₂dba₃ (11.4 mg, 0.025 mmol). The crude residue was purified by flash chromatography (20 % v/v EtOAc/hexanes) affording a white solid (165 mg, 89 %). ¹H NMR (400 MHz, CDCl₃): δ 7.78-7.82 (m, 2H), 7.64-7.68 (m, 2H), 7.40 (d, *J* = 9.6 Hz, 2 H), 7.28 (d, *J* = 9.6 Hz, 2 H), 7.047 (t, *J* = 2.2 Hz, 2 H), 6.32 (t, *J* = 2.2 Hz, 2 H), 5.27 (s, 1 H), 5.06 (s, 1 H), 3.66 (t, *J* = 7.1 Hz, 2 H), 2.54 (t, *J* = 7.1 Hz, 2 H), 1.70 (quint., *J* = 7.5 Hz, 2 H), 1.49 (quint., *J* = 7.5 Hz, 2 H); ¹³C NMR (175 MHz, CDCl₃): δ 168.4, 146.9, 139.8, 138.2, 133.8, 132.1, 127.2, 123.1, 120.1, 119.2, 112.8, 110.3, 37.7, 34.7, 28.0, 25.2; mp = 84-86

°C; IR (thin film): 2939, 1769, 1708, 1520, 1396, 1330, 1070, 1037, 840, 719 cm^{-1} ;
HRMS (ESI) (m/z): $[\text{M}+\text{H}]^+$ calc for $\text{C}_{24}\text{H}_{22}\text{N}_2\text{O}_2$, 371.1754; found, 371.1757.

Undec-1-en-2-ylbenzene (3-52) (Scheme 3-6)



THF (25 mL) was added to a solid mixture of IPr^{OMe} **3-29** (213 mg, 0.225 mmol) and Pd_2dba_3 (103 mg, 0.112 mmol) at rt. After stirring for 10 min at rt, the reaction mixture turned bright red and dimethylethoxysilane (0.618 mL, 4.5 mmol) was added. The reaction mixture was stirred for 5 min at rt followed by dilution with THF (75 mL) and addition of undeca-1,2-diene (685 mg, 4.5 mmol) neat by syringe. The reaction mixture was stirred at rt for 2.5 h and the reaction was complete by observed consumption of starting material as determined by thin-layer chromatography. TBAF (6.75 mL, 6.75 mmol, 1.0 M in THF) was then added slowly by hand with a syringe over 5 minutes (**caution, a strong exotherm is generated!**) to the stirring solution. After 10 minutes at rt, iodobenzene (0.502 mL, 4.5 mmol) was added. The reaction vessel was then heated at 50 °C in an oil bath until the reaction was determined complete by the disappearance of iodide, within 1 h, as determined by thin-layer chromatography. The reaction mixture was filtered through silica gel eluting with 50% v/v EtOAc/hexanes. The solvent was removed *in vacuo*, and the crude residue was purified via flash column chromatography (100% hexanes) on silica gel to afford the desired product as a clear oil (910 mg, 88%). Spectral data matched that previously published.⁵⁹

Chapter 4

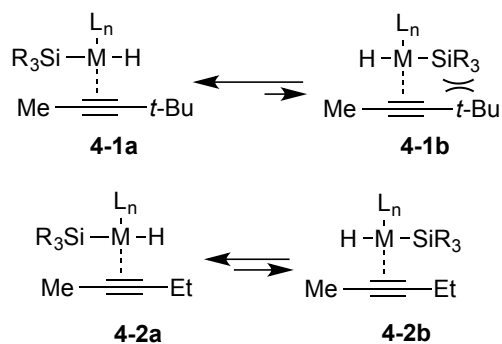
Access to Regio- and Stereodefined *E*-Allylic- and *Z*-Alkenylsilanes via 1,3-Disubstituted Allene Hydrosilylation

4.1 Introduction

A significant challenge presented in transition-metal catalyzed hydrosilylations of unbiased π systems is the lack of regio- and stereocontrol. Systems lacking either significant steric or electronic biases tend to afford mixtures of inseparable isomers, resulting in the loss of raw materials. This is particularly evident in additions to internal alkynes in the absence of electronic or steric biases.⁶⁰

For the majority of processes, the regioselectivity achieved in the hydrosilylations of internal alkynes is primarily due to the lowest energy insertion transition state. As discussed previously, either hydrometalation or silylmetalation occurs depending on the catalyst employed and these steps are typically the rate-determining steps and also the regiochemistry-determining steps. For internal alkyne hydrosilylations without strong electronic biases (i.e. $R_2 = \text{EWG}$), the steric interaction of the silyl group with the alkyne substituent tends to direct the positioning of the ligands prior to the insertion (Scheme 4-1)

Scheme 4-1 Challenge of Regiocontrol in Hydrosilylations of Internal Alkynes



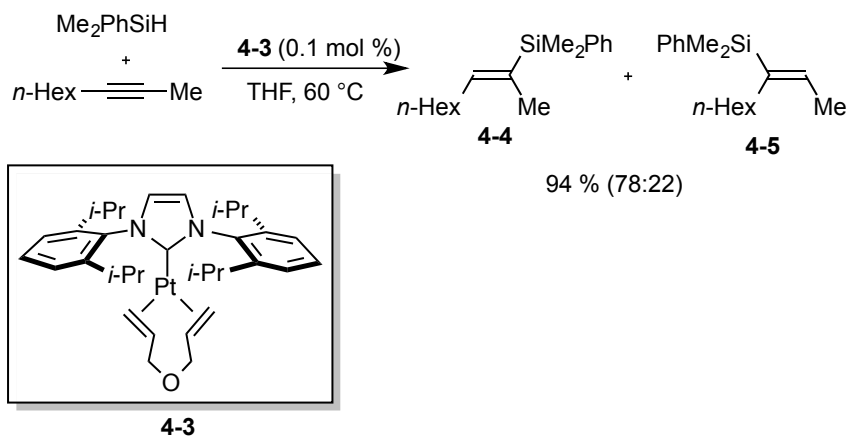
For example, in the hydrosilylations of internal alkynes substituted with Me vs. *t*-Bu, the steric interaction of the silyl ligand with the larger substituent (*t*-Bu) in π -complex **4-1b** results in the formation of primarily complex **4-1a**, which has a lower kinetic barrier for migratory insertion. Under these circumstances, the regioselectivity would be predicted to be high, favoring hydride addition next to the *t*-Bu substituent with the silyl group added closer to the less sterically encumbered substrate. In cases where alkyne substitution results in closely similar steric environments (**4-2a** and **4-2b**), the regioselectivity is typically low due to the inability of the metal catalyst to differentiate the two complexes resulting in two migratory insertion transition states of similar energy and therefore relatively equal populations.

Despite the inherent challenges in commanding coupling reactions of silanes and alkynes, numerous successful approaches have been developed that afford stereo- and regiodefined alkenylsilanes (including those discussed in Chapter 1). In addition, numerous other indirect approaches have been developed that creatively and effectively install silyl groups albeit via alternate mechanisms.

4.2 Internal Alkyne Hydrosilylation Procedures

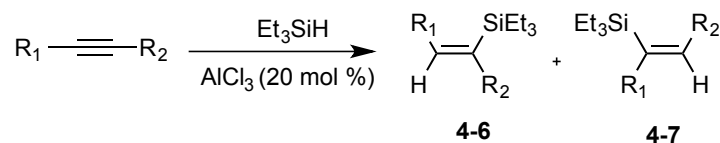
A useful procedure for the hydrosilylation of internal alkynes employs the IPr-Pt-AE catalyst **4-3** to selectively deliver dimethylphenylsilyl groups to the least hindered carbon of 2-nonyne in 78:22 regioselectivity to afford *E*-alkenylsilanes (Scheme 4-2).⁶¹ It was determined that including an NHC ligand as part of the catalyst structure drastically improved the catalytic activity in comparison with the popular Karstedt's catalyst (AE-Pt-PR₃ system), which is also useful in hydrosilylations of a variety of π components. However, this procedure drastically and unpredictably drops in regioselectivity upon selection of other silane substructures.

Scheme 4-2 Pt-Catalyzed Hydrosilylations of Internal Alkynes



Access to *Z*-alkenylsilanes is achieved in the Lewis-acid catalyzed hydrosilylations of internal alkynes (Scheme 4-3).⁶² In this protocol, the hydride and silyl group add across the alkyne but ultimately reside on opposite faces of the π -bond.

Scheme 4-3 Lewis-Acid-Catalyzed Hydrosilylations of Alkynes

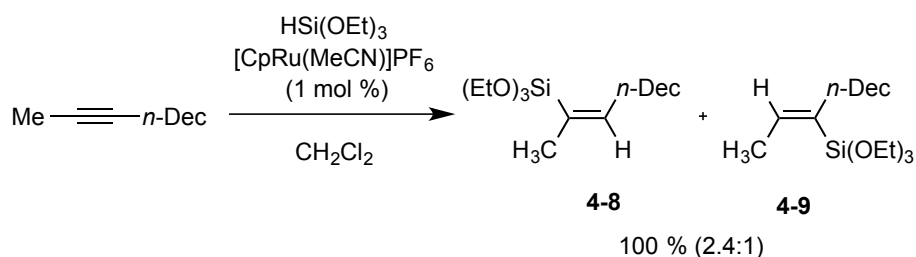


R ₁	R ₂	product (% yield, regioselect. (4-6:4-7))
<i>n</i> -Dec	H	4-6a (93 %, >98:2)
Ph	Me	4-6b (86 %, 88:12)
Ph	Et	4-6c (80 %, 68:32)

Terminal alkynes were found to be regio- and stereoselectively hydrosilylated due to the electronic and steric biases associated with these substrates (Scheme 4-3, **4-6a**). In addition, internal alkynes containing aryl groups functioned under the reaction conditions to afford **4-6b** and **4-6c** in moderate regioselectivities and high yields. Internal alkyne substrates without aryl groups were not tolerated under these conditions and another important consideration is the use of a strong Lewis acid limits the substrate scope.

Another example of a *trans*-addition process was developed by Trost and coworkers through the development of a cationic Ru complex that hydrosilylates internal alkynes affording trisubstituted *Z*-alkenylsilanes (Scheme 4-4).⁶³ This protocol works well with a variety of internal alkynes; however, in the absence of alkynes with steric differences or alcohol directing-groups, the regioselectivity is poor for a variety of silane coupling partners (Scheme 4-4).

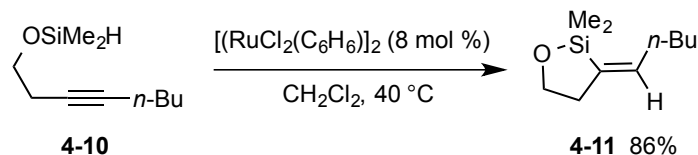
Scheme 4-4 Hydrosilylations with Cationic Ruthenium Complexes



For example, unhindered alkynes functionalized with triethoxysilane afford a mixture of **4-8** and **4-9** in 2.4:1 selectivity (Scheme 4-4). A series of deuterium-incorporation experiments verified the addition process and computational studies have explained the addition process as undergoing an isomerization process discussed in Chapter 1.

An intriguing solution to the challenge of gaining regiocontrol in additions to unbiased internal alkynes involves use of tethered homopropargylic silylether substrates to direct the hydrosilylation reaction affording only *Z*-alkenylsilane **4-11** (Scheme 4-5).⁶⁴ The advantage to use of this protocol is that the silyl ether is readily generated by treatment of homopropargyl alcohol with a chlorosilane.

Scheme 4-5 Intramolecular *Trans*-Hydrosilylations



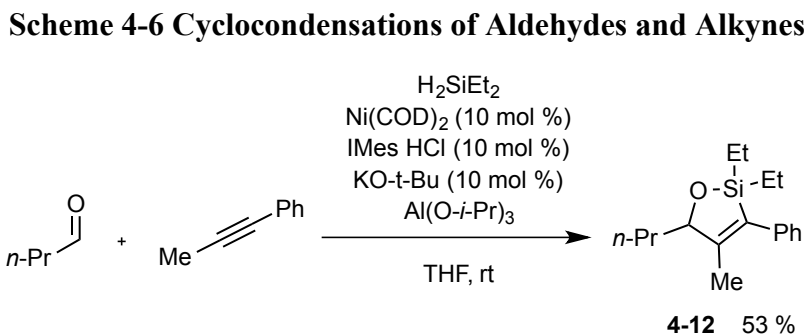
Use of a Ru catalyst allows for the reaction to take place in the *trans*-addition pathway similar to Trost's catalyst while the favored cyclic conformation directs the regiochemistry. However, if the reactant silyl ether is spaced further from the π -component, the reaction affords a mixture of regioisomers due to the more degrees of freedom in conformational flexibility. Use of Karstedt's catalyst with this system permits access to the opposite stereochemistry via a *syn*-addition pathway.

Despite the numerous successes in catalysts with high activities in the hydrosilylation of internal π -components, harnessing regio- and stereocontrol is still a significant impediment in the implementation of alkenylsilanes in synthetic protocols. Reactions that are highly efficient in installing Si and H across π -components, both to the same and opposite faces, often result in a mixture of inseparable constitutional isomers.

4.3 Methods for the Synthesis of Stereo- and Regiodefined Alkenylsilanes

There are several other non-hydrosilylative reactions that result the net addition of silane across a unit of unsaturation to afford stereodefined metalated intermediates. Although these particular protocols may not be the most efficient means of introducing silane functionality to a substrate, the benefit to their use is clear in the highly stereo- and regioselective formation of only one isomer.

An example of a highly effective procedure for the synthesis of tetrasubstituted alkenylsilanes is the cyclocondensation of alkynes with aldehydes (Scheme 4-6).⁶⁵ In this protocol, widely available starting materials are combined through a metallacyclic pathway with a nickel/IMes catalyst system to furnish silane **4-12** in 53 % yield.



In this mechanism, oxidative cyclicization is followed by sigma-bond metathesis with H_2SiEt_2 affords a Ni-H that rapidly extrudes hydrogen gas via sigma-bond metathesis, affording a new metallacycle with a Ni-Si bond. This intermediate reductively eliminates the silyl group to afford the cyclized product.

In contrast, the reductive coupling of chiral aldehydes and terminal TMS acetylenes diastereoselectively affords trisubstituted *Z*-alkenylsilanes **4-14** through the use of nickel/IMes catalytic systems with a silane reductant (Scheme 4-7).⁶⁶ This protocol introduces the silane in the C-C bond formed in the metallacycle, but not by means of action of the reductant as in the previous example.

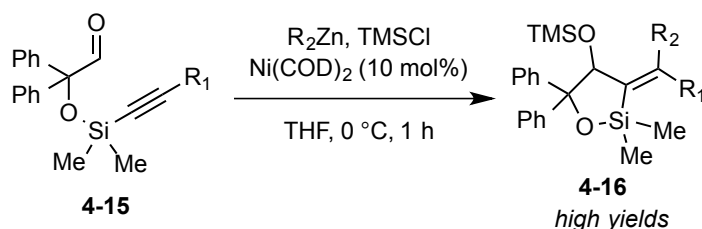
Scheme 4-7 Reductive Couplings of Silylalkynes and Chiral Aldehydes



The stereochemistry of the alpha-chiral center induces a diastereoselective metallacyclic transition state that results in enantioenriched silane **4-14**. This method is however limited to TMS groups that are not active in Pd-catalyzed cross-coupling reactions.

Stereodefined tetrasubstituted silanes are also afforded in the nickel-catalyzed intramolecular alkylative coupling of tethered silylether ynals (Scheme 4-8).⁶⁷ In this protocol, ynal **4-15** undergoes *exo*-cyclization to afford **4-16** in good yields.

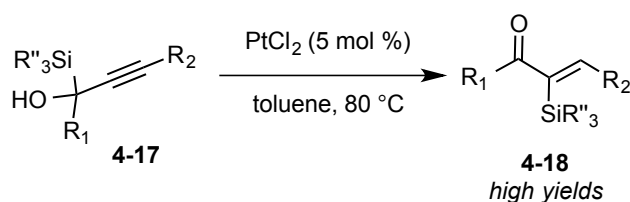
Scheme 4-8 Intramolecular Alkylative Couplings



This example is yet another indirect method for introducing silyl functionality that affords a substitution pattern not readily available by direct hydrosilylation of alkynes.

The rearrangement of alkynyl silyl alcohols **4-17** was found to also afford trisubstituted *Z*-alkenylsilanes with catalytic PtCl₂ (Scheme 4-9).⁶⁸ Although the products in this reaction are net hydrosilylation isomers, the mechanism actually involves a protosilylation, whereby coordination by the Pt catalyst results in 1,2-silyl migration and protonation of the vinyl-Pt intermediate restores the active catalyst resulting in the formation of *Z*-alkenylsilane **4-18**.

Scheme 4-9 Rearrangement of Alkynols



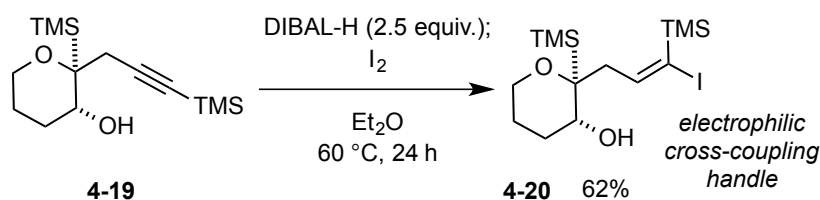
This procedure tolerates a wide scope of silanes, including motifs that are functional in cross-coupling procedures. It is also noteworthy that silyl-enone **4-18** is formed as many hydrosilylation catalysts often readily reduce enone substrates via 1,2- or 1,4-reductions.

4.4 Uncatalyzed Hydroalumination Methods Towards *Z*-Alkenylsilanes

In contrast with the catalytic methods previously discussed, reactions have been developed that utilize stoichiometric reagents to afford stereodefined alkenylsilanes. These methods typically involve hydrometalation pathways followed by quenching of the formed nucleophile with an electrophile source.

For example, the hydroalumination of alkynylsilanes exclusively affords *Z*-alkenylsilanes.^{69a} This protocol usually utilizes diisobutylaluminum hydride (DIBAL-H) for the *syn*-delivery of a hydride and aluminum to the face of an alkyne. Upon forming this vinyl-aluminum species, treatment with iodine quenches the nucleophile and affords **4-20**. The product afforded can then be transformed as an electrophile in a cross-coupling reaction to further elaborate the substitution pattern of the alkene.

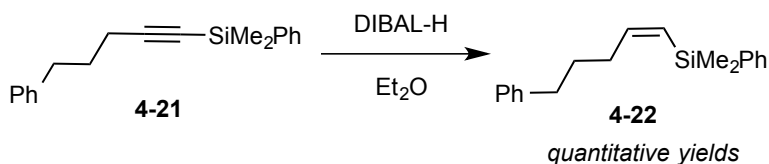
Scheme 4-10 Hydroalumination/ Iodination Procedure



Although this procedure overrides the traditional challenges in directing the hydrosilylations of alkynes, substrate incompatibility is an issue through the use of such a

strong reductant and electrophile. A similar approach to afford disubstituted *Z*-alkenylsilanes utilizes DIBAL-H with silylalkynes.^{69b} In a similar pathway to the previous example, hydroalumination followed by quenching with protic work-up affords only one stereoisomer of the alkenylsilane **4-22** in excellent yields.

Scheme 4-11 Hydrometalations of Silyl Alkynes



These types of procedures, however, are limited to relatively simple substrates without other reduction sites exist (i.e. esters, other alkynes, base labile groups...).

Successful indirect approaches towards *Z*-alkenylsilanes exist; however, a consistent theme exists in the requirement for the silyl group to already be installed in the molecule prior to either a coupling reaction or rearrangement. Although this often results in very stereo- and regioselective outcomes, affording silylalkynes typically requires use of strong bases and other substrate elaboration steps. This can make late-stage introduction of the silane in more complex settings challenging and less efficient. Creative catalyst designs for the efficient hydrosilylations of π -components in access to stereo- and regiodefined alkenylsilanes remain to be an atom-economical and attractive protocol in access to alkenyl- and allylsilanes.

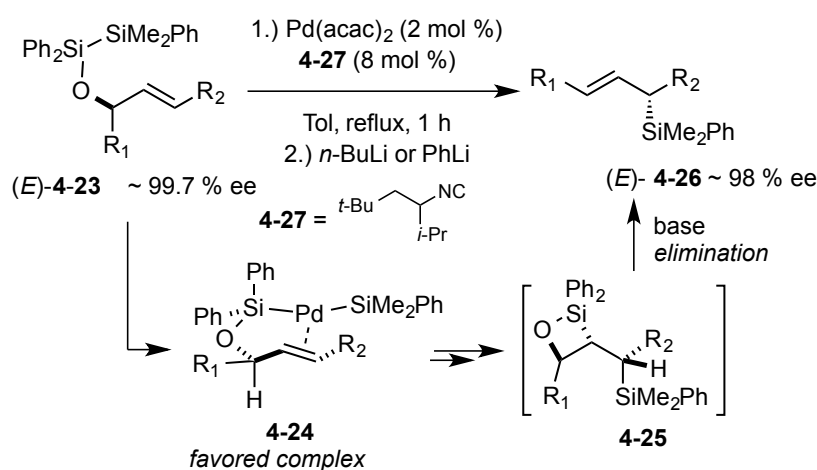
4.5 Access to *E*-Allylsilanes

Although the direct hydrosilylation of 1,3-dienes, previously discussed in Chapter 1, is typically the most direct method in access to *E*-allylsilanes, there are inherent challenges in preparing this type of diene substrate class, especially with increasing substitution patterns. As a result of the challenges in preparing *E*-allylsilanes and interest

in their use in synthesis, many indirect methods have been developed that introduce allylsilane functionality by alternate catalytic methods.

An example of a method that stereoselectively affords *E*-allylsilanes via indirect methods is the Pd-catalyzed disilylation and subsequent Peterson olefination reaction to afford chiral *E*-allylsilanes (Scheme 4-12).⁷⁰ In this transformation, enantioenriched chiral alcohols are protected with disilanes to afford **4-26**.

Scheme 4-12 Disilylation Route to Chiral Allylsilanes

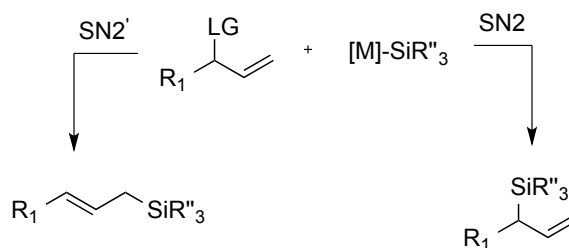


The palladium catalyst undergoes oxidative addition to the Si-Si bond and then coordinates to the *E*-alkene affording π -complex **4-24**. *Syn*-Migratory insertion then sets the stereochemistry of the dimethylsilyl group and subsequent reductive elimination affords intermediate **4-25** (Scheme 4-12). Treatment with a strong base then initiates the Peterson elimination that affords **4-26** with excellent transfer of chirality 98 % ee. This process simultaneously installs a silyl chiral center with retained olefin geometry; however, it requires a pre-functionalized allylic alcohol that is likewise a challenging substrate class.

Many other successful approaches have also been developed that exploit metal-catalyzed allylic substitutions to install allylsilane functionality. These methods require

more elaborate starting materials since direct hydrometalation of the majority of π -components would not afford allylic silanes, but alkenylsilane isomers. For example, many of these reactions utilize stereodefined allylic acetates, allylic halides, and allylic phosphonates with numerous catalysts.⁷¹ However, there are significant challenges with these types of operations including the difficulty in preparing allylic stereodefined substrates and harnessing regiocontrol in SN2' versus direct SN2 metal-catalyzed displacements affording mixtures of **4-28** and **4-29**.

Scheme 4-13 Allylic Substitution Pathways to Allylsilanes



4.6 Research Plan

Due to the challenge in accessing regio- and stereodefined alkenyl- and allylsilane reagent classes, we became interested in exploring the hydrosilylations of 1,3-disubstituted allenes. In contrast with additions to monosubstituted allenes, the addition across 1,3-disubstituted allenes would necessarily result in the formation of an alkene functionalized with a stereochemical configuration. Additionally, we were inspired by the challenge of controlling regio- and stereoselectivity for unsymmetrical allene substrates. We envisioned this substrate class as being an ideal opportunity to exploit differences in reaction mechanism to afford motifs not readily accessible via traditional alkyne and 1,3-diene hydrosilylation. Work presented in this chapter was performed in collaboration with visiting student Ruth Dorel (from ICIQ).

4.7 Evaluation of NHC Ligand Effects in 1,3-Disubstituted Allene Hydrosilylation

At the start of our exploration, we employed a strategy for catalyst generation that employed use of NHC hydrochloride salts, KO-*t*-Bu base, with either Pd₂dba₃ or Ni(COD)₂ pre-catalysts (Table 7). In additions to symmetrically *n*-Hexyl substituted allene, it was found that bulky IPr*OMe ligand **4-35** was ineffective for promoting the Pd-catalyzed hydrosilylation as only starting material was recovered (Entry 1, Table 7). Suspecting that the steric demands placed on the system by ligand **4-35** prevented reactivity, smaller NHC ligand IMes **4-33** was instead employed with Pd and favored the formation of *E*-allylsilane **4-32** in excellent regioselectivity (>98:2 allyl:vinyl) but in only moderate d.r. (75:25 *E/Z*) in 80 % yield (Table 7, entry 2). However, by changing the NHC ligand to larger ligand IPr **4-34** resulted in the formation of *E*-allylsilane **4-32** in excellent regio- and stereoselectivity (>98:2 regioSEL., >98:2 *E/Z*) in 75 % yield (Table 1, entry 3).

Table 7 Optimization Studies: 1,3-Disubstituted Allene Hydrosilylations

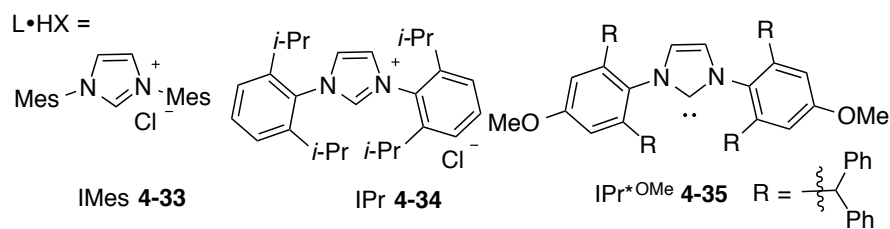
entry	precatalyst ^a	L•HX ^b	% yield, (regiosel. 4-31 : 4-32) ^c	4-31 (Z/E)	4-32 (E/Z)
1	Pd ₂ dba ₃	4-35	no reaction	not detected	not detected
2	Pd ₂ dba ₃	4-33	80 (<2:>98)	not detected	75:25
3	Pd ₂ dba ₃	4-34	75 (<2:>98)	not detected	>98:<2
4	Ni(COD) ₂	4-34	84 (60:40)	>98:<2	75:25
5	Ni(COD) ₂	4-35	89 (>98:<2)	>98:<2	not detected

^aReactions conducted with Ni(COD)₂/L•HX/KO-*t*-Bu: 10 mol %/ 10 mol %/ 10 mol %.

Reactions conducted with Pd₂dba₃/L•HX/KO-*t*-Bu: 2.5 mol %/5.0 mol %/ 5.0 mol %

^bReactions conducted with IPr*OMe were conducted in absence of base

^cRegioselectivity determined by GCMS and ¹H-NMR of crude material



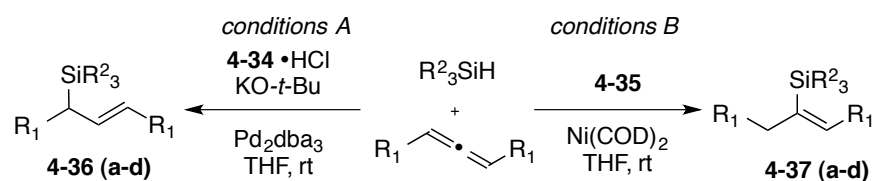
After locating the conditions that favored *E*-alkenylsilanes with Pd, we wondered whether stereodefined alkenylsilanes could be afforded with similar levels of regio- and stereocontrol with nickel-catalysis (Table 7, entries 4-5). Using the same catalyst generation strategy, it was found that reactions with Ni and ligand IPr **4-34** primarily afforded *Z*-alkenylsilane **4-31** in moderate regioselectivity (60:40 vinyl:allyl) and in 84 % yield, with a mixture of diastereomeric allylsilanes (75:25 *E/Z*) (Table 7, entry 4). However, increasing the steric bulk of the NHC ligand through the use of IPr*OMe **4-35** provided an efficient solution for *Z*-alkenylsilane generation, as **4-31** was exclusively

formed with exceptional regio- and stereoselectivity (>98:2 regioselect. & d.r.) in excellent yield 89 % (Table 7, entry 5).

4.8 Allene Substrate Exploration

Further exploration of these complementary methods commenced with the evaluation of symmetrically substituted 1,3-disubstituted allenes with Me₂PhSiH and BnMe₂SiH for both Ni (conditions B) and Pd based procedures (conditions A) (Table 8). Reactions with *n*-aliphatic substrates using conditions A afforded allylsilanes functionalized with BnMe₂SiH (**4-36a**) or Me₂PhSiH (**4-36b**) in excellent yields and stereoselectivities (Table 8, entries 1,2). More hindered aliphatics (**4-36c**) and silylether-containing Me₂PhSiH moieties (**4-36d**) were also afforded using the palladium protocol with high stereo- and regioselectivities (Table 8, entries 3-4). The protocol with Ni afforded *Z*-alkenylsilanes with *n*-aliphatics (**4-37a** and **4-37b**) for both BnMe₂SiH and Me₂PhSiH respectively (Table 8 entries 4-5). More hindered aliphatics (**4-37c**) and silylether-containing allenes (**4-37d**) were likewise coupled with Me₂PhSiH in high yields and selectivities (Table 8, entries 7-8).

Table 8 Metal-Directed 1,3-Disubstituted Allene Hydrosilylation



entry	R ₁	conditions ^a	silane	product, (% yield, regioselect. 4-37 : 4-36) ^b	d.r. (<i>E/Z</i>)
1	<i>n</i> -Hex	A	BnMe ₂ SiH	4-36a , 75 (<2:>98)	>98:<2
2	<i>n</i> -Hex	A	Me ₂ PhSiH	4-36b , 84 (<2:>98)	>98:<2
3	Cy	A	Me ₂ PhSiH	4-36c , 58 (<2:>98)	96:4
4	TBSO	A	Me ₂ PhSiH	4-36d , 64 (<2:>98)	>98:<2
5	<i>n</i> -Hex	B	BnMe ₂ SiH	4-37a , 89 (>98:<2)	<2:>98
6	<i>n</i> -Hex	B	Me ₂ PhSiH	4-37b , 75 (>98:<2)	<2:>98
7	Cy	B	Me ₂ PhSiH	4-37c , 65 (>98:<2)	<2:>98
8	TBSO	B	Me ₂ PhSiH	4-37d , 75 (>98:<2)	10:90

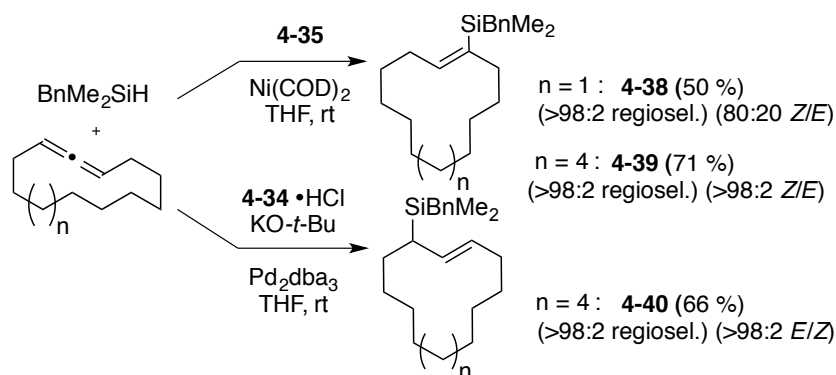
^aReactions conducted with Ni(COD)₂/L: 10 mol %/ 10 mol %/ 10 mol %.

Reactions conducted with Pd₂dba₃/L•HX/KO-*t*-Bu: 2.5 mol %/5.0 mol %/ 5.0 mol %

^bRegioselectivity determined by GCMS and ¹H-NMR of crude material

Cyclic allenes were also tolerated in the nickel- and palladium-based procedures to afford cyclic *Z*-alkenylsilanes or *E*-allylsilanes. Use of 12-membered cyclic allene with the nickel procedure afforded **4-38** in 50 % yield with excellent regioselectivity (>98:2) and good stereoselectivity (80:20 *Z/E*) (Scheme 4-14). By lowering the conformational restrictions imposed by the allene, a 15-membered cyclic allene was synthesized and afforded alkenylsilane **4-39** in excellent yield and exceptional stereoselectivity (>98:2 *Z/E*) (Scheme 4-14). Reactions with the same substrate only with the Pd protocol, afforded the complementary *E*-allylsilane **4-40** in good yield 66 % and exceptional regio- and stereoselectivity >98:2 (Scheme 4-14).

Scheme 4-14 Hydrosilylation of Cyclic Allenes



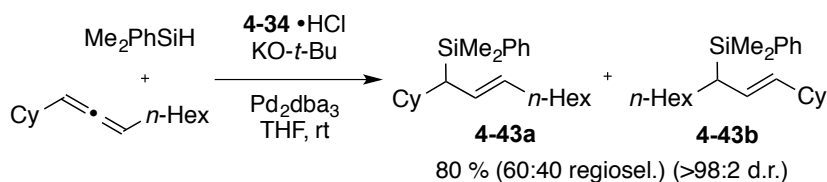
Especially challenging substrates were also tolerated with the nickel-based procedure as unsymmetrically substituted allenes were coupled with silanes to afford *Z*-alkenylsilanes in exceptional selectivities (Table 9). For selectivity to be consistently achieved, it was observed that one substituent (R_1 or R_2) needs to be sterically larger than the other. For example, it was found that an allene functionalized with *i*-Bu and *n*-Hex afforded an equal mixture of *Z*-alkenylsilanes in moderate yield 49 % (**4-41a** and **4-42a**, Table 9). However, by increasing one of the substituents to *i*-Pr while maintaining less hindered *n*-Hex afforded *Z*-alkenylsilane **4-41b** in exceptional regio- and stereoselectivities ($>98:2$) in 64 % yield. This effect was further explored with sterically differentiated allenes of Cy vs. *n*-Hex (**4-41c** and **4-41d**, Table 9) for both Me_2PhSiH and BnMe_2SiH and *t*-Bu vs. *n*-Hex (**4-41e**), all favoring *Z*-alkenylsilanes where the hydride adds to the carbon of the allene closest to the larger substituent. Further elaboration of the less hindered substituent while maintaining one substituent with greater steric encumbrance is also possible as aromatic containing (**4-41f**) and benzyl ether (**4-41g**) allenes resulted in highly regio- and stereoselective outcomes favoring the same *Z*-alkenylsilane isomers in high diastereomeric ratios.

Table 9 Additions to Unsymmetrically Substituted Allenes

entry ^a	R ₁	R ₂	silane	product, (% yield, regioisel. 41:42)	regioisel. (alkenyl:allyl)	d.r. (Z/E)
1	<i>i</i> -Bu	<i>n</i> -Hex	BnMe ₂ SiH	4-41a , (49, 50:50)	(91:9)	>98:2
2	<i>i</i> -Pr	<i>n</i> -Hex	BnMe ₂ SiH	4-41b , (64, 98:2)	(98:2)	>98:2
3	Cy	<i>n</i> -Hex	Me ₂ PhSiH	4-41c , (51, >98:2)	(>98:2)	>98:2
4	Cy	<i>n</i> -Hex	BnMe ₂ SiH	4-41d , (70, >98:2)	(>98:2)	>98:2
5	<i>t</i> -Bu	<i>n</i> -Hex	BnMe ₂ SiH	4-41e , (52, >98:2)	(>98:2)	>98:2
6	Cy	Ph	BnMe ₂ SiH	4-41f , (66, >98:2)	(>98:2)	90:10
7	Cy	BnO	BnMe ₂ SiH	4-41g , (72, >98:2)	(>98:2)	95:5

In contrast with the nickel based procedure, the Pd-catalyzed procedure results in only moderate regioselectivity with unsymmetrical substitution (Scheme 4-15). For example, *E*-dimethylphenylallylsilane **4-43a** was afforded in excellent yield and stereoselectivity; however, as a mixture (60:40) of regioisomers **4-43a** and **4-43b** (Scheme 4-15).

Scheme 4-15 Pd-Catalyzed Hydrosilylations of Unsymmetrical Substrates

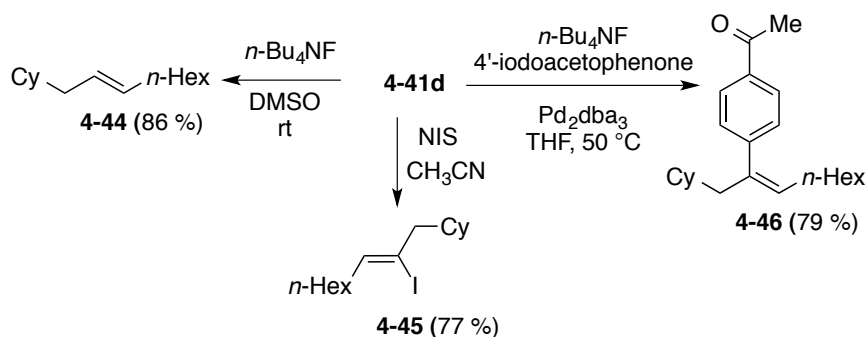


4.9 Synthetic Manipulations of Alkenylsilanes

The ability to transform unsymmetrically substituted allenenes into regio- and stereodefined *Z*-alkenylsilane intermediates can be a potentially powerful synthetic

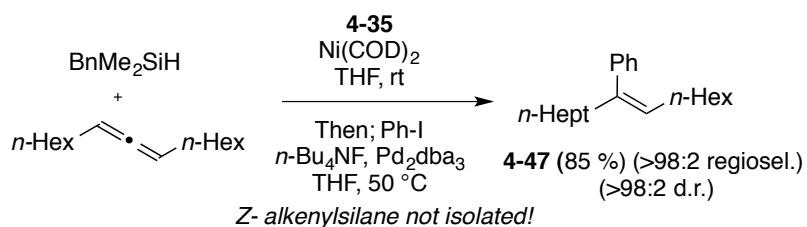
handle for a variety of synthetic manipulations (Scheme 4-16). For example, intermediate **4-41d**, afforded by direct regio- and stereoselective allene hydrosilylation, can afford net reduced *trans*-alkene **4-44** in 86 % yield, an alternate protocol to hydrogenative protocols with harsh conditions. Treatment of **4-41d** with NIS also afford stereodefined iodide **4-45** in 77 % yield as only one isomer (Scheme 4-16). In addition, the Pd-catalyzed cross-coupling reaction of **4-41d** with 4'-iodoacetophenone furnishes trisubstituted *Z*-arylalkene **33** in excellent yield 79%.

Scheme 4-16 Synthetic Manipulations of Stereo- and Regiodefined Alkenylsilanes



Reactions with symmetrically substituted allenes are also potentially appealing synthons in access to stereodefined trisubstituted alkenes. A demonstration of this is presented (Scheme 4-17), whereby coupling the hydrosilylation reaction in tandem with a Pd-cross-coupling reaction in one-pot affords net hydroarylation products without the requirement of subsequent isolation and purification steps. For example, *n*-hexyl disubstituted allene was hydrosilylated by action of the nickel NHC catalyst and then subsequently treated with an activator, Pd_2dba_3 , and iodobenzene furnished trisubstituted olefin **4-47** in excellent yield 85 % as one stereo- and regioisomer (Scheme 4-17).

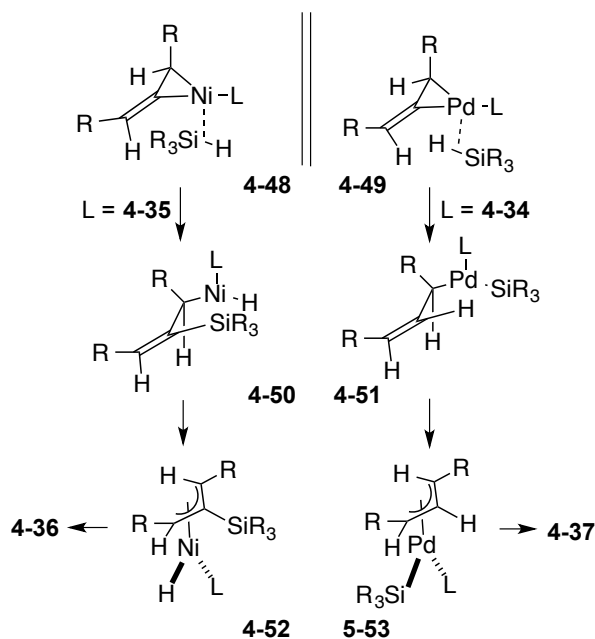
Scheme 4-17 One-Pot Hydroarylation



4.10 Proposed Mechanisms

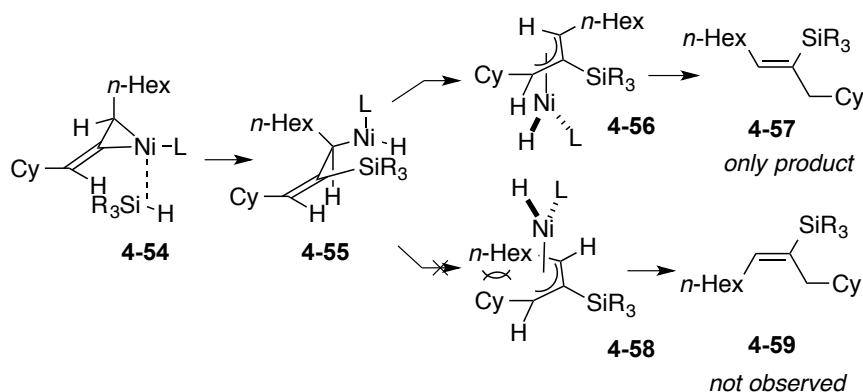
Based on these studies, we propose two metal-divergent mechanisms for the hydrosilylations of 1,3-disubstituted allenes (Scheme 4-18). Based on the cross-over studies from Chapter 2, the silane structure remains associated with the metal catalyst and recent computational studies have demonstrated that oxidative addition/migratory insertion happens in one step. This disfavors a mechanism that involves disproportionation to a Ni-H or Ni-SiR₃. Coordination to the allene at the least sterically hindered face by Ni and Pd affords **4-34** and **4-35** respectively. When the ligand is bulky with Ni, the π complex favors arrangement with the silane directed away from this impending steric interaction (Scheme 4-18). As observed in our previous studies, the palladium catalyst inherently prefers hydrometalation pathways, so **4-51** forms with the hydride ligand closest to the central allene carbon.

Scheme 4-18 Proposed Hydrosilylation Mechanisms



Both processes undergo migratory insertion/oxidative addition sequences affording **4-50** with Ni and **4-51** with Pd. Stereoselective bond rotation then occurs forming π -allyl intermediate **4-52** (with Ni) and **4-53** (with Pd), therefore avoiding potential allylic 1,3-strain. Reductive elimination occurs directly from these intermediates as governed by the geometry of the trigonal π -complex, as a high kinetic barrier for ligand exchange is predicted to exist based on previous studies. Elimination at the carbon of the complex with the least steric interactions between NHC ligand L and R affords products **4-36** with Ni and **4-37** with Pd. Significant insights in allene/aldehyde nickel-catalyzed reductive couplings likewise provide evidence for metal-catalysts interacting with 1,3-disubstituted allenes to afford *Z*-stereodefined allylic alcohols.⁷²

Scheme 4-19 Origin of Selectivity with Unsymmetrical Substrates

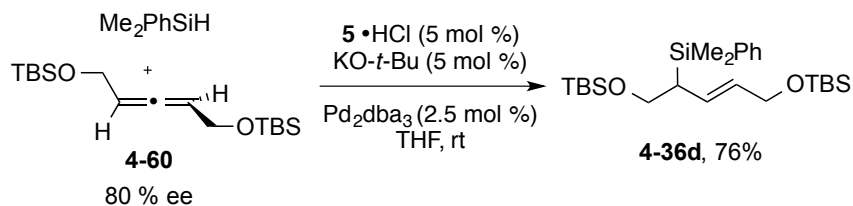


For cases with unsymmetrically substituted allenes with the nickel protocol, a similar sequence is invoked where selective coordination occurs with minimized steric interactions to afford **4-54** (Figure 4-19). Oxidative addition/migratory insertion then affords **4-55** and reductive elimination at the more congested carbon affords the observed products **4-57** (Figure 4-19). Formation of intermediate **4-58** is disfavored as mentioned above, and products **4-59** that would be formed through this route are not routinely observed. Similar additions with Pd NHC catalysts affording mixtures of allylsilanes (Scheme 4-15) are likely unselective due to differences in steric repulsions afforded by having a metal-silyl (instead of metal-hydride) reductive elimination step. In these cases, the ligand likely imposes a more significant repulsion to the allene substituents R, making the transition states closer in energy; and thus more unselective for a regioisomer.

An experiment that was performed to gain more information about the operative mechanistic pathways was the hydrosilylation of enantioenriched allenes (Scheme 4-20). In accordance with our proposed pathways, we envisioned a high degree of chirality transfer to occur in Pd-catalyzed additions to enantioenriched substrates. Enantioenriched

allene **4-60** was synthesized from the respective enantioenriched propargyl alcohol. The enantioenriched secondary carbinol was afforded following Carreira's protocol and this intermediate was transformed into **4-60** by Myers' protocol employing the well-studied sigmatropic reductive pathways of diazene intermediates.^{73,74}

Scheme 4-20 Additions to Enantioenriched Allenes



We found that addition of Me_2PhSiH to an enantioenriched allene afforded the allylsilane in high yield; however, finding assay conditions with modern HPLC chiral columns that directly resolved both enantiomers were not located. Transformation of the allylsilane to more polar silyl alcohols by regio- and stereoselective hydroboration/oxidation sequence proved unsuccessful as the afforded products were not consistent with the anticipated product.⁷⁰ Future work in re-designing this experiment, mainly in selection of substrate and method for determination of the chirality transfer and absolute stereochemistry is warranted as it could definitively outrule a *syn*-migratory insertion pathway.

4.11 Conclusions and Outlook

In summary, the hydrosilylation of 1,3-disubstituted allenes is an effective protocol in the synthesis of *E*-allylsilanes and *Z*-alkenylsilanes. It was found that the metal identity Pd vs. Ni could be exploited to not only direct the regiochemical outcome but to also dictate the olefin geometry to afford useful products not readily available by other means. It is predicted that the pathways undergo *anti*-migratory insertion pathways

that differ by silylmetalation (with Ni) and hydrometalation (with Pd) pathways. This work demonstrates that NHC ligands are useful with transition-metal catalysts in controlling the regiochemical and stereochemical outcome in simple, two-component couplings. Future work in exploring the utility of NHC catalysts in related classes of two-component couplings are currently underway.

4.12 Experimental

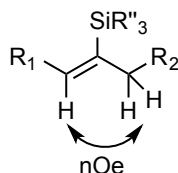
General: All reagents were used as received unless otherwise noted. Solvents were purified under nitrogen using a solvent purification system (Innovative Technology, Inc. Model # SPS-400-3 and PS-400-3). *Tris*(dibenzylideneacetone)-dipalladium (Pd₂dba₃) was purchased from Sigma Aldrich and was stored in a glovebox and on the benchtop. All reactions were conducted under an atmosphere of nitrogen with magnetic stirring in flame-dried or oven-dried (120 °C) glassware. All acyclic allenes were made according to literature precedent from the terminal alkyne and aldehyde.⁷⁵ Cyclic allenes were made according to literature precedent from the respective ketones.⁷⁶ Ligand **4-35** (IPr*^{OMe}) was purchased from Strem and was stored in a glovebox. NHC Ligands **4-33** (IMes·HCl) and **4-34** (IPr·HCl) were purchased from Sigma-Aldrich and stored and weighed in a glovebox. Dimethylphenylsilane and dimethylbenzylsilane (purchased from Sigma-Aldrich) were used as received. A solution of tetra-*n*-butylammonium (TBAF, 1.0 M in THF, purchased from Sigma-Aldrich). Cyclohexylallene, propylsilane, and *d*-triethylsilane (>99% purity) were purchased from Sigma-Aldrich and was used as received. Iodobenzene, 4'-iodoacetophenone, and *N*-iodosuccinimide were purchased from Sigma-Aldrich and used as received. ¹H and ¹³C spectra were obtained in CDCl₃ at rt (25 °C), unless otherwise noted, on a Varian Mercury 400 MHz instrument, Varian Unity 500 MHz instrument, or Varian Unity 700 MHz instrument. Chemical shifts of ¹H NMR spectra were recorded in parts per million (ppm) on the δ scale from an internal standard of residual chloroform (7.24 ppm). Chemical shifts of ¹³C NMR spectra were recorded in ppm from the central peak of CDCl₃ (77.0 ppm) on the δ scale. High-resolution mass spectra (HRMS) were obtained on a VG-70-250-s spectrometer

manufactured by Micromass Corp. (Manchester UK) at the University of Michigan Mass Spectrometry Laboratory. Regioisomeric ratios were determined on crude reaction mixtures using NMR or GC. GC analyses were carried out on an HP 6980 Series GC System with HP-5MS column (30 m x 0.252 mm x 0.25 μ m). When noted, a Biotage purification system (model # SP1) was utilized with SNAP (10 g) silica columns. Reported regioselectivities were determined by GCMS analysis and confirmed by ^1H NMR analysis by comparing the ratios of detectable alkenyl protons of the major and minor regioisomers in the crude reaction mixture. In cases where >98:2 regio- or stereoselectivity is reported, minor isomers were not detected by either GCMS or NMR based methods.

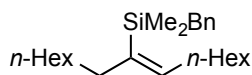
General Procedure I for the $\text{Ni}(\text{COD})_2/\text{IPr}^*\text{OMe}$ – promoted hydrosilylation of 1,3-disubstituted allenes:

THF (1.0 mL) was added to a solid mixture of IPr*OMe **4-35** (0.05 mmol) and $\text{Ni}(\text{COD})_2$ (0.05 mmol) at rt. After stirring for 10 min at rt the silane (0.5 mmol) was added. The reaction mixture was stirred for 10 min at rt followed by the addition of allene (0.5 mmol) in THF (3.0 mL) over 1 h by syringe pump. The reaction mixture was stirred at rt until TLC analysis indicated disappearance of the allene. The reaction mixture was filtered through silica gel eluting with 50% v/v EtOAc/hexanes. The solvent was removed *in vacuo*, and the crude residue was purified via flash column chromatography on silica gel to afford the desired product.

The configuration of the olefin was determined by 1D NOE for all products where relevant, where alkenyl protons for all major isomers were determined to have the following observable correlation (verifying *Z* stereochemistry):

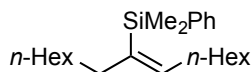


(Z)-Benzyl dimethyl(tetradec-7-en-7-yl)silane (4-37a) (Table 8, entry 1)



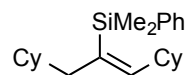
General procedure I was followed with Ni(COD)₂ (13.8 mg, 0.05 mmol), IPr*OMe **4-35** (47.2 mg, 0.05 mmol), benzyldimethylsilane (79 μ L, 0.5 mmol), and pentadeca-1,7-diene (104 mg, 0.5 mmol). The crude residue was purified by flash chromatography (100% hexanes) affording a clear oil (159 mg, 89% yield). ¹H NMR (400 MHz, CDCl₃): δ 7.19 (t, J = 7.8 Hz, 2H), 7.05 (m, 1H), 7.00 (m, 2H), 5.97 (t, J = 7.2 Hz, 1H), 2.20 (s, 2H), 2.01 – 2.08 (m, 2H), 1.93 – 1.99 (m, 3H), 1.15 – 1.36 (m, 21H), 0.88 (m, 7H), 0.080 (s, 6H); ¹³C NMR (100 MHz, CDCl₃): δ 144.0, 140.3, 137.4, 128.32, 128.27, 128.0, 123.9, 38.4, 32.3, 31.9, 31.8, 30.0, 29.4, 29.2, 29.1, 28.5, 26.7, 22.7, 22.6, 14.1, -1.7; IR (thin film): ν 2953.5, 2923.7, 2853.6, 1716.2, 1600.8, 1493.2, 1452.2, 1377.5, 1248.7, 1056.5, 826.3 cm⁻¹; HRMS (EI⁺) (m/z): [M⁺] calc for C₂₄H₄₂Si, 358.3056; found, 358.3066.

(Z)-Dimethyl(phenyl)(tetradec-7-en-7-yl)silane (4-37b) (Table 8, entry 2)



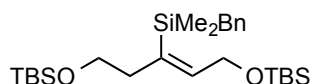
General procedure I was followed with Ni(COD)₂ (13.8 mg, 0.05 mmol), IPr*OMe **4-35** (47.2 mg, 0.05 mmol), dimethylphenylsilane (77 μ L, 0.5 mmol), and pentadeca-1,7-diene (104 mg, 0.5 mmol). The crude residue was purified by flash chromatography (100% hexanes) affording a clear oil (147 mg, 85 % yield). ¹H NMR (400 MHz, CDCl₃): δ 7.52 (m, 2H), 7.33 (m, 3H), 6.04 (t, J = 7.2 Hz, 1H), 2.08 (t, J = 7.2 Hz, 2H), 1.91 (q, J = 7.2 Hz, 2H), 1.16 – 1.36 (m, 16H), 1.08 – 1.15 (m, 5H), 0.87 (t, J = 8.0 Hz, 3H), 0.83 (t, J = 8.0 Hz, 3H), 0.369 (s, 6H); ¹³C NMR (100 MHz, CDCl₃): δ 144.8, 140.2, 136.9, 133.8, 128.6, 127.6, 38.6, 32.5, 31.9, 31.7, 31.0, 29.8, 29.4, 29.2, 28.9, 22.7, 22.6, 14.12, 14.06, -0.83; IR (thin film): 2954.0, 2923.6, 2855.0, 1708.5, 1610.1, 1465.0, 1427.5, 1248.5, 1110.7, 831.2 cm⁻¹; HRMS (EI⁺) (m/z): [M-CH₃]⁺ calc for C₂₂H₃₇Si, 329.2665; found 329.2669.

(Z)-(1,3-Dicyclohexylprop-1-en-2-yl)dimethyl(phenyl)silane (4-37c) (Table 8, entry 3)



General procedure I was followed with Ni(COD)₂ (13.8 mg, 0.05 mmol), IPr*OMe **4-35** (47.2 mg, 0.05 mmol), dimethylphenylsilane (77 μL, 0.5 mmol), and 1,3-dicyclohexylpropa-1,2-diene (102 mg, 0.5 mmol). The crude residue was purified by flash chromatography (100% hexanes) affording a clear oil (110.7 mg, 65%). ¹H NMR (500 MHz, CDCl₃): δ 7.50 - 7.57 (m, 2H), 7.30 - 7.36 (m, 3H), 5.75 (d, *J* = 10.4 Hz, 1H), 1.99 - 2.05 (m, 1H), 1.97 (dd, *J* = 6.8, 0.6 Hz, 2H), 1.63 - 1.71 (m, 5H), 1.50 - 1.60 (m, 4H), 1.41 - 1.36 (m, 2H), 1.11 - 1.22 (m, 4H), 0.91 - 1.01 (m, 4H), 0.74 - 0.84 (m, 2H), 0.38 (s, 6H); ¹³C NMR (100 MHz, CDCl₃): δ 151.72, 140.51, 133.70, 132.89, 128.48, 127.50, 46.62, 41.24, 37.65, 33.11, 32.95, 26.77, 26.49, 25.92, 25.65, -0.81; IR (thin film): ν 2918.4, 2846.8, 1609.5, 1446.8, 1426.3, 1245.8, 1108.6, 903.4, 830.3, 812.1, 768.4, 727.2, 698.0, 675.0 cm⁻¹; HRMS (EI⁺) (*m/z*): [*M*⁺] calc for C₂₃H₃₆Si, 340.2586; found, 340.2585.

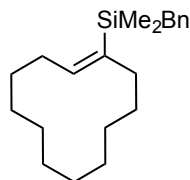
(Z)-7-(benzyltrimethylsilyl)-2,2,3,3,11,11,12,12-octamethyl-4,10-dioxa-3,11-disilatridec-6-ene (4-37d) (Table 8, entry 4)



General procedure I was followed with Ni(COD)₂ (2.9 mg, 0.00105 mmol), IPr*OMe **4-35** (9.8 mg, 0.00105 mmol), benzyltrimethylsilyl (33 μL, 0.21 mmol), and 2,2,3,3,11,11,12,12-octamethyl-4,10-dioxa-3,11-disilatrideca-6,7-diene (70 mg, 0.21 mmol). The crude residue was purified by flash column chromatography (10% EtOAc: hexanes) affording a clear oil (75 mg, 75 % yield). ¹H NMR (500 MHz): δ 7.18 (t, *J* = 9.0 Hz, 2H), 7.05 (t, *J* = 9.0 Hz, 1H), 6.97 (d, *J* = 9.0 Hz, 2H), 6.13 (t, *J* = 7.4, 1 H, major isomer), 5.90 (t, *J* = 7.4 Hz, 0.1H, minor isomer), 4.04 (d, *J* = 9.4 Hz, 2H), 3.42 (t, *J* = 8.5 Hz, 2H), 2.23 (t, *J* = 7.4 Hz, 2H), 2.16 (s, 2H), 0.88 (s, 10H), 0.86 (s, 10H), 0.098 (s, 6H), 0.035 (s, 6H), 0.0093 (s, 6H); ¹³C NMR (125 MHz, CDCl₃): δ 145.4, 143.9 (minor), 139.6, 139.4 (minor), 135.3, 128.3, 128.1, 124.2, 124.0 (m

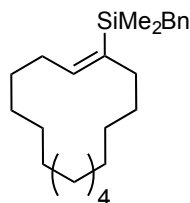
inor), 63.9, 62.7, 40.9, 26.5, 26.02, 26.00, 18.4, -0.09, -1.9, -5.1, -5.2; IR (thin film): ν 2953.5, 2926.2, 2856.6, 1704.1, 1601.0, 1462.4, 1250.7, 1089.8, 831.8, 697.8 cm^{-1} ; HRMS (ESI⁺) (m/z): [M+Na]⁺ calc for C₂₆H₅₀S₃O₂, 501.3011; found, 501.3009.

(Z)-Benzyl(cyclododec-1-en-1-yl)dimethylsilane (4-38) (Scheme 4-14)



General procedure I was followed with Ni(COD)₂ (5.5 mg, 0.02 mmol), IPr*OMe **4-35** (18.9 mg, 0.02 mmol), benzyldimethylsilane (32 μL , 0.2 mmol), and cyclododeca-1,2-diene (33 mg, 0.2 mmol). The crude residue was purified by flash chromatography (100% hexanes) affording a clear oil (78.6 mg, 50 %), *Z/E*= 79:21. ¹H NMR (400 MHz, CDCl₃): δ 7.24 – 7.16 (m, 2H), 7.06 (t, *J* = 7.4 Hz, 1H), 7.03 – 6.97 (m, 2H), 6.18 (t, *J* = 7.6 Hz, 1H), 2.23 (s, 2H), 2.22 – 2.18 (m, 2H), 2.17 – 2.12 (m, 2H), 1.71 – 1.60 (m, 2H), 1.58 – 1.51 (m, 2H), 1.48 – 1.21 (m, 12H), 0.10 (s, *J* = 3.1 Hz, 6H); ¹³C NMR (100 MHz, CDCl₃): δ 146.62, 140.24, 136.11, 128.32, 128.00, 123.89, 37.58, 32.18, 26.92, 26.82, 26.67, 26.47, 25.92, 25.81, 24.92, 24.43, 24.13, -1.73; IR (thin film): ν 3060.1, 3024.0, 2920.6, 2850.6, 1600.5, 1492.8, 1449.9, 1406.8, 1345.7, 1247.5, 1204.7, 1153.1, 1056.2, 1029.7, 901.7, 811.8 cm^{-1} ; HRMS (EI⁺) (m/z): [M⁺] calc for C₂₁H₃₄Si, 314.2430; found 314.2428.

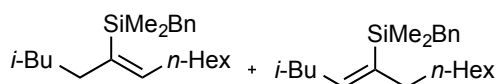
(Z)-Benzyl(cyclopentadec-1-en-1-yl)dimethylsilane (4-39) (Scheme 4-14)



General procedure I was followed with Ni(COD)₂ (6.6 mg, 0.024 mmol), IPr*OMe **4-35** (22.7 mg, 0.024 mmol), benzyldimethylsilane (37.9 μL , 0.24 mmol), and cyclopentadeca-1,2-diene (50 mg, 0.24 mmol). The crude residue was purified by flash chromatography (100% hexanes) affording a clear oil (61 mg, 71% yield). ¹H NMR (500 MHz, CDCl₃):

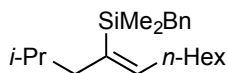
δ 7.18 (t, $J = 9.9$ Hz, 2H), 7.04 (t, $J = 9.9$ Hz, 1H), 7.00 (d, $J = 9.9$ Hz, 2H), 5.94 (t, $J = 8.6$ Hz, 1H), 2.21 (s, 2H), 2.17 (m, 2H), 2.07 (m, 2H), 1.39 – 1.47 (m, 2H), 1.16 – 1.38 (m, 20H), 0.069 (s, 6H); ^{13}C NMR (175 MHz, CDCl_3): 145.2, 140.3, 137.3, 128.3, 128.0, 123.9, 37.6, 31.2, 29.4, 29.0, 27.7, 27.6, 27.25, 27.20, 27.1, 26.9, 26.8, 26.7, 26.5, 26.0, -1.7; IR (thin film): ν 2925.9, 2855.4, 1493.2, 1451.4, 1248.6, 1151.4, 828.7 cm^{-1} ; HRMS (EI^+) (m/z): $[\text{M}]^+$ calc for $\text{C}_{24}\text{H}_{40}\text{Si}$, 356.2899; found, 356.2901.

(Z)-Benzyldimethyl(2-methyldodec-5-en-5-yl)silane and (Z)-benzyldimethyl(2-methyldodec-4-en-5-yl)silane (4-41 a and 4-42a) (Table 9, entry 1)



General procedure I was followed with $\text{Ni}(\text{COD})_2$ (13.8 mg, 0.05 mmol), IPr^*OMe **4-35** (47.2 mg, 0.05 mmol), benzyldimethylsilane (79 μL , 0.5 mmol), and 2-methyldodeca-14,5-diene (90.2 mg, 0.5 mmol). The crude residue was purified by flash chromatography (100% hexanes) affording a clear oil (114 mg, 69% yield). ^1H NMR (400 MHz, CDCl_3): δ 7.21 (t, $J = 8.0$ Hz, 4H), 7.07 (t, $J = 8.0$ Hz, 2H), 7.01 (d, $J = 7.1$ Hz, 4H), 6.02 (t, $J = 8.0$ Hz, 1H), 5.99 (t, $J = 8.0$ Hz, 1H), 5.09 (m, 0.19H (minor allyl isomer)), 2.22 (s, 4H), 2.13 (m, 1H), 1.94 -2.09 (m, 9H), 1.61 (m, 1H), 1.48 (m, 2H), 1.20 – 1.39 (m, 25H), 1.05 – 1.12 (m, 2H), 0.88 – 0.94 (m, 15H), 0.87 (s, 4H), 0.85 (s, 3H), 0.10 (s, 4H), 0.097 (s, 4H), 0.07 (s, 2H); ^{13}C NMR (100 MHz, CDCl_3): δ 146.2, 143.9, 142.9, 140.4, 140.29, 140.27, 139.7, 134.9, 128.3, 128.0, 125.1, 123.9, 123.8, 45.3, 41.1, 40.5, 38.6, 37.2, 36.3, 32.3, 31.9, 31.8, 31.02, 30.1, 29.6, 29.4, 29.2, 29.1, 29.0, 28.3, 27.9, 26.8, 26.7, 26.5, 22.64, 22.60, 22.46, 14.1, -1.64, -1.7, -1.9; IR (thin film): ν 2952.9, 2924.8, 1600.8, 1493.1, 1465.3, 1248.1, 1205.2, 1153.5, 1055.9, 826.1 cm^{-1} ; HRMS (EI^+) (m/z): $[\text{M}]^+$ calc for $\text{C}_{22}\text{H}_{38}\text{Si}$, 330.2743; found, 330.2739.

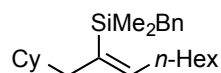
(Z)-Benzyldimethyl(2-methylundec-4-en-4-yl)silane. (4-41b) (Table 9, entry 2)



General procedure I was followed with $\text{Ni}(\text{COD})_2$ (13.8 mg, 0.05 mmol), IPr^*OMe **4-35** (47.2 mg, 0.05 mmol), benzyldimethylsilane (79 μL , 0.5 mmol), and 2-methylundeca-

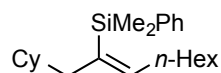
3,4-diene (83.2 mg, 0.5 mmol). The crude residue was purified by flash chromatography (100% hexanes) affording a clear oil (101.3 mg, 64%). ^1H NMR (500 MHz, CDCl_3): δ 7.27 – 7.22 (m, 2H), 7.11 (t, $J = 7.4$ Hz, 1H), 7.08 – 7.05 (m, 2H), 5.99 (t, $J = 7.5$ Hz, 1H), 2.27 (s, 2H), 2.15 (d, $J = 7.3$ Hz, 2H), 1.94 (d, $J = 6.9$ Hz, 2H), 1.55 – 1.45 (m, 1H), 1.43 – 1.30 (m, 8H), 0.95 (t, $J = 7.0$ Hz, 3H), 0.88 (d, $J = 6.6$ Hz, 6H), 0.14 (s, $J = 12.2$ Hz, 6H); ^{13}C NMR (125 MHz, CDCl_3): δ 145.62, 140.29, 136.17, 128.29, 128.07, 123.96, 48.37, 32.48, 31.88, 30.17, 29.21, 28.18, 26.77, 22.69, 22.34, 14.12, -1.70. IR (cm^{-1}): ν 2951.5, 2921.7, 2851.0, 1601.2, 1492.6, 1461.3, 1451.2, 1363.5, 1247.3, 1204.7, 1153.3, 1055.9, 901.0, 825.2, 789.5, 759.3, 696.5 cm^{-1} ; HRMS (EI^+) (m/z): [M^+] calc for $\text{C}_{21}\text{H}_{36}\text{Si}$, 316.2586; found, 316.2590.

(Z)-Benzyl(1-cyclohexylnon-2-en-2-yl)dimethylsilane (4-41c) (Table 9, entry 4)



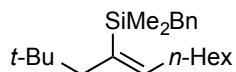
General procedure I was followed with $\text{Ni}(\text{COD})_2$ (13.8 mg, 0.05 mmol), IPr^*OMe **4-35** (47.2 mg, 0.05 mmol), benzyldimethylsilane (79 μL , 0.5 mmol), and nona-1,2-dienylcyclohexane (103 mg, 0.5 mmol). The crude residue was purified by flash chromatography (100% hexanes) affording a clear oil (124 mg, 71%). ^1H NMR (500 MHz, CDCl_3): δ 7.25 – 7.19 (m, 2H), 7.09 (t, $J = 7.4$ Hz, 1H), 7.05 – 7.01 (m, 2H), 5.93 (t, $J = 7.5$ Hz, 1H), 2.23 (s, 2H), 2.11 (d, $J = 7.4$ Hz, 2H), 1.90 (d, $J = 6.8$ Hz, 2H), 1.73 – 1.63 (m, 5H), 1.41 – 1.27 (m, 8H), 1.21 – 1.12 (m, 3H), 1.11 – 1.04 (m, 1H), 0.92 (t, $J = 7.0$ Hz, 3H), 0.86 – 0.74 (m, 2H), 0.10 (s, $J = 2.7$ Hz, 6H); ^{13}C NMR (125 MHz, CDCl_3): δ 145.51, 140.29, 135.36, 128.24, 128.05, 123.92, 46.79, 37.67, 33.21, 32.43, 31.82, 30.14, 29.18, 26.76, 26.74, 26.47, 22.66, 14.09, -1.70; IR (thin film): ν 2918.5, 2849.2, 1600.9, 1492.4, 1448.8, 1246.7, 1205.0, 1153.4, 1055.7, 900.8, 826.8, 789.5, 759.1, 696.3 cm^{-1} ; HRMS (EI^+) (m/z): [M^+] calc for $\text{C}_{24}\text{H}_{40}\text{Si}$, 356.2899; found, 356.2894.

(Z)-(1-Cyclohexylnon-2-en-2-yl)dimethyl(phenyl)silane (4-41c) (Table 9, entry 3)



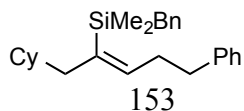
General procedure I was followed with Ni(COD)₂ (13.8 mg, 0.05 mmol), IPr*OMe **4-35** (47.2 mg, 0.05 mmol), dimethylphenylsilane (77 μL, 0.5 mmol), and nona-1,2-dien-1-ylcyclohexane (103 mg, 0.5 mmol). The crude residue was purified by flash chromatography (100% hexanes) affording a clear oil (87.3 mg, 51%). ¹H NMR (500 MHz, CDCl₃): δ 7.57 – 7.52 (m, 2H), 7.37 – 7.32 (m, 3H), 6.00 (t, *J* = 7.5 Hz, 1H), 2.01 (d, *J* = 6.8 Hz, 2H), 1.96 (q, *J* = 7.4 Hz, 2H), 1.74 – 1.67 (m, 4H), 1.67 – 1.62 (m, 1H), 1.28 – 1.11 (m, 12H), 0.93 – 0.77 (m, 2H), 0.86 (t, *J* = 7.3 Hz, 3H), 0.40 (s, 6H); ¹³C NMR (125 MHz, CDCl₃): δ 146.12, 140.23, 134.89, 133.73, 128.52, 127.58, 46.90, 37.72, 33.19, 32.54, 31.70, 29.81, 28.96, 26.75, 26.47, 22.58, 14.05, -0.84; IR (thin film): ν 2918.3, 2848.9, 1609.0, 1447.8, 1426.7, 1246.4, 1109.0, 831.0, 812.4, 769.2, 726.6, 698.3, 669.5 cm⁻¹; HRMS (EI⁺) (*m/z*): [M⁺] calc for C₂₃H₃₈Si, 342.2743; found 342.2740.

(Z)-Benzyl(2,2-dimethylundec-4-en-4-yl)dimethylsilane (4-41e) (Table 9, entry 5)



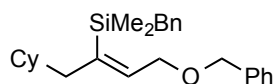
General procedure I was followed with Ni(COD)₂ (13.8 mg, 0.05 mmol), IPr*OMe **4-35** (47.2 mg, 0.05 mmol), benzyltrimethylsilane (79 μL, 0.5 mmol), and 2,2-dimethylundeca-3,4-diene (90.2 mg, 0.5 mmol). The crude residue was purified by flash chromatography (100% hexanes) affording a clear oil (86.0 mg, 52%). ¹H NMR (500 MHz, CDCl₃): δ 7.22 (t, *J* = 7.6 Hz, 2H), 7.08 (t, *J* = 7.4 Hz, 1H), 7.05 – 7.01 (m, 2H), 6.05 (t, *J* = 7.6 Hz, 1H), 2.26 (s, 2H), 2.17 (d, *J* = 7.6 Hz, 2H), 1.97 (s, 2H), 1.45 – 1.38 (m, 2H), 1.37 – 1.28 (m, 6H), 0.92 (t, *J* = 7.0 Hz, 3H), 0.87 (s, 9H), 0.10 (s, *J* = 4.4 Hz, 6H); ¹³C NMR (126 MHz, CDCl₃): δ 148.74, 140.56, 134.38, 128.32, 128.05, 123.90, 49.36, 32.99, 32.04, 31.85, 30.14, 29.87, 29.25, 26.90, 22.66, 14.11, -1.18. IR (cm⁻¹): ν 2949.6, 2853.0, 1600.2, 1492.4, 1451.1, 1361.0, 1247.7, 1203.8, 1153.8, 1056.5, 826.5, 790.3, 759.8, 696.5; HRMS (EI⁺) (*m/z*): [M⁺] calc for C₂₂H₃₈Si [M-H]⁺ 315.2508, found 315.2508.

(Z)-Benzyl(1-cyclohexyl-5-phenylpent-2-en-2-yl)dimethylsilane (4-41f) (Table 9, entry 6)



General procedure I was followed with Ni(COD)₂ (13.8 mg, mmol), IPr*OMe **4-35** (16.3 mg, 0.03 mmol), benzyldimethylsilanesilane (79 μ L, 0.5 mmol), and (5-cyclohexylpenta-3,4-dien-1-yl)benzene (113 mg, 0.5 mmol). The crude residue was purified by flash chromatography (100% hexanes) affording a clear oil (141 mg, 71 % yield). ¹H NMR (400 MHz, CDCl₃): δ 7.27 (m, 2H), 7.16 (m, 4H), 7.04 (m, 1H), 6.95 (m, 3H), 5.93 (t, *J* = 7.3 Hz, 1H), 2.65 (t, *J* = 8.0 Hz, 2H), 2.40 (q, *J* = 8.0 Hz, 2H), 2.15 (s, 2H), 2.04 (s, 2H), 1.86 (d, *J* = 7.1 Hz, 2H), 1.56 – 1.70 (m, 9H), 1.04 – 1.23 (m, 6H), 0.732 (m, 3H), 0.043 (s, 6H); ¹³C NMR (175 MHz, CDCl₃): δ 144.0, 141.9, 140.1, 136.5, 128.5, 128.3, 128.2, 128.1, 125.8, 124.0, 46.7, 37.6, 36.4, 34.3, 33.2, 26.7, 26.6, 26.4, -1.74; IR (thin film): ν 2361.1, 2339.1, 2177.6, 1134.0, 667.9, 437.8 cm⁻¹; HRMS (EI⁺) (m/z): [M-Me]⁺ calc for C₂₅H₃₃Si, 261.2352; found, 361.2359.

(Z)-Benzyl(4-(benzyloxy)-1-cyclohexylbut-2-en-2-yl)dimethylsilane (4-41 g) (Table 9, entry 7)

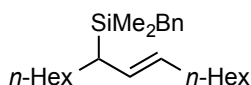


General procedure I was followed with Ni(COD)₂ (13.8 mg, 0.05 mmol), IPr*OMe **4-35** (47.2 mg, 0.05 mmol), benzyldimethylsilane (79 μ L, 0.5 mmol), and (((4-cyclohexylbuta-2,3-dien-1-yl)oxy)methyl)benzene (121 mg, 0.5 mmol). The crude residue was purified by flash chromatography (5 % EtOAc: hexanes) affording a clear oil (130 mg, 66 % yield). ¹H NMR (400 MHz, CDCl₃): 7.32 (d, *J* = 4.5 Hz, 4H), 7.27 (m, 1H), 7.17 (t, *J* = 7.4 Hz, 2H), 7.05 (t, *J* = 7.4 Hz, 1H), 6.931 (d, *J* = 7.4 Hz, 2H), 6.09 (t, *J* = 6.9 Hz, 1H), 4.46 (s, 2H), 3.93 (d, *J* = 6.9 Hz, 2H), 2.12 (s, 2H), 1.93 (d, *J* = 6.5 Hz, 2H), 1.56 – 1.70 (m, 6H), 1.11 (m, 4H), 0.796 (m, 2H), 0.030 (s, 6H); ¹³C NMR (100 MHz, CDCl₃): δ 140.9, 140.5, 139.7, 138.2, 128.4, 128.3, 128.1, 128.0, 127.7, 124.1, 72.5, 69.4, 46.6, 37.3, 33.2, 26.6, 26.4, -1.8; IR (thin film): 2920.1, 2849.3, 1599.7, 1493.4, 1449.7, 1248.7, 1096.0, 1027.8 cm⁻¹; HRMS (APCI) (m/z): [M+H]⁺ calc for C₂₃H₃₆OSi, 393.2608; found, 393.2627.

General Procedure II for the Pd₂dba₃/ IPr·HCl – promoted hydrosilylation of 1,3-disubstituted allenes

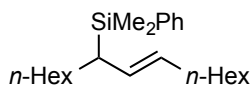
THF (1.0 mL) was added to a solid mixture of IPr·HCl **4-34** (0.025 mmol), *t*-BuOK (0.025 mmol), and Pd₂dba₃ (0.0125 mmol) at rt. After stirring for 10 min at rt, the reaction mixture turned dark red and the silane (0.5 mmol) was added. The reaction mixture was stirred for 10 min at rt followed by addition of the allene (0.5 mmol) neat by syringe. The reaction mixture was stirred at rt for 2 h. The reaction mixture was filtered through silica gel eluting with 50% v/v EtOAc/hexanes. The solvent was removed *in vacuo*, and the crude residue was purified via flash column chromatography on silica gel to afford the desired product.

(E)-Benzyl(dimethyl)(pentadec-8-en-7-yl)silane (4-36a) (Table 8, entry 5)



General procedure II was followed with Pd₂dba₃ (11.4 mg, 0.0125 mmol), IPr·HCl salt **4-34** (10.6 mg, 0.025 mmol), *t*-BuOK (2.8 mg, 0.025 mmol), benzyl(dimethyl)silane (79 μL, 0.5 mmol), and pentadeca-1,7-diene (104 mg, 0.5 mmol). The crude residue was purified by flash chromatography (100% hexanes) affording a clear oil (135 mg, 75 % yield). ¹H NMR (400 MHz, CDCl₃): 7.19 (t, *J* = 7.6 Hz, 2H), 7.04 (t, *J* = 6.8 Hz, 1H), 6.98 (t, *J* = 7.6 Hz, 2H), 5.22 (dt, *J* = 15.5, 6.8 Hz, 1H), 5.14 (dd, *J* = 15.5, 8.8 Hz, 1H), 2.07 (s, 2H), 1.98 (q, *J* = 7.0 Hz, 2H), 1.36 – 1.48 (m, 3H), 1.14 – 1.34 (m, 17H), 0.87 (t, *J* = 6.6 Hz, 6H), -0.10 (s, 3H), -0.11 (s, 3H); ¹³C NMR (100 MHz, CDCl₃): δ 140.5, 131.0, 129.0, 128.2, 128.1, 123.8, 32.9, 31.9, 31.8, 31.7, 30.0, 29.2, 29.2, 28.9, 28.7, 23.9, 22.7, 14.1, -5.10, -5.15; IR (thin film): ν 2954.8, 2924.4, 2856.0, 1703.5, 1600.0, 1493, 1452, 1057, 827.8, 697.7 cm⁻¹; HRMS (EI⁺) (*m/z*): [*M*]⁺ calc for C₂₄H₄₂Si, 358.3056; found, 358.3068.

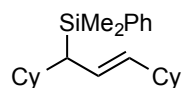
(E)-Dimethyl(pentadec-8-en-7-yl)(phenyl)silane (4-36b) (Table 8, entry 6)



General procedure II was followed with Pd₂dba₃ (11.4 mg, 0.0125 mmol), IPr·HCl salt **4-34** (10.6 mg, 0.025 mmol), *t*-BuOK (2.8 mg, 0.025 mmol), dimethylphenylsilane (77 μL,

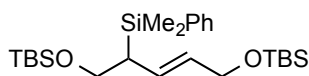
0.5 mmol), and pentadeca-1,7-diene (104 mg, 0.5 mmol). The crude residue was purified by flash chromatography (100% hexanes) affording a clear oil (151 mg, 84 % yield). ¹H NMR (500 MHz, CDCl₃): δ 7.46 (m, 2H), 7.32 (m, 3H), 5.17 (dt, *J* = 15.9, 6.2 Hz, 1H), 5.11 (dd, *J* = 15.9, 6.2 Hz, 1H), 1.95 (q, *J* = 6.5 Hz, 2H), 1.60 (t, *J* = 11.7 Hz, 1H), 1.10 – 1.39 (m, 21H), 0.87 (t, *J* = 6.8 Hz, 3H), 0.83 (t, *J* = 6.8 Hz, 3H), 0.22 (s, 3H), 0.21 (s, 3H); ¹³C NMR (125 MHz, CDCl₃): δ 138.4, 134.1, 130.9, 129.0, 128.7, 127.5, 32.9, 32.4, 31.83, 31.80, 30.0, 29.2, 29.0, 28.9, 28.8, 22.70, 22.68, 14.12, 14.10, -4.25, -5.10; IR (thin film): ν 2954.0, 2925.1, 2857, 1709.7, 1465.4, 1427.5, 1249.4, 1117.7, 829.3, 698.2 cm⁻¹; HRMS (EI⁺) (*m/z*): [*M*]⁺ calc for C₂₃H₄₀Si, 344.2899; found, 344.2907.

(*E*)-(1,3-Dicyclohexylallyl)dimethyl(phenyl)silane (4-36c) (Table 8, entry 7)



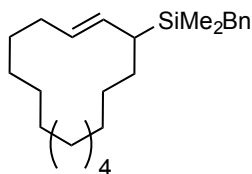
General procedure II was followed with Pd₂dba₃ (13.7 mg, 0.015 mmol), IPr-HCl salt **4-34** (12.8 mg, 0.03 mmol), *t*-BuOK (3.6 mg, 0.03 mmol), dimethylphenylsilane (46 μL, 0.3 mmol), and 1,3-dicyclohexylpropa-1,2-diene (61 mg, 0.3 mmol). The crude residue was purified by flash chromatography (100% hexanes) affording a clear oil (98.7 mg, 58 % yield). ¹H NMR (400 MHz, CDCl₃): δ 7.54 – 7.46 (m, 2H), 7.37 – 7.29 (m, 3H), 5.31 – 5.21 (m, 1H), 5.13 (ddd, *J* = 15.2, 6.7, 1.8 Hz, 1H), 1.93 (dd, *J* = 10.6, 7.0 Hz, 1H), 1.76 – 1.56 (m, 11H), 1.50 – 1.38 (m, 2H), 1.33 – 0.90 (m, 11H), 0.30 (d, *J* = 2.0 Hz, 3H), 0.27 (d, *J* = 2.0 Hz, 3H); ¹³C NMR (100 MHz, CDCl₃) δ 139.43, 136.25, 133.96, 128.50, 127.43, 125.88, 41.11, 40.14, 38.69, 34.08, 33.64, 33.48, 31.48, 26.77, 26.74, 26.32, 26.26, 26.14, -2.64, -3.37; IR (thin film): ν 2917.9, 2847.5, 1446.9, 1426.0, 1245.3, 1109.7, 997.9, 966.1, 891.9, 851.1, 811.4, 767.3, 732.3, 697.5, 641.7 cm⁻¹; HRMS (EI⁺) (*m/z*): [*M*]⁺ calc for C₂₃H₃₆Si, 340.2586; found, 340.2589.

(*E*)-8-(dimethyl(phenyl)silyl)-2,2,3,3,11,11,12,12-octamethyl-4,10-dioxa-3,11-disilatrisc-6-ene (4-36d) (Table 8, entry 8)



General procedure II was followed with Pd₂dba₃ (4.8 mg, 0.0052 mmol), IPr·HCl salt **4-34** (4.5 mg, 0.0105 mmol), *t*-BuOK (1.2 mg, 0.0105 mmol), dimethylphenylsilane (32 μL, 0.21 mmol), and 2,2,3,3,11,11,12,12-octamethyl-4,10-dioxa-3,11-disilatrideca-6,7-diene (70 mg, 0.21 mmol). The crude residue was purified by flash chromatography (10% EtOAc:hexanes) affording a clear oil (60 mg, 64 % yield). ¹H NMR (500 MHz, CDCl₃): δ 7.52 (m, 2H), 7.35 (m, 3H), 5.63 (dd, *J* = 15.0, 9.0 Hz, 1H), 5.40 (dt, *J* = 15.0, 6.1 Hz, 1H), 4.12 (d, *J* = 5.8 Hz, 2H), 3.73 (m, 2H), 2.00 (m, 1H), 0.912 (s, 9H), 0.872 (s, 9H), 0.322 (s, 3H), 0.309 (s, 3H), 0.063 (s, 6H), -0.0047 (s, 3H), -0.014 (s, 3H); ¹³C NMR (125 MHz, CDCl₃): δ 134.0, 133.0, 130.0, 128.8, 128.4, 127.5, 64.2, 63.9, 36.6, 26.0, 18.3, -3.7, -4.0, -5.11, -5.14, -5.40, -5.43; IR (thin film): ν 2953.5, 2926.2, 1704.1, 1462.4, 1250.7, 1089.8, 831.8 cm⁻¹; HRMS (ESI⁺) (*m/z*): [M+Na]⁺ calc for C₂₅H₄₈O₂Si₃, 487.2854; found, 487, 2851.

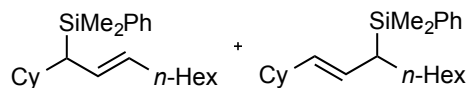
(*E*)-Benzyl(cyclopentadec-2-en-1-yl)dimethylsilane (4-40) (Scheme 4-14)



General procedure II was followed with Pd₂dba₃ (5.5 mg, 0.006 mmol), IPr·HCl salt **4-34** (5.1 mg, 0.012 mmol), *t*-BuOK (1.3 mg, 0.012 mmol), benzyldimethylsilane (37.9 μL, 0.24 mmol), and cyclopentadeca-1,2-diene (50 mg, 0.24 mmol). The crude residue was purified by flash chromatography (100% hexanes) affording a clear oil (57 mg, 66 % yield). ¹H NMR (700 MHz, CDCl₃): δ 7.19 (t, *J* = 7.5 Hz, 2H), 7.05 (t, *J* = 7.5 Hz, 1H), 6.983 (d, *J* = 7.5, 2H), 5.15 (m, 2H), 2.15 (m, 1H), 2.07 (s, 2H), 1.96 (m, 1H), 1.09 – 1.5 (m, 26H), -0.103 (s, 3H), -0.118 (s, 3H). ¹H NMR (700 MHz, C₆D₆): 7.21 (m, 2H (overlapping signals)), 7.03-7.10 (m, 3H), 5.20 (dd, *J* = 15.8, 10.2 Hz, 1H), 5.15 (ddd, *J* = 15.8, 10.2, 4.0 Hz, 1H), 2.21 (m, 1H), 2.10 (s, 2H), 2.04 (m, 1H), 1.25 – 1.52 (m, 26H), -0.0039 (s, 6H); ¹³C NMR (175 MHz, CDCl₃): δ 140.5, 131.7, 129.1, 128.2, 128.1, 123.8, 31.9, 31.5, 29.0, 28.7, 28.2, 27.2, 27.1, 26.9, 26.8, 26.7, 25.4, 23.8, -5.2, -5.3; IR (thin

film): ν 2926.0, 2856.4, 1599.8, 1451.8, 1257.8, 1152.4, 826.8 cm^{-1} ; HRMS (EI^+) (m/z): $[\text{M}]^+$ calc for $\text{C}_{24}\text{H}_{40}\text{Si}$, 356.2899; found, 356.2902.

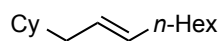
(E)-(1-Cyclohexylnon-2-en-1-yl)dimethyl(phenyl)silane and (E)-(1-cyclohexylnon-1-en-3-yl)dimethyl(phenyl)silane (4-43a and 4-43b) (Scheme 4-15)



General procedure II was followed with Pd_2dba_3 (22.9 mg, 0.025 mmol), IPr-HCl salt **4-34** (21.3 mg, 0.05 mmol), *t*-BuOK (5.6 mg, 0.05 mmol), dimethylphenylsilane (77 μL , 0.5 mmol), and nona-1,2-dien-1-ylcyclohexane (103.2 mg, 0.5 mmol). The crude residue was purified by flash chromatography (100% hexanes) affording a clear oil (mg, 80 % yield). ^1H NMR (500 MHz, CDCl_3): δ 7.53 (m, 4 H), 7.37 (m, 6H), 5.33 (dd, $J = 16$, 11 Hz, 1H), 5.21 (dt, $J = 16$, 11 Hz, 1H), 5.19 (dd, $J = 16$, 11 Hz, 0.7 Hz), 5.14 (dd, $J = 16$, 9.2 Hz, 0.7H), 2.02 (m, 2H), 1.94 (m, 1H), 1.57 – 1.76 (m, 11H), 1.10 – 1.38 (m, 26H), 0.936 (t, $J = 10$ Hz, 3H), 0.90 (t, $J = 10$ Hz, 3H), 0.33 (s, 3H), 0.30 (s, 3H), 0.29 (2H), 0.278 (s, 2H); ^{13}C NMR (125 MHz, CDCl_3): δ 139.5, 138.4, 135.1, 134.2, 134.0, 130.3, 128.7, 128.60, 128.55, 128.2, 127.5, 41.1, 40.3, 38.8, 34.2, 33.7, 33.6, 32.9, 32.4, 31.9, 31.8, 31.5, 30.0, 29.10, 29.06, 28.9, 28.8, 26.82, 26.80, 26.4, 26.2, 22.74, 22.71, 14.2, 14.1, -2.6, -3.3, -4.3, -5.1; IR (thin film); ν 2925.4, 2852.1, 1725.7, 1448.5, 1427.5, 1249.4, 1117.9, 1061.8, 971.7, 828.9, 698.7, 418.6 cm^{-1} ; HRMS (EI^+) (m/z): $[\text{M}]^+$ calc for $\text{C}_{23}\text{H}_{38}\text{Si}$, 342.2743; found, 342.2749.

Synthetic Manipulations of Alkenylsilane 10d:

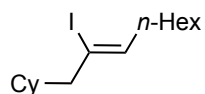
(E)-Non-2-en-1-ylcyclohexane (4-44) (Scheme 4-16)



Alkenylsilane **4-41d** (70 mg, 0.196 mmol) in DMSO (50 μL) was added to a 6 mL dram vial with stir bar. TBAF (1.96 mL, 1.96 mmol, 1.0 M in THF) was then slowly added and the vessel was subsequently heated at 50 $^\circ\text{C}$ for 6 h when the reaction was judged complete by TLC analysis. The solvent was removed *in vacuo* and the crude material was purified by flash column chromatography (100 % hexanes) affording a clear oil (35.2 mg,

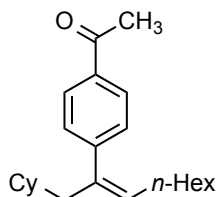
86 %). ^1H NMR (500 MHz, CDCl_3): δ 5.38 (m, 2H), 1.98 (m, 2 H), 1.88 (m, 2H), 1.614-1.78 (m, 6H), 1.14 – 1.42 (m, 15H), 0.894 (t, $J = 8.7$ Hz, 6H); ^{13}C NMR (175 MHz, CDCl_3): δ 131.4, 128.7, 40.7, 38.1, 33.1, 32.6, 31.7, 29.6, 28.8, 26.6, 26.3, 22.6, 14.1; IR (thin film): ν 2920.3, 2851.3, 1707.9, 1448.0, 1259.5, 966.2 cm^{-1} ; HRMS (EI^+) (m/z): $[\text{M}]^+$ calc for $\text{C}_{15}\text{H}_{29}$, 208.2191; found, 208.2189.

(Z)-(2-Iodonon-2-en-1-yl)cyclohexane (4-45) (Scheme 4-16)



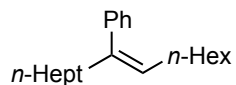
Alkenylsilane **4-41d** (70 mg, 0.196 mmol) in CH_3CN (1 mL) was added to a 6 mL dram vial equipped with a stir bar. The reaction vessel was cooled in an ice bath to 0 °C and then NIS (110 mg, 0.491 mmol) was added. The reaction was then removed from the ice bath and warmed to RT. After 12 h the reaction was judged complete by TLC analysis and sodium thiosulfate was added (2 mL) to quench the reaction. The solution was then extracted with EtOAc (3 X 2 mL) and washed with water (3 X 3 mL) and subsequently dried over anhydrous MgSO_4 . The solvent was then removed in vacuo and the crude material was purified by flash column chromatography (100 % hexanes) affording a clear oil (50 mg, 77 %). ^1H NMR (500 MHz, CDCl_3): δ 5.43 (t, $J = 7.2$ Hz, 1H), 2.32 (d, $J = 7.5$ Hz, 2H), 2.09 – 2.16 (m, 2H), 1.60 – 1.75 (m, 8H), 1.22 – 1.46 (m, 12H), 1.10-1.19 (m, 1H), 0.90 (t, $J = 7.2$ Hz, 3H), 0.84 – 0.88 (m, 2H); ^{13}C NMR ((175 MHz, CDCl_3): δ 135.8, 108.2, 52.6, 36.4, 36.3, 32.6, 31.7, 28.8, 28.4, 26.5, 26.2, 26.1, 22.6, 14.0; IR (thin film): ν 2925.6, 2852.2, 1972.0, 1718.2, 1449.4, 1249.4, 1118.1, 827.3, 698.5 cm^{-1} ; HRMS (EI^+) (m/z): $[\text{M}]^+$ calc for $\text{C}_{15}\text{H}_{27}\text{I}$, 334.1158; found, 334.1161.

(Z)-1-(4-(1-Cyclohexylnon-2-en-2-yl)phenyl)ethan-1-one (4-46) (Scheme 4-16)



Alkenylsilane **4-41d** (125 mg, 0.7 mmol) in THF (1 mL) was added to a flame-dried 6 mL dram vial with a stir bar. TBAF (2.1 mL, 2.1 mmol, 1.0 M in THF) was then slowly added followed by addition of 4'-iodoacetophenone (172 mg, 0.7 mmol) and Pd₂dba₃ (16 mg, 0.0175 mmol). The reaction vessel was then heated at 50 °C for 30 min when the reaction was judged complete by TLC analysis. DCM (1 mL) was added to the vial and the solution was filtered with 50 % EtOAc:hexanes and the solvent was removed *in vacuo*. The crude material was purified by flash column chromatography (5 – 15% EtOAc:hexanes) affording a clear oil (180 mg, 79 %). ¹H NMR (500 MHz, CDCl₃): δ 7.90 (d, *J* = 8.2, 2H), 7.21 (d, *J* = 8.2 2H), 5.43 (t, *J* = 7.2 Hz, 1H), 2.59 (s, 3H), 2.31 (d, *J* = 7.5 Hz, 2H), 1.89 (q, *J* = 7.0 Hz, 2H), 1.54 – 1.67 (m, 6H), 1.14 – 1.34 (m, 10H), 1.00 – 1.11 (m, 5H), 0.824 (t, *J* = 7.5 Hz, 5H); ¹³C NMR (175 MHz, CDCl₃): δ 197.9, 147.0, 138.3, 135.2, 130.0, 128.6, 128.1, 47.2, 35.4, 33.1, 31.6, 30.0, 28.9, 28.9, 26.6, 26.1, 22.6, 14.0; IR (thin film): ν 2925.3, 1682.0, 1604.1, 1358.0, 1263.3, 1120.1, 833.1 cm⁻¹; HRMS (ESI⁺) (*m/z*): [M+H]⁺ calc for C₂₃H₃₄O, 327.2682; found, 327.2682.

(Z)-Pentadec-7-en-8-ylbenzene (4-47) (Scheme 4-17)

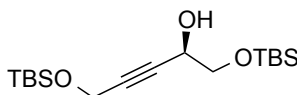


General procedure I was followed with Ni(COD)₂ (13 mg, 0.05 mmol), IPr*OMe **4-35** (47.2 mg, 0.05 mmol), mmol), benzyldimethylsilane (79 μL, 0.5 mmol), and pentadeca-1,7-diene (104 mg, 0.5 mmol). After 1 h the reaction was judged complete by TLC analysis and TBAF (1 mL, 1 mmol, 1.0 M in THF) was slowly added to the stirring solution, followed by iodobenzene (x mg, x mmol) and Pd₂dba₃ (11.3 mg, 0.025 mmol). The reaction vessel was then heated at 50 °C for 30 min when the reaction was judged complete by TLC analysis. DCM (1 mL) was added to the solution and then filtered (50 % EtOAc:Hex). The solution was removed *in vacuo* and the crude material was purified by flash column chromatography (100 % hexanes) to afford a clear oil (121 mg, 85 %). ¹H NMR (400 MHz, CDCl₃): δ 7.31 (t, *J* = 7.1 Hz, 2H), 7.22 (m, 1H), 7.12 (d, *J* = 7.9 Hz, 2H), 5.41 (t, *J* = 8.0 Hz, 1H), 2.30 (m, 2H), 1.90 (q, *J* = 8.0 Hz, 2H), 1.14 – 1.35 (m, 21H), 0.852 (q, *J* = 5.2 Hz, 7H); ¹³C NMR (100 MHz, CDCl₃): δ 141.6, 140.9, 128.4, 127.9, 127.3, 126.1, 39.3, 31.8, 31.7, 30.1, 29.1, 28.9, 28.2, 22.62, 22.59, 14.1; IR (thin

film): ν 2925.8, 2856.4, 1689.9, 1598.7, 1448.6, 1377.2, 1177.5, 1028.0, 762.9, 700.0 cm^{-1} ; HRMS (EI⁺) (m/z): [M]⁺ calc for C₂₁H₃₄, 286.2661; found, 286.2656.

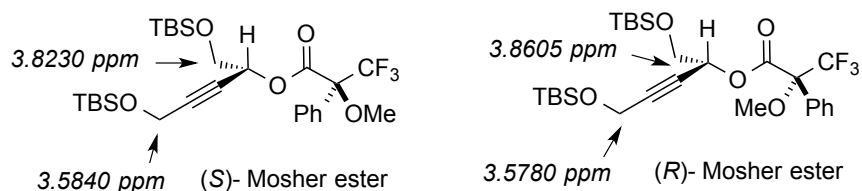
Synthesis of Chiral Allene Substrate 4-60:

(R)-2,2,3,3,11,11,12,12-octamethyl-4,10-dioxa-3,11-disilatridec-7-yn-6-ol (Scheme 4-20)



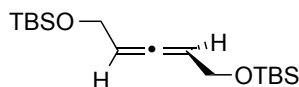
Following the Carreira procedure,⁷³ zinc trifluoromethanesulfonate (2.032 g, 5.6 mmol) was added to a flame dried round bottom flask, and the solid was dried under vacuum at 130 °C for 12 h then allowed to cool to rt. (1*R*, 2*S*)-(-)-*N*-methylephedrine (1.07 g, 6.0 mmol) was then added as a solid, and the solid mixture was put under vacuum for 20 min. Toluene (25 mL) was added, followed by dropwise addition of freshly distilled triethylamine (835 μL , 6.0 mmol). After the white slurry was stirred for 2 h under nitrogen at rt, a 12 mL toluene solution of *tert*-butyldimethylsilylpropargyl ether (1.02 g, 6.0 mmol) was added dropwise via syringe pump over 20 min at rt. The reaction was stirred for 30 min, then a 12 mL toluene solution of *tert*-butyldimethylsilylacetaldehyde (0.915 mL, 4.0 mmol) was added dropwise over 22 h at rt. The reaction was quenched with sat. NH₄Cl, extracted 3x with diethyl ether, and the extract was dried over MgSO₄. The solvent was removed under vacuum, and the crude product was purified with silica gel column chromatography (10:1 pentane/diethyl ether) to yield a colorless oil (910 mg, 65 %, 90 % ee). ¹H NMR (500 MHz, CDCl₃): δ 4.41 (m, 1H), 4.32 (m, 2H), 3.75 (dd, *J* = 12.8, 4.6 Hz, 1H), 3.62 (dd, *J* = 12.8, 8.5 Hz, 1H), 0.889 (s, 9H), 0.884 (s, 9H), 0.096 (s, 6H), 0.076 (s, 6H).; ¹³C NMR (175 MHz, CDCl₃): δ 84.2, 82.5, 66.9, 63.1, 51.7, 25.83, 25.81, -5.16, -5.35; IR (thin film): ν 3324.2, 2961.8, 2928.2, 2859.5, 1463.6, 1362.5, 1253.8, 1124.9, 1089.0, 835.6, 777.9 cm^{-1} ; HRMS (ESI⁺) (m/z): [M+Na] calc for C₁₇H₃₇O₃Si₂, 367.2095; found, 367.2094.

Mosher ester absolute configuration determination:



Aryl groups on the Mosher esters are documented to impose an anisotropic shielding effects on protons residing above the plane of the aryl ring.⁷⁷ The synthesis of the (*S*)- and (*R*)- Mosher esters demonstrated that the doublet absorbance at 3.8230 ppm was less shielded in the (*R*)-Mosher ester 3.8605 ppm, as predicted by this model. Further supporting this assignment is the shielding of the singlet absorbance when comparing the (*S*)- to the (*R*)- Mosher esters (3.5840 ppm to 3.5780 ppm). These observations are consistent with the proposed (*R*) stereochemistry of the carbinol. The % ee was determined by comparing the ¹⁹F-NMR chemical shifts at -71.765 ppm and -71.613 ppm of the enantioenriched and racemic (*S*)-Mosher esters (spectra included in appendix).

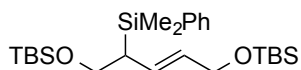
Enantioenriched 4-60 preparation (Scheme 4-20):



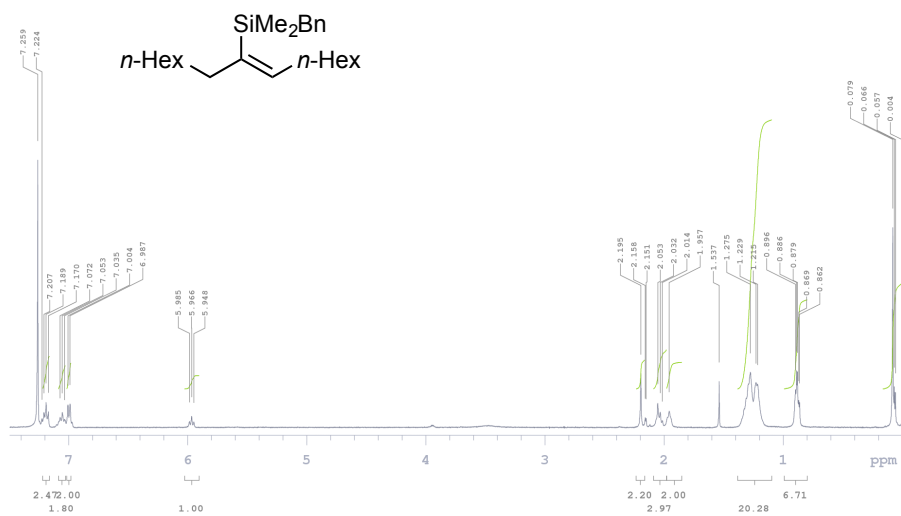
Following the Myers protocol for allene synthesis,⁷⁴ triphenylphosphine (314 mg, 1.2 mmol) was loaded to a flame dried flask, and 10 mL of dry THF was added. The solution was cooled to -15 °C (materials crystallize out of solution when temperature falls below -20 °C) and DEAD (209 mg, 188 μL, 1.2 mmol) was added dropwise. The reaction was stirred at -15 °C for another 10 min, and 8 mL THF solution of the alcohol (500 mg, 1.45 mmol) was added over 5 min. After 10 min, a 10 mL THF solution of NBSH (260 mg, 1.2 mmol) was added dropwise. The reaction mixture was stirred at -15 °C for 2 h, then brought to rt and stirred for 12 h, quenched with sat. NH₄Cl, and extracted 3 times with diethyl ether. The ether solution was dried over MgSO₄, and the solvent was removed in vacuo. The crude product was purified by column chromatography (hexane/ethyl acetate, 50:1) to yield (182 mg, 48 %, 80 % ee) a yellow oil. The % ee of this reaction was determined by ¹H NMR analysis of the formed allene in presence of Yb(hfc)₃-Ag(FOD) as a chiral shift reagent according to the following ratio: allene:Ag:Yb = 1:2:1.5 (7.5 mg

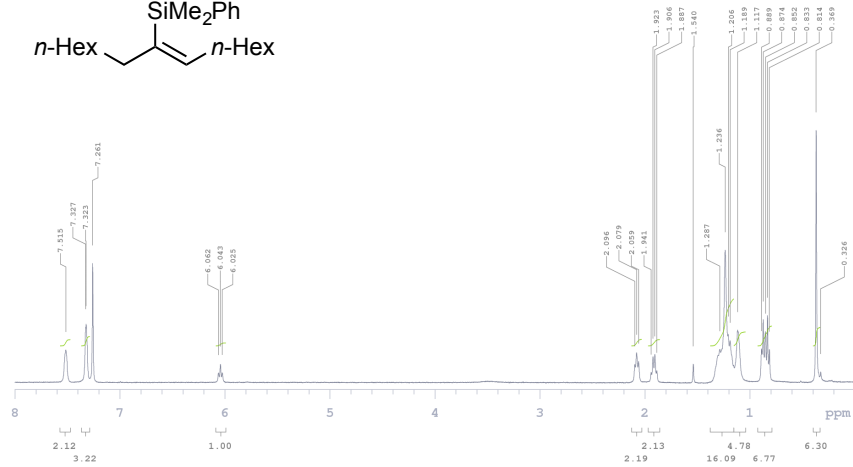
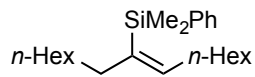
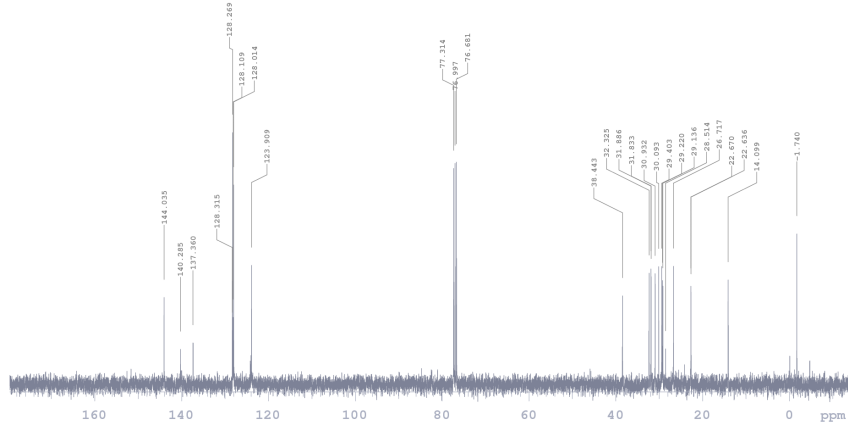
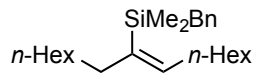
of allene, 17.0 mg of Ag(FOD), and 34.0 mg of Yb(hfc)₃ in 1.5 mL CDCl₃) and its racemate. The ee was determined by comparison of the ¹H NMR signals at δ = 5.48 and δ = 5.41. ¹H NMR (500 MHz, CDCl₃): δ 5.33 (pent., *J* = 4.5 Hz, 2H), 4.21 (q., *J* = 4.5 Hz, 4H), 0.913 (s, 18H), 0.885 (s, 12 H); ¹³C NMR (125 MHz, CDCl₃): δ 202.8, 93.1, 61.5, 25.9, -5.10, -5.14; IR (thin film): ν 2177.5, 2135.6, 1985.5, 1083.9 cm⁻¹; HRMS (ESI+) (m/z): [M+Na] calc for C₁₇H₃₆O₂Si₂, 329.2327; found, 329.2325.

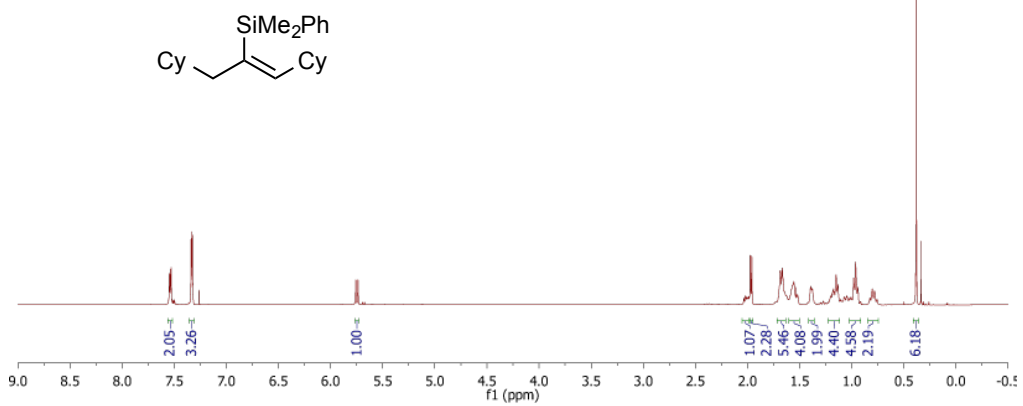
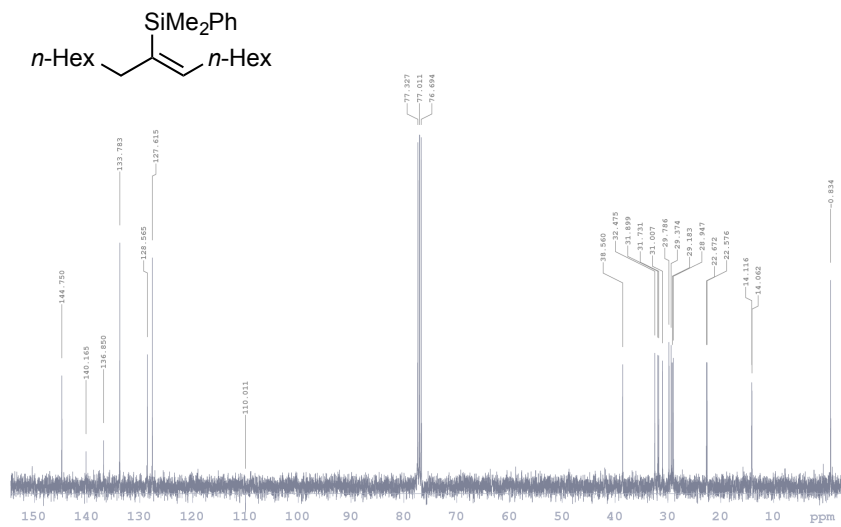
(*E*)-8-(dimethyl(phenyl)silyl)-2,2,3,3,11,11,12,12-octamethyl-4,10-dioxa-3,11-disilatridec-6-ene (4-36d), Scheme 4-20)

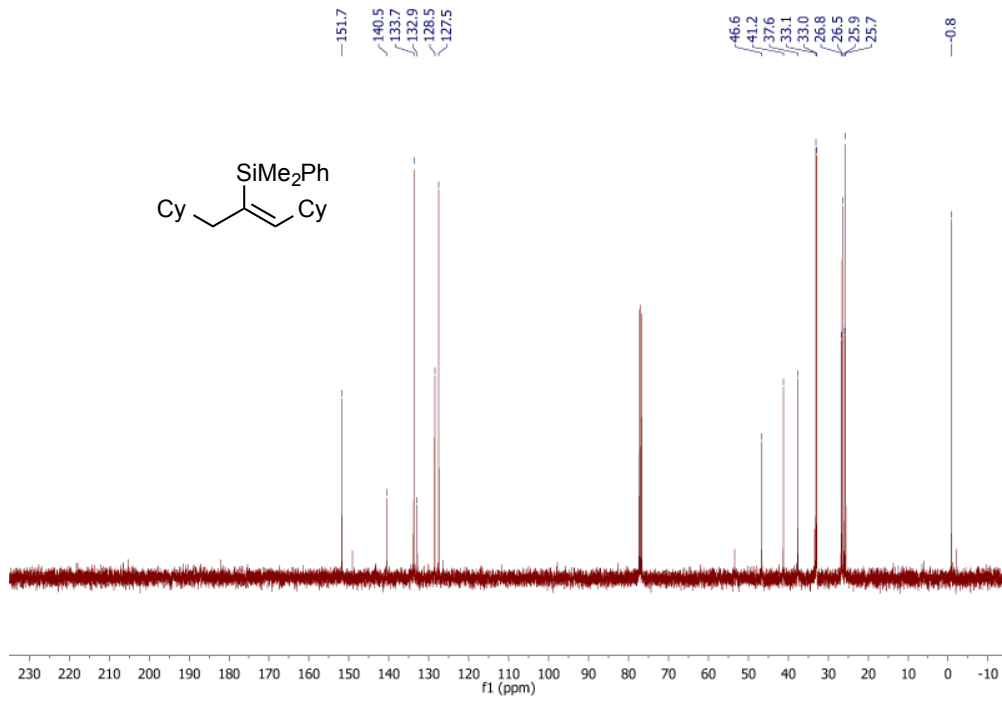


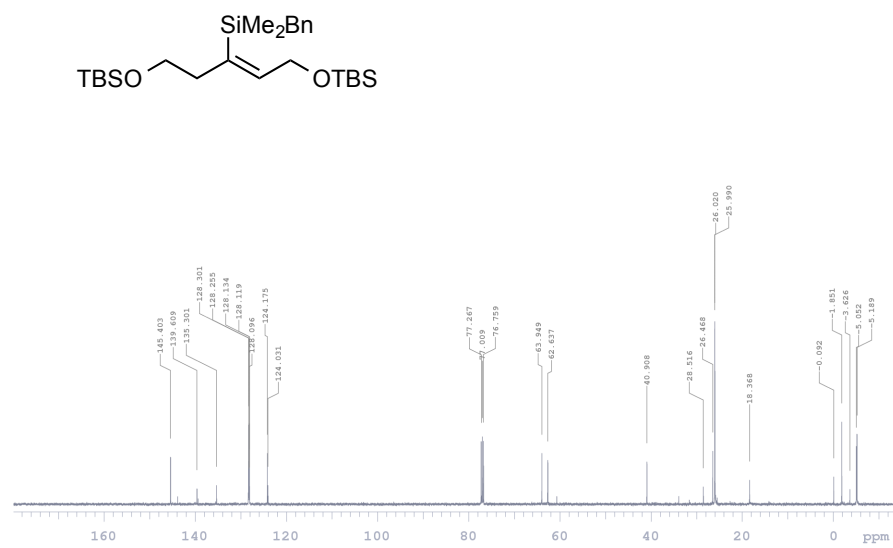
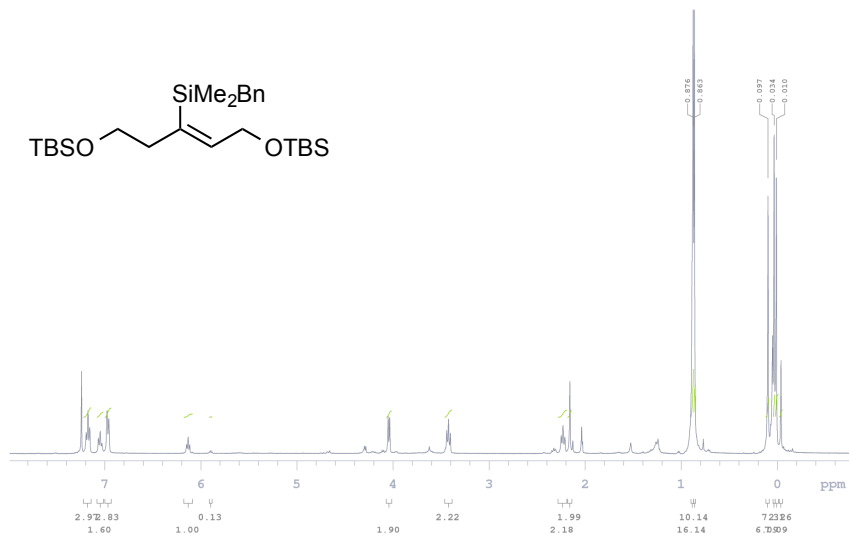
General procedure II was followed with Pd₂dba₃ (4.8 mg, 0.0052 mmol), IPr·HCl salt **4-34** (4.5 mg, 0.0105 mmol), *t*-BuOK (1.2 mg, 0.0105 mmol), dimethylphenylsilane (32 μL, 0.21 mmol), and 2,2,3,3,11,11,12,12-octamethyl-4,10-dioxa-3,11-disilatrideca-6,7-diene (70 mg, 0.21 mmol). The crude residue was purified by flash chromatography (10 % EtOAc:hexanes) affording a clear oil (73 mg, 76 % yield). ¹H NMR (500 MHz, CDCl₃): δ 7.52 (m, 2H), 7.35 (m, 3H), 5.63 (dd, *J* = 15.0, 9.0 Hz, 1H), 5.40 (dt, *J* = 15.0, 6.1 Hz, 1H), 4.12 (d, *J* = 5.8 Hz, 2H), 3.73 (m, 2H), 2.00 (m, 1H), 0.912 (s, 9H), 0.872 (s, 9H), 0.322 (s, 3H), 0.309 (s, 3H), 0.063 (s, 6H), -0.0047 (s, 3H), -0.014 (s, 3H); ¹³C NMR (125 MHz, CDCl₃): δ 134.0, 133.0, 130.0, 128.8, 128.4, 127.5, 64.2, 63.9, 36.6, 26.0, 18.3, -3.7, -4.0, -5.11, -5.14, -5.40, -5.43; IR (thin film): ν 2953.5, 2926.2, 1704.1, 1462.4, 1250.7, 1089.8, 831.8 cm⁻¹; HRMS (ESI⁺) (m/z): [M+Na]⁺ calc for C₂₅H₄₈O₂Si₃, 487.2854; found, 487, 2851.

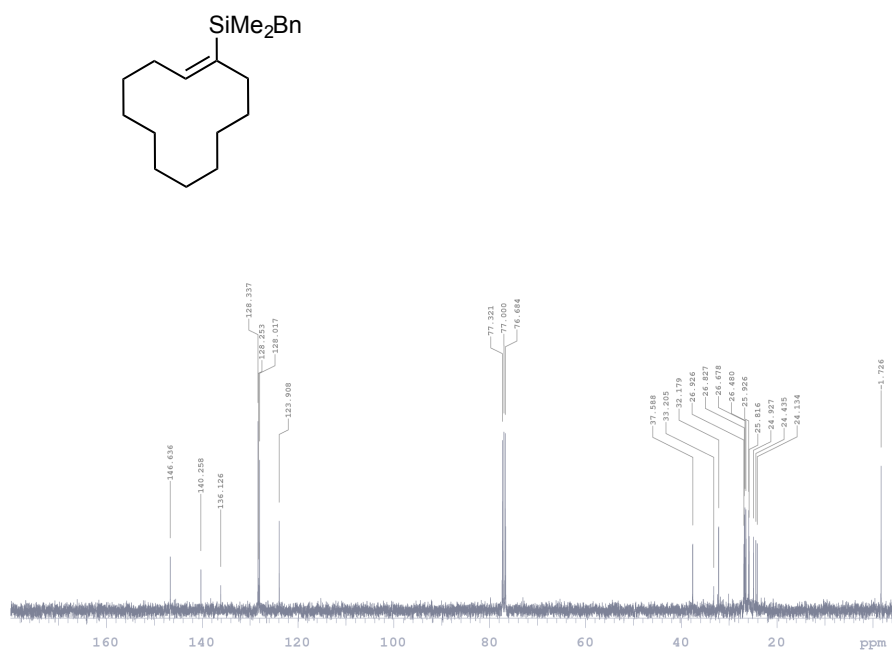
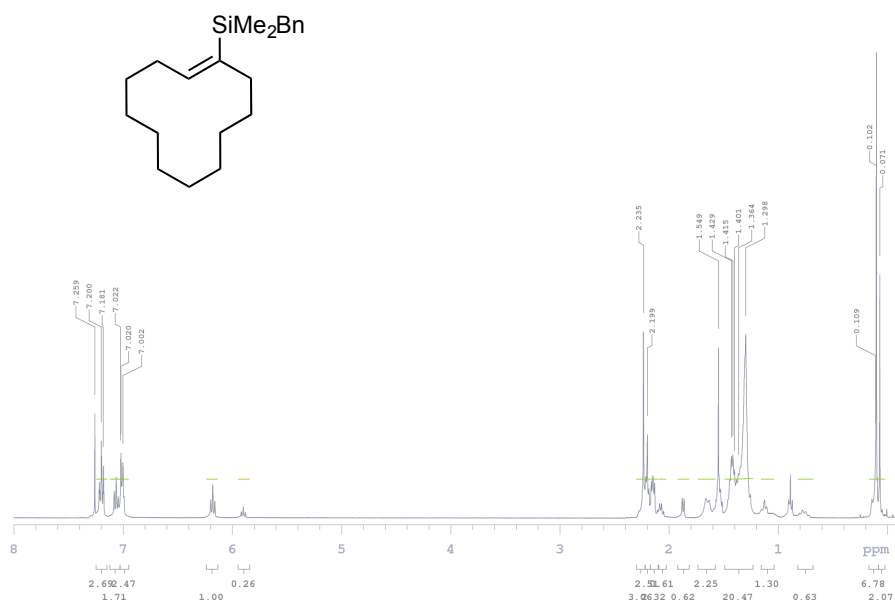


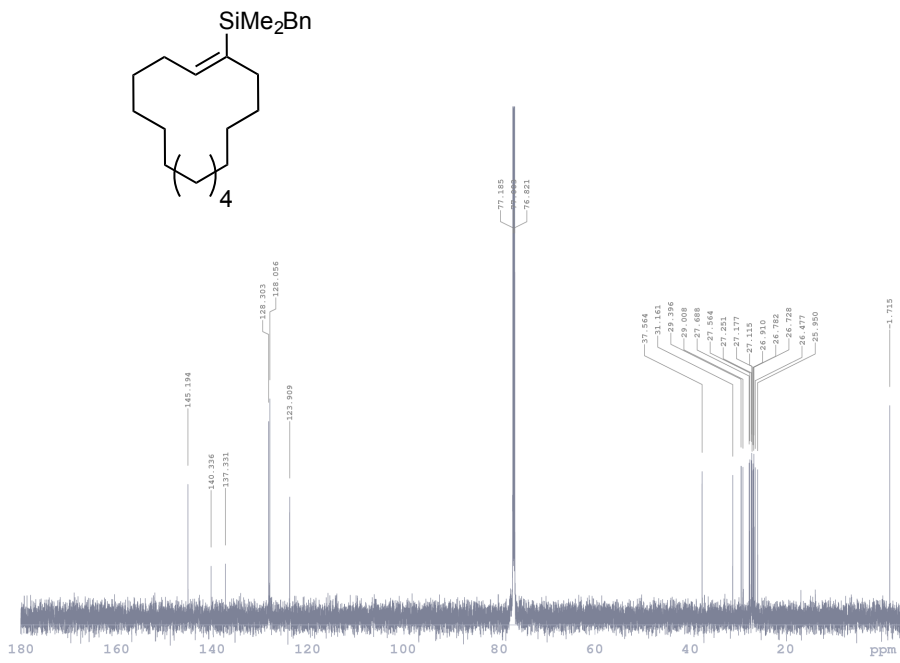
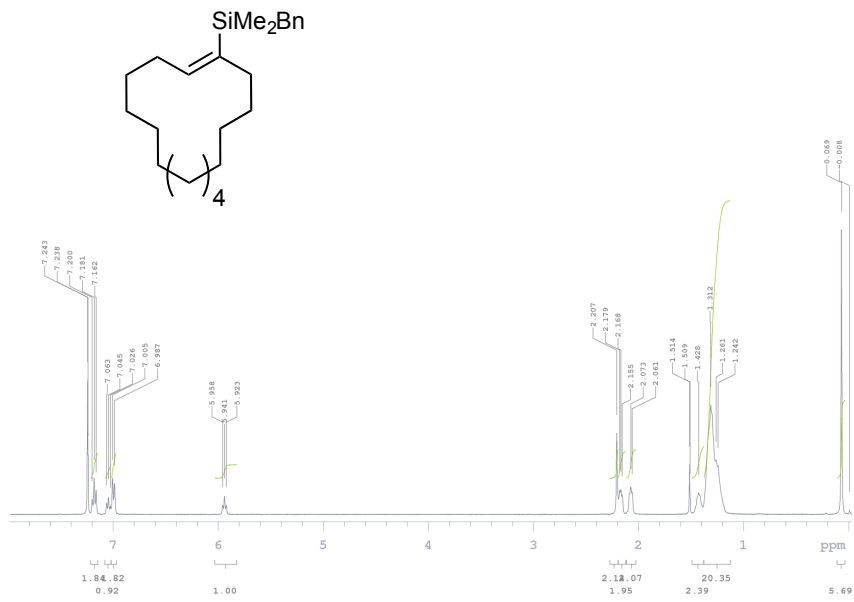


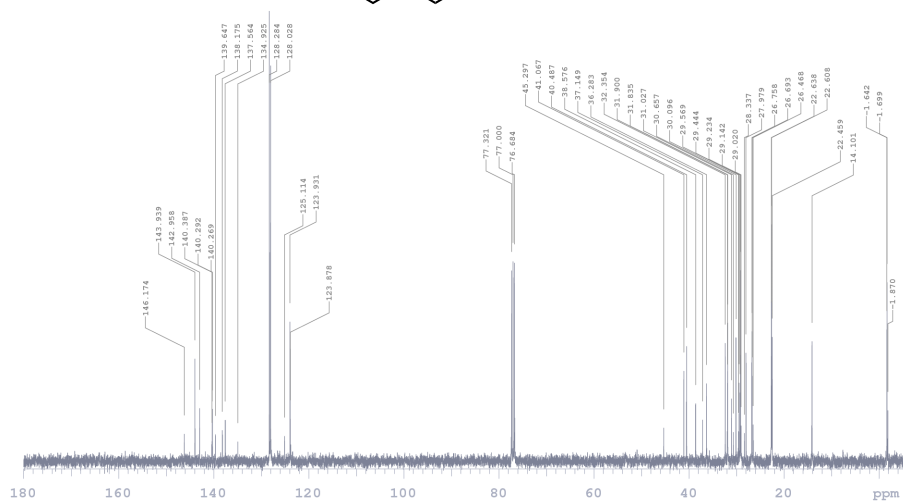
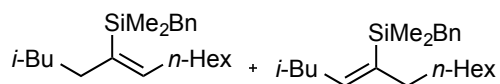
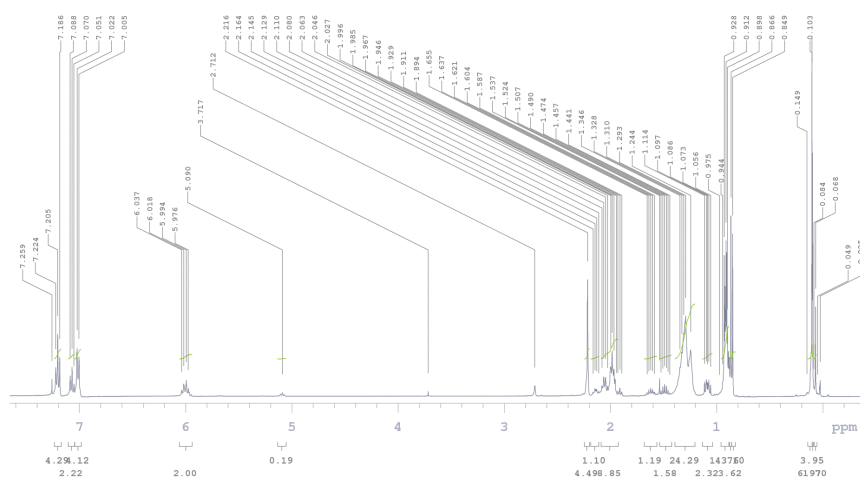
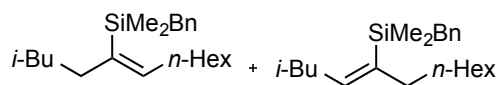


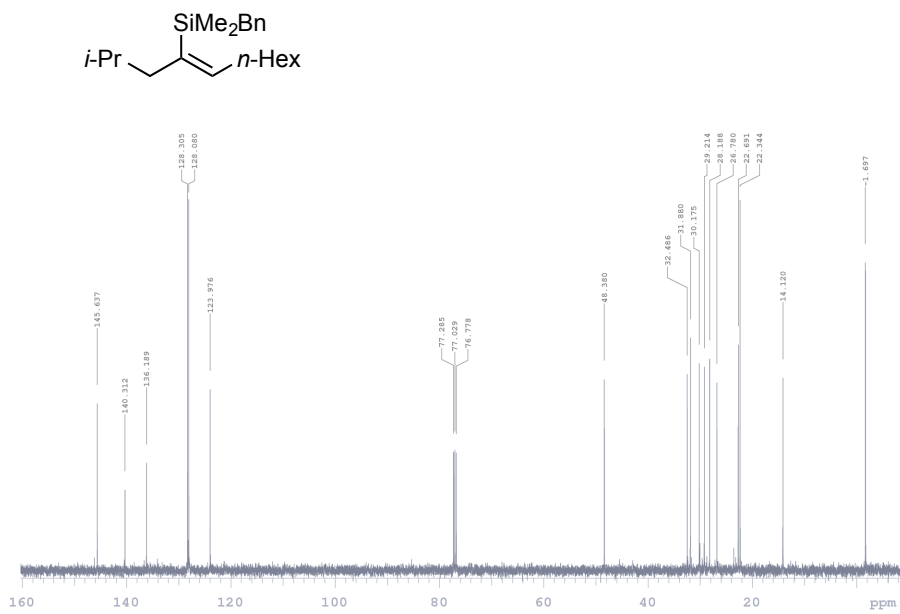
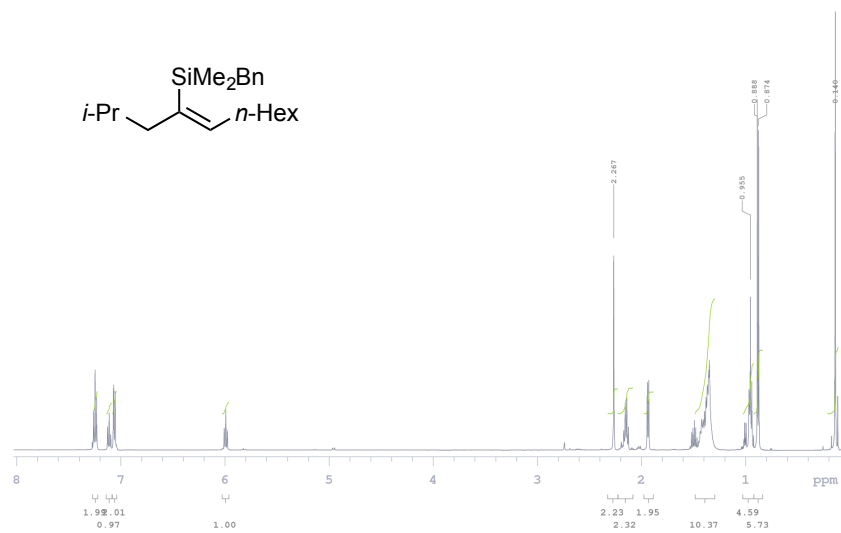


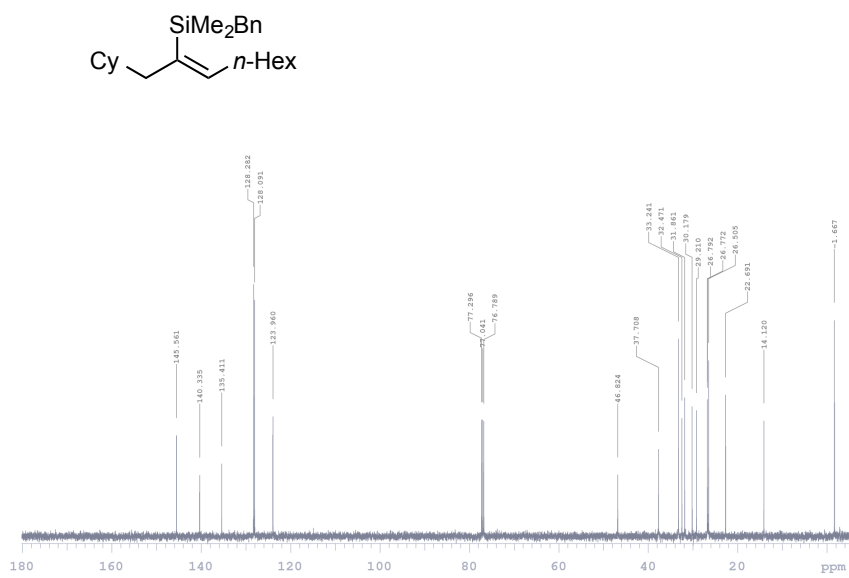
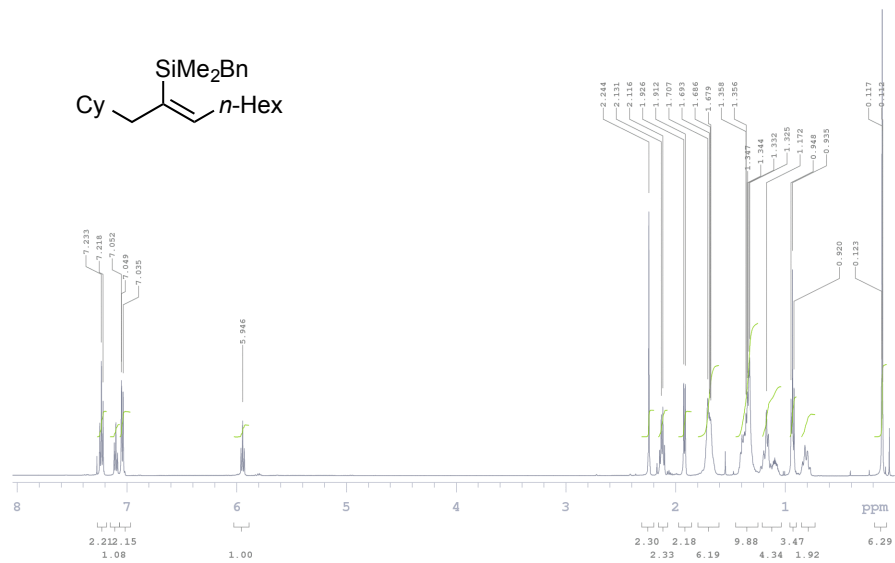


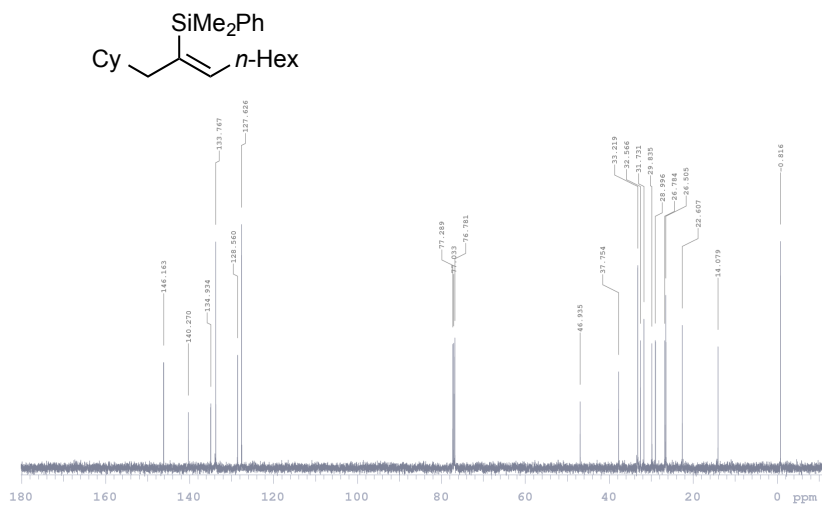
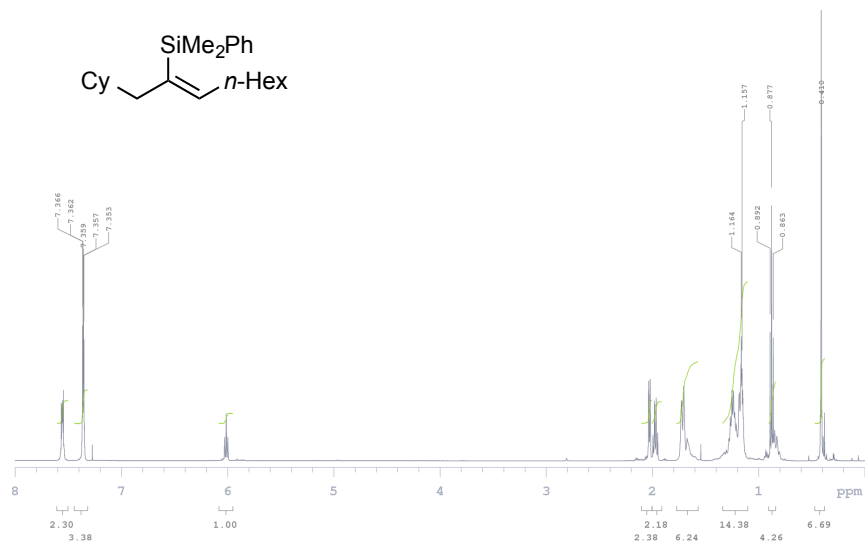


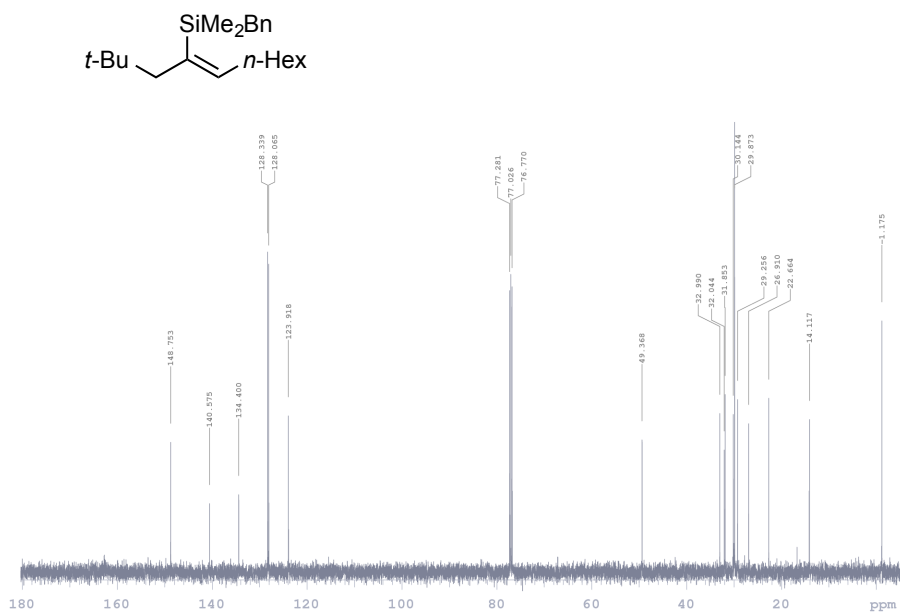
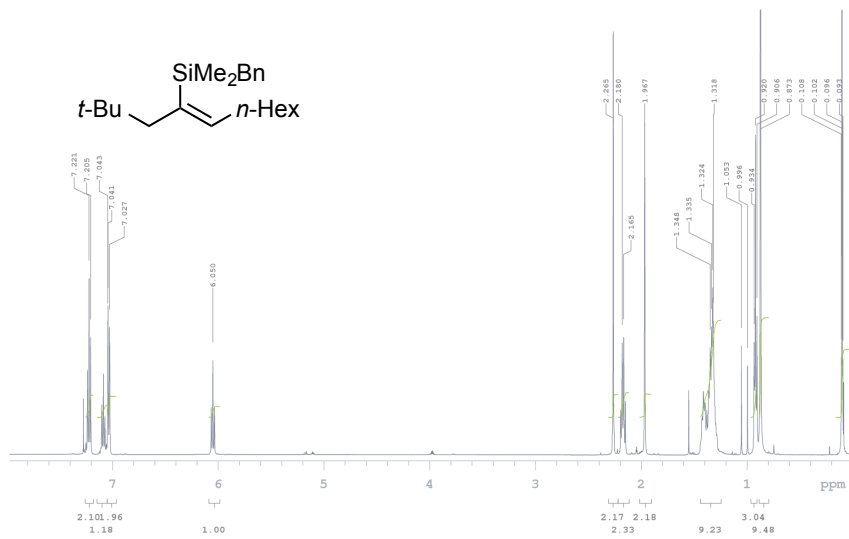


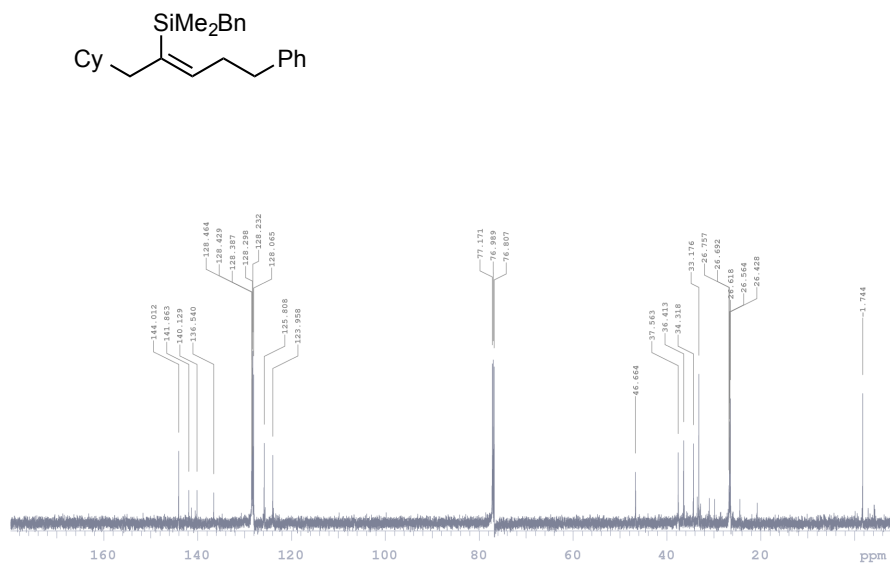
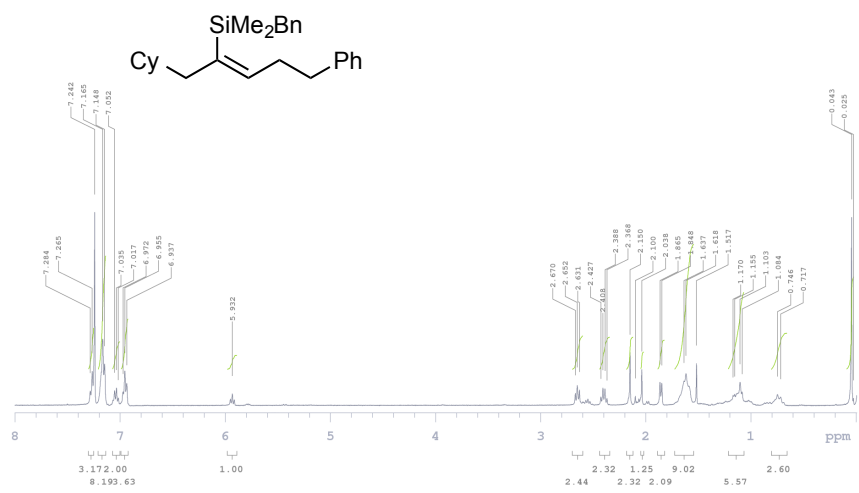


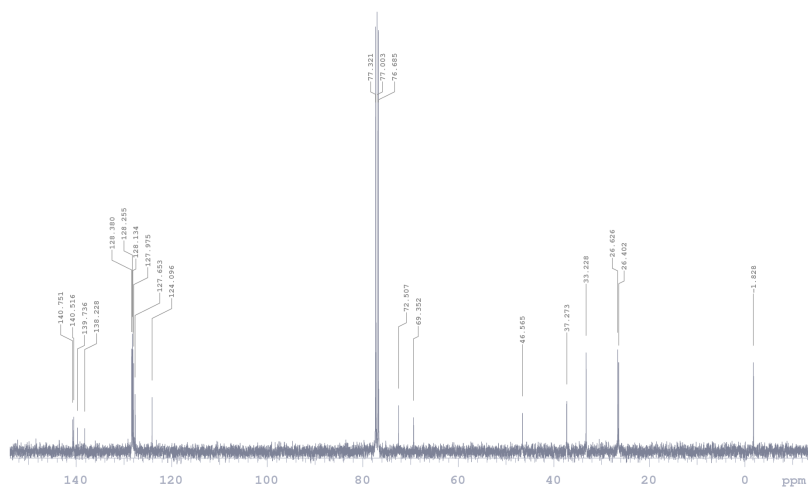
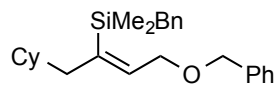
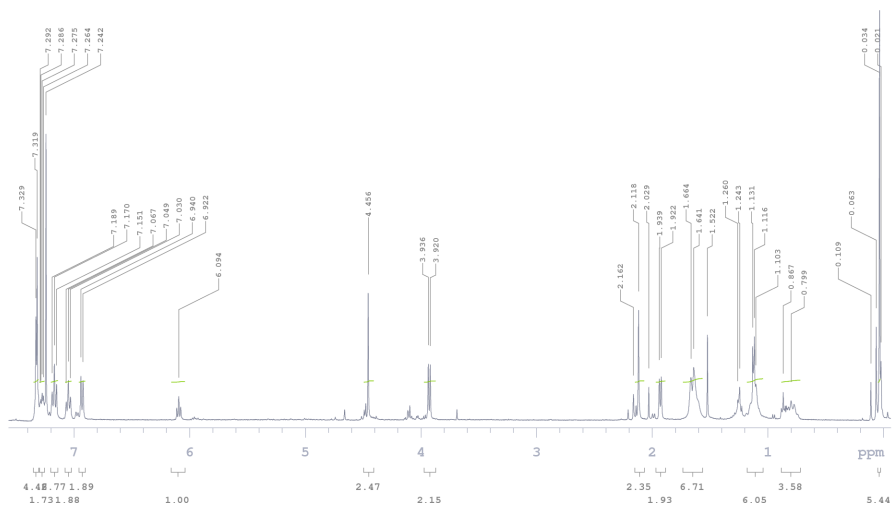
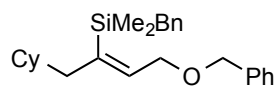


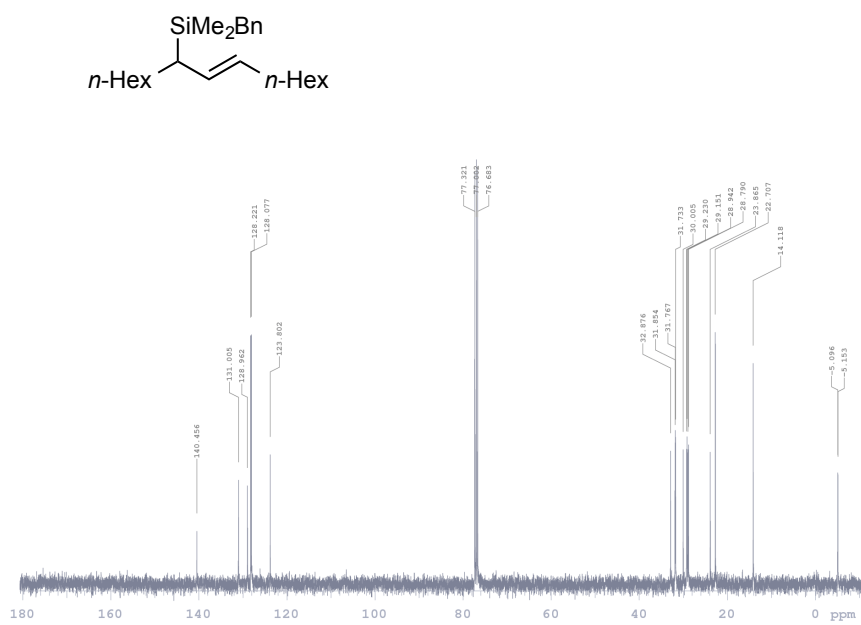
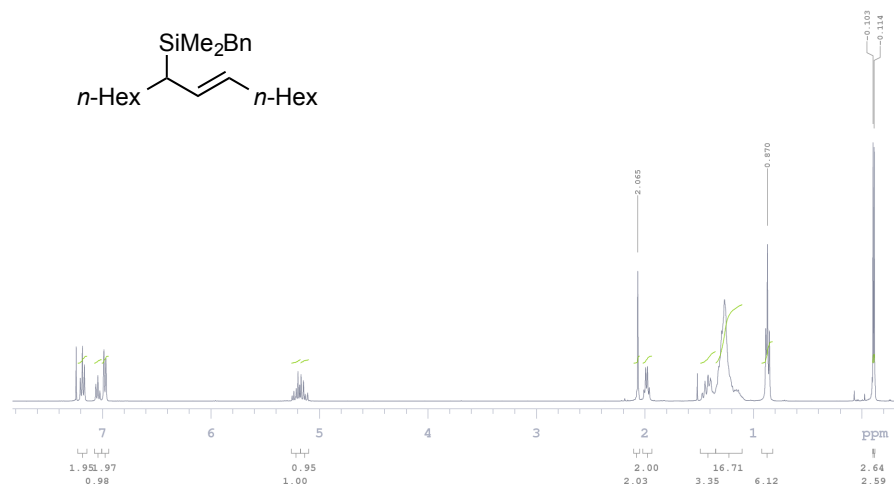


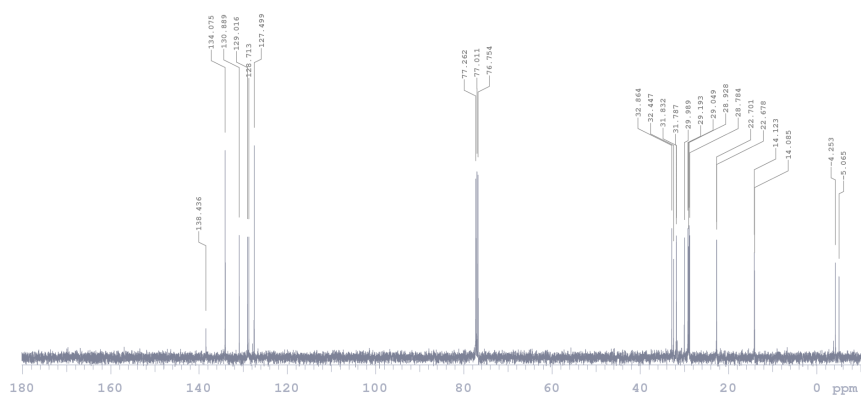
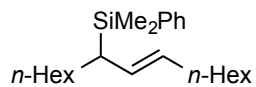
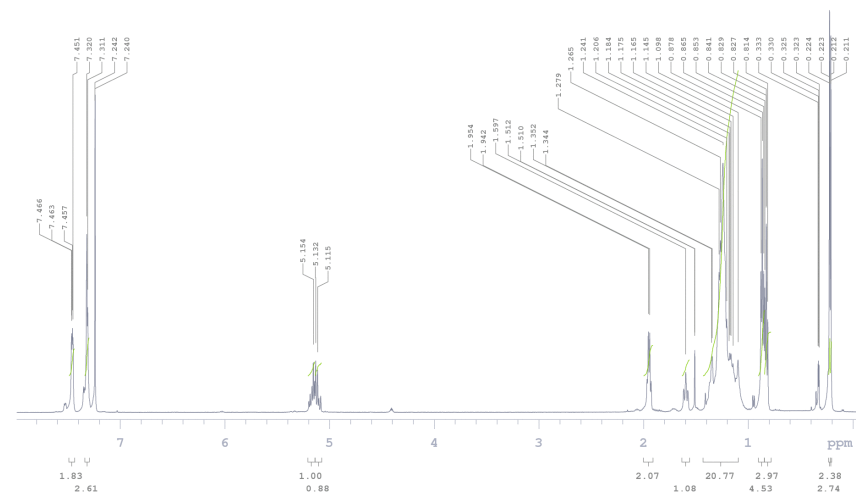
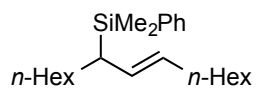


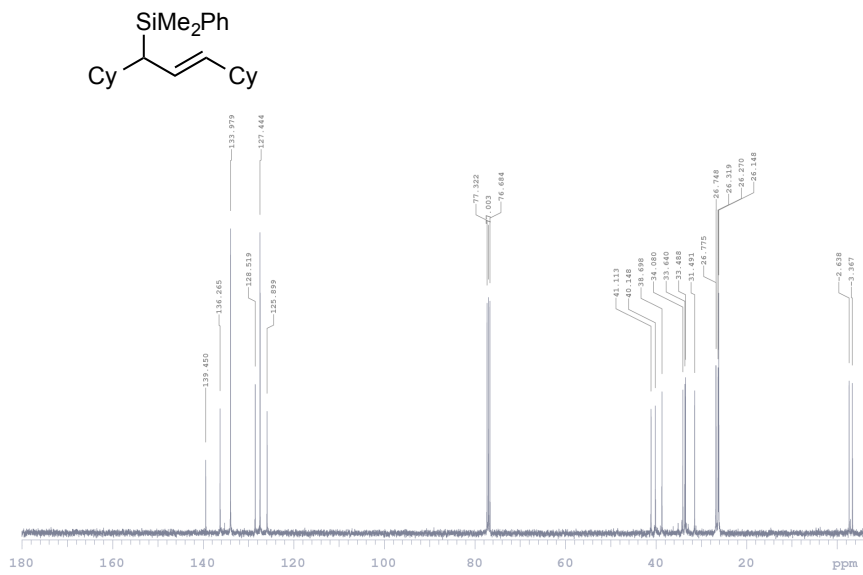
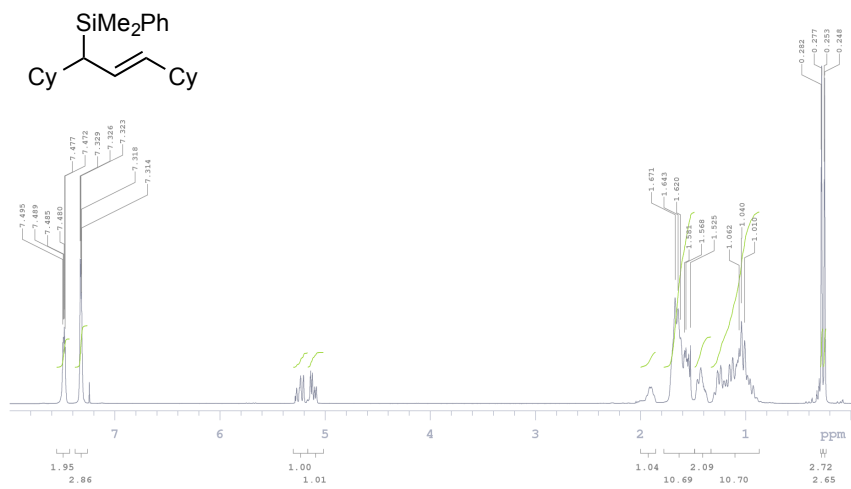


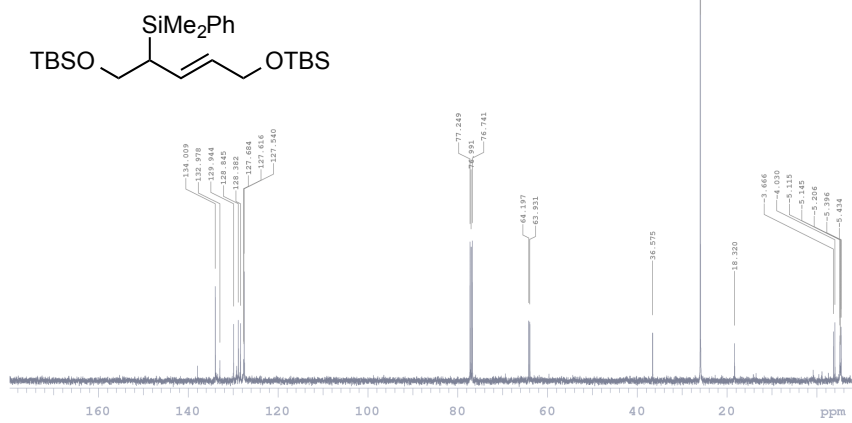
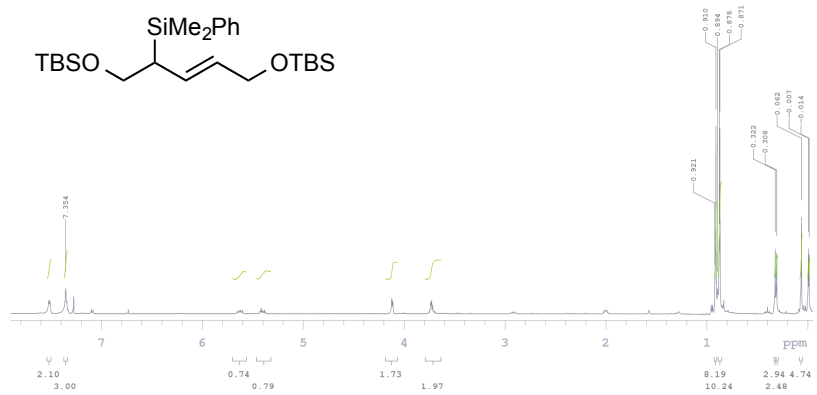


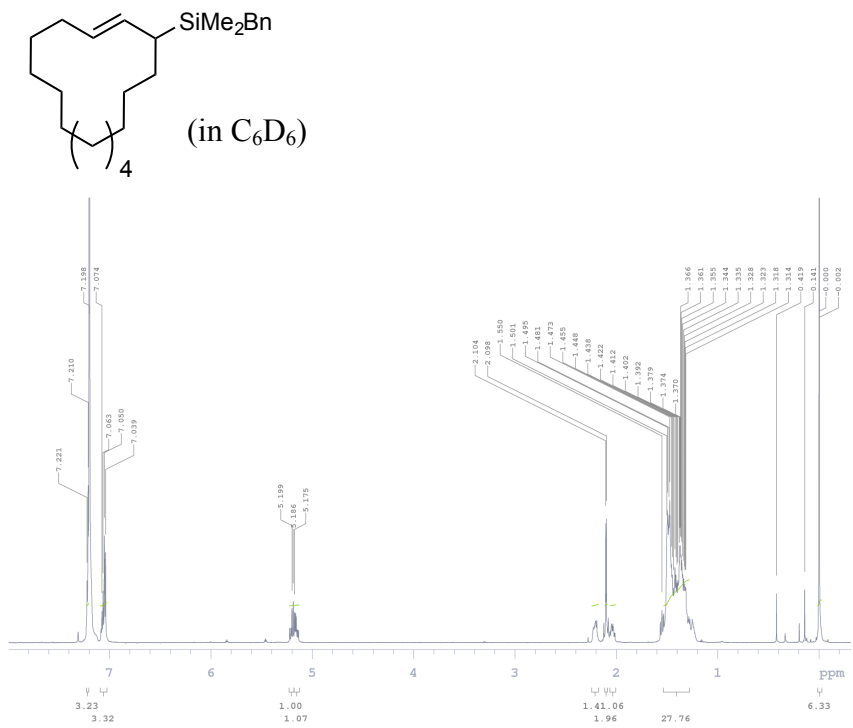
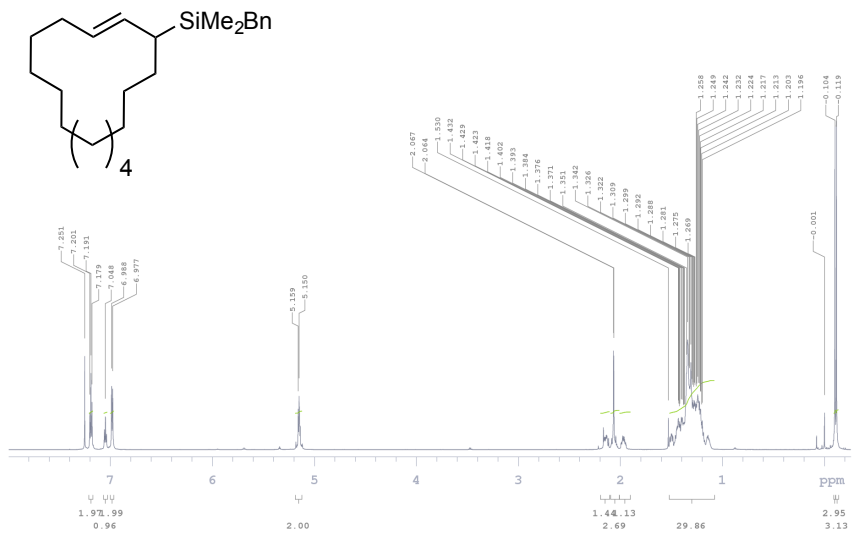


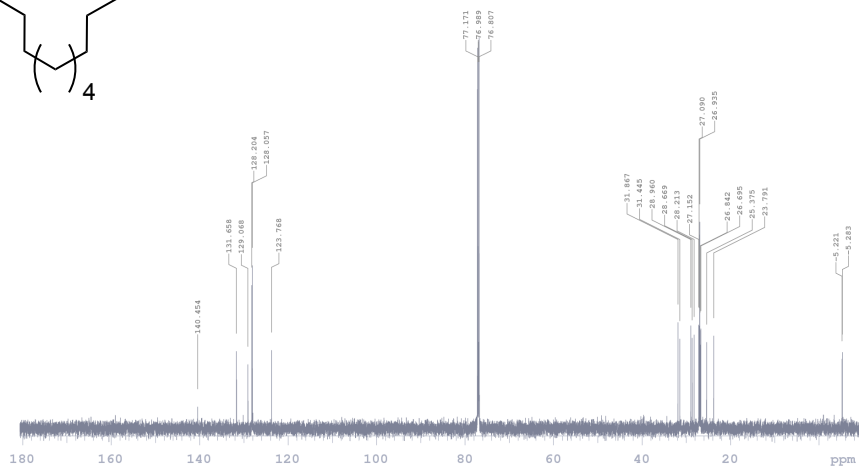
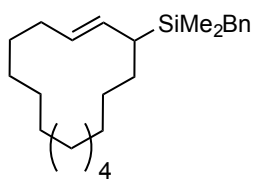
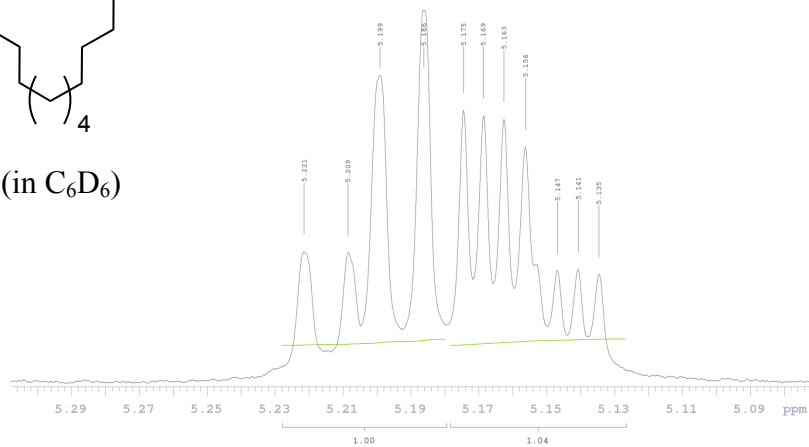
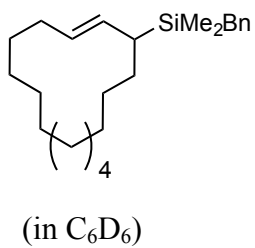


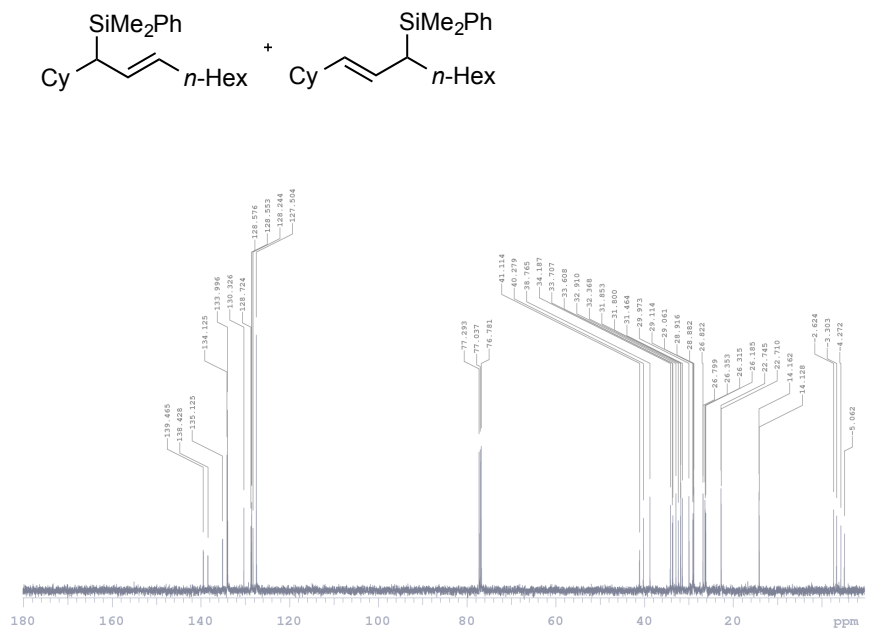
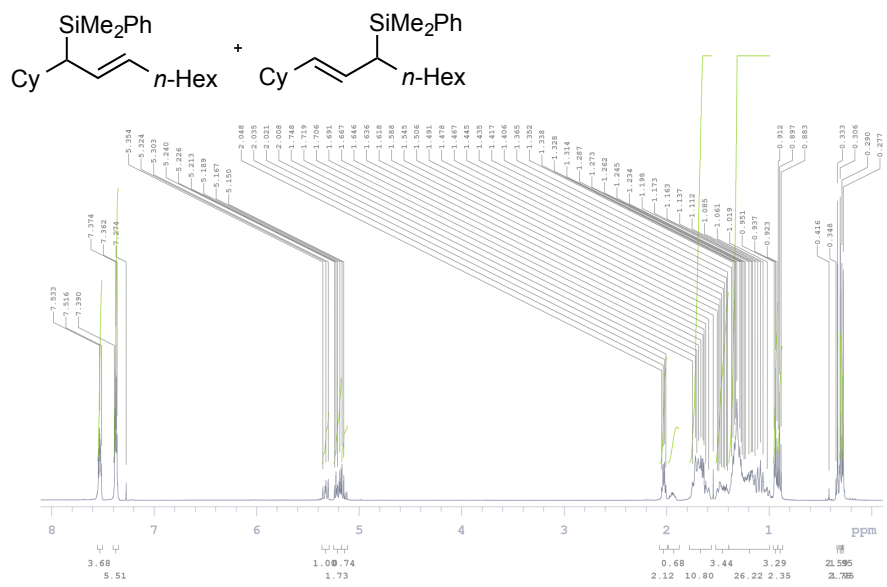


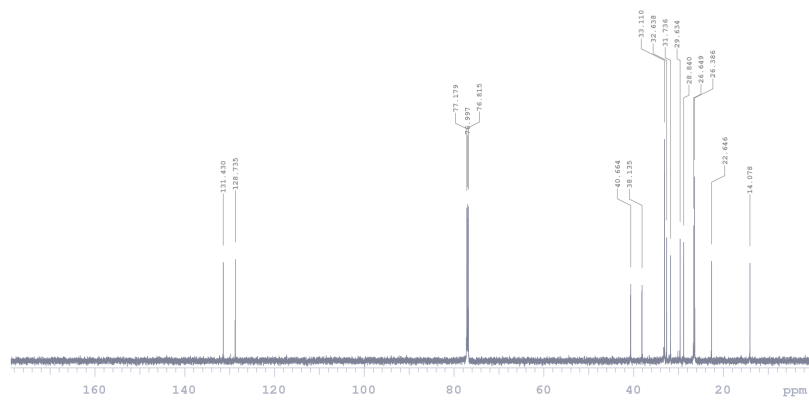
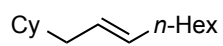
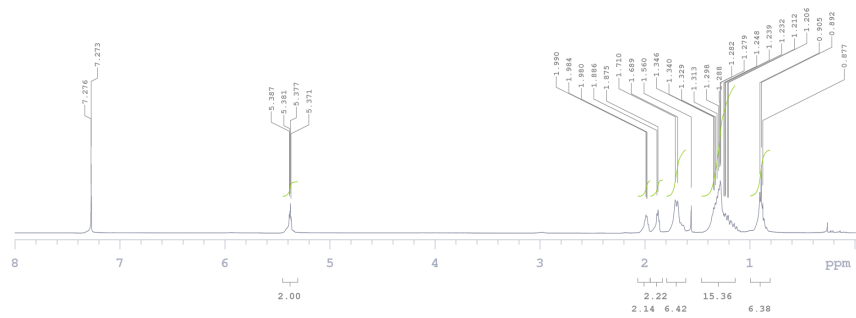
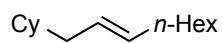


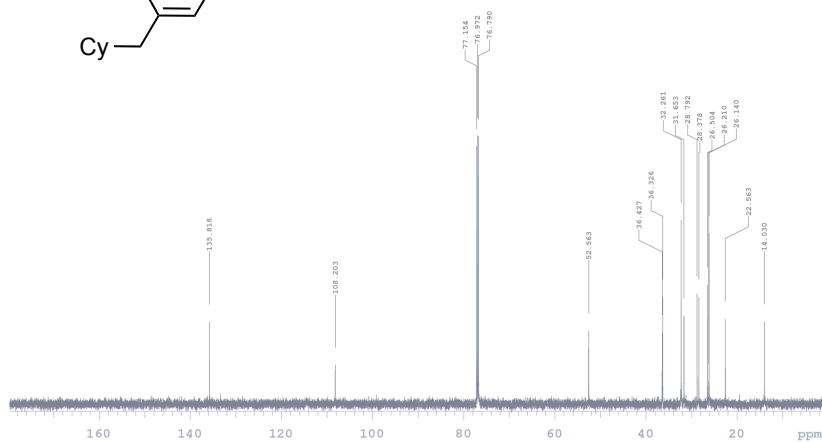
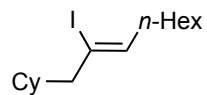
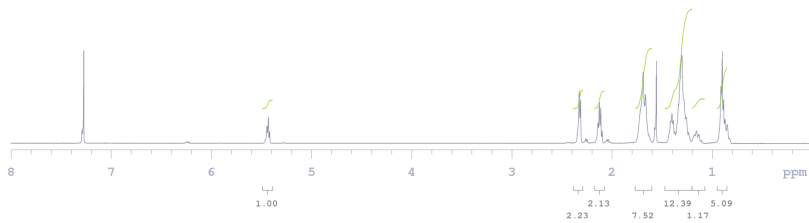
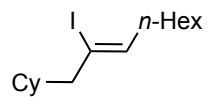


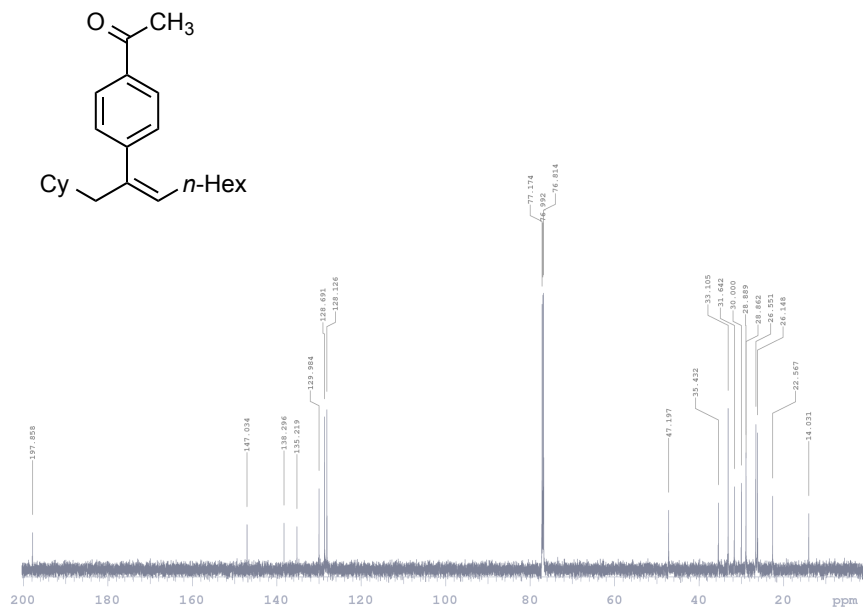
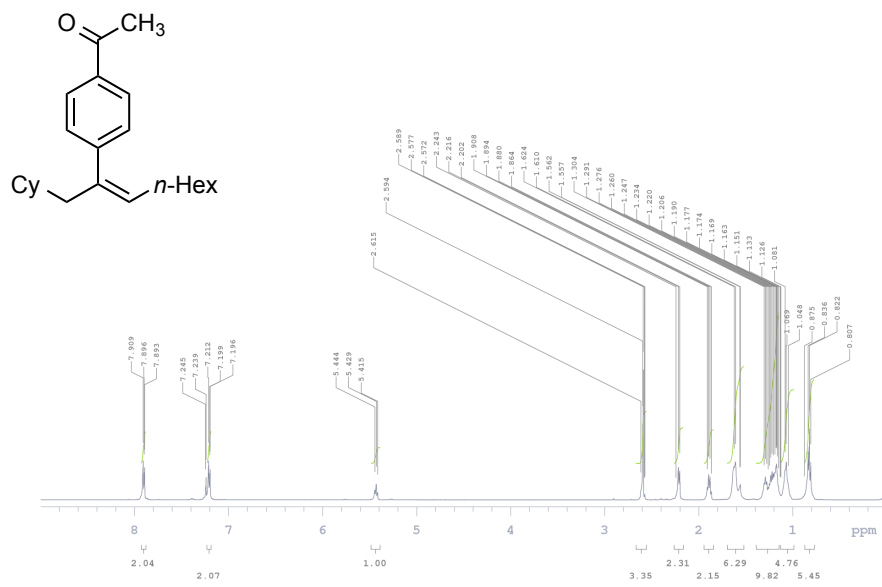


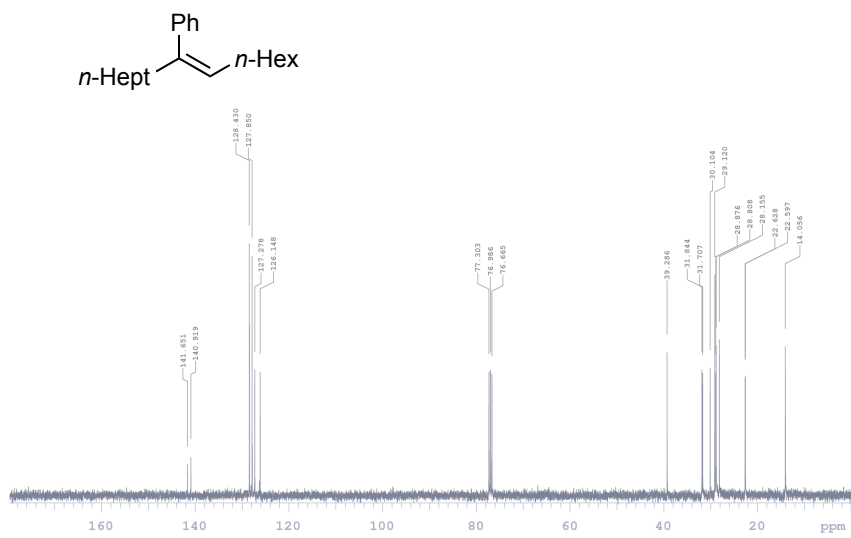
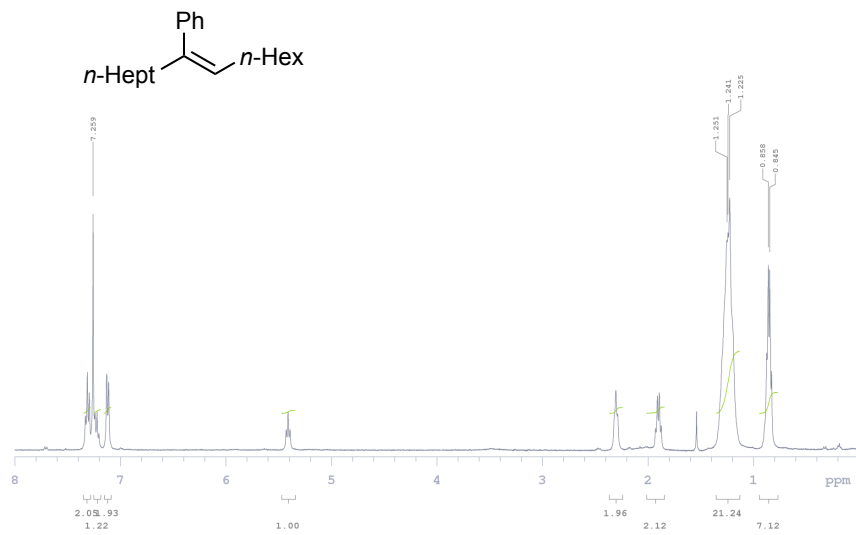


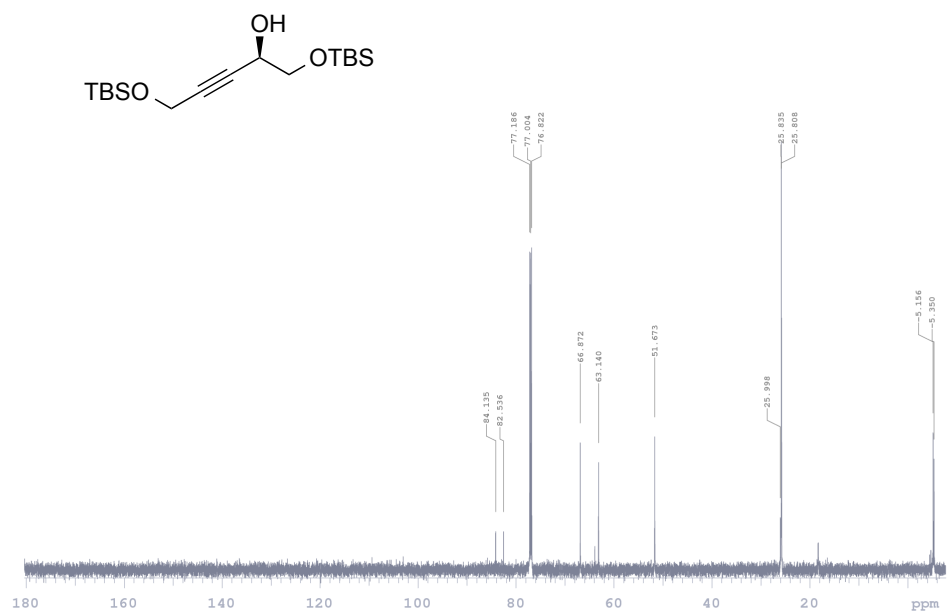
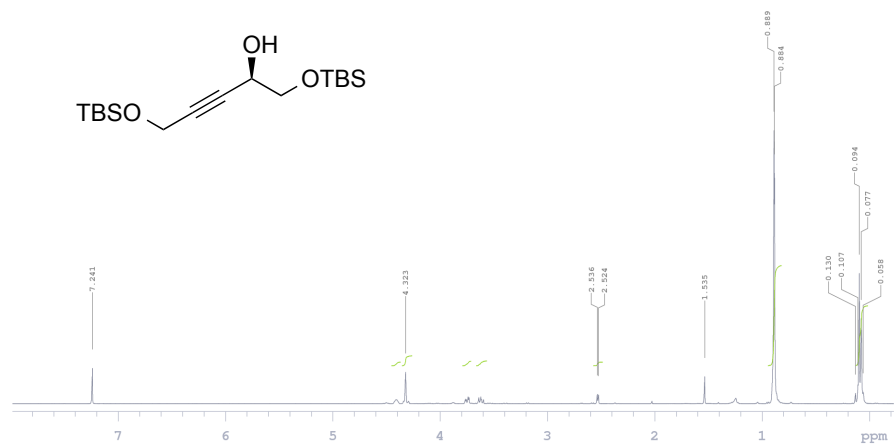




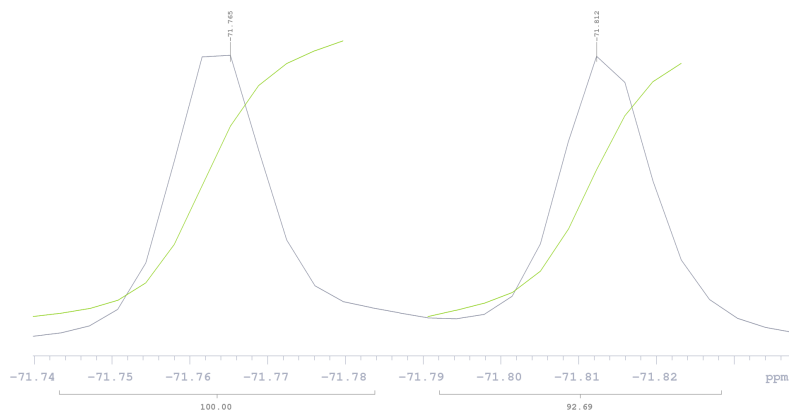




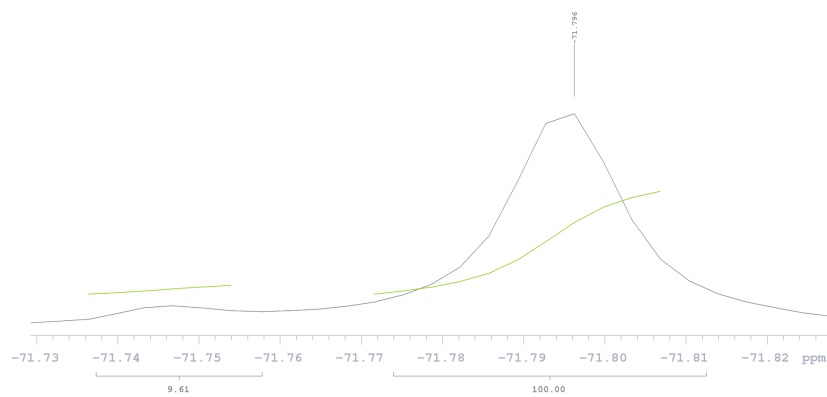


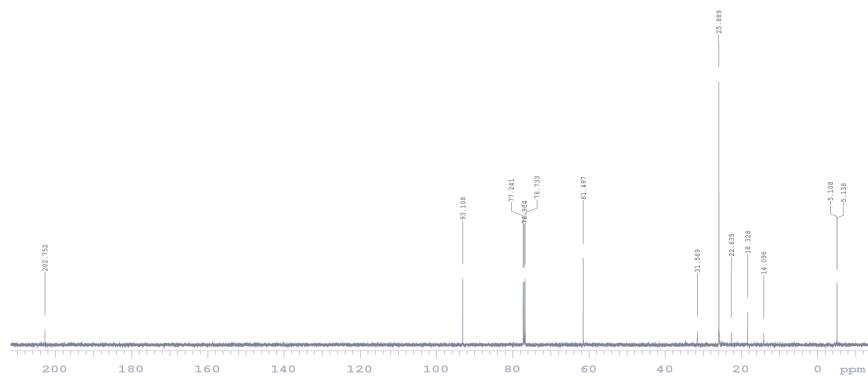
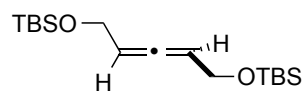
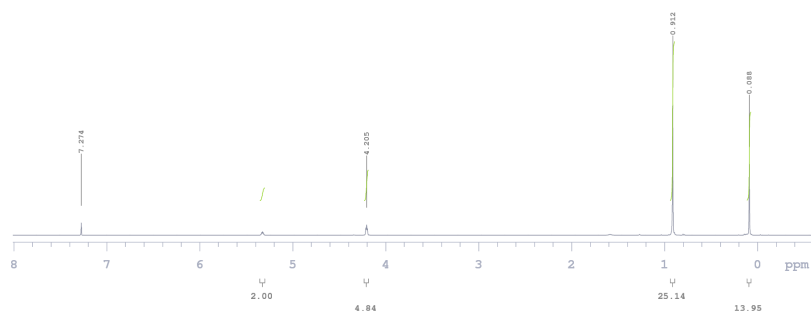
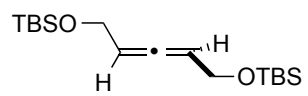


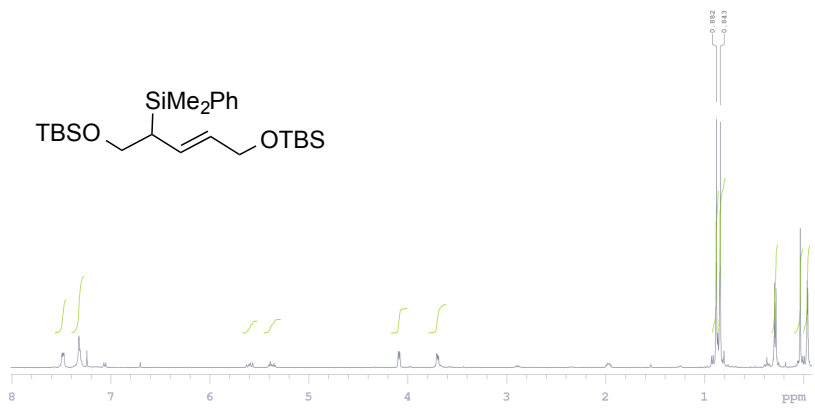
^{19}F NMR of racemic sample: From (*S*)-Mosher ester:



^{19}F NMR of enantioenriched sample: From (*S*)-Mosher Ester:







Chapter 5

Summary and Outlook

The work described in this thesis has primarily focused on the reduction of allenes by silane reducing agents, with an emphasis on controlling the stereo- and regiochemical outcomes in these transformations. In our preliminary studies described in detail in Chapter 2, we made the discovery that through the exploitation of metal identity, base metals in the same catalytic triad favored different regioisomers. For example, reactions with Pd(0) catalysts resulted in highly regioselective formations of allylsilanes, while reactions with Ni(0) catalysts afforded primarily alkenylsilanes. In the context of organometallic chemistry, this rare example of metal-directed regiocontrol strategy has not been widely explored or observed in other contexts. We had expected that either both reactions would afford the same regioisomeric product to similar levels of regioselectivity or that one of the catalysts would simply prove inefficient for the given transformation.

In our subsequent exploration of allene hydrosilylation, we considered designing more NHC complexes of Pd(0) in order to improve access to useful alkenylsilane structures. In all of our prior studies, we had observed that use of traditional NHC ligands afforded primarily allylsilanes in the hydrosilylations of allenes. We envisioned gaining access to a regime where Pd(0) hydrometalation was disfavored due to unfavorable steric

interactions between the silane ligand and NHC ligand. This would in turn favor silylmetalation and effectively reverse the regiochemical outcome to afford alkenylsilanes. In our studies, we discovered that two alterations were effective in promoting alkenylsilane formation: 1.) Including substituents (eg. methyl groups) on the bridgehead of the imidazolium ring as observed in regioreversals employing DM-IPr. 2.) Significantly increasing the sterics of the *N*-aryl groups to increase the encumbrance of the NHC ligand (eg. use of IPr*^{OMe} ligand) (See Chapter 3 for more detail). The optimized reaction conditions were also demonstrated to be effective in C-C bond-forming protocols when coupled in one-pot with a Pd(0)-catalyzed cross-coupling reaction to afford a variety of functionalized 1,1-disubstituted alkenes. This work also clearly demonstrates in its rare observation of ligand-controlled regioreversals that this is an effective protocol for converting a common starting material into a variety of products by simple alterations of the catalyst structure.

The hydrosilylations of 1,3-disubstituted allenes is also presented and describes useful catalytic protocols in access to stereodefined (*E*)-allylsilanes with Pd(0) catalysis and (*Z*)-alkenylsilanes with Ni(0) catalysis. In addition to the challenge of controlling their regiochemical outcomes in these transformations, the issue of favoring only one stereoisomer due to the possible configurations of the olefin geometry is also noteworthy. These particular classes of organosilicon-containing compounds are especially challenging to access in high regio- and stereoselectivity by other direct hydrometalation protocols. Using the same metal-directed strategy (Ni(0) vs. Pd(0) for controlling the regiochemistry in the migratory insertion, we found that (*Z*)-alkenylsilanes were favored with Ni(0)-catalysis and (*E*)-allylsilanes were primarily favored with Pd(0) catalysis

achieving high levels of regio- and stereocontrol. An interesting finding in this investigation is that products afforded in this manifold afford products with stereochemistry rarely achieved in transition-metal catalyzed additions with other π -components. Additionally, the Ni(0) catalyzed protocol permitted use of unsymmetrically substituted 1,3-disubstituted allenes with high levels of regio- and stereocontrol, favoring the reductive elimination of hydride at the more sterically encumbered carbon. This has permitted access to useful structures not readily accessible via alkyne hydrometalation that are useful in the synthesis of heavily substituted alkenes.

Future work should be dedicated to further exploring the discoveries made in this work within the context of other transformations involving different classes of π -components. There are numerous simple addition reactions that would tremendously benefit by a similar regiodivergent strategy employing metal or ligand identity as a means for regiocontrol. For example, developing hydrothiolation reactions with alkene substrates could be an important new direction that would enable C-S bond formation to take place in a controllable fashion. In addition to exploring other coupling reactions, studying electronically differentiated NHC ligands and the effects this has on catalysis could be an interesting direction for unlocking fundamentally new reactivity. This could also open the door for developing new strategies for regiocontrol that do not rely on steric effects experienced prior to migratory insertions.

In summary, strategies for gaining regio- and stereocontrol in simple additions of silane reductants to allene substrates have been described. Effective means for gaining regiocontrol include exploiting metal identity (Ni vs. Pd) in access to either alkenylsilanes or allylsilanes respectively. This observation clearly demonstrates that

NHC ligand scaffolds effectively enable metals in the group to undergo fundamentally different mechanisms. It has also been observed that use of ligand identity is an effective means for reversing the inherent preference for Pd(0) catalysts to undergo hydrometalation. This when strategy, when combined with a cross-coupling reaction, permits access to functionalized 1,1-alkenes without the requirement for isolation and purification steps of the alkenylsilane intermediate. In addition, the development of NHC catalysts of Ni(0) and Pd(0) have demonstrated that the stereochemistry of the allyl- and alkenylsilanes afforded can be controlled through the modifications of ligand structure, whereby the regiochemistry is set by metal identity. This has improved access to important alkenyl- and allylsilane structures otherwise not directly available by other hydrometalative protocols.

References

- 1.) a.) Huang, W. S.; Chan, J.; Jamison, T. F. *Org. Lett.* **2000**, *2*, 4221. b) Miller, K. M.; Huang, W. S.; Jamison, T. F. *J. Am. Chem. Soc.* **2003**, *125*, 3442.
- 2.) a.) Tang, X. Q.; Montgomery, J. *J. Am. Chem. Soc.* **1999**, *121*, 6098. b.) Tang, X. Q.; Montgomery, J. *J. Am. Chem. Soc.* **2000**, *122*, 6950. c.) Mahandru, G. M.; Liu, G.; Montgomery, J. *J. Am. Chem. Soc.* **2004**, *126*, 3698. d.) Chaulagain, M. R.; Sormunen, G. J.; Montgomery, J. *J. Am. Chem. Soc.* **2007**, *129*, 9568.
- 3.) a.) Baxter, R. D.; Montgomery, J. *J. Am. Chem. Soc.* **2011**, *133*, 5728. b.) McCarren, P. R.; Liu, P.; Cheong, P. H. Y.; Jamison, T. F.; Houk, K. N. *J. Am. Chem. Soc.* **2009**, *131*, 6654. c.) Liu, P.; McCarren, P. R.; Cheong, P. H. Y.; Jamison, T. F.; Houk, K. N. *J. Am. Chem. Soc.* **2010**, *132*, 2050.
- 4.) a.) Malik, H. A.; Sormunen, G. J.; Montgomery, J. *J. Am. Chem. Soc.* **2010**, *132*, 6304. b.) Liu, P.; Montgomery, J.; Houk, K. N. *J. Am. Chem. Soc.* **2011**, *133*, 6956. c.) Jackson, E. P.; Montgomery, J. *J. Am. Chem. Soc.* **2015**, *137*, 958.
- 5.) a.) Ng, S.-S.; Jamison, T. F. *J. Am. Chem. Soc.* **2005**, *127*, 7320. b) Amarasinghe, K. K. D.; Montgomery, J. *J. Am. Chem. Soc.* **2002**, *124*, 9366. c.) Wei, L.; Chen, N.; Montgomery, J. *Angew. Chem. Int. Ed.* **2010**, *49*, 8712.
- 6.) Gao, F.; Hoveyda, A. H. *J. Am. Chem. Soc.* **2010**, *132*, 10961.
- 7.) Wu, J. Y.; Moreau, T.; Ritter, T. *J. Am. Chem. Soc.* **2009**, *131*, 12915.
- 8.) Ohmura, T.; Oshima, K.; Taniguchi, H.; Suginome, M. *J. Am. Chem. Soc.* **2010**, *132*, 12194.
- 9.) a) Marciniak, B. *Hydrosilylation In Advances in Silicon Science*; Marciniak, B. Ed.; Springer: Dordrecht, Netherlands, 2009, Chapters 1-2. b.) Trost, B. M.; Ball, Z. T. *Synthesis* **2005**, 853-887.
- 10.) a.) Chalk, A. J.; Harrod, J. F. *J. Am. Chem. Soc.* **1965**, *87*, 16. b.) Mo, Z.; Xiao, J.; Gao, Y.; Deng, L. *J. Am. Chem. Soc.* **2014**, *136*, 17414.
- 11.) Berthon-Gelloz, G.; Schumers, J.-M.; De Bo, G.; Markó, I. E. *J. Org. Chem.* **2008**, *73*, 4190.
- 12.) Trost, B. M.; Ball, Z. T. *J. Am. Chem. Soc.* **2005**, *127*, 17644.
- 13.) Rooke, D. A.; Mendar, Z. A.; Ferreira, E. M. *Tetrahedron* **2014**, *70*, 4232.
- 14.) Kawasaki, Y.; Ishikawa, Y.; Igawa, K.; Tomooka, K. *J. Am. Chem. Soc.* **2011**, *133*, 20712.
- 15.) Chaulagain, M. R.; Mahandru, G. M.; Montgomery, J. *Tetrahedron* **2005**, *62*, 7560.
- 16.) a.) Wu, J. Y.; Stanzl, B. N.; Ritter, T. *J. Am. Chem. Soc.* **2010**, *132*, 13214. b.) Parker, S. E.; Börgel, J.; Ritter, T. *J. Am. Chem. Soc.* **2014**, *136*, 4867.
- 17.) Wang, P.; Yeo, X.-L.; Loh, T.-P. *J. Am. Chem. Soc.* **2011**, *133*, 1254.
- 18.) a.) McAtee, J. R.; Martin, S. E. S.; Ahneman, D. T.; Johnson, K. T.; Watson, D.

- A. *Angew. Chem. Int. Ed.* **2012**, *51*, 3663. b.) Martin, S. E. S.; Watson, D. A. *J. Am. Chem. Soc.* **2013**, *135*, 13330. c.) McAtee, J. R.; Yap, G. P. A.; Watson, D. A. *J. Am. Chem. Soc.* **2014**, *136*, 10166.
- 19.) Zhang, Y.; Panek, J. S. *Org. Lett.* **2007**, *9*, 3141.
- 20.) a) M. A. Brook, *Silicon in Organic, Organometallic, and Polymer Chemistry*, Wiley, Chichester, 2000. b) Fleming, I.; Barbero, A.; Walter, D. *Chem. Rev.* **1997**, *97*, 2063-2192; c) Fleming, I.; Dunoguès, J.; Smithers, R. *Org. React.* **1989**, *37*, 57. d) Ojima, I.; Li, Z. Y.; Zhu, J. W. *In Chemistry of Organic Silicon Compounds*; Rappoport, Z., Apeloig, Y. Eds.; John Wiley & Sons Ltd; Chichester, England, 1998.
- 21.) a) Liu, P.; Montgomery, J.; Houk, K. N. *J. Am. Chem. Soc.* **2011**, *133*, 6956. b) Li, W.; Chen, N.; Montgomery, J. *Angew. Chem. Int. Ed.* **2010**, *49*, 8712.
- 22.) Sudo, T.; Asao, N.; Gevorgyan, V.; Yamamoto, Y. *J. Org. Chem.* **1999**, *64*, 2494.
- 23.) Huang, G.; Isobe, M. *Tetrahedron* **2001**, *57*, 10241.
- 24.) a) Abe, Y.; Kuramoto, K.; Ehara, M.; Nakatsuji, H.; Suginome, M.; Murakami, M.; Ito, Y. *Organometallics* **2008**, *27*, 1736. b) Ohmura, T.; Taniguchi, H.; Suginome, M. *J. Am. Chem. Soc.* **2006**, *128*, 13682. c) Ito, Y.; Suginome, M. *J. Organomet. Chem.* **2003**, *680*, 43.
- 25.) Burks, H. E.; Liu, S.; Morken, J. P. *J. Am. Chem. Soc.* **2007**, *129*, 8766.
- 26.) For uncatalyzed hydroborations: a) Kister, J.; DeBaillie, A. C.; Lira, R.; Roush, W. R. *J. Am. Chem. Soc.* **2009**, *131*, 14174. b) Chen, M.; Handa, M.; Roush, W. R. *J. Am. Chem. Soc.* **2009**, *131*, 14602. c) Ess, D. H.; Kister, J.; Chen, M.; Roush, W. R. *Org. Lett.* **2009**, *11*, 5538. d) Gonzalez, A. Z.; Roman, J. G.; Alicea, E.; Canales, E.; Soderquist, J. A. *J. Am. Chem. Soc.* **2009**, *131*, 1269. e) Brown, H. C.; Liotta, R.; Kramer, G. W. *J. Am. Chem. Soc.* **1979**, *101*, 2966.
- 27.) For catalyzed hydroborations: a) Semba, K.; Shinomiya, M.; Fujihara, T.; Terao, J.; Tsuji, Y. *Chem.-Eur. J.* **2013**, *19*, 7125. b) Yamamoto, Y.; Fujikawa, R.; Yamada, A.; Miyaura, N. *Chem. Lett.* **1999**, 1069.
- 28.) a) Martín, C.; Molina, F.; Alvarez, E.; Belderrain, T. R. *Chem. Eur. J.* **2011**, *17*, 14885. b) Iglesias, M. J.; Blandez, J. F.; Fructos, M. R.; Prieto, A.; Álvarez, E.; Belderrain, T. R.; Nicasio, M. C. *Organometallics* **2012**, *31*, 6312.
- 29.) Searles, S.; Li, Y.; Nassim, B.; Lopes, M. T. R.; Tran, P. T.; Crabbé, P. *J. Chem. Soc., Perkin Trans. 1.* **1984**, 747. For the preparation of tert-butyl dimethylsiloxy-containing allene, the respective alkynol was treated with TBSCl and imidazole: Cheng, X.; Jiang, X. F.; Yu, Y. H.; Ma, S. M. *J. Org. Chem.* **2008**, *73*, 8960.
- 30.) Malik, H. A.; Sormunen, G. J.; Montgomery, J. *J. Am. Chem. Soc.* **2010**, *132*, 6304.
- 31.) Tanouchi, N.; Takeuchi, R. *J. Chem. Soc., Perkin Trans. 1.* **1994**, 2909.
- 32.) Fürstner, A.; Kollegger, G.; Weidmann, H. *J. Organomet. Chem.* **1991**, *414*, 295.
- 33.) Iwamura, H.; Uozumi, Y.; Hayashi, T. *Tet. Lett.* **1994**, *35*, 4813.
- 34.) Seki, Y.; Takeshita, K.; Kawamoto, K.; Murai, S.; Sonoda, N. *J. Org. Chem.* **1986**, *51*, 3890.
- 35.) Delvos, L. B.; Vyas, D. J.; Oestreich, M. *Angew. Chem. Int. Ed.* **2013**, *52*, 4650.
- 36.) a) Hatanaka, Y.; Hiyama, T. *J. Org. Chem.* **1989**, *54*, 268. b) Tamao, K.; Kobayashi, K.; Ito, Y. *Tetrahedron Lett.* **1989**, *30*, 6051. c) Itami, K.; Nokami, T.; Ishimura, Y.; Mitsudo, K.; Kamei, T.; Yoshida, J.-I. *J. Am. Chem. Soc.* **2001**, *123*,

11577. d) Denmark, S. E.; Wehrli, D. *Org. Lett.* **2000**, *2*, 565-568. e) K. Hirabayashi, K.; Mori, A.; Kawashima, J.; Suguro, M.; Hiyama, T. *J. Org. Chem.* **2000**, *65*, 5342. f) S. E. Denmark, T. Kobayashi, *J. Org. Chem.* **2003**, *68*, 5153. g) Denmark, S. E.; Yang, S.-M. *Org. Lett.* **2001**, *3*, 1749.
- 37.) Allen, A. E.; MacMillan, D. W. *Chem. Sci.* **2012**, *3*, 633.
- 38.) a) *Metal-Catalyzed Cross-Coupling Reactions*, 2nd Ed.; de Meijere, A., Diederich, F.; Eds.; Wiley-VCH: Weinheim, Germany, 2004. b) Nakao, Y.; Hiyama T. *Chem. Soc. Rev.* **2011**, *40*, 4893. c) Chang, W.-T. T.; Smith, R. C.; Regens, C. S.; Bailey, A. D.; Werner, N. S.; Denmark, S. E. *Organic Reactions*; Denmark, S. E., Ed.: John Wiley & Sons: 2011; Vol. 75, pp 213-746.
- 39.) a) Mizoroki, T.; Mori, K.; Ozaki, A. *Bull. Chem. Soc. Jpn.* **1971**, *44*, 581. b) Heck, R. F.; Nolley, J. P. *J. Org. Chem.* **1972**, *37*, 2320. c) *The Mizoroki-Heck Reaction*; Oesterirch, M., Ed.; John Wiley & Sons: Chichester, UK, 2009.
- 40.) a) Hatanaka, Y.; Hiyama, T. *J. Org. Chem.* **1988**, *53*, 918. b) Hiyama, T.; Hatanaka, Y. *Pure Appl. Chem.* **1994**, *66*, 1471. c) Hiyama, T. *J. Organomet. Chem.* **2002**, *653*, 58.
- 41.) a) Denmark, S. E.; Sweis, R. F. *J. Am. Chem. Soc.* **2001**, *123*, 6439. b) Denmark, S. E.; Sweis, R. F. *Acc. Chem. Res.* **2002**, *35*, 835. c) Denmark, S. E.; Baird, J. D. *Chem.-Eur. J.* **2006**, *12*, 4954. d) Denmark, S. E.; Regens, C. S. *Acc. Chem. Res.* **2008**, *41*, 1486.
- 42.) Denmark, S. E.; Wang, Z. *Org. Lett.* **2001**, *3*, 1073.
- 43.) a) Takahashi, K.; Minami, T.; Ohara, Y.; Hiyama, T. *Tetrahedron Lett.* **1993**, *34*, 8263. For other examples: b) Tamao, K.; Kobayashi, K.; Ito, Y. *Tetrahedron Lett.* **1989**, *30*, 6051. c) Mori, A.; Takahisa, E.; Hiyama, T. *Bull. Chem. Soc. Jpn.* **1995**, *68*, 2649. d) Mori, A.; Takahisa, E.; Kajiro, H.; Hirabayashi, K.; Nishihara, Y.; Hiyama, T. *Chem. Lett.* **1998**, 443.
- 44.) Miller, Z. D.; Li, W.; Belderrain, T. R.; Montgomery, J. *J. Am. Chem. Soc.* **2013**, *135*, 15282.
- 45.) a) Gaillard, S.; Bantreil, X.; Slawin A. M. Z.; Nolan, S. *Dalton Trans.* **2009**, 6967. b) Van Ausdall, B. R.; Glass, J. L.; Wiggins, K. M.; Aarif, A. M.; Louie, J. *J. Org. Chem.* **2009**, *74*, 7935.
- 46.) a) Anderson, J. C.; Munday, R. H. *J. Org. Chem.* **2004**, *69*, 8971. b) Spivey, A. C.; Gripton, C. J. G.; Hannah, J. P. *Curr. Org. Synth.* **2004**, *1*, 211.
- 47.) Trost, B. M.; Xie, J. *J. Am. Chem. Soc.* **2006**, *128*, 6044.
- 48.) Searles, S.; Li, Y.; Nassim, B.; Lopes, M. T. R.; Tran, P. T.; Crabbé, P. *J. Chem. Soc., Perkin Trans. 1.* **1984**, 747
- 49.) Meiries, S.; Speck, K.; Cordes, D. B.; Slawin, A. M. Z. ; Nolan, S. P. *Organometallics* **2013**, *32*, 330.
- 50.) a) Van Ausdall, B. R.; Glass, J. L. Wiggins, K. M.; Aarif, A. M.; Louie, J. *J. Org. Chem.* **2009**, *74*, 7935. b) Marko, I. E., et. al. *Dalton Trans.*, **2010**, 39, 1444.
- 51.) Miller, Z. D.; Montgomery, J. *Org. Lett.* **2014**, *16*, 5486.
- 52.) Nakamura, S.; Uchiyama, M.; Ohwada, T. *J. Am. Chem. Soc.* **2004**, *126*, 11146.
- 53.) Berthon-Gelloz, G.; Schumers, J.-M.; De Bo, G.; Markó, I. E. *J. Org. Chem.* **2008**, *73*, 4190.
- 54.) Andavan, G. T. S.; Bauer, E. B.; Letko, C. S.; Hollis, T. K.; Tham, F. S. *J. Organomet. Chem.* **2005**, *690*, 5938.

- 55.) Dai, Y.; Wu, F.; Zang, Z.; You, H.; Gong, H. *Chem. -Eur. J.* **2012**, *18*, 808.
- 56.) Guo, H.; Ma, S. *Synthesis* **2007**, *17*, 2731.
- 57.) Standley, E. A.; Jamison, T. F. *J. Am. Chem. Soc.* **2013**, *135*, 1584.
- 58.) Lebel, H.; Davi, M.; Díez-González, S.; Nolan, S. P. *J. Org. Chem.* **2007**, *72*, 144.
- 59.) Delcamp, J. H.; Brucks, A. P.; White, M. C. *J. Am. Chem. Soc.* **2008**, *130*, 11270.
- 60.) Lim, D. S. W.; Anderson, E. A. *Synthesis* **2012**, *44*, 983–1010. b) Blumenkopf, T. A.; Overman, L. E. *Chem. Rev.* 1986, *86*, 857–873. c) Langkopf, E.; Schinzer, D. *Chem. Rev.* **1995**, *95*, 1375–1408. d) Ojima, I.; Li, Z. Y.; Zhu, J. W. *The Chemistry of Organosilicon Compounds*; Rappoport, Z., Apeloig, Y., Eds.; John Wiley & Sons Ltd.: Chichester, U.K., 1998; Vol. 2, pp 1687–1792.
- 61.) Berthon-Gelloz, G.; Schumers, J.-M.; De Bo, G.; Markó, I. E. *J. Org. Chem.* **2008**, *73*, 4190.
- 62.) Sudo, T.; Asao, N.; Gevorgyan, V.; Yamamoto, Y. *J. Org. Chem.* **1999**, *64*, 2494.
- 63.) Trost, B. M.; Ball, Z. T. *J. Am. Chem. Soc.* **2005**, *127*, 17644.
- 64.) Denmark, S. E.; Pan, W. *Org. Lett.* **2002**, *4*, 4163.
- 65.) Baxter, R. D.; Montgomery, J. *J. Am. Chem. Soc.* **2008**, *130*, 9662.
- 66.) a) Sa-ei, K.; Montgomery, J. *Org. Lett.* **2006**, *8*, 4441. b) Montgomery, J. *Acc. Chem. Res.* **2000**, *33*, 467.
- 67.) a) Lozanov, M.; Montgomery, J. *Tetrahedron Lett.* **2001**, *42*, 3259. b) Oblinger, E.; Montgomery, J. *J. Am. Chem. Soc.* **1997**, *119*, 9065.
- 68.) Rooke, D. A.; Ferreira, E. M. *J. Am. Chem. Soc.* **2010**, *132*, 11926.
- 69.) a) Heffron, T. P.; Simpson, G. L.; Merino, E.; Jamison, T. F. *J. Org. Chem.* **2010**, *75*, 2681. b) Ley, S. V. *Comprehensive Organic Functional Group Transformations* Vol. 2, 1st Ed.; Cambridge University Press, **1995**.
- 70.) Suginome, M.; Iwanami, T.; Ohmori, Y.; Matsumoto, A.; Ito, Y. *Chem. -Eur. J.* **2005**, *11*, 2954.
- 71.) a) Tsuji, Y.; Kajita, S.; Isobe, S.; Funato, M. *J. Org. Chem.* **1993**, *12*, 4051. b) Masumoto, Y.; Ohno, A.; Hayashi, T. *Organometallics* **1993**, *12*, 4051.
- 72.) a) Ng, S. -S.; Jamison, T. F. *J. Am. Chem. Soc.* **2005**, *127*, 7320. b) Ng, S.-S.; Jamison, T. F. *Tetrahedron.* **2005**, *61*, 11405.
- 73.) El-Sayed, E.; Ananda, K.; Carreira, E. M. *Org. Lett.* **2001**, *3*, 3017.
- 74.) Myers, A. G.; Zheng, B. *J. Am. Chem. Soc.* **1996**, *118*, 4492.
- 75.) Hossain, M. L.; Ye, F.; Zhang, Y.; Wang, J. *J. Org. Chem.* **2013**, *78*, 1236.
- 76.) Brummond, K. M.; Dingess, E. A.; Kent, J. L. *J. Org. Chem.* **1996**, *61*, 6096.
- 77.) Hoyer, T. R.; Jeffrey, C. S.; Shao, F. *Nat. Prot.* **2007**, *2*, 2451.